Institutionen för vattenbyggnad
Chalmers Tekniska Högskola

Department of Hydraulics
Chalmers University of Technology

Slurry Transportation of Ores and Industrial Minerals in a Vertical Pipe by Centrifugal Pumps

A Pilot-plant Investigation of Hydraulic Hoisting

Anders Sellgren

Report
Series A:4
ISSN 0348-1050 Göteborg 1979

Adress: Institutionen för vattenbyggnad
Chalmers Tekniska Högskola
S-412 96 Göteborg, Sweden
Telephone: 031/81 01 00

ACKNOWLEDGMENTS

The experimental portion of this work was conducted partly under a grant from the Swedish Board of Technical Development (STU). Pump equipment was supplied by Morgårdshammar AB and Aros Electronics AB. Ores taken from in-plant processing were supplied by LKAB and Boliden AB. The author wishes to acknowledge and thank these organizations for their support.

Mr. Bengt Carlsson, Georg Nilsson and Ahti Vanninen did the machining work in connection with the building and instrumentation of the pilot-plant facility. Mr. Anders Ahlström, Per Lindvall, Jan Rogbeck, Håkan Sellgren, and Svante Wahlström have in various ways taken part in the experimental test programme. I am most grateful to all these individuals who helped make the experimental work possible.

My advisor Professor Anders Sjöberg made valuable comments during the final part of my work. Mr. Per-Johan Kindlund and Anders Nilsson did the programming in connection with their Master of Science thesis. Mrs. Göta Bengtsson and Mrs. Ann-Marie Holmdahl typed my manuscripts, Mrs. Alicja Janiszewska drew the figures and Mrs. Gerd Eng and her associates corrected the language. To these and to all others involved I am very thankful.

SUMMARY

The demand for higher productivity as well as health and safety considerations are the main reasons for the increasing international interest in the development of hydraulic transportation in underground mining and tunneling. A hydraulic hoisting system can replace, or partly replace, a shaft hoisting system, and thus influence the load carrying capacity of the main haulage system. The hoisting capacity can also be increased without necessitating the sinking of new shafts.

In the metal mining industry, conversion into a slurry of fine particles is often a part of the normal processing of the ore. Therefore, from a systems point of view, slurry transportation would be considered as a natural alternative, all the way from the working face to the final processing.

It is also believed that the same type of hydraulic transportation as is used for land-based underground mines will be able to be applied in future exploitation of consolidated undersea mineral deposits.

The present study is a pilot-plant investigation of slurry transportation in a vertical pipe with a diameter of 0.094 m, and of the effect of suspended solids on the performance of a rubber-lined centrifugal pump. In addition, the experimental results obtained in a horizontal laboratory-scale test loop (with a diameter of 0.027 m) are compared with some well-known computational models.

Based on the experimental results, the pressure requirement and energy consumption in a vertical slurry transportation system are represented in a simple graph. The technical-economic feasibility of hydraulic hoisting is also discussed and exemplified.

In a mining system for which hydraulic hoisting is being considered, the grade of size reduction before hoisting is a key parameter. Therefore, the solids used in this study were taken directly from in-plant crushing and milling processing, which, in most cases, provided a wide particle size distribution.

In the pilot-plant facility, important design factors such as velocities, concentrations, and energy consumption were investigated for complex ore, lead ore, two iron ores, perlite mineral and granite. The upper limit of particle size was about 8 mm and the densities varied from 2300 kg/m^3 to 4200 kg/m^3.

Experimentally determined energy losses are related to a Darcy-Weissbach friction factor and a modified Reynolds number. With the exception of the greatest velocities, there was a tendency towards greater friction factors than the ordinary friction factor-Reynolds number relationship expresses. For the coarsest solids investigated, this tendency may partly be attributed to a difference in velocity between the solid component and the water (slip).

From the experimental results of the iron ores, lead ore, and perlite it is concluded that the total pressure gradient can, in practice, be determined by considering the solid-water mixture as a homogeneous Newtonian fluid. In most applications, the corresponding energy losses can be determined from the ordinary Darcy-Weissbach equation for clear water, where the gradient thus obtained is expressed in metres of slurry per metre of pipe.

The effect of attrition of most solids investigated was almost negligible because the solid particles were relatively inert. However, experience obtained in this study with long-term exposed solids demonstrates the importance of controlling the effect of attrition and other time-dependent variables in a recirculating test-system.

The performance of the centrifugal pump was investigated in connection with the pilot-plant study on vertical transportation, using the same ores and industrial minerals. Pump head and efficiency are generally lowered by the presence of solids. For example, the clear water head and efficiency were lowered 30%-40% by the coarsest iron ore investigated.

With the exception of the complex ore and the granite, all experimental data is correlated to a formula expressing the influence of solid concentration and solid properties on the reduction in pump head. The drop in efficiency was equivalent to the drop in head up to concentrations by volume of 20%-25%. With higher concentrations, the drop in efficiency became greater than the drop in head.

A computational model developed by Wasp et al. (1963) for determination of energy losses in horizontal slurry transportation systems is analysed. It is demonstrated that the usefulness of the model is attributable to the dominant influence of the Darcy-Weissbach equation, when the model is applied to long-distance slurry pipeline systems.

TABLE OF CONTENTS Page

INTRODUCTION

Numerous technical and economic benefits derived from long-distance pipeline transportation of minerals, mainly coal and fine-grade ores, have been shown through approximately 15 years of international experience. In 1977 the world´s longest and largest iron ore pipeline went into operation in Brazil. This pipeline which runs from an inland mine to a pellet plant on the coast 400 km away, has a capacity of 12 Mtonnes of ore per year.

In 1974 the Swedish Board of Technical Development commissioned the Department of Hydraulics, Chalmers University of Technology(CTH), to perform a state-of-the-art study on slurry transportation in pipes. From that study it was concluded that any Swedish research and development (R and D) contributions should be directed towards transportation of mineral ores, peat and wood, the latter in connection with a conceivable future utilization of biomass as an energy resource. In the overall survey of the R and D requirements, it was pointed out, Sellgren (1975), that the work should concentrate on:

1. Applications where hydraulic transportation can be an integral part of the successive processing of raw material, thus leading to elimination and rationalisation of processing steps.

2. Improvements of some components and better understanding of specific problems, which together were believed to be of great importance in Swedish slurry transportation applications.

In Sweden there is no tradition of long-distance pipeline transportation, not even of oil or gas. The use of hydraulic transportation of minerals is mainly restricted to waste products in the mining industry, with pipelines no longer than about 5 km. In addition, slurry transportation technology is also an interdisciplinary field of chemical, civil, mechanical, and mining engineering, where the choice of organization strategy is a question of utmost importance if long-term R and D work is considered.

In connection with the possible opening of a new iron ore mine north of the arctic circle, the LKAB mining company analysed very intensively the feasibility of pipeline transportation of the ore to the coast,

Eriksson et al. (1976). It is believed that an increasing part of the LKAB iron ore handling will be in the form of pellets. A factor of great importance is that railway transportation of pellet feed in arctic climates is at present not economically feasible because of freezing. LKAB also delivers mineral products with particle sizes larger than pellet feed. There is great interest in alternative modes of transportation of these products in large volumes over long distances. It is generally believed that future improvements in slurry technology must also include transportation of coarser particles than today. System design and operating experience available for conveying large particle slurries is scarce as compared to those of fine particle systems now used extensively all over the world.

Swedish ore production is dominated by iron ore from large underground mines. Complex sulphide ores (copper, zink, etc.) are usually extracted from rather small mines in conjunction with cut- and fill mining methods. Conversion into a slurry of fine particles is often a part of the normal processing of the ore. There is in general a considerable inflow of groundwater which has to be pumped out. Therefore, from a system point of view, slurry transportation would be considered as a natural alternative of transportation, all the way from working face to final processing of the ore. Hard-rock, full-face techniques and continuous mining methods in softer minerals will, in the future, use slurry transportation technology.

In 1975 the Board of Technical Development granted money for a pilot-plant study at CTH on hydraulic hoisting of ores, as a continuation of the previously mentioned state-of-the-art study. Parallel to the work on the hydraulic hoisting pilot-plant facility at CTH, a system-oriented project was organised in 1976 by the LKAB-mining company and CTH, in cooperation with manufacturers and inventors. The project can be seen as a part of an overall program to meet long-term requirements for alternative modes of transportation in the Swedish mining industry. The development work on hydraulic transportation was initially concentrated on improvements of some components and better understanding of specific problems. No major organisation was ever built up. The work was organised in a very flexible way, with continually changing forms and partners. Necessary mining and processing expertise was obtained through the LKAB long-range planning function. The system-oriented work in close cooperation with different inventors

has to date inspired much innovative thinking among the people involved. The development work carried out so far was presented at the "5th International Conference on the Hydraulic Transport of Solids in Pipes" in May 1978. Eriksson et al. (1977).

There are a number of technical-economic reasons for studying hydraulic hoisting as a possible alternative to conventional hoisting methods. A hydraulic hoisting system can replace or partly replace a shaft hoisting system, and thus influence the load carrying capacity of the main haulage system. The hoisting capacity can also be increased without necessitating the sinking of new shafts.

Most large Swedish mines today work with relatively new and highly effective transportation facilities. Hydraulic hoisting in these mines, therefore, should be seen as an alternative in the overall mining system of tomorrow. However, the planning of a new main level in a large underground mine must start 10-15 years before the production starts, because of the long establishment and utilization times that are involved. To find the best overall solution, alternative technical solutions must be studied and weighed against each other at an early stage.

In present underground mining technology, the ore is comminuted to a rock size of about 0.1 - 0.2 m underground before being hoisted to the surface. Additional underground grinding and handling of the ore is necessary if the ore is to be hoisted hydraulically. The grade of size reduction before hoisting is a key parameter in the total economy of a hydraulic hoisting system.

A large number of pilot-plant studies on slurry transportation of industrial minerals in horizontal pipes have been carried out during the last decades. Consequently, large amounts of data have been published for a wide range of mineral commodities. Transportation of coarse, highly concentrated slurries would be desirable, but the technical feasibility of such systems still requires extensive research. The flow of slurry through vertical pipes has traditionally been considered to be a simpler problem, because of the axisymmetric behaviour with no particle deposition. Therefore, vertical slurry transportation has not merited the extensive research carried out for horizontal pipeline systems. Little work has been reported in the vertical slurry trans-

portation of mineral ores taken from in-plant processing, and with a wide range of particle sizes. Most available investigations have utilized relatively low concentrations of natural sediments such as sand and gravel. An adequate method of predicting the influence of slurry on centrifugal pump performance does not exist, and the number of published studies in this field is relatively small.

The present study involves an experimental investigation of the hydrodynamic properties of hydraulic hoisting of industrial minerals of different particle sizes and densities, which are taken from representative in-plant processing steps.

In the beginning of the present report some characteristics of the operation and of the hydraulic design of a slurry transportation sys- are reviewed. This is followed by some theoretical considerations and hydraulic design proposals of a single slurry system and a detailed description of the pilot-plant experimental work, as well as a discussion of the results. A model proposed for hydraulic design of long-distance slurry pipeline transportation systems has been analysed and compared to some experimental results here obtained in a laboratory-scale test loop. Finally, the feasibility of hydraulic hoisting is exemplified. These examples are, mainly based on the experimental results. The section dealing with the technical-economic feasibility of hydraulic hoisting is primarily a continuation of a report delivered to the Swedish Board of Technical Development, Sellgren (1977). A summary of the experimental work with coarse iron ore was also included in that report.

1. DESCRIPTION OF THE PROBLEM

1.1 Hydraulic design considerations of a slurry pipeline system

When designing a long-distance slurry pipeline, one must consider a number of design factors that are not normally part of an oil, gas, or water pipeline system. A long-distance slurry pipeline system should be designed so that the velocity can be kept at a moderate level causing no abrasive wear and so that the slurry flow can be stopped and re-started in the pipeline without difficulty. Carbon steel pipes without interior treatment are used. For a long-distance system, normal practice is to employ positive displacement pumps because of the large amount of pressure required.

The slurry design parameters were initially obtained from large-scale tests, and full-scale industrial operation has completed the test work. The organisations involved in the design work have successively built up an extensive foundation of knowledge. It is believed that the experience gained is sufficient to establish the technical feasibility of large-diameter, long-distance conventional slurry pipeline systems.

Transported solids can be classified in a homogeneous or a heterogeneous flow regime, according to the flow situation and the properties of the solids. Homogeneous slurries have the solid particles uniformly distributed in a liquid even at low flow rates. These slurries usually contain a high concentration of fine particles. One typical example of such slurries is sewage sludge. The operational velocity must be high enough to ensure turbulent flow conditions in a homogeneous slurry, because even fine-grained industrial minerals contain traces of coarse particles capable of settling at laminar flow conditions. The range of velocities where the flow changes from laminar to turbulent conditions in a homogeneous slurry is very sensitive to the system rheology, which means that the mixture may behave in a non-Newtonian way. Fluids are called Newtonian if shear stress, τ , is directly proportional to rate of velocity gradient, du/dy, starting with zero stress and zero gradient:

$$\tau = \mu \frac{du}{dy} \qquad (1.1)$$

where μ is the dynamic viscosity. Water is an example of a Newtonian fluid.

Fluids having a variable proportionality between stress and deformation rate are called non-Newtonian. Homogeneous mixtures often exhibit non-Newtonian behaviour particularly if the solid concentration is high and if the portion of solids less than 0.1 mm predominate. The rheological properties are normally identified in laboratory viscosimetric studies.

Heterogeneous slurries tend to separate, and there is a solid concentration gradient in horizontal pipe flow even at relatively high flow rates. A typical example of a heterogeneous slurry is sand in water. As the mean pipeline velocity is decreased, the nonuniform concentration profile becomes more and more pronounced until a moving or stationary bed of solids builds up in the pipe. Operation at too low a velocity in a homogeneous or heterogeneous slurry system would result in unstable flow situations with possible settling of solids. The operational velocity must exceed critical deposition conditions by a safety margin.

As a general rule of thumb, Aude et al. (1971) defined as homogeneous those flows with particles of median sieve size, d_{50}, of less than 0.05 mm and as heterogeneous those flows with d_{50} of more than 0.15 mm.

A long-distance pipeline system is operated in such a way that the particles are nearly uniformly distributed, i.e. the settling rate of the solid component is small under typical flow conditions. The flow can be classified as being in a pseudohomogeneous state. In the pseudohomogeneous flow in a horizontal pipe the extent of different velocities between the components can in most cases be neglected.

Design of mine-tailing pipelines involves many of the considerations of long-distance pipeline transportation and is further complicated by the variability in particle sizes and solid throughput. In mine-tailing pipelines or other short-distance applications, centrifugal pumps are traditionally used because of the moderate pressures required.

The operation and the hydraulic control of Swedish mine-tailing pipelines and cut-and fill systems are not always working at their best efficiency. Traditionally, the cost of energy has been low, and the availability of water has been good. Escalating energy costs and serious environmental problems, such as leakage of toxic metallic salts

from tailing disposal areas, point out the need of more detailed hydraulic design methods. This would result in benefits in many areas. For example, if a mine-tailing slurry is pumped with a solid concentration by weight equal to 50% instead of 30%, then the consumption of energy could be lowered by about 30% per tonne of solids pumped.

A hydraulic hoisting system based on centrifugal pumps

A hydraulic hoisting system based on staged centrifugal pumps is schematically shown in Fig. (1.1).

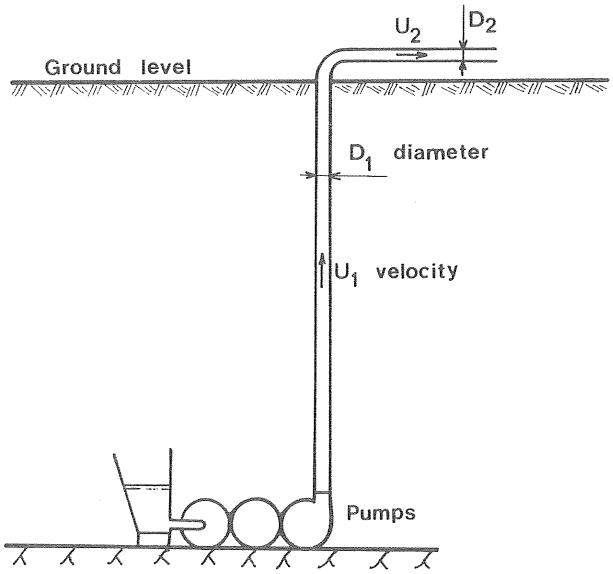

Fig. 1.1 Schematic lay-out of a hydraulic hoisting system.

Hoisting systems using centrifugal pumps are limited to shallow shafts because the number of pumps required in deep shafts would probably adversely affect the reliability. Pumping with centrifugal pumps or positive displacement pumps limits the maximum particle size to about 10 and 1 mm, respectively. If conventional overland, long-distance pipeline transportation is considered, the ore has to be ground to a maximum particle size of 0.1 - 0.2 mm.

Centrifugal pump characteristics supplied by pump manufacturers are mostly developed for clear water only. However, pump head and effi-

ciency are generally lowered by the presence of solids, especially if the solids are coarse and heavy. For example, pump tests carried out by a manufacturer in Sweden showed that the pump head and efficiency were nearly unaffected for iron ore composed to 90% of particles of less than 0.07 mm and a concentration by volume of up to 25%. However, the pump head and efficiency were lowered by about 40% for the same mineral and concentration, but with a mean particle size of about 0.3 mm. In order to correctly match the pump to the pipeline system, one has to know how the performance of the pump is affected in slurry service, Fig. (1.2).

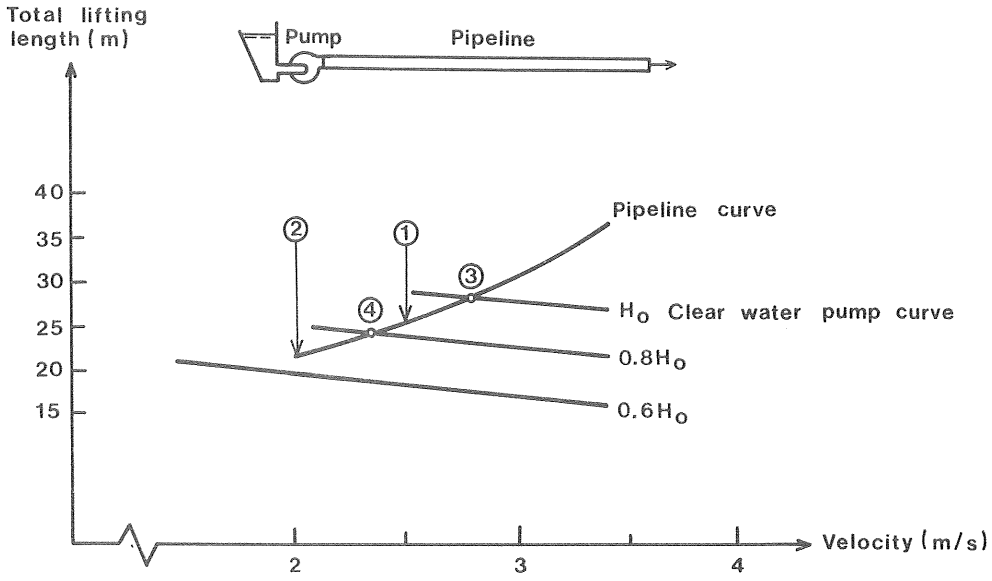

Legend

① Formation of moving dunes on the bottom of the pipe

② Formation of a stationary bed on the bottom of the pipe

③ Operational point with the pump clear water head unaffected

④ Operational point with the pump clear water head curve lowered by 20%

Fig. 1.2 *Deflection of the operational point due to effects of solids on a centrifugal pump head curve. Pipeline data from Haas et al (1973a). Transportation of a sand of mean particle size = 0.15 mm with a concentration by volume = 24% in a pipe of diameter = 0.16 m.*

Having seen the relationship between the pump and pipeline curves in Fig. (1.2), one can easily explain certain operational difficulties. The selection of the operational point is considerably complicated by the flat pump head curve, i.e. a small change in head produces a large change in flow. If the operational point moves to the left, Fig. (1.2), then the flow rate decreases, and solids settle with the possibility of plugging the pipe. At the other extreme, overcapacity results in excess velocity in the system.

In a vertical pipe flow of slurry the static part of the total pressure drop normally dominates over the friction loss. The total head for the vertical transportation of a relatively fine-grained, abrasive iron ore slurry is shown in Fig. (1.3). The friction loss term has been calculated for the two most often proposed approaches, which are based on a homogeneous flow pattern and a two-component flow pattern, A and B respectively, in Fig. (1.3).

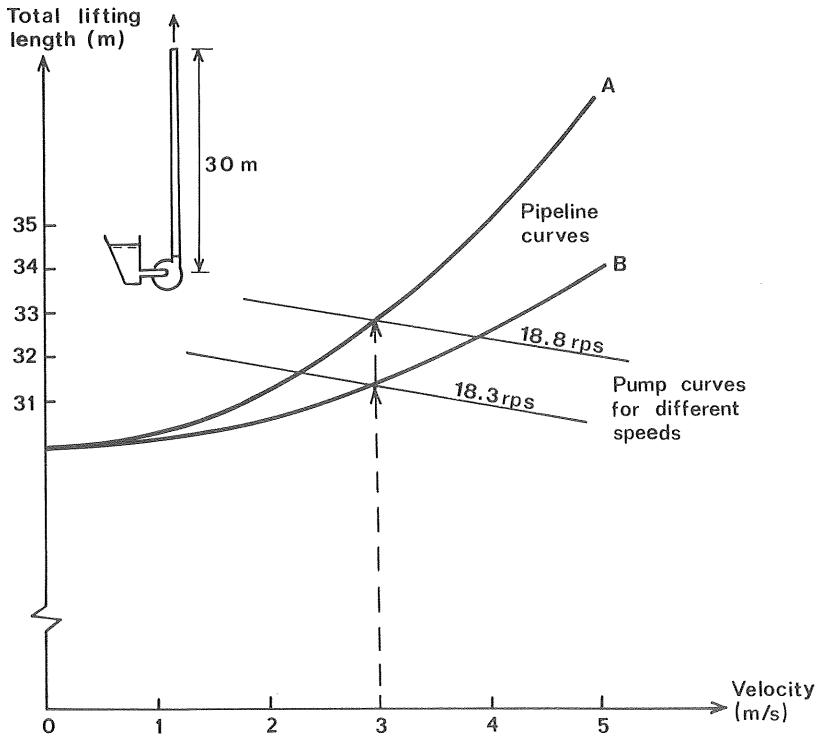

Fig. 1.3 *Transportation of a fine-grained iron ore with a centrifugal pump in a vertical pipe of diameter = 0.1 m. Comparison between two pipeline curves and pump speeds. Solid density = 5000 kg/m^3 and concentration by volume = 20%.*

Assume that the system outlined in Fig. (1.3) was designed to operate at a velocity of 3 m/s, based on pipeline-curve B in Fig. (1.3). If the actual pipeline friction loss is higher than estimated (curve A), then the pump speed must be increased from 18.3 rps to 18.8 rps to restore the flow. The operational point for practical application cannot be explicity established, because the performance is affected by the successive wear inside the pump and by changes in slurry characteristics. However, even a small deviation, over a long period of time, from a predetermined average pump speed may be expensive. The slight increase in rotary speed from 18.3 rps to 18.8 rps in the outlined example might increase the wear inside the pump with up to 8%, equivalent to a possible extra cost of about 10,000 Sw. Crowns[1] per year.

1.2 Objectives and scope of this study

There is no general relationship available for the determination of energy loss and pump performance in a slurry transportation system. The aim of this work is to establish a method of predicting the energy loss in a vertical pipe and the characteristics of a rubber-lined, centrifugal slurry pump within the range of pilot-scale tests with ores and industrial minerals. The behaviour of these industrial slurries was studied in a pilot-test facility, which provides an opportunity for observing flow phenomena and for measurements of energy loss and pump performance.

The minerals used are of different particle sizes (0-8 mm) and densities (2300-5000 kg/m^3). They were delivered from the following plants or mineral deposits, Fig. (1.4).

1 Iron ore from the LKAB-mines in Kiruna and Malmberget
2 Lead ore from the Boliden AB-mine at Laisvall
3 Complex ore from the Boliden AB-mine at Garpenberg
4 Crushed granite mineral from a crushing plant in Göteborg
5 Beach sand from a deposit in Baskarp
6 Perlite mineral from a deposit in Iceland

---

1) One Sw. Crown is about US$ 0.23 in November 1978.

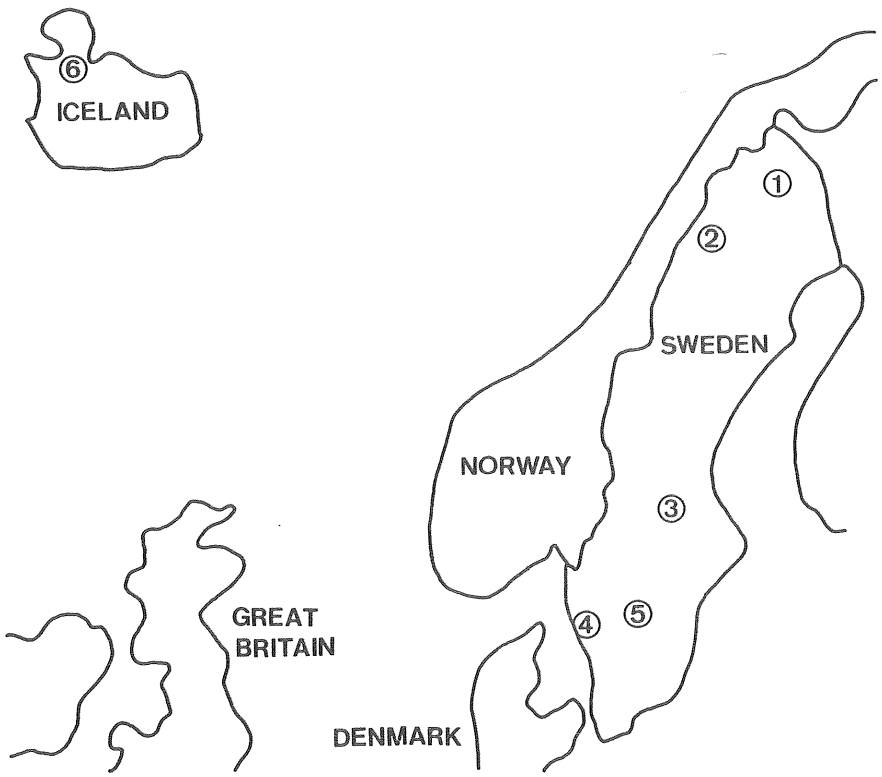

Fig. 1.4 *Locations of plants and deposits from which the ores and minerals used in the experimental study were taken.*

The hydraulic characteristics of the slurries of the most fine-grained minerals and ores used in this study were investigated in a laboratory-scale horizontal test loop. The friction losses and the operational conditions obtained from the tests were compared to some empirical models.

2. CHARACTERISTICS OF INDUSTRIAL SLURRIES

2.1 Classification

The flow of a particle-liquid mixture forms a complex multiphase system. However, the solids can in many cases be represented as one particulate phase in a carrier liquid. The particle-liquid mixture is then generally treated as a two-phase (two-component) system, assuming no change of state and no chemical reactions. The leading variables attending the flow of industrial suspensions in pipes are listed in Table (2.1).

Table 2.1 Leading variables attending the flow of solid-water mixtures in industrial pipeline applications

Properties of solid particle	Properties of water	Properties of pipe	Properties of flow
density (ρ_s)	density (ρ_o)	diameter (D)	concentration of solids (C)
size (d)	dynamic viscosity (μ_o)	inclination (θ)	
size distribution (Z)		absolute roughness (k)	rheological behaviour
shape factor (Ψ)			mean velocity of mixture (U)

Truly homogeneous solid-water mixtures are those for which separational effects due to the higher density of the solids are negligible. Such slurries may be treated hydraulically as if they were single-phase fluids.

If separational effects cannot be neglected, then various flow regimes may be defined, Fig. (2.1). The concept of defining distinguished flow regimes is, however, only applicable to mixtures of particles of similar size, while most slurries of industrial interest contain a considerable range of particle sizes.

In the heterogeneous flow regime the vertical distribution of solids in the pipe is clearly asymmetric. At lower velocities in horizontal pipes some particles indicate traces of a moving deposit on the bot-

tom of the pipe. With further reduction in velocity the coarser particles will form a sliding or stationary bed with the uppermost particles moving by saltation (rolling or jumping).

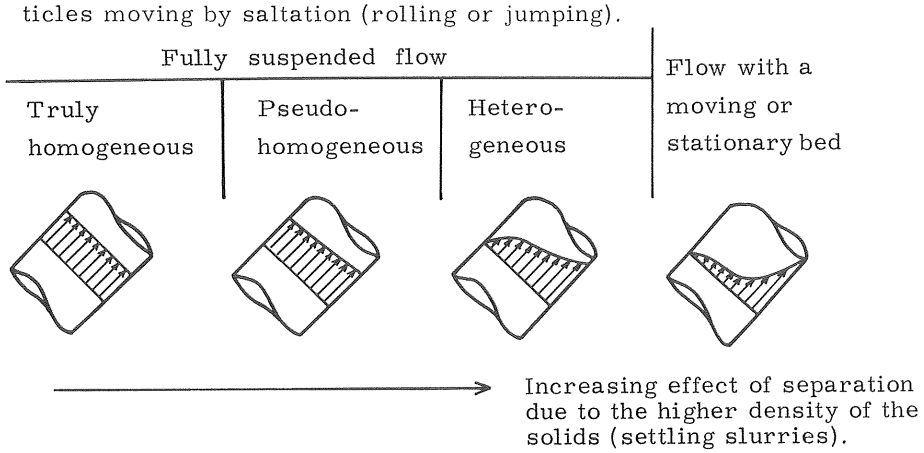

Fig. 2.1 *Illustration of slurries in different flow regimes.*

The flow of industrial slurries can generally be described as consisting of a homogeneous fluid medium formed with the water and the finer particles. The coarser particle sizes then act heterogeneously in this medium. Fig. (2.2) provides a rough means of classifying an industrial slurry, based on maximum particle size and density of the solids, Aude et al. (1971).

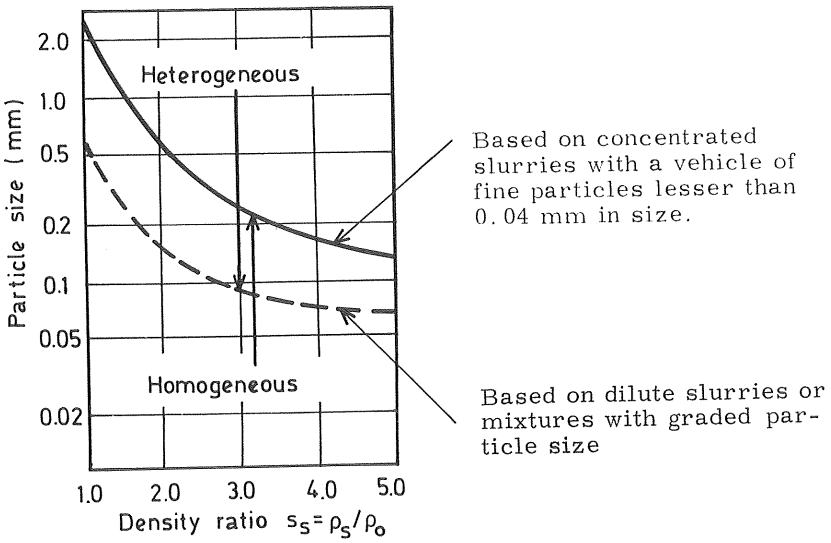

Fig. 2.2 *Schematic classification of slurries operation at velocities of from 1.2 m/s to 2.1 m/s in industrial pipeline applications. According to Aude et al. (1971).*

2.2 Rheological behaviour of slurries

Truly homogeneous mixtures of small particles may behave in a non-Newtonian way, which involves the complex field of rheology. The behaviour of the mixture is dominated by particle surface interaction forces, and therefore chemical properties such as the pH-value may be of importance. For example, fine-disperse systems of clay-minerals often exhibit non-Newtonian behaviour for concentrations as low as a few percent.

For the one-dimensional flow of a time-independent non-Newtonian fluid the shear stress within the slurry is a function (ϕ) of the applied velocity gradient:

$$\tau = \phi \left(\frac{du}{dy}\right) \qquad (2.1)$$

The parameters required to define the rheological behaviour are in general defined by empirical rheological models, Fig. (2.3).

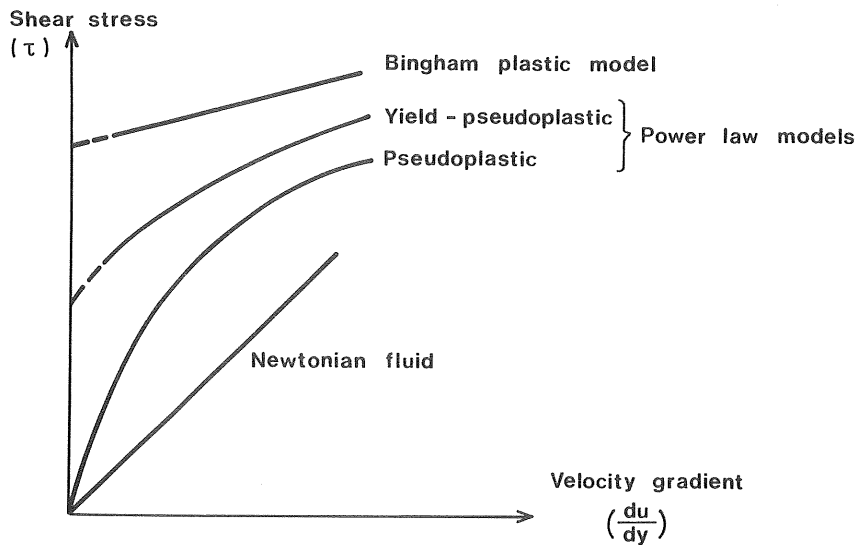

Fig. 2.3 Common rheological models used in slurry pipeline design.

The Bingham plastic model is defined by the relationship:

$$\tau = \tau_B + \eta_r \frac{du}{dy} \qquad (2.2)$$

where τ_B is the yield stress and η_r is the coefficient of rigidity. The Power law model reads:

$$\tau = K \left(\frac{du}{dy}\right)^n \qquad (2.3)$$

where K is the power law coefficient and n is the power law exponent. These two models are those most frequently used in slurry pipeline design. In Newtonian fluids the shear stress is proportional to the velocity gradient, i.e. $K = \mu$, and $n = 1$ in Eq. (2.3), as expressed in Eq. (1.1).

In practice, it is believed that the slurry is not adequately described by one of the simple models shown in Fig. (2.3). Most industrial slurries with nearly homogeneous flow behaviour are essentially Newtonian up to concentrations of about 10%-15%. For higher concentrations, the slurry may behave in a pseudoplastic or yield-pseudoplastic way. At very high concentrations (30%-40%), the mixture may behave as a Bingham plastic substance.

Dilute suspensions of uniform spherical particles generally exhibit Newtonian behaviour. Thomas (1965) proposed an empirical equation for the determination of the Newtonian viscosity, μ, of a solid-water mixture:

$$\mu / \mu_o = 1 + 2.5\,C + 10.05\,C^2 + 0.0027 \exp(16.6\,C) \qquad (2.4)$$

where μ_o is the viscosity of water. C is the volume concentration of solids expressed by the ratio between the solid discharge and the total discharge delivered:

$$C = \frac{Q_s}{Q_o + Q_s} \qquad (2.5)$$

where

Q_s = volumetric flow rate of solids

Q_o = volumetric flow rate of water

The total volumetric flow rate, Q, is:

$$Q = Q_o + Q_s \qquad (2.6)$$

It has been shown, however, that the relative Newtonian viscosity, μ/μ_o, depends upon the ratio between C and the maximum concentration, C_{max}, rather than upon the concentration itself, Aziz et al.(1972). A simple empirical relationship from determined values of metallic powders was obtained by Landel et al. (1963).

$$\frac{\mu}{\mu_o} = (1 - C/C_{max})^{-2.5} \qquad (2.7)$$

The maximum concentration for uniform spheres corresponding to a possible flow of a mixture in a pipe may be between 50% and 60%.

The particles in slurries of industrial interest are generally too coarse for rheological measurements. A representative viscosity of a slurry might be defined if the coarse particles are removed from the slurry and the viscosity of the fine particle part is identified.

2.3 Energy losses

Homogeneous slurries

The energy loss in pipe flow is normally represented by the energy loss gradient which can be related to the pipe wall shear stress by means of a simple force balance. Thus, it follows that:

$$\text{Energy loss gradient} = \frac{4\tau_w}{\rho g D} \qquad \left[\frac{\text{metres of slurry}}{\text{metre of pipe}}\right] \qquad (2.8)$$

where

τ_w = wall shear stress
ρ = density of slurry
g = acceleration of gravity
D = diameter of pipe

Assuming that:

$$\tau_w = c_1 \rho U^2, \qquad (2.9)$$

where

c_1 = dimensionless constant
U = average velocity of slurry

Eqs. (2.8) and (2.9) can be transformed to:

$$\text{Energy loss gradient} = \frac{f\,U^2}{2\,g\,D} \qquad \left[\frac{\text{metres of slurry}}{\text{metre of pipe}}\right] \tag{2.10}$$

where $f = c_1 \cdot 8$, is called the Darcy-Weissbach friction factor.

For laminar flow, τ_w, (and thus also f) can be obtained for any given rheological model. For a Newtonian slurry the following relationship can be found

$$f = \frac{\tau_w\, 8}{\rho\, U^2} = \frac{64}{Re} \tag{2.11}$$

where Re is the Reynolds number of the slurry:

$$Re = \frac{U\,D\,\rho}{\mu} \tag{2.12}$$

For turbulent flow conditions the absolute roughness, k, of the pipe wall also has to be considered, which leads to the relationship:

$$f = \phi\left(\frac{k}{D},\ Re\right) \tag{2.13}$$

where k/D is the relative roughness. For full turbulent flow, Eq. (2.13) is independent of Re, i.e.

$$f = \phi\,(k/D) \tag{2.14}$$

For industrial pipeline applications, the function ϕ in Eqs. (2.13) and (2.14) is often expressed in graphical form by the Moody-diagram, see page 183. The concept of Darcy-Weissbach friction factor will be used throughout this work.

Non-Newtonian properties are less severe under turbulent flow conditions, and Newtonian fluid methods may apply. A common method of determining the turbulent friction loss is to use the conventional Moody-diagram, where Reynolds number is calculated with a limiting viscosity obtained as an asymptotic value. For the non-laminar flow of Bingham plastic slurries Thomas (1962) suggested that the friction factor could be obtained with a Reynolds number, Re_B, based on the coefficient of rigidity, η_r

$$Re_B = \frac{U\,D\,\rho}{\eta_r} \tag{2.15}$$

The Darcy-Weissbach friction factor of a Bingham plastic fluid and a Newtonian fluid are compared schematically in Fig. (2.4).

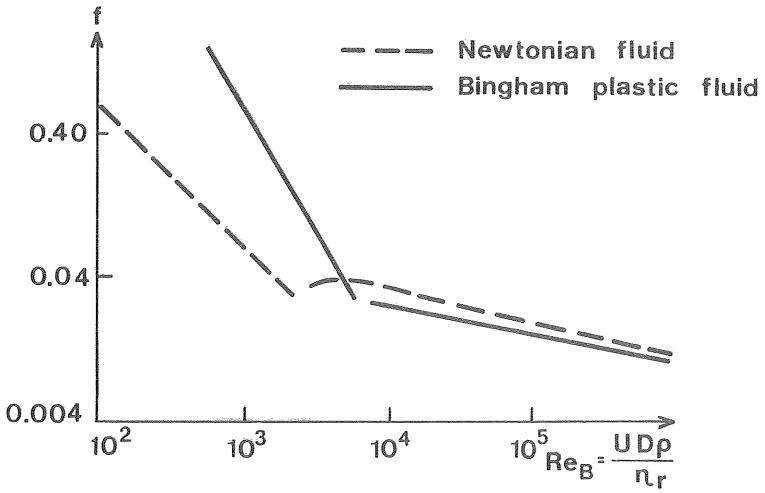

Fig. 2.4 *The Darcy-Weissbach friction factor versus the Reynolds number relationship for a Bingham plastic fluid and a Newtonian fluid.*

Heterogeneous slurries

The energy losses are often measured in U-tube manometers containing water and some heavy oil or mercury. Therefore, it is common practise to represent the slurry losses in terms of clear water. The contributions of water and solid to the energy loss gradient are not independent since the particles in suspension will almost certainly modify the flow pattern. However, in the determination of the energy loss gradient of non-homogeneous slurries it is generally assumed that the components can be treated independently:

$$i = i_o + i_s \qquad (2.16)$$

where

i = energy loss gradient of mixture.

i_o = the energy loss gradient that would arise in the water in the absence of solids (the clear water energy loss gradient).

i_s = excess energy loss gradient due to the solids in the mixture.

All gradients are expressed here in metres of water per metre of pipe. Furthermore, all gradients are related to the mean velocity of the solid-water flow, Fig. (2.5)

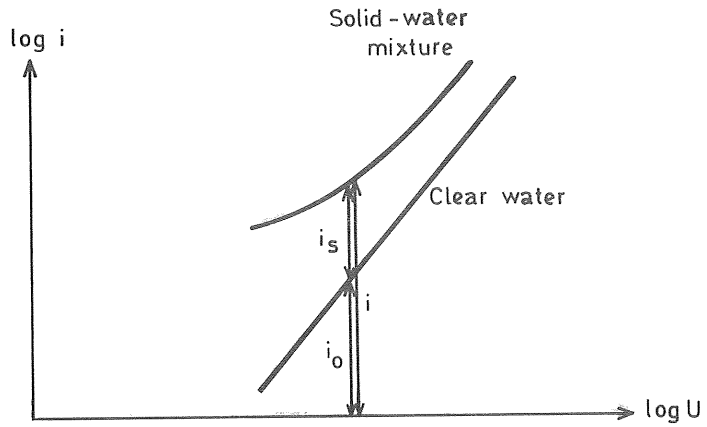

Fig. 2.5 *Characteristic energy loss gradient-velocity curve of a slurry compared with the clear water curve.*

The excess energy gradient $i - i_o$, Fig. (2.5), is traditionally expressed as a function of the variables listed in Table (2.1). If these variables are grouped into dimensionless parameters, the energy loss gradient can be expressed by, Duckworth (1969),

$$i = i_o + \phi(Re_o, Fr, \frac{k}{D}, C, s_s, \frac{d}{D}, Z, \Psi, \theta) \qquad (2.17)$$

where

$$Re_o = \frac{U D \rho_o}{\mu_o} \qquad (2.18)$$

is the Reynolds number of the flow of water, and where

$$Fr = \frac{U}{(gD)^{1/2}} \qquad (2.19)$$

is the Froude number. The parameter

$$s_s = \frac{\rho_s}{\rho_o} \qquad (2.20)$$

is the density ratio of the solids and the water.

The function ϕ in Eq. (2.17) is often expressed in the form of simplified empirical models developed from laboratory or pilot-plant test data. It is, however, important to know under which conditions the various models are applicable. For example, in an extreme transport situation with a stationary bed of solids on the bottom of a horizontal pipe with water flowing in the reduced cross-sectional area of the pipe, it is of little significance to relate the parameters in Eq. (2.17) to the mean velocity of the mixture.

Pseudohomogeneous slurries

O´Brien et al. (1937) found, for heterogeneous flow without saltation and with a nearly uniform concentration profile (pseudohomogeneous) that the energy loss gradient expressed in metres of delivered slurry per metre of pipe was approximately equal to the energy loss gradient of water, flowing at the same mean velocity. This result was based on experiments with sands in horizontal pipes having diameters of 0.055 m and 0.075 m.

If the energy loss of a solid-liquid mixture is analysed in terms of the Darcy-Weissbach parameters, it should by definition be related to the density, ρ, of the flowing mixture. The energy loss gradient of slurry, i, expressed in metres of water per metre of pipe, is converted to metres of slurry per metre of pipe by:

$$i/s \quad \left[\frac{\text{metres of slurry}}{\text{metre of pipe}}\right]$$

where s is the mixture density ratio = ρ/ρ_o. Thus, the experimental results by O´Brien et al. can be expressed by the following relationship:

$$i/s \quad \left[\frac{\text{metres of slurry}}{\text{metre of pipe}}\right] \approx i_o \left[\frac{\text{metres of water}}{\text{metre of pipe}}\right] \qquad (2.21)$$

where i_o is the energy loss gradient of water.

If the flow is assumed to be in the fully turbulent zone then the friction factor is not a function of Reynolds number. Thus, if Eq. (2.21) is an equality, and if Eq. (2.14),

$$f = \phi\left(\frac{k}{D}\right)$$

is applied to the flow of mixture with friction factor, f, and to the same flow of water with friction factor, f_o, respectively, then it follows that:

$$f = f_o \tag{2.22}$$

O'Brien et al. (1937) were among the earliest investigators who related the energy loss to the Darcy-Weissbach equation. In their original work they represented some of their experimental data in the form of f-U graphs. For the sand-water mixtures they investigated, the flow was usually well into the turbulent region where the friction is little affected by the viscosity. However, more generally, it is not clear whether f would be defined by a Reynolds number determined from the density and viscosity of the liquid or from the slurry. In applications where the flow of the mixture can be considered to be pseudohomogeneous, Graf (1971) stated that f in general can be taken from the Darcy-Weissbach equation based on a modified Reynolds number, Re', calculated on the basis of the density of the mixture and the viscosity of the carrier water, i.e.

$$Re' = s\, Re_o \tag{2.23}$$

where

$$s = \rho/\rho_o$$

$$Re_o = \frac{U D \rho_o}{\mu_o}$$

In systems encountered industrially, Eq. (2.21) seems to be valid in any pipe of given orientation provided the velocity is sufficiently high. Thus, more generally:

$$|f - f_o| \approx 0 \quad \text{if } Re > Re_c \tag{2.24}$$

where Re_c defines a "critical" Reynolds number dependent on the properties of the system and the slurry.

2.4 Discussion of some experimental observations

Pilot-plant studies by Haas et al.(1973 a)with silica sand slurries in horizontal pipes having diameters of 0.055 to 0.31 m may here exemplify the converging tendency of f to f_o for growing Reynolds numbers. The sand was of uniform size distribution with median sieve size, d_{50} = 0.15 mm. The experiments were conducted in smooth pipes with absolute roughness, k = 10^{-6} m. The energy loss gradients in Table (2.2) are related to a concentration of 23 to 24% and to a velocity just above that which has been observed for moving dunes on the bottom of the pipe.

Table 2.2 Energy loss convergence for growing pipe diameters and velocities. Based on experimental data from Haas et al. (1973 a).

Pipe diameter, D(m)	0.055	0.11	0.16	0.26	0.31
Velocity, U (m/s)	1.64	1.95	2.56	2.83	2.98
Energy loss gradient ratio, i/si_o	1.33	1.30	1.22	1.11	1.08

A decreasing energy loss gradient for concentrations from about 10 to about 25% can be found for heavy solid slurries in horizontal pipes as schematically illustrated in Fig. (2.6)

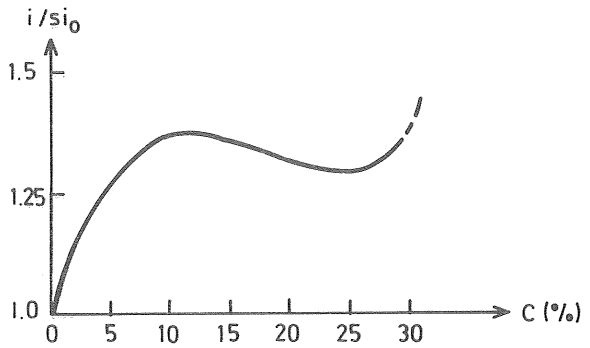

Fig. 2.6 *Energy loss gradient ratio of heavy solid slurries versus concentration for constant velocity.*

Cave (1978) described this behaviour as a typical flow pattern in pipes of diameters of 0.05 m to 0.35 m with mineral ore slurries of particle sizes and solid densities in the range of 0.15 mm to 0.20 mm and 4500 to 5000 kg/m^3, respectively.

The effect of particle size distribution on the energy loss in general is very complex. From the pilot-plant studies by Haas et al. (1973 a) with sand slurries, it was in some cases found that the energy loss of mixture containing solids having a broad size distribution was less than that of a mixture of uniform solids with comparable mean particle size. This effect, however, depended on the pipe diameter, and with concentrations below 20-25% the energy loss was lower for the uniform sand than for the sand having the broad particle size distribution.

Based on extensive pilot-plant test data of settling industrial slurries in horizontal pipes, Faddick (1972) correlated the experimental energy loss data with the Darcy-Weissbach friction factor, f, and a modified Reynolds number defined by Eq. (2.23):

$$Re' = s\, Re_o$$

The single-component parameters (f, Re, k/D) were thought to be related to (s_s, Z, C, d/D), where d is a characteristic particle size, Z is a particle size distribution factor, and s_s is the slurry density ratio. The influence of all these parameters was found to be very complex. It was observed that the divergence from the clear water curve for decreasing values of Re' mainly differentiates full suspension flow and non-suspension flow, Fig. (2.7).

Similar observations were reported by Lazarus et al. (1978), who analysed experimental friction loss data for the flow of settling mixtures of uniform particle sizes in horizontal hydraulically smooth pipes.

The convergence of the slurry curve, shown in Fig. (2.7), illustrates schematically the decreasing relative significance of separational tendencies of solid particles or laminar non-Newtonian behaviour. This is related to the increase in velocity. A comparison of Fig. (2.7) with Fig. (2.4) may illustrate the complex influence of separational effects due to higher density of the solids and non-Newtonian behaviour in industrial slurries.

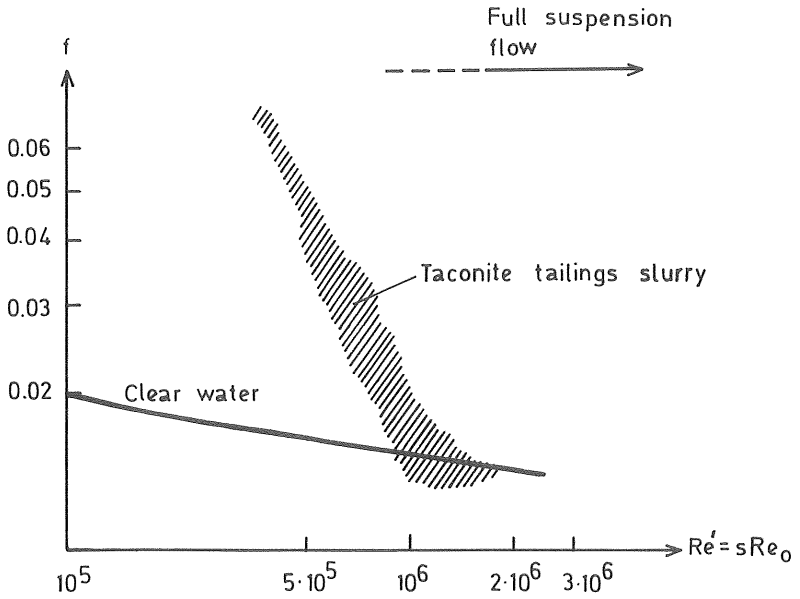

Fig. 2.7 *Schematic representation of experimental data with the Darcy-Weissbach friction factor versus a modified Reynolds number, according to Faddick (1972). Taconite tailings, D = 0.15 m, ρ_s = 2630 kg/m^3, d_{50} = 0.37 mm, maximum particle size, d_{max} = 0.85 mm, and C = 26% to 38%.*

Prediction of energy losses in the laminar/turbulent transitional region is not a well-defined phenomenon, not even for Newtonian fluids. With the combined non-Newtonian and separational effects in a slurry flow, it is not expected that unique criteria for distinguishing between flow regimes can be found.

In the analysis of energy loss data from experiments and full scale operation of non-homogeneous slurries, it is sometimes found that

$$i/s \left[\frac{\text{metres of mixture}}{\text{metre of pipe}}\right] < i_o \left[\frac{\text{metres of water}}{\text{metre of pipe}}\right] \qquad (2.25)$$

i.e. the energy loss in metres of slurry is less than the energy loss for the flow of water compared at equivalent velocities. Such behaviour has generally been observed under various operational conditions. The behaviour demonstrated by Eq. (2.25) has usually been attributed to a dampening effect of particles on transporting turbulence eddies, re-

sulting in a lowering of the energy losses.

Under certain flow conditions it has been observed by, for example, Brühl (1976) and Zandi (1967), that the energy loss is reduced when relatively small concentrations of fine particles (less than about 0.05 mm) are added to the non-laminar flow of a solid-water mixture.

As stated before, the effect of particle size distribution is very complex. The slurry may behave in a non-Newtonian way with small particles, whereas larger particle sizes may make the slurry behave in a Newtonian way. However, even in systems where fine particles are not present and where non-Newtonian behaviour is unlikely, experimental results confirming Eq. (2.25) have been reported.

2.5 Problems encountered in experimental studies

Limited laboratory bench tests may be sufficient to characterize the rheological properties of a pseudohomogeneous mixture. In many cases, such small scale tests must be completed with pumping in larger diameter pipes, which are usually carried out in recirculating test facilities. Evaluation of experimental data to full scale application is not only a scaling up problem, loop tests present a number of problems, which must be interpreted carefully.

Viscosimetric studies indicate changes of the hydraulic characteristics of a slurry. For example, the maximum solid concentration may be taken as the concentration at which a small increase in concentration results in a large change in the measured viscosity. Conventional viscosimeters are not always suitable for measurements of slurry viscosities and measured rheological variables are not independent of the type of viscosimeter used. Stratification of particles can cause considerable errors, Cheng et al. (1972). Rotational viscosimeters cannot, for example, handle coal particles of sizes over about 0.2 mm, Lavingia et al. (1974). The rheological properties should be evaluated up to the expected wall shear stress in the actual pipeline application. At such high shear rate a finite viscosity may be reached.

The degradation of solid grains in a transported slurry is an important

design factor, because a system working at optimal conditions may be very sensitive to small changes in the particle size distribution. Experience of long-distance transportation of coal and limestone has shown that attritional effects usually occur very gradually. However, in a recirculating test system such effects can occur very rapidly, mainly because of repeated passages through the pumps. The number of passages per hour in an ordinary pilot-plant test loop may be 50 to 100. In addition, the elbows in a test loop introduce changes in the flow direction similar to the changes that occur in centrifugal pumps.

The effect of attrition generally shows up as a wearing away of sharp projections on irregularly shaped particles. Wasp et al. (1968) point out the important role of circulating effects in test loops in the general "pumpability" of slurries. The effect of circulation in experimental studies is difficult to determine and to interpret to full-scale applications. The long-term stability of the flow, i.e. the influence of particle segregation in a long-distance pipeline, cannot be fully interpreted from test-loop studies.

The recirculating solids and the secondary flow introduced in bends and fittings may have a considerable influence on the settling conditions. Deposition conditions are mostly observed visually in short transparent pipe test sections. The interpretion of the influence of upstream disturbances on friction loss in straight pipe sections in a loop is complicated by the fact that the extra turbulence generated may be transferred downstream in a different way for slurry and clear water, respectively, Cave (1978).

3. SOLID-WATER FLOW IN A VERTICAL PIPE

3.1 Two-component definitions

Spatial concentration and delivered concentration

In a solid-water mixture the components are considered to be incompressible, and no transfer of mass is assumed to occur within the mixture. Only steady one-dimensional flow in a circular pipe is studied, and all variables are considered as averages over the area of the pipe. When the components move at different velocities in a pipe, the energy required cannot be determined without knowledge of the mixture density inside the pipe.

The spatial concentration of solids, E, is defined by the ratio:

$$E = \frac{A_s}{A} \tag{3.1}$$

where A_s is the cross-sectional area occupied by the solid component and A is the total area of the pipe, Fig. (3.1),

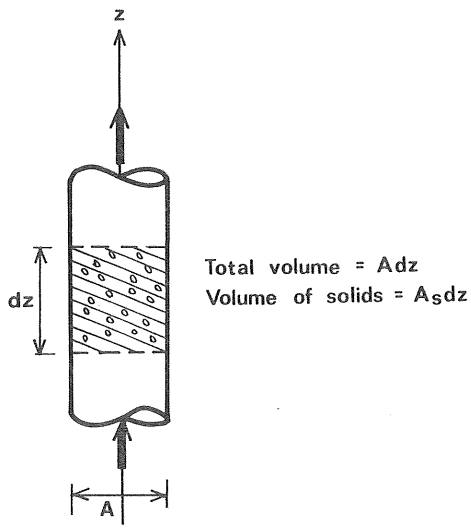

Fig. 3.1 Definition sketch of the spatial concentration of solids in a pipe.

The concentration of water is (1-E), and the density of the mixture in the pipe is given by:

$$\rho' = (1 - E)\,\rho_o + E\,\rho_s \tag{3.2}$$

which is equivalent to:

$$\rho' = \rho_o (1 + E(s_s - 1)) \qquad (3.3)$$

where s_s is the solid density ratio = ρ_s/ρ_o. The density ratio of the mixture in the pipe is defined by:

$$\frac{\rho'}{\rho_o} = 1 + E(s_s - 1) \qquad (3.4)$$

In general, there will be a relative velocity between the solid and water component. The mean value of the relative velocity is often defined by the slip velocity S, Fig. (3.2), as follows:

$$S = U_o - U_s \qquad (3.5)$$

where U_o is the mean velocity of the water and U_s is the mean velocity of the solids.

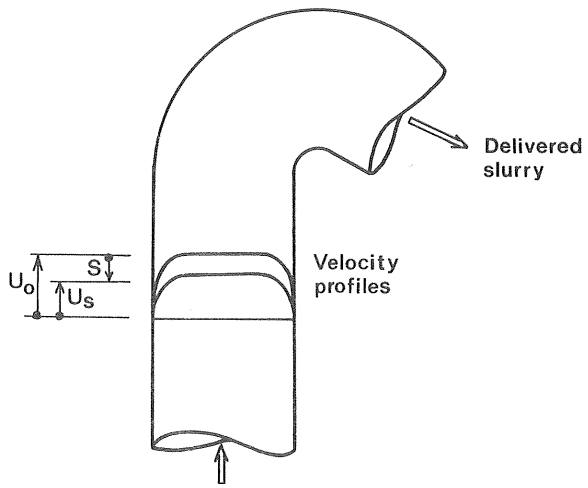

Fig. 3.2 Sketch of a vertical two-component flow.

Due to the relative velocity between the components the concentration, E, in the pipe is not the same as the concentration, C, in which the components are introduced into or delivered from the system.

The delivered mass flow rate, M, at the discharge end of a pipe is, Fig.

(3.2),

$$M = M_o + M_s \tag{3.6}$$

where

M_o = mass flow rate of water
M_s = mass flow rate of solids

The mass flow rates can be expressed by:

$$M_o = Q_o \rho_o \tag{3.7 a}$$

$$M_s = Q_s \rho_s \tag{3.7 b}$$

The delivered concentration is defined by the ratio between the discharge of solid and the total discharge from the pipe, Eqs. (2.5) and (2.6):

$$C = \frac{Q_s}{Q_o + Q_s} = \frac{Q_s}{Q}$$

The density ratio of the delivered mixture, s, is obtained in a similar way to Eqs (3.2) to (3.4) but with the delivered concentration, C, i.e.

$$s = \frac{\rho}{\rho_o} = 1 + C\,(s_s - 1) \tag{3.8}$$

The average velocity, U, of the mixture is defined as the total volumetric flow rate of the components per unit area:

$$U = \frac{Q}{A} = \frac{Q_o + Q_s}{A} \tag{3.9}$$

The true velocity of each component in the pipe is obtained by:

$$U_o = \frac{Q_o}{A(1 - E)} \tag{3.10}$$

$$U_s = \frac{Q_s}{A\,E} \tag{3.11}$$

From Eqs. (3.9), (3.10),, and (3.11), it then follows that:

$$U = U_o\,(1 - E) + U_s\,E \tag{3.12}$$

The conservation law of mass for the steady-state flow of a mixture in a pipe gives for the solid and water component, respectively,

$$Q C \rho_s = A E U_s \rho_s \tag{3.13}$$

$$Q(1 - C) \rho_o = A (1 - E) U_o \rho_o \tag{3.14}$$

which together with Eqs (3.5) and (3.12) give:

$$S = U_o - U_s = \frac{U - U_s}{1 - E} \tag{3.15}$$

$$U_s = U \frac{C}{E} \tag{3.16 a}$$

$$U_o = U \frac{1 - C}{1 - E} \tag{3.16 b}$$

Eqs. (3.15) and (3.16 a) then finally give the ratio between delivered and spatial concentration:

$$\frac{C}{E} = 1 - \frac{S(1 - E)}{U} \tag{3.17 a}$$

or

$$E - C = \frac{ES(1 - E)}{U} \tag{3.17 b}$$

Thus, the delivered concentration C is less than the concentration E within the pipe if the relative velocity, $S > 0$.

Flow behaviour

In a vertical pipe flow the velocity and concentration profiles are always symmetric but not necessarily uniform. Investigations by Durand (1953), Newitt et al. (1961), and Toda et al. (1969) have shown that the turbulent water-velocity profile is flattened somewhat by the presence of the solids, Fig. (3.3).

With relatively dilute suspensions the previously mentioned authors also observed that the particles were uniformly distributed over the entire cross section for low or modest velocities (less than about 1.5 m/s). At higher velocities and coarse particles, Newitt et al. (1961) and Toda et al. (1969) observed a concentrated peaking of solids in the centre of the pipe with almost clear surroundings of water.

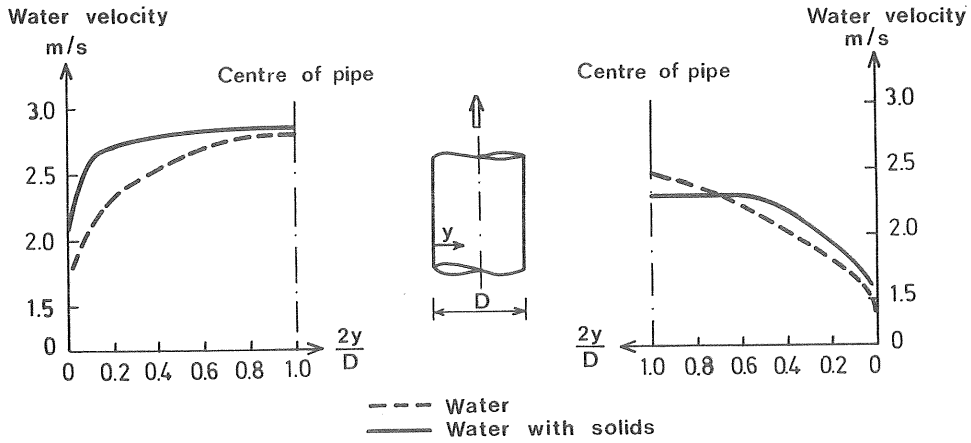

Fig. 3.3 *Water velocity profiles. Data from Newitt et al. (1961) (left), and Toda et al. 1969 (right).*

For solid-water mixtures transported industrially the distribution of water and solids tends to be approximately uniform with a modest peaking in the centre of the pipe.

Aziz et al. (1972) reported that experimental observations on the solid velocity, U_s, are very few but that available data confirm that U_s can be approximately determined by the following expression:

$$U_s \approx U_o - w \tag{3.18}$$

where w is a characteristic terminal settling velocity of the solids. Thus, for the steady flow of a solid-water mixture in a vertical pipe, it follows from Eq. (3.5), $S = U_o - U_s$, that:

$$S \approx w$$

3.2 Terminal settling velocity, drag coefficient

The terminal settling velocity, w, for a single particle is the uniform velocity the particle attains under the influence of gravity in a still fluid which is infinite in extent. The relative steady-state motion is

expressed by counterbalancing the hydrodynamic forces by gravitational forces. If this relationship is applied to a single smooth non-rotating solid sphere of diameter d_o, and density ρ_s, in water of density ρ_o, and viscosity μ_o, then the terminal settling velocity of the sphere w_o, is given by:

$$w_o = \left[\frac{4g}{3} \cdot \frac{d_o (s_s - 1)}{C_D}\right]^{1/2} \qquad (3.19)$$

where s_s is the solid density ratio = ρ_s/ρ_o, and C_D is the drag coefficient. C_D is uniquely related to a particle Reynolds number,

$$Re_{w_o} = \frac{w_o d_o \rho_o}{\mu_o} \qquad (3.20a)$$

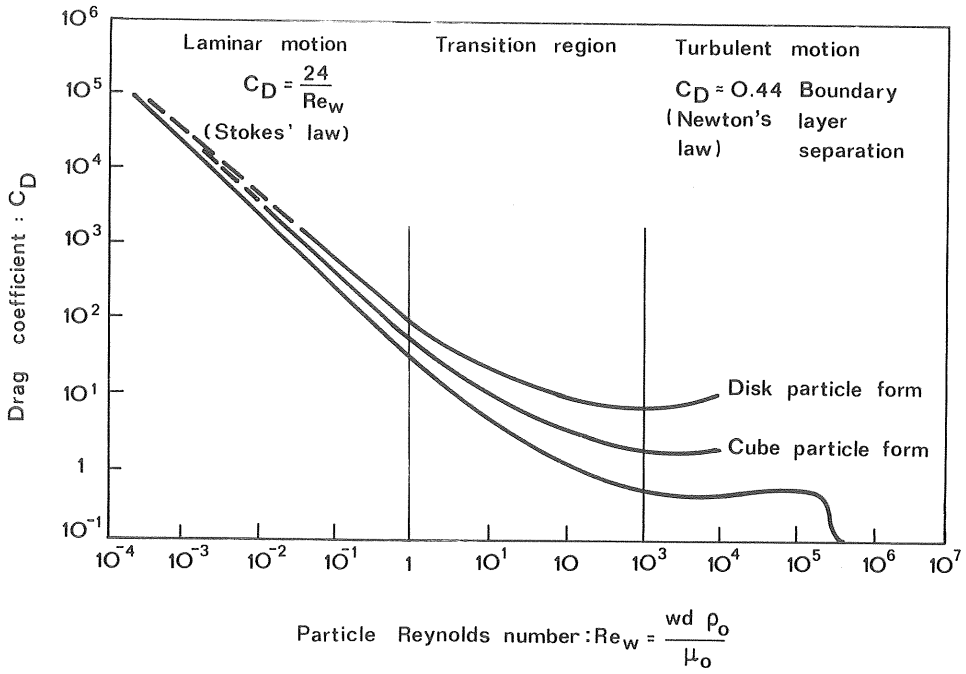

Fig. 3.4 *Dependence of drag coefficient on particle Reynolds number for spheres and irregular particles for which d is defined as the diameter of a sphere having the same volume as the particle (the nominal diameter).*

through the so-called standard drag curve for spheres, Fig. (3.4). With non-spherical particles the particle Reynolds number is defined by:

$$Re_w = \frac{w\, d\, \rho_o}{\mu_o} \qquad (3.20b)$$

where d is a characteristic diameter of the particle and w is the corresponding terminal settling velocity.

Solid particles from industrial slurries mostly have terminal settling velocities or C_D-coefficients in the transition region. Some examples of sphere diameters and the corresponding terminal settling velocities at the limits of the transition region are shown in Table (3.1).

Table 3.1 Examples of sphere diameters and the corresponding terminal settling velocities at the approximate limits of the transition region.

Solid density	$Re_{w_o} = 1$ (Stokes' law)		$Re_{w_o} = 1000$ (Newton's law)	
ρ_s (kg/m^3)	w_o (m/s)	d_o (mm)	w_o (m/s)	d_o (mm)
2500	0.009	0.12	0.37	3.2
4000	0.012	0.10	0.47	2.5

The irregular shape of a crushed solid particle normally reduces the terminal settling velocity substantially, for example w can be reduced by about 50% for a cube-shaped particle compared to a sphere of equivalent volume.

When there are a number of particles in a still fluid, the interference between neighbouring particles will reduce the terminal settling velocity, provided no agglomerative effects are acting. This is referred to as the hindered settling velocity, w'. Experimental data in vertical ducts has shown that:

$$w' = w(1 - E)^{\alpha} \qquad (3.21)$$

where α is a constant > 2, Kranenburg et al. (1974). For example, from Eq. (3.21) it can be seen that w' will be less than about half the

value of w in a mixture with E = 25%.

It should be pointed out that $w(C_D)$ so far has been defined for ideal conditions without the influence of pipe-flow turbulence, which will exist in practice. The impart of turbulence is not well understood, and experimental evidence is conflicting. Gauvin et al. (1960) stated that turbulence may reduce the point of starting boundary layer separation (see Fig. 3.4) by a factor of about 100 in solid-gas flow, and Ingebo (1956) found from experiments with solid spheres in gas flow that turbulence reduced the C_D-coefficient. Adams (1968) found an increase in C_D for spheres of glass and iron (diameter = about 4 mm) in the flow of water in horizontal pipes ($10^4 \leqslant Re_o \leqslant 3 \cdot 10^5$). These measurements indicate a similar influence as is caused by irregularly shaped particles. Wasp et al. (1977) reported similar findings by Ho (1964) in an oscillating flow of water.

Most slurries of industrial interest, covering a considerable range of particle sizes and characteristic values of d, w, and C_D, cannot be uniquely defined. These variables are together with s_s interrelated by Eq. (3.18), and C_D can be expressed by:

$$C_D = \frac{4g}{3} \frac{d(s_s - 1)}{w^2} \qquad (3.22)$$

In the following, d and w will not only represent the size and the terminal settling velocity, respectively, of a single particle, but they will also stand for characteristic values of all solid particles in the mixture. Thus a characteristic diameter, d, must be chosen according to some convenient method of measurement.

A representative particle diameter may be represented by the mean value of each sieve size, d_j, i.e. although the particle size represents a square mesh opening, it is considered as a diameter. If p_j is the weight fraction of solid particles of diameter d_j, then a weighted value, $\bar{d}$, may be obtained as:

$$\bar{d} = \sum_{j=1}^{N} p_j d_j \qquad (3.23)$$

where N is the number of fractions.

Different weighting methods have been proposed in the representation of w, but direct measurements in still water for each size fraction seem to be as reliable as any method. An average estimate may be

defined by a weighted value, $\bar{w}$,

$$\bar{w} = \sum_{j=1}^{N} p_j W_j \qquad (3.24)$$

where W_j is an average value of randomly chosen particles from each fractional part p_j.

3.3 Equations of momentum and energy

In contrast to what occurs in single-phase flow, the weight of a column of a two-component mixture ("hydrostatic head") does not truly represent the potential energy because of the difference in velocity between the components. A term in the energy equation, which accounts for energy dissipation including wall shear stress of mixture and relative motion between the components, will therefore be determined.

The components are considered together, but their velocities are allowed to differ. Under such conditions, the conservation laws of mass, momentum, and energy can be conveniently used for the entire mixture, rather than separate formulations for each component, Wallis (1969).

For the flow of a solid-water mixture in a straight vertical pipe of constant diameter, Fig. (3.5), the conservation law of momentum is reduced to a simple balance of forces. This balance is expressed by the relationship:

$$-Adp - \rho' g A dz - dF = 0 \qquad (3.25)$$

where p is the pressure, ρ' is the density of the mixture within the element, and dF is the resulting force of the average wall shear stress

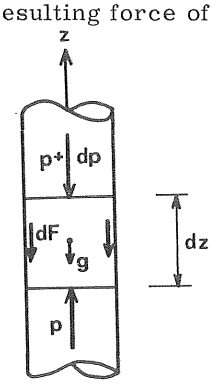

Fig. 3.5 Considered variables for the steady flow of a solid-water mixture in a vertical pipe.

around the pipe within the element.

The pressure required to maintain a steady flow may be expressed as a gradient in the direction of motion:

$$i_{Tot} = - \frac{dp}{\rho_o \, g \, dz} \tag{3.26}$$

where the gradient, i_{Tot}, is expressed in metres of water per meter of pipe. Eqs. (3.25), (3.26) and (3.3) then give:

$$i_{Tot} = 1 + E \, (s_s - 1) + \frac{dF}{\rho_o \, g \, A \, dz} \tag{3.27}$$

This equation will now be combined with a relationship based on the energy equation.

The law of conservation of energy or the first law of thermodynamics balances the time rate of change of internal, kinetic and potential energy with the rate of heat transfer for a flowing fluid (shaft work omitted). With negligible transfer of heat to the surroundings, then the energy equation in differential form is reduced to:

$$de + dp/\rho g + dz = 0 \tag{3.28}$$

where e is the internal energy which for the incompressible medium here studied accounts for all energy degraded as a result of irreversibilities. The density, ρ, in Eq. (3.28) represents the ratio of the mass flow rate and the volume flow rate, i.e. the density entering the infinitesimal element in Fig. (3.5) per unit time:

$$\rho = \frac{M_o + M_s}{Q} \tag{3.29}$$

Expressing the pressure required in Eq. (3.28) in the form of the total gradient defined in Eq. (3.26), then Eq. (3.28) may be written:

$$\frac{\rho}{\rho_o} \frac{de}{dz} - i_{Tot} + \frac{\rho}{\rho_o} = 0 \tag{3.30}$$

The first term in Eq. (3.30) represents the irreversible energy (energy losses) expressed in metres of water per metre of pipe, i_{Irr}. The last term in Eq. (3.30) represents the rate of change of reversible (potential) energy, i_{Rev}, expressed in metres of water per metre of pipe. Thus,

$$i_{Irr} - i_{Tot} + i_{Rev} = 0 \qquad (3.31)$$

where i_{Rev} is equal to the term ρ/ρ_o in Eq. (3.30) which together with Eq. (3.29) can be expressed by:

$$i_{Rev} = s = \frac{M_o + M_s}{\rho_o Q} = \frac{Q_o\rho_o + Q_s\rho_s}{\rho_o Q} = \qquad (3.32)$$

$$= \frac{Q(1 - C) + Q\ s_s\ C}{Q} = 1 + C(s_s - 1)$$

For the upward transportation of a two-component solid-water mixture in a vertical pipe of constant diameter, the conservation laws of momentum and energy expressed by Eqs. (3.27), (3.31) and (3.32) give:

$$i_{Irr} = (E - C)(s_s - 1) + \frac{dF}{\rho_o g A dz} \qquad (3.33)$$

where i_{Irr} is expressed in metres of water per metre of pipe.

The pressure gradient required to transport the flow vertically in a pipe may thus be written:

$$i_{Tot} = \underbrace{1 + C(s_s - 1)}_{i_{Rev}} + \underbrace{((E - C)(s_s - 1) + \left[\begin{matrix}\text{pipe wall}\\ \text{friction}\end{matrix}\right]}_{i_{Irr}} \qquad (3.34\,a)$$

which is equivalent to:

$$i_{Tot} = 1 + E(s_s - 1) + \left[\begin{matrix}\text{pipe wall}\\ \text{friction}\end{matrix}\right] \qquad (3.34\,b)$$

The first two terms in Eq. (3.34 b) represent the weight of the mixture per unit area.

In Eq. (3.34a), i_{Irr}, i_{Rev}, C, and s_s can easily be measured. However, the equation shows that thorough analysis of the composition of i_{Irr} should also include the determination of E, which is much more difficult. It is thus almost impossible to distinguish the different influences of the slip velocity and the pipe wall friction on i_{Irr}.

If the term (E - C) (s_s - 1) in Eq. (3.33) is to be determined, then the density in the pipe must be known in order to obtain the spatial concentration E. However, this requires sophisticated techniques, as for example by gamma-ray scanning.

The second term in Eq. (3.33) is the common pipe wall friction loss gradient, which can be expressed by means of an average shear stress, τ_w. For axisymmetric flows:

$$\frac{dF}{A\,dz} = \frac{4 \cdot \tau_w}{D}$$

which inserted in Eq. (3.33) gives:

$$i_{Irr} = (E - C)(s_s - 1) + \frac{4\tau_w}{\rho_o g D} \qquad (3.35)$$

Most correlations used to estimate the pipe wall friction losses are based on standard single-component methods. With the wall shear stress, τ_w, expressed by the Darcy-Weissbach relationship, Eq. (2.9), for the flow of water, it follows that:

$$\tau_w = \tau_{w_o} = \frac{f_o \rho_o U_o^2}{8}$$

which inserted in Eq. (3.35) then gives:

$$i_{Irr} = (E - C)(s_s - 1) + \frac{f_o U_o^2}{2 g D} \qquad (3.36)$$

3.4 Pressure requirement in a two-component system

According to Eq. (3.36), Eqs. (3.34 a) or (3.34 b), the total pressure gradient can then be expressed by:

$$i_{Tot} = 1 + E(s_s - 1) + \frac{f_o U_o^2}{2 g D} \qquad (3.37)$$

This is the relationship most often proposed for the determination of the total pressure requirement in a vertical solid-water system. The water velocity, U_o, in Eq. (3.37) is obtained from Eq. (3.16 b):

$$U_o = U \frac{1 - C}{1 - E}$$

i.e. the pipe wall friction term cannot be determined without knowledge of E.

A model of optimal operation

With the assumption, $S \approx w$, where S is the slip velocity and w is the terminal settling velocity, inserted in Eq. (3.17 a):

$$1 - \frac{C}{E} = \frac{S(1 - E)}{U}$$

it follows that:

$$1 - \frac{C}{E} \approx \frac{w(1 - E)}{U} \leqslant \frac{w(1 - C)}{U} \leqslant \frac{w}{U} \qquad (3.38)$$

The spatial concentration, E, can then be estimated from Eq. (3.38):

$$E \leqslant C(1 - \frac{w}{U})^{-1} \qquad (3.39)$$

If E is considered to be equal to, $C(1 - \frac{w}{U})^{-1}$, in Eq. (3.37):

$$i_{Tot} = 1 + C(1 - \frac{w}{U})^{-1}(s_s - 1) + \frac{f_o U_o^2}{2g D} \qquad (3.40)$$

where

$$U_o = U \frac{1 - C}{1 - E}$$

then it follows that there exist a minimum of i_{Tot} with respect to the average velocity, U, for constant values of C, w, s_s, f_o and D.

According to Eq. (3.40), the consumption of energy in a vertical solid-water mixture can be expressed by:

$$P = \rho_o g Q L i_{Tot} \qquad (3.41)$$

where

P = power
ρ_o = water density
Q = flow rate of mixture
L = vertical pipe length

The mass flow rate of solids, M_s, is obtained from Eq. (2.6):

$$C = \frac{Q_s}{Q_o + Q_s} = \frac{Q_s}{Q}$$

and Eq. (3.7 b):

$$M_s = Q_s \rho_s$$

which thus can be expressed by:

$$M_s = Q \rho_s C \qquad (3.42)$$

The power consumption per unit mass of hoisted solids, P/M_s, is then obtained from Eq. (3.41) with Eqs. (3.40) and (3.42). Thus, P/M_s can be expressed as a function with a minimum respect to the average velocity, U, or with respect to the pipe diameter D, if U is constant, Fig. (3.6).

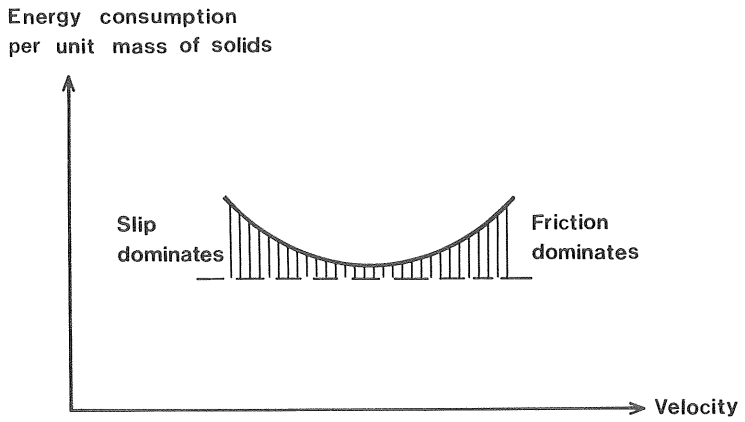

Fig. 3.6 *Schematic representation of energy consumption when the components move at different velocities.*

Condolious et al. (1963), Brebner et al. (1964), Laubcher (1973), and others have analysed optimal conditions of operation in vertical two-component systems mainly based on simplified approaches, as illustrated here by Eq. (3.38). However, the optimal conditions obtained with these approaches sometimes correspond to operational velocities which are only slightly higher than the terminal settling velocity. At present, there is no experience of operation at such low velocities in industrial applications.

Based on a similar analysis, Weber (1973) demonstrated the optimal conditions for the vertical transportation of spherical particles in water from a depth of 1000 m in a hypothetical example:

Capacity	300 tonnes/h
Solid density (ρ_s)	3000 kg/m^3
Water density (ρ_o)	1025 kg/m^3
Delivered concentration (C)	5%
Particle diameter (d)	16.5 mm
Terminal settling velocity (w)	1 m/s
Spatial concentration (E)	7.1%
Velocity (U)	3.13 m/s
Pipe diameter (D)	0.475 m
Solid velocity (U_s)	2.2 m/s
Water velocity (U_o)	3.2 m/s

In-plant operation

In a hydraulic hoisting application the operational velocity must be sufficiently high to maintain a continuous flow of solids at the discharge end. In a vertical slurry transportation system, Aziz et al. (1972) proposed a minimum operational velocity, U_{min}, based on:

$$U_{min} = 2\, w_{max}$$

where w_{max} was defined as "the terminal settling velocity of the largest solid particles if there is a range of particles".

In-plant experience of hydraulic hoisting of coal and ores has usually shown that the operational velocity must be considerably higher than two times the terminal settling velocity. Most known applications operate at velocities which exceed the terminal settling velocity of the largest particles by 4 to 6 times. In fact, most plants operate under conditions where the relative velocity between the components seems to be almost negligible.

Gamma-ray measurements of the density inside the pipe in an industrial application for iron ore (Lengede mine, West Germany), showed that no measurable difference in E and C occurred, Ilseder Hütte, (1969). The principal hydraulic data from that plant and another representative industrial application, are shown in Table (3.2).

Table 3.2 Principal hydraulic data from two industrial application of hydraulic hoisting

	Lengede-mine (Federal Republic of Germany)	Hansa-mine (Federal Republic of Germany)
Mineral	Iron ore	Coal
Solid density (kg/m^3)	3000	1500
Mean particle size (d_{50} mm)	4	10
Max. particle size (d_{max} mm)	30	60
Terminal settling velocity, w, corresponding to d_{50}	0.4	0.4
Max. terminal settling velocity (w_{max} m/s)	0.65	0.9
Delivered concentration (%)	20	up to 30
Pipe diameter (m)	0.225	0.250
Operational velocity (m/s)	3.4	4.1
$2 \cdot w_{max}$	1.30	1.80
$\frac{w_{max}}{U}$	0.22	0.19
$\frac{w}{U}$	0.10	0.12

Operational conditions of negligible slip

From the hydraulic data in Table (3.2) it was found that $\frac{w}{U} \approx 0.1$. Due to Eq. (3.38),

$$1 - \frac{C}{E} \leqslant \frac{w}{U}$$

with $w/U = 0.1$, it follows that:

$$C/E \geqslant 0.9$$

However, the measurements at the Lengede plant indicate that, if $w/U \approx 0.1$ then $E \approx C$, i.e. the slip was negligible.

From experimental data on crushed magnetite, Kostuik (1966) quantified that E could be taken as equal to C, provided that:

$$w/U < 0.1$$

where w may be taken as an average value. The solids used in Kostuik´s study had a weighted terminal settling velocity, $\bar{w} = 0.19$ m/s. The principal hydraulic data from Kostuik´s investigation will be shown later.

An operational velocity corresponding to negligible slip between the components can be estimated in the following way. Solid particles continually tend to settle downward in direction of gravity relative to the flow of a solid-water mixture. The average turbulent fluctuations are typically of the order of 10% of the average velocity, U, in the longitudinal direction of the flow of water in a pipe. Therefore, the steady state capability of a turbulent flow of water to transport a single solid particle vertically under stable conditions with no average velocity difference between the components can be expressed by:

$$0.1\ U > w$$

or

$$U > 10\,w$$

where w is the characteristic terminal settling velocity of the solids.

Based on the previous estimations and investigational experience already discussed, it is reasonable to assume that E can be taken as equal to C if w/U is less than about 0.1. Thus, the estimation given by Eq. (3.38):

$$1 - \frac{C}{E} \leqslant \frac{w}{U}$$

seems to be conservative in connection with industrial systems where the concentration is high and w may be reduced because of hindered settling effects.

Estimation of energy losses (negligible slip)

The following discussion will be based on situations where E is taken as equal to C and no attempts will be made to identify E separately. The irreversible energy for the two-component system is expressed by Eq. (3.36):

$$i_{Irr} = (E - C)(s_s - 1) + \frac{f_o U_o^2}{2 g D}$$

In order to relate i_{Irr} to the average velocity,

$$U = Q/A$$

which is easily measurable, Eq. (3.16 b),

$$U_o = U \frac{1 - C}{1 - E}$$

can be rewritten as:

$$U_o = U \left(1 + \frac{E - C}{1 - E}\right)$$

With this expression inserted in Eq. (3.36) it follows that:

$$i_{Irr} = (E - C)\left[(s_s - 1) + \frac{f_o U^2 (E - C)}{2g D (1 - E)^2} + \frac{f_o U^2}{g D (1 - E)}\right] + \frac{f_o U^2}{2g D} \qquad (3.43)$$

Thus, in the limit:

$$E \longrightarrow C$$

it follows in Eq. (3.43) that:

$$i_{Irr} = \frac{f_o U^2}{2g D} = i_o \qquad (3.44)$$

where i_o is the ordinary Darcy-Weissbach equation for the flow of water with velocity U, and where:

$$f_o = \phi (Re_o, k/D)$$

Some investigational data

Some investigational data often referred to in the field of vertical pumping of slurries are summarized in Table (3.3).

Table 3.3 Some investigational data dealing with two-component mixtures.

Investigator	Pipe diameter (m)	Solids	Density (kg/m^3)	Particle sizes d_{50} (mm)	Maximum concentration by volume (%)
Durand (1953 a)	0.150	Gravel	2670	4.36	7.3
		Sand	2670	1.0	7.9
		Sand	2670	0.18	8
Newitt et al. (1961)	0.025 and 0.051	Manganese-dioxide	4200	1.3	7
		Pebbles	2590	3.6	20
		Sand B	2640	0.19	30
		Sand C	2590	0.7	25
		Sand D	2590	1.3	25
		Sand A	2620	0.10	35
		Zircon sand	4560	0.11	10
Einstein et al. (1966)	0.076	Sand	2700	1.70	17.5
		Sand	2700	1.15	11.8
Kostuik (1966)	0.076	Iron ore	4060	2.5	20
Toda et al. (1969)	0.043	Glass	2500	0.5-3.6	less than 10%
		Plastic coated steel	4900	10	
		Plastic	1200	6-10	
		Steel	7700	8	

The criterion of negligible slip previously discussed, $w/U < 0.1$, was here compared to the settling conditions of the solids and the operational velocities in the experimental studies in Table (3.3). It was found that most investigational results in Table (3.3) correspond to flow situations where slip is negligible, i.e. E can be approximately taken as equal to C. Furthermore, many investigators found that their measured energy loss data was well-correlated with Eq. (3.44):

$$i_{Irr} = \frac{f_o U^2}{2g D}$$

Alternatively, if the energy loss gradient, i_{Irr}, is expressed in metres of mixture per metre of pipe, then Eq. (3.44) is equivalent to:

$$i_{Irr}/s = \left[\frac{\text{metres of mixture}}{\text{metre of pipe}}\right] = i_o/s \qquad (3.45)$$

where i_o is expressed in metres of water per metre of pipe and where

$$s = \rho/\rho_o = 1 + C\,(s_s - 1)$$

The conclusion reached by means of Eqs. (3.44) and (3.45) is that the energy loss of the flow of a mixture expressed in metres of mixture is less than the energy loss of water flowing at the same velocity, i.e.

$$i_{Irr}/s \left[\frac{\text{metres of mixture}}{\text{metre of pipe}}\right] < i_o \left[\frac{\text{metres of water}}{\text{metre of pipe}}\right]$$

This relationship corresponds to Eq. (2.25), discussed earlier in section 2.4.

Total pressure gradient

The total pressure gradient required to maintain a steady state flow in a vertical pipe is obtained from Eq. (3.34 a):

$$i_{Tot} = i_{Rev} + i_{Irr}$$

where

$$i_{Rev} = s = 1 + C(s_s - 1) \qquad \text{Eq. (3.32)}$$

and

$$i_{Irr} = i_o \qquad \text{Eq. (3.44)}$$

The total pressure gradient required in Eq. (3.34 a) is then:

$$i_{Tot} = s + i_o \qquad (3.46)$$

Alternatively, if the gradients are expressed in metres of mixture per metre of pipe, then Eq. (3.46) corresponds to:

$$i_{Tot}/s = 1 + i_o/s \qquad \left[\frac{\text{metres of mixture}}{\text{metre of pipe}}\right] \qquad (3.47)$$

3.5 Pressure requirement in a homogeneous system

From a strictly phenomenological point of view, a solid-liquid mixture can be treated as a single-component homogeneous fluid medium only if the particle size is much smaller than the fine structure of the turbulence, where the particles follow all fluctuations of the turbulence field. In the classification of industrial slurries, truly homogeneous mixtures were defined as those for which the action of the gravitational force on the particles is negligible under non-laminar flow conditions. Independently of the orientation of the flow, Newtonian or non-Newtonian single-component methods have been successfully applied to such systems.

The pipe wall friction loss of a homogeneous Newtonian mixture is traditionally treated as a loss from a true fluid by use of the Darcy-Weissbach equation, where f is determined by use of the density and the viscosity of the mixture:

$$i/s = \frac{f\,U^2}{2\,g\,D} \qquad \left[\frac{\text{metres of mixture}}{\text{metre of pipe}}\right] \tag{3.48}$$

$$f = \phi\,(Re,\ k/D)$$

where

i = energy loss gradient expressed in metres of water per metre of pipe

s = mixture density ratio = ρ/ρ_o

$\rho = \rho_o\,(1 + C(s_s - 1))$

$$Re = \frac{U\,D\,\rho}{\mu}$$

μ = Newtonian viscosity of the mixture

The viscosity must be measured or otherwise identified. If the whole solid-liquid mixture is considered as a continuum, then the viscosity may be estimated by the empirical Eq. (2.4):

$$\mu/\mu_o = 1 + 2{,}5\,C + 10.05\,C^2 + 0.0027\,(\exp 16.6\,C))$$

Aude et al. (1971) proposed Eq. (3.48) together with Eq. (2.4) for industrial applications of Newtonian slurry transportation in vertical pipes. Einstein et al. (1966) and Graf et al. (1967) found from experi-

mental results with sand-water slurries that $f = f_o$ in Eq. (3.48) was a good general approximation.

Total pressure gradient

The total pressure gradient required in the case of a homogeneous flow pattern is obtained from Eq. (3.34 a)

$$i_{Tot} = \underbrace{1 + C(s_s - 1)}_{i_{Rev}} + \underbrace{(E - C)(s_s - 1) + \left[\begin{matrix}\text{pipe wall} \\ \text{friction}\end{matrix}\right]}_{i_{Irr}}$$

In a homogeneous mixture:

$$E = C$$

and the pipe wall friction is expressed by Eq. (3.48). Thus, the irreversible gradient, i_{Irr}, in Eq. (3.34 a) is expressed by:

$$i_{Irr}/s = i/s = \frac{f U^2}{2 g D} \quad \left[\frac{\text{metres of mixture}}{\text{metre of pipe}}\right]$$

and the reversible gradient, i_{Rev}, is obtained from Eq. (3.32):

$$i_{Rev} = s = 1 + C(s_s - 1)$$

The pressure gradient required in metres of water per metre of pipe, i_{Tot}, in Eq. (3.34 a) is then:

$$i_{Tot} = s + i \tag{3.49}$$

Alternatively, with the gradients expressed in metres of mixture per metre of pipe it follows that:

$$i_{Tot}/s = 1 + i/s \quad \left[\frac{\text{metres of mixture}}{\text{metre of pipe}}\right] \tag{3.50}$$

The ratio of the Reynolds number of the flow of mixture and the flow of water is:

$$\frac{Re}{Re_o} = \frac{UD\mu_o\rho}{\mu UD\rho_o} =$$

$$= \frac{1 + C(s_s - 1)}{1 + 2.5C + 10.05C^2 + 0.0027 (\exp (16.6C))} \qquad (3.51)$$

where

$$\rho = \rho_o (1 + C(s_s - 1)$$

and where the viscosity ratio μ/μ_o was obtained from Eq. (2.4).

The physical properties of the solids influence the development and the scale of turbulence in a way which cannot be quantified by comparing the Reynolds numbers of the mixture and the liquid, respectively. However, the relationship in Eq. (3.51) will still be used to show schematically that the friction factor in Eq. (3.48) can be approximately determined by use of the density and the viscosity of the water.

For the Newtonian non-laminar flow in a pipe, Eq. (2.13),

$$f = \phi (Re, k/D)$$

where ϕ is a decreasing function defined for Re larger than about $0.5 \cdot 10^4$. The maximum gradient of f in Eq. (2.13) with respect to k/D corresponds to a hydraulically smooth flow ($k \rightarrow 0$), where f can be expressed by a simple empirical relationship, Brebner et al. (1964):

$$f = \frac{c_3}{Re^{c_4}} \qquad (3.52)$$

where c_3 and c_4 are constants of less value than about 0.32. The maximum gradient of f with respect to Re corresponds to the largest value of c_4. For Re less than about 10^5, f can be expressed by the following well-known relationship, Blasius (1913):

$$f = \frac{0.316}{Re^{0.25}} \qquad (3.53)$$

The maximum ratio of the mixture friction factor, f, to the clear water friction factor, f_o, is then:

$$\frac{f}{f_o} = \left(\frac{Re_o}{Re}\right)^{0.25} \qquad (3.54)$$

Eq. (3.51) is now schematically applied to Eq. (3.54), i.e.

$$\frac{f}{f_o} = \left[\frac{1 + 2.5C + 10.05C^2 + 0.0027\,(\exp(16.6C))}{1 + C(s_s - 1)}\right]^{0.25} \qquad (3.55)$$

The largest scatter of taking $f = f_o$ in Eq. (3.48) was estimated from Eq. (3.55) to be below about 15%, for mixtures of water and industrial minerals or ores of densities of 2600 kg/m^3 - 5000 kg/m^3 and concentrations of 20% - 30%. Thus, if a Newtonian behaviour of a mixture is recognized and if the viscosity can be related to Eq. (2.4), then the friction factor, f, in Eq. (3.48) can be approximately calculated from the clear water viscosity and density, i.e.

$$f \approx f_o$$

With Eq. (2.22),

$$f = f_o$$

where

$$f_o = \phi\,(Re_o,\ k/D)$$

then Eqs. (3.49) and (3.50) can be expressed by:

$$i_{Tot} = s(1 + i_o)\left[\frac{\text{metres of water}}{\text{metre of pipe}}\right] \qquad (3.56)$$

or

$$i_{Tot}/s = 1 + i_o\left[\frac{\text{metres of slurry}}{\text{metre of pipe}}\right] \qquad (3.57)$$

3.6 Discussion

Based on negligible slip and a continuum description by Darcy-Weissbach equation, Eq. (3.44) and (3.48) represent two energy loss approaches which can be expressed in the form of the wall shear stress, τ_w. Eq. (3.44) corresponds to:

$$\tau_w = \tau_{w_o} = \frac{f_o \rho_o U^2}{8} \qquad (3.58)$$

where τ_{w_o} is the wall shear stress developed in clear water flow. Eq. (3.48) corresponds to:

$$\tau_w = \frac{f \rho U^2}{8} \qquad (3.59)$$

As discussed earlier, f can be taken as equal to f_o without serious error. The question whether wall shear stress should be computed from the density of the water, or from the density of the mixture leads to doubt in the choice of Eq. (3.44) or (3.48).

Recommended design methods for the flow of industrial slurries in vertical pipes reflect this uncertainty. In practical applications where E approximately may be taken as C, Aziz et al. (1972) suggested that the energy losses should be calculated with the approach based on Eq. (3.44) but added: "in some cases the use of a density corresponding with that of the mixture seems preferable". On the other hand, Aude et al. (1971) stated: "in a vertical pipe the solids are uniformly distributed so the friction loss is calculated as for a homogeneous slurry", i.e. Eq. (3.48) was suggested. An intermediate flow pattern, with the value of the wall shear stress between the two approaches given above seems reasonable in practice. However, such a pattern is difficult to interpret phenomenologically.

A transported slurry is often described as a "heavy medium" of the liquid and the solid particles of sizes less than 0.04 to 0.07 mm, in which coarser particles then act with their separate identities. The homogeneous part may then be characterized by its density and rheological properties. The remaining solid particles are then considered separately in distinct size fractions, where each fraction is represented by a reduced settling velocity in the modified carrier substance. However, it does not seem possible to state a physically sound criteria that would enable division of an industrial slurry into a heterogeneous and a homogeneous part. For example, the viscosity of a suspension is a manifestation of the energy dissipated due to electrochemical interaction between the components, while the transfer mechanism of coarse particles depends on mechanical forces due to collisions.

Radial migration

Many investigators have observed that particles in low concentration slurries may not be uniformly distributed over the entire cross-section of the pipe. Investigations reporting radial migration of particles toward the centre of the pipe in upward slurry flow were mentioned previously in section 3.2.

Radial migration of particles in turbulent solid-water flow was also observed by Willets (1970), in a vertical pipe of diameter = 0.077 m and with low concentration of sand particles of diameter = 0.6 mm. Willets observed a systematic shift of the particle distribution. The particles tended to migrate away from the pipe wall in upward flow and toward the pipe wall in downward flow. Similar observations have been reported for spherical particles under steady laminar conditions (Poiseuille flow) in vertical pipes, see for example Jeffrey (1965). Jeffrey used particles of density = 1190 kg/m^3 with a diameter of 0.15 mm in the flow of glycerol in a pipe of a diameter of 0.033 m.

In effect, the findings in a laminar pipe flow corresponds to the observations by Willets in a turbulent flow. Willets explained partly the systematic shift of radial migration to an action of a lateral force. The existence of a lateral force on a rigid sphere which is both rotating and translating in a fluid is usually known as the Magnus effect. In the upward flow of water with constant average velocity in a vertical pipe a spherical particle may start spinning and, on entering the wall region, it may perhaps propel itself out again. It can be shown from hydrodynamics, that a transversal force can be created perpendicular to the direction of motion and the rotating axis, Fig. (3.7).

If the particle were free to move transversely due to the force, F_y, then it would have a velocity component towards the centre of the pipe. However, a radial velocity component due to the Magnus effect can only develop if there is a difference in velocity between the components, i.e. the local spatial concentration cannot be equal to the locally delivered concentration due to slip. Therefore, irreversible energy, over and above that of the pipe wall friction, will be generated. Thus, an explanation as to why the wall shear stress of the flow of slurry is the same as that for clear water cannot be directly related to the presence of an annulus of clear water at the pipe wall due to the

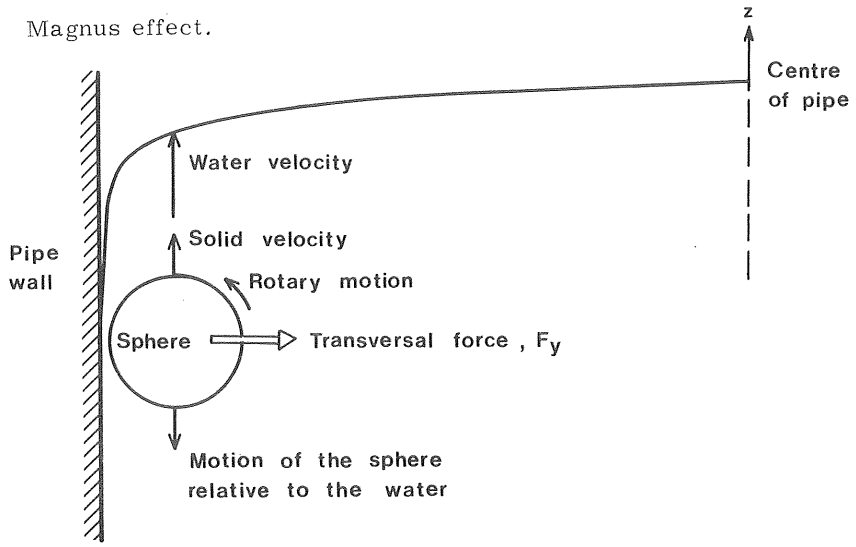

Fig. 3.7 *Schematic representation of the movement of a single solid spherical particle near the wall in a vertical pipe flow.*

There is experimental evidence of radial migration of solid particles in the upward flow of slurries, at least at low concentrations. However, it is doubtful if the effect can be developed in the flow of industrial slurries at higher concentrations. For example, operational experience from the Hansa mine (principal hydraulic data on page 48) shows that the total wear in the vertical pipe did not vary appreciably from the wear observed in horizontal pipe parts, Gaessler et al. (1976). This observation indicates that solid particles also create erosive action in vertical pipes.

The erosion may generally be lesser in the axisymmetric flow in a vertical pipe than in a horizontal pipe, but the combined effect of erosion-corrosion can still be substantial. Corrosion studies with slurries by Holdner et al. (1975, 1976) show that the rate of wall mass transfer of dissolved oxygen is much higher in slurry flow than in clear water flow, independent of the orientation of the pipe. However, the mechanism of momentum transfer leading to different energy losses depending on the orientation of the slurry flow can not be related to the same factors that lead to wall mass transfer.

Some turbulent related phenomena

The basic structure of the turbulenc is, at present, not completely understood, not even for single-phase fluids. Energy loss phenomena in mixtures are coupled to the kinetic energy spectrum of turbulence. Mechanical energy which is transformed into turbulence is not necessarily directly dissipated into heat, but part of the kinetic energy generated may be used to create lifting of the solids. Therefore, relationships in the form of Eq. (2.16):

$$i = i_o + i_s$$

(see Fig. 2.5, page 25) represent simplifications of basically very complex phenomena.

Some variables dealing with the scale of turbulence and the size of solid particles in the near wall region in a vertical pipe will be discussed based on some general definitions for the turbulent flow of a solid-water mixture in a pipe. The instantaneous velocity, $\hat{u}$, at a point in one direction in a steady turbulent flow over a period of time is given by the sum of a mean value, u, plus a fluctuating component, u',

$$\hat{u} = u + u'$$

Because the fluctuation is both plus and minus, the mean of the fluctuating component, $\bar{u'}$, is equal to zero. The spread is defined by the standard deviation, $(\overline{u'^2})^{1/2}$.

Consider the flow of water in a straight circular pipe of constant diameter. The average velocity is parallel to the axis of the pipe but in any point there are three-dimensional velocity fluctuations.

The turbulence field of the flow of water, in a circular pipe, is anisotropic. The degree of anisotropy increases toward the wall region, Fig. (3.8).

The maximum fluctuation occurs at the region of maximum production of turbulence, which is near the viscous sublayer, Fig. (3.9), in which viscous forces dominate.

The viscous sublayer is approximately defined by:

$$\frac{u_{ж}\, y\, \rho_o}{\mu_o} < 4 \qquad (3.60)$$

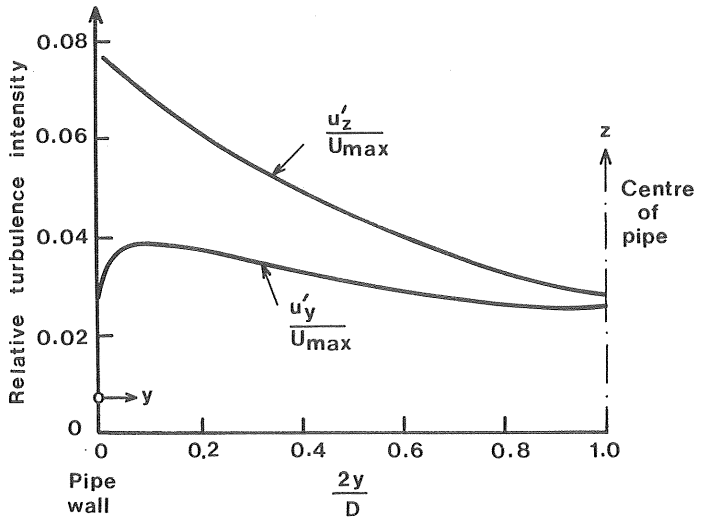

Fig. 3.8 *Turbulence intensities for fully-developed pipe flow. Reynolds number = $5 \cdot 10^5$. According to Laufer (1954).*

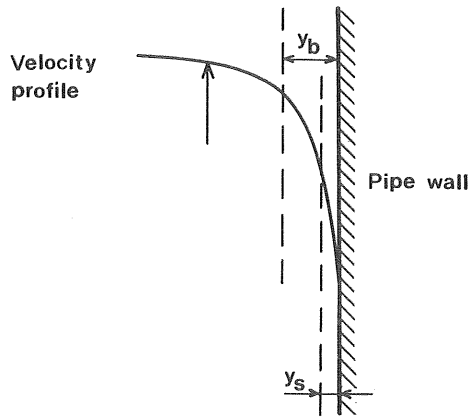

Fig. 3.9 *The near wall region of turbulent pipe flow.*

where

$$u_* = \left[\frac{\tau_{w_o}}{\rho_o}\right]^{1/2} \tag{3.61}$$

is the friction velocity. The motion in the sublayer undergoes a change toward intensive turbulence in the so-called buffer zone

which is approximately limited to:

$$4 < \frac{u_{ж}\, y\, \rho_o}{\mu_o} < 50 \qquad (3.62)$$

For the flow of water, in a hydraulically smooth pipe at a Reynolds number of about 10^5 the extension, y_s, of the viscous sublayer can be roughly estimated by the following expression:

$$\frac{y_s^{\,2}}{D} = 10^{-3} \qquad (3.63)$$

The thickness of the buffer zone, y_b, can be considered to be:

$$\frac{y_b^{\,2}}{D} = 10^{-2} \qquad (3.64)$$

The behaviour of a solid-water mixture depends largely on the size of the particles in relation to the scale of turbulence. Howard (1974) found, from laboratory tests in a vertical pipe of diameter = 0.184 m and with particles in the size range of 2 mm to 5 mm, that radial particle dispersion generally increased with particle diameter if:

$$\frac{d}{\lambda} > 1$$

where λ is the turbulent microscale.

The microscale represents the average dimensions of the smallest eddies that are mainly responsible for dissipation. For the flow of water in a pipe with $Re_o = 10^5$, the dimension of the smallest eddies in the wall region will be between the size of the viscous sublayer and the buffer layer Eqs. (3.63) and (3.64), respectively.

The relative length of viscous sublayer, buffer layer, and representative particle diameters is shown in Fig. (3.10).

The momentum transfer mechanism depends on the state of the turbulent motion, which varies across the mixture in the pipe. In the near wall region, it is mainly the physical properties of the flowing medium, that are attributable to the wall transfer mechanism. From Fig. (3.10) it can be seen that the thickness of the viscous sublayer in general is much smaller than the length of the transported solid particles. Therefore, it is not possible to define a physically valid

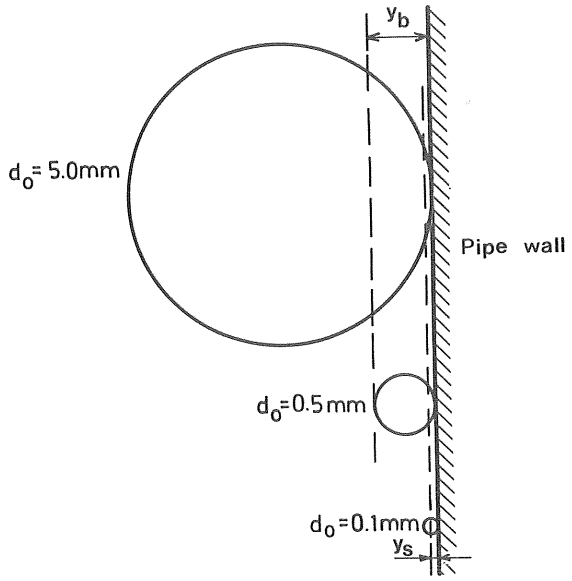

Fig. 3.10 *Relative thickness of the viscous sublayer and buffer layer compared with the diameter of different spherical particles in a hydraulically smooth flow in a pipe of diameter = 0.1 m.*

property defining a mixture viscosity, at least not for particles which are of larger dimension than the viscous sublayer.

Newitt et al. (1961) obtained greater energy losses for the fine-grained solids, sand A and zircon sand, than for the other solids in their experimental study (see Table (3.3) page 51). They related the higher energy losses to a possible increase of the rate of shear within the viscous sublayer, because the diameter of the particles were of the same order as the thickness of the viscous sublayer. However, the opposite effect of decreased rate of shear, due to an addition of fine particles of similar or lesser order as the sublayer, has also been related to changes in the near wall region.

A reduction of the energy dissipation can also be produced by the addition of small quantities of certain polymers into the flow of water in a pipe. No measurable change of the density or the viscosity occurs. The reductional effect is related to changes of turbulent transfer mechanism, mainly in the buffer layer. However, it is at present not possible to interpret a physically valid analogy between the mechanism of possible suppression action of fine particles and

and the effect of polymers.

Application of a pseudohomogeneous approach to the determination of the energy losses

The pseudohomogeneous flow pattern was discussed earlier in section 2.3 in connection with the experimental results by O´Brien et al. (1937) in horizontal pipes. Moreover, Graf (1971) suggested that the Darcy-Weissbach friction factor, f , could be approximately determined on the basis of a modified Reynolds number, Re´, in situations where the flow could be considered to be pseudohomogeneous:

$$Re' = s Re_o \quad \text{(Eq. 2.23)}$$

This is an obvious approach to the axisymmetric flow of industrial slurries in vertical pipes where the particle sizes mainly are in the range of 0.1 mm to 10 mm. The Reynolds number parameters can be considered as the ratio of inertial forces to viscous forces. For the flow in a pipe of diameter D the inertial force may be expressed by $\rho D^2 U^2$, which is a function of the mass flow rate. The density, $\rho = \rho_o(1 + C(s_s - 1))$, expresses thus the influence of C and s_s.

The viscous force, μDU, is a function of the average velocity. The portion of small particles less than the size of the viscous sublayer, i.e. less than about 0.1 mm, will generally be low for the transport situations studied here. Therefore, it is believed that the viscous properties of the mixture can be represented by the viscosity of water. This behaviour may also be reinforced by the possible radial migration tendencies of particles in the near wall region.

The observed flattening of the velocity-profile curves, exemplified in Fig. (3.3) page 37 indicate also that the slurry flow corresponds to a higher Reynolds number than that of clear water flow. This can in turn be related to a reduction of the thickness of the viscous sublayer. Solid particles penetrate the viscous sublayer and may strip away the upper part of the sublayer.

The energy losses may thus be determined from the Darcy-Weissbach equation, with f determined from a Reynolds number based on

the density of the slurry and the viscosity of water, i.e.

$$i_{Irr}/s = i/s = \frac{f\,U^2}{2\,g\,D} \qquad \left[\frac{\text{metres of mixture}}{\text{metre of pipe}}\right] \tag{3.65}$$

with

$$f = \phi\,(\frac{k}{D},\ Re')$$

where ϕ can be obtained from the ordinary Moody-diagram. If a representative Newtonian viscosity, μ, can be defined, then the homogeneous approach, Eq. (3.48) may apply, i.e. Darcy-Weissbach equation with:

$$f = \phi\,(k/D,\ Re)$$

where

$$Re = \frac{U\,D\,\rho}{\mu}$$

Comparison with some experimental data

In a recent pilot-scale investigation on oil shale minerals in a vertical pipe of diameter = 0.154 m, the f-Re' relationship was found to be adequite for predicting the hoisting energy requirement, Pouska et al. (1978).

Most investigational data shown in Table (3.3) page 51 corresponds to relatively low concentrations, at least for slurries composed of particles of greater mean particle size, d_{50}, than 0.50 mm. However, some experimental data by Newitt et al. (1961) also included concentrations of industrial interest. Their experimental results were originally presented in graphs in the form of measured clear water head loss versus mean velocity on a linear plot.

Newitt et al. concluded from their experimental results with manganese-dioxide, pebbles, sand A, sand B, and sand C, see Table(3.1), that: the energy loss of slurry expressed in metres of water are either identical with the clear water energy loss at all velocities or slightly higher at low velocity but tend to the water-losses at high velocities.

In order to study the results of Newitt et al., some of their experimental data was converted into the f-Re' parameters, Fig. (3.11).

The alternative representation in Fig. (3.11) shows that the experimental result obtained by Newitt et al. (1961) can be related approxi-

mately to the f-Re´ parameters. It can also be seen from Fig. (3.11) that there is a tendency towards a growing friction factor when the velocity (Re´) decreases.

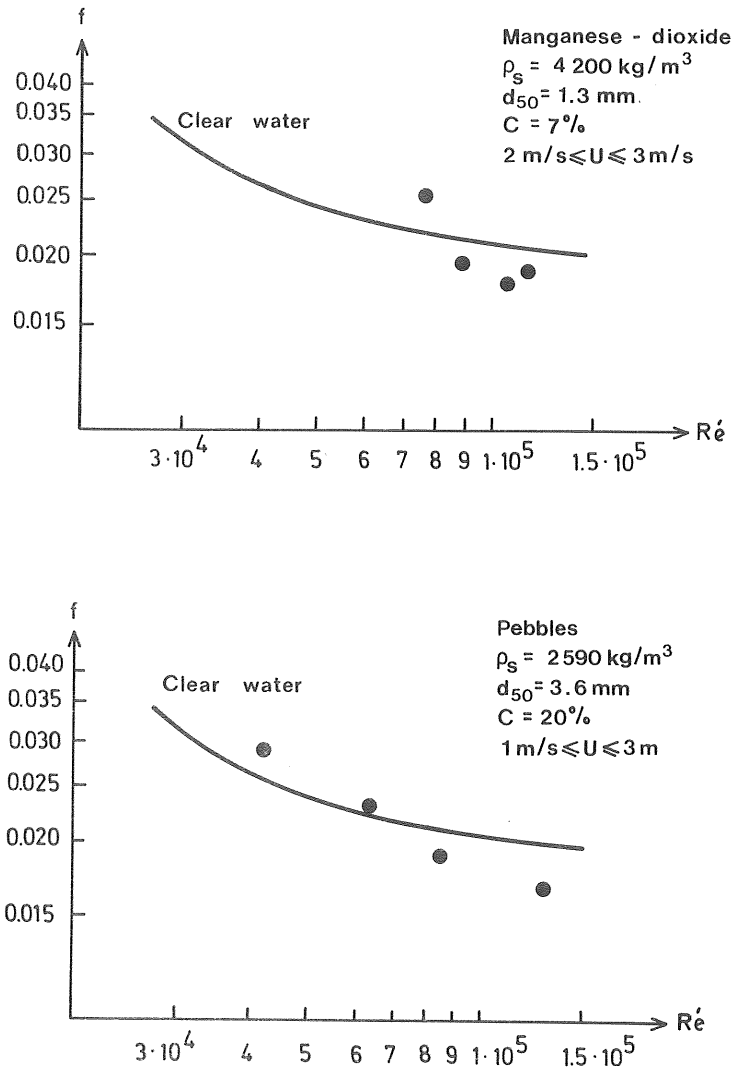

Fig. 3.11 *Representation of experimental data by Newitt et al. (1961) in the form of the f-Re´ parameters. D = 0.0255 m.*

4. ESTIMATION OF ENERGY LOSSES IN HORIZONTAL PIPES

4.1 Flow regimes - operational velocity

The concept of defining flow regimes was discussed in Chapter 2. Classification of slurries into different regimes is only applicable to mixtures of particles of similar size. Criteria for distinguishing between flow regimes are generally empirical formulas based on limited experimental data. For slurries composed of particles of wide size distribution, Fig. (2.2) page 19 may indicate the dominant regime of the flow.

Based on experimental tests with different minerals in a pipe of diameter 0.025 m, Newitt et al. (1955) separated heterogeneous flow from homogeneous flow and flow with moving bed, respectively:

$$\underset{\text{(flow with moving bed)}}{U_{Mb}} < \underset{\text{(heterogeneous flow)}}{U_{Het}} < \underset{\text{(pseudohomogeneous flow)}}{U_{Ph}} \qquad (4.1)$$

where

$U_{Mb} = 17\ w$

$U_{Ph} = (1800\ gDw)^{1/3}$

w = representative terminal settling velocity

D = pipe diameter

U_{Mb} defines the velocity below which solids form a deposit on the bottom of the pipe. For velocities larger than U_{Ph} the mixture flows as a pseudohomogeneous suspension. The limits defined by Eq. (4.1) were obtained by the investigators by making a continuous function of their empirical energy loss relationships.

The velocity at which the particle settle out at the bottom of a horizontal pipe (the deposition velocity, U_D) is generally determined by visual observations of the flow through a transparent pipe section in pilot-plant studies. The deposition velocity of a slurry system represents the lowest velocity at which the system can be operated. From a design standpoint it is advisable to operate at a somewhat higher velocity. Aude et al. (1971) and many others, suggested that the operational velocity should be about 0.3 m/s higher than U_D.

In the literature different criteria and empirical formulas have been presented for determination of the deposition velocity. Most relationships have been expressed in the following form

$$U_D = \phi D^{1/2} \tag{4.2}$$

where the function ϕ depends on d, C, and s_s. The relationship most often proposed goes back to Durand (1953), who related his experimental results to a modified Froude number expressed by a diagram factor, F_L,

$$\frac{U_D}{(2gD\,(s_s - 1))^{1/2}} = F_L \tag{4.3}$$

where F_L varies with the particle size and the concentration as shown in Fig. (4.1).

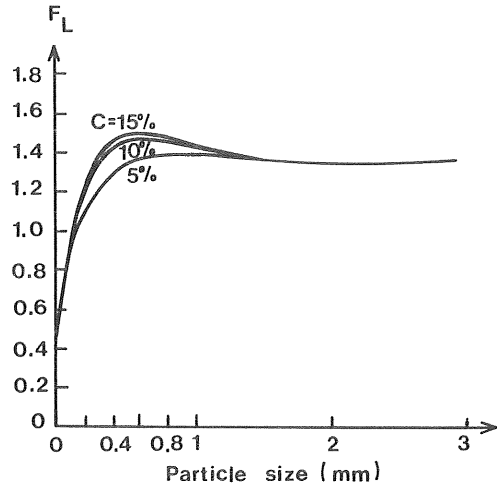

Fig. 4.1 *The factor F_L versus the particle size and some concentrations. According to Durand (1953).*

Eq. (4.3) was originally obtained for uniformly sized particles. The experimental background to Eq. (4.3) and Fig. (4.1) will be considered in the next section.

4.2 Heterogeneous flow - Durand's equation for energy loss

Great research effort has been concentrated on this flow regime but, unfortunately no generally accepted criteria to describe energy loss under various flow conditions have yet been established. About thirty more or less empirical formulas were recently presented in a survey of existing criteria to predict energy losses in horizontal pipes, Kazanski (1978).

The relationship most used to predict energy loss in a heterogeneous flow of a slurry composed of uniformly sized particles goes back to Durand (1953). The now classical expression given by Durand includes the parameters, Fr, C, s_s, and C_D reads:

$$i = i_o \left(1 + c_5 C \left(Fr^{-2}(s_s - 1)\, C_D^{-1/2}\right)^{3/2}\right) \qquad (4.4)$$

where

i = energy loss gradient of slurry expressed in metres of water per metre of pipe

i_o = energy loss gradient of water

c_5 = constant equal to 81

C = delivered concentration

$F_r = \dfrac{U}{(gD)^{1/2}}$ (Froude number)

$s_s = \rho_s / \rho_o$

C_D = drag coefficient defined by Eq. (3.22)

It is not difficult to find experimental or full-scale operational data which contradict Eq. (4.4). However, in comparison with many other published relationships, it has been proved to be useful in representing a broad range of slurries. Eq. (4.4) was based on extensive tests for D = 0.04 m to 0.58 m, d = 0.2 mm to 25 mm, s_s = 1.60 to 3.95, and U = 0.6 m/s to 6 m/s. Most experimental data was obtained for sand and gravel with concentrations not exceeding 22%. Some data undoubtedly must be classified as belonging to a pseudohomogeneous flow situation. Furthermore, the larger particle sizes were only investigated in pipes of diameter of less than 0.2 m.

In practice, the mineral in the slurry cover a considerable range of particle sizes. Eq. (4.4) has been modified, Aude et al. (1971), to yield mixtures covering a wide span of particle sizes and solids of different physical properties. Each size fraction (based on standard screen analyse) is treated as a separate entity. If a representative value of C_D of each fraction is used, then Eq. (4.4) is separately applied to each size fraction. The sum of the individual contributions then gives the corresponding energy loss gradient for the whole system:

$$i = i_o(1 + c_5(Fr^{-2}(s_s - 1))^{3/2} \sum_{j=1}^{N} C_{D_j}^{-3/4} C_j) \qquad (4.5)$$

where N is the number of fractions and C_j is the volume concentration of fraction p_j. The corresponding, C_{D_j}, is a representative value for particles within that fraction, Fig. (4.2):

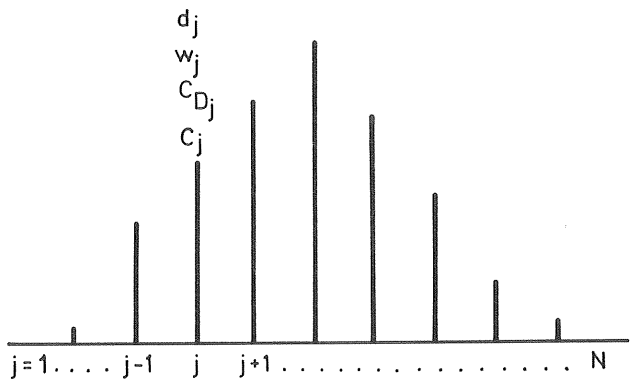

Fig. 4.2 *Variables defined for each particle size fraction.*

In Eq. (4.5) the solid density ratio, s_s, has not been defined for individual sieve fractions. Thus, the solid density is represented by an average value. This assumption will be used throughout in this study.

4.3 The Wasp et al. computational model

Wasp et al. (1963) applied a classical relationship from sedimentation technology to determine the distribution of solids in a solid-liquid flow in a pipe. The calculated distribution was used to define a split between a heterogeneous and a homogeneous part of the slurry. They then suggested determination of the energy loss due to the homogeneous part and the heterogeneous part, separately. The model will be described here in the case of a Newtonian slurry.

Background

The classical model for the distribution of solid particles in a steady uniform flow in wide open channels is based on the assumption that the flow of solids through a horizontal area, z = constant, is zero, Fig. (4.3).

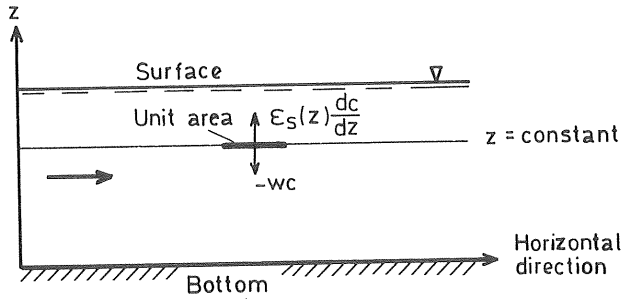

Fig. 4.3 *Schematic representation of the vertical movement of particles in the steady uniform flow in a wide open-channel.*

The equilibrium between the upward rate of particle motion due to turbulent diffusion and the volumetric rate of solid transfer per unit area due to gravity is expressed by:

$$wc + \varepsilon_s(z)\frac{dc}{dz} = 0 \qquad (4.6)$$

where

w = terminal settling velocity of a single particle

c = local concentration of solid particles

ε_s = diffusion coefficient for solid particles

By integrating Eq. (4.6) and letting (z; $0 \leqslant z \leqslant h$) be the domain on which the equation is integrated, then it follows that:

$$c = c_o \exp\left[-w \int_0^h \frac{d\xi}{\varepsilon_s(\xi)}\right]$$

where

c = local concentration of solids at level z

c_o = local concentration of solids at level $z = 0$

h = water depth

ξ = integration variable

Physically, the solution to Eq. (4.6) cannot be applied to the complete domain (z; $0 \leqslant z \leqslant h$), because ε_s is not defined for $z = 0$. The suspension does not exist close to the bed, where the physical situation is extremely difficult to define. Therefore, solutions to Eq (4.6) have referred to a concentration a distance $z = z_o$ from the bed. The boundary condition at the free water surface is based on the fact that the net vertical transfer of solids must be zero at the free surface, i.e.

$$w\,c + \varepsilon_s(z)\frac{dc}{dz} = 0 \qquad \text{for } z = h$$

Under these conditions, Eq. (4.6) can be easily integrated with the case of constant diffusion coefficient. O'Brien (1933) integrated Eq. (4.6) based on the triangular shear distribution of the open-channel flow and a logarithmic velocity profile, and arrived at the now classical expression:

$$c/c_{z_o} = \left(\frac{h - z}{z}\,\frac{z_o}{h - z_o}\right)^Y \tag{4.7}$$

where c_{z_o} represents the concentration at a level $z = z_o$, and where h is the water depth. The exponent in Eq. (4.7) is:

$$Y = \frac{w}{\varkappa\beta \cdot u_*} \tag{4.8}$$

where $\varkappa$ is the universal von Kármán constant, and u_* is the friction velocity defined in Eq. (3.61). The factor β in Eq. (4.8) is considered as a constant in the relation

$$\varepsilon_s = \beta \varepsilon \qquad (4.9)$$

where ε is the momentum transfer coefficient for the flow of water.

Description of the model

From experimental results in closed rectangular channels, Ismail (1952) found an empirical relationship between the exponent, Y, and the distribution of solid particles. This findings was applied by Wasp et al. (1963) on observed distributions in a coal slurry pipeline with a diameter of 0.60 m. By relating the concentration of solids at the top of the pipe to the concentration of solids in the centre-line of the pipe, they obtained the following relationship:

$$c_{0.08D}/c_{0.50D} = \exp(-1.8\ Y) \qquad (4.10)$$

where $c_{0.08D}$ is the concentration of solids at 0.08D below the top of the pipe and $c_{0.50D}$ is the concentration in the centre-line of the pipe, Fig. (4.4).

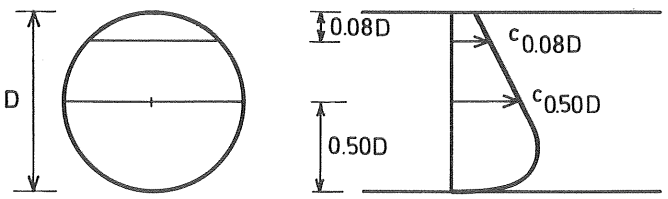

Fig. 4.4 *Diagram of the distribution of solids in a circular pipe.*

The exponent Y in Eq.(4.10) was defined by Eq. (4.8). Wasp et al. used Eq.(4.10) under the assumption that the concentration at the centre-line of the pipe was equal to the average solid concentration, C,

$$c_{0.50D} = C \qquad (4.11)$$

The friction velocity can be expressed in the form of the average velocity and the Darcy-Weissbach friction factor. With Eq. (2.9):

$$\tau_w = \frac{f \rho U^2}{8}$$

in Eq. (3.61) with τ_w and ρ:

$$u_* = (\tau_w/\rho)^{1/2}$$

it follows that:

$$u_* = U (f/8)^{1/2} \qquad (4.12)$$

Following the general assumptions, $\varkappa = 0.4$ and $\beta = 1$, with Eqs. (4.11) and (4.12) in Eq. (4.10) then it follows that:

$$c_{0.08D}/C = \exp\left[-12.7 \frac{w}{Uf^{1/2}}\right] \qquad (4.13)$$

Wasp et al. used Eq. (4.13) to define a limit between a homogeneous and a heterogeneous part of the slurry. Eq. (4.13) was applied successively to each particle size range interval, j. The concentration and the size distribution of the particles occuring at a depth of 0.08D below the top of the pipe were taken to exist at all other points in the pipe, i.e. the conditions at that level represent the homogeneous part of the slurry. Thus, for each size fraction the homogeneous part, C_j^{Hom}, is assumed to be equal to the concentration ratio defined by Eq. (4.13) multiplied by the average volume concentration, C_j, of that size fraction, i.e.

$$C_j^{Hom} = C_j \exp(-Y_j) \qquad (4.14)$$

where

$$Y_j = \frac{12.7\, w_j}{Uf^{1/2}}$$

where w_j is the terminal settling velocity in the fractional homogeneous part defined by its viscosity and density. The remainder of the solids:

$$C_j^{Het} = (1 - \exp(-Y_j))C_j \qquad (4.15)$$

was considered to be a heterogeneous suspension conveyed by the homogeneous part, Fig. (4.5).

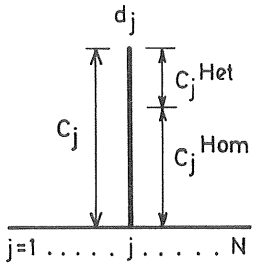

Fig. 4.5 *Schematic representation of the homogeneous and heterogeneous portion for each particle size fraction.*

The total energy loss was then calculated by summing up the homogeneous energy loss and the excess energy loss due to the heterogeneity of the remainder of the solids. The excess energy loss that may be attributed to the solids in heterogeneous suspension was obtained by applying Durand's equation to each size fraction, as discussed earlier, using the properties of water when calculating the drag coefficient, C_D. The calculation procedure to determine the energy loss of the heterogeneous part is schematically shown in Fig. (4.6).

Heterogeneous part

Fraction	Fractional concentration	Concentration	Energy loss gradient
1 ⋮ j-1 j j+1 ⋮ N	C_j	$C_j^{Het} = (1 - \exp(-Y_j))C_j$	$i_j^{Het} = C_j^{Het}\,\phi_o$

i_j^{Het} = fractional energy loss gradient of mixture (heterogenous part)

$i^{Het} = \sum_{j=1}^{N} i_j^{Het}$

i^{Het} = energy loss gradient of mixture (heterogeneous part)

These gradients are expressed in metres of water per metre of pipe.

Fig. 4.6 *Calculation procedure to determine the energy loss of the heterogeneous part in the Wasp et al. model. The function* ϕ_o *is here equal to:* $i_o c_5 (Fr^{-2} (s_s - 1) C_{D_j})^{-1/2})^{3/2}$

The total homogeneous part of the slurry, C^{Hom}, is obtained from Eq. (4.14):

$$C^{Hom} = \sum_{j=1}^{N} C_j^{Hom} \tag{4.16}$$

The density of the total homogeneous part is then obtained from Eq. (3.8):

$$\rho^{Hom} = \rho_o \ (1 + C^{Hom} \ (s_s - 1) \tag{4.17}$$

The viscosity of the total homogeneous part is simply related to Eq. (2.4):

$$\mu^{Hom} = \mu_o \ (1 + 2.5 \ C^{Hom} + 10.05 \ C^{Hom} + 0.0027 \exp (16.6 \ C^{Hom}) \tag{4.18}$$

The energy loss of the homogeneous part, i^{Hom}, is calculated with the Darcy-Weissbach equation, according to section 3.5. Finally, Wasp et al. related the pressure gradient, i_{Tot}, as the sum of the heterogeneous and the homogeneous part, respectively:

$$i_{Tot} = i^{Het} + i^{Hom} \tag{4.19}$$

where all gradients are expressed in metres of water per metre of pipe.

To find C_j^{Het}, iterations are required because the fractional viscosity μ_j^{Hom} depends on Y_j, where the fractional terminal settling velocity, w_j, in turn, is related to the fractional homogeneous part defined by its viscosity and density. Furthermore, the friction factor, f, depends on the pressure gradient, i_{Tot}.

4.4 Discussion

The deposition velocity in large diameter pipes may be roughly predicted by scaling-up of pilot-plant data by the exponential relationship in Eq. (4.2). Scale effects on the deposition conditions might be anticipated when pipes of different roughness are compared, according to Kazanskij (1976).

Durand's equation must be used with caution for solid-liquid mixtures other than those for which the formula has been verified through experiment. The equation represents an oversimplification of very complex phenomena.

The computational model developed by Wasp et al. (1963) is empirical in nature because it, among other things, involves the use of Durand's formula. The split between the heterogeneous and homogeneous part is one of the central features of the computational model. The criterion used goes back to the mathematical model of the distribution of small solid particles in low concentration in a two-dimensional open-channel flow, where Eq. (4.7) has been found to apply to laboratory and field data. However, it is not possible to determine the value of Y in Eq. (4.8) from an independent physical interpretation of the variables, w, β, $\varkappa$, and $u_{\varkappa}$. Available analytical and experimental work gives no assurance that a model based on Eq. (4.6) is more valid when applied to the flow of industrial slurries in pipes with much higher solid concentrations.

The use of the Wasp et al. model has generally been associated with the design of long-distance slurry pipelines, where the flow can be classified as being in a pseudohomogeneous state. Therefore, if the Wasp et al. model is applied to a pseudohomogeneous flow, then the homogeneous part, C^{Hom}, is considerably larger than the heterogeneous part, C^{Het}, in the relationship:

$$C = C^{Hom} + C^{Het}$$

where C is the total concentration of solids in the slurry. The pressure gradient in metres of water per metre of pipe is expressed by:

$$i_{Tot} = i^{Hom} + i^{Het} \qquad \text{(Eq. 4.19)}$$

The heterogeneous part of the mixture is low and the heterogeneous term in Eq. (4.19) will be small, compared with the homogeneous energy loss term. Therefore, the usefulness of the model in a pseudohomogeneous flow is attributable to the dominant influence of the Darcy-Weissbach equation and the usefulness of this relationship.

The iteration procedures described earlier in section 4.3 were formulated for computer calculation. The computer programming was carried out at the Department of Hydraulics as a part of a Master of Science thesis, Kindlund et al. (1977).

The previous discussion of the determination of the energy loss with the Wasp et al. model will now be demonstrated in an example, with iron ore slurry in a horizontal pipe.

Example

Mineral	Iron ore concentrate
Solid density (kg/m^3)	4947
Mean particle size (d_{50} mm)	0.06
Max. particle size (d_{max} mm)	0.2
Concentration (%)	21.3
Pipe diameter (m)	0.1
Absolute roughness of pipe (m)	10^{-6}
Temperature (^oC)	15

The deposition velocity, U_D, was estimated from Eq. (4.3) and Fig. (4.1) with $d_{50} = 0.06$ mm.

$$\frac{U_D}{(2gD(s_s - 1))^{1/2}} = F_L$$

$$\frac{U_D}{(2g \cdot 0.1 \cdot 3.947)^{1/2}} \approx 0.6$$

$$U_D \approx 1.65 \text{ m/s}$$

The operational velocity was chosen to:

$$U = 1.65 + 0.3 = 1.95 \text{ m/s}$$

In the application of the model the fractional drag coefficient, C_{D_j}, was related to the standard curve for spheres, Fig. (3.4), based on the size distribution of the particles given as input.

The following results were obtained from the computer calculations:

$$C^{Hom} = 17.7\%$$

$$C^{Het} = 3.6\%$$

$$i^{Het} + i^{Hom} = i_{Tot}$$

$$0.0100 + 0.0539 = 0.0639$$

With the gradient, i_{Tot}, expressed in metres of slurry, i_{Tot}/s, then with $s = 1.84$ it follows that:

$$i_{Tot}/s = 0.035 \left[\frac{\text{metres of slurry}}{\text{metre of pipe}}\right]$$

If the total energy loss is determined directly with the Darcy-Weissbach equation based on the density and viscosity for the total solid content, C, then Eq. (3.48) applies to the flow in the horizontal pipe, i.e.

$$i_{Tot}/s = i/s = \frac{f\,U^2}{2g\,D} \left[\frac{\text{metres of slurry}}{\text{metre of pipe}}\right]$$

The gradient, i/s, was determined and it follows that:

$$i_{Tot}/s = 0.031 \left[\frac{\text{metres of slurry}}{\text{metre of pipe}}\right]$$

Thus, the value of i_{Tot}/s calculated directly by the Darcy-Weissbach equation is, in this case, only slightly less than the value obtained with the model.

The particle size distribution of the iron ore in the example corresponds to sizes which are slightly larger than those normally encountered in long-distance slurry transportation of iron ore in pipelines.

The calculations in the example have been carried out under the assumptions of non-laminar flow and Newtonian behaviour of the slurry. These are reasonable assumptions for the operational conditions given in this example.

5. PERFORMANCE OF CENTRIFUGAL PUMPS

Solids in suspension adversely influence both the head developed and the energy consumed in a centrifugal pump. Because of the reliability of the transportation system and the wear on pump parts, centrifugal slurry pumps mostly operate at flow rates lower than those corresponding to the highest efficiency.

5.1 Hydraulic characteristics of pumping liquids

In a centrifugal pump the mechanical energy is transferred to the fluid to produce mostly kinetic energy within the small passages of the impeller, which is then transformed to potential energy in the larger passages of the volute and discharge piping of the pump casing. The losses in a centrifugal pump when pumping liquid are schematically shown in Fig. (5.1).

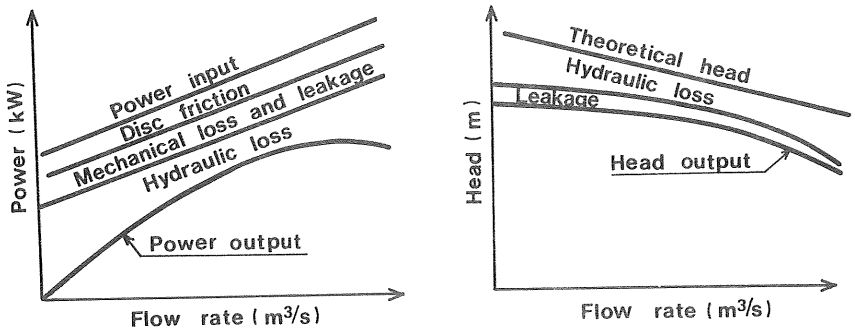

Fig. 5.1 *Schematic illustration of the losses in a centrifugal pump. According to Cruger (1974).*

The disc friction is a result of friction between the outer sides of the impeller and the pumped media. Media which have passed the impeller leak back and cause losses. The hydraulic losses are mainly eddy and separation losses due to changes in direction and magnitude of the velocity of the flow.

The head developed by a centrifugal pump pumping a true liquid generally is a function of the following variables, Hansen (1967):

$$H = \phi (Q, N, D, \mu, \rho, k, g) \tag{5.1}$$

where H is the head, Q is the flow, N is the rotary speed of the impeller, D is the impeller diameter, k is the absolute roughness, and g is the acceleration of gravity. After grouping the variables in Eq. (5.1) in dimensionless parameters, then:

$$\frac{Hg}{N^2D^2} = \phi \left(\frac{Q}{ND^3}, \frac{\rho N D^2}{\mu}, \frac{k}{D}\right). \tag{5.2}$$

The highly turbulent flow usually encountered in pumping liquids causes negligible viscous influence and the dependence on viscosity is therefore omitted. The influence of the roughness is also normally neglected. Then,

$$\frac{Hg}{N^2D^2} = \phi \left(\frac{Q}{ND^3}\right) \tag{5.3}$$

$$\eta = \phi \left(\frac{Q}{ND^3}\right) \tag{5.4}$$

where η is the efficiency of the pump determined by:

$$\eta = \frac{\rho g Q H}{P}$$

where P is the power delivered to the pump.

The influence on the performance of pumping fluids of higher (Newtonian) viscosities or densities than those of water is schematically shown in Fig. (5.2).

If the viscosity of a pumped fluid of constant density is increased, then the head and efficiency are lowered, and the power needed to maintain a constant capacity is increased. If the density of a fluid of constant viscosity is increased, then the head and efficiency curves will be unaffected, but the energy requirement will be increased to maintain the capacity. In this case, no change of the internal flow characteristics within the pump occurs, compared to the pumping of water. The power input is proportional to the density ratio of fluid and water.

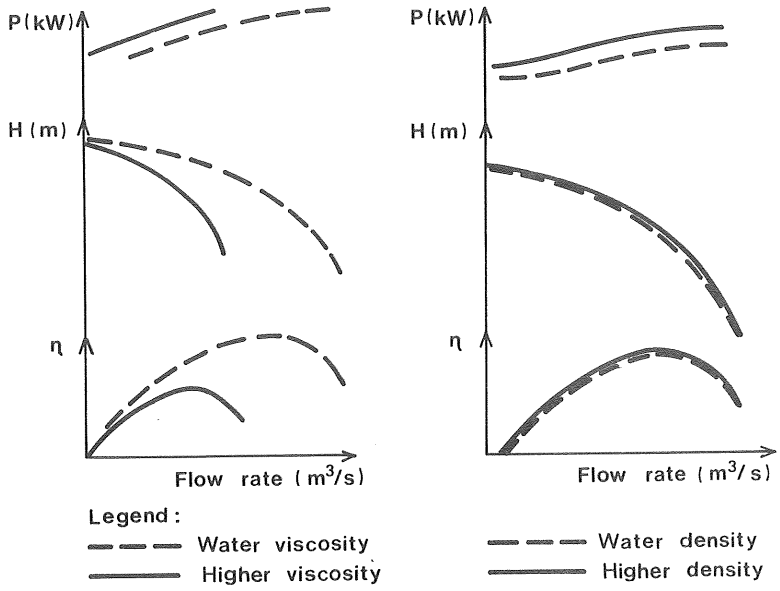

Fig. 5.2 *Schematic representation of the influence of pumping fluids of higher viscosity or density than water.*

5.2 Effects of solids on pump performance

The pump head and efficiency are generally lowered by the presence of solids. When pumping slurries, the relative reduction of the clear water head and efficiency for a constant flow rate and rotary speed may be defined by the following two ratios:

the head ratio: H/H_o

the efficiency ratio: η/η_o

where

H = head developed in slurry service, metres of slurry

H_o = head developed in water service, metres of water

η = pump efficiency in slurry service

η_o = pump efficiency in water service

These variables are schematically defined in Fig. (5.3).

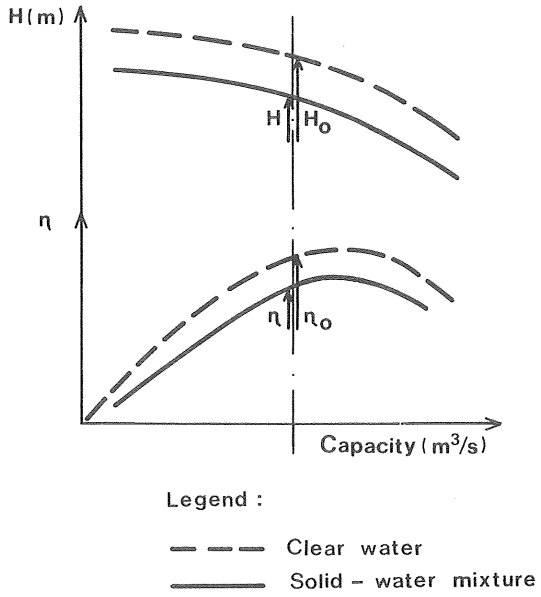

Fig. 5.3 *Sketch defining the reduction in head and efficiency of a centrifugal pump pumping a solid-water mixture.*

Most investigational work carried out on performance tests with industrial slurries in centrifugal pumps has shown that the power consumption increases proportionally to the density ratio:

$$P = s\,P_o \tag{5.5}$$

where

P = power input to pump when pumping a mixture

P_o = power input to pump when pumping water

s = mixture density ratio, ρ/ρ_o

and that a lower head output of the pump is directly related to a reduction in efficiency:

$$\frac{H}{H_o} = \frac{\eta}{\eta_o} \tag{5.6}$$

see for example, Stepanoff (1965) and Vocadlo et al. (1974).

Eqs. (5.5) and (5.6) are in fact equivalent statements:

$$\frac{P}{P_o} = \frac{\rho g H Q}{\eta} \cdot \frac{\eta_o}{\rho_o g H_o Q} = s \frac{H/H_o}{\eta/\eta_o} = s \qquad (5.7)$$

The slurry absorbs the same kinetic energy as a heavy fluid with density ρ. In principle, pump head can only be developed by the energy imparted to the liquid by the impeller. The diminution of the area for the liquid in the impeller channels may reduce the amount of energy transfer to the liquid in the pump. Based on this assumption, Frazier (1968) explained that the head and efficiency of a centrifugal pump were reduced in the following way:

$$\frac{H}{H_o} = \frac{\eta}{\eta_o} = \frac{\frac{1-C}{\rho}}{\frac{1}{\rho_o}} = \frac{1-C}{s} \qquad (5.8)$$

which corresponds to the ratio of energy imparted per mass unit of mixture and water, respectively. However, experience has shown that the particle size has a marked influence on the performance, and therefore Eq. (5.8) alone does not present a complete representation of the flow situation in the pump.

The flow of solids through the pump causes additional hydraulic losses due to relative motion of coarse particles or viscous effects by a high concentration of small particles. Because of the different densities of solids and liquid, a separation of the two components will take place in the acceleration field of the pump, which also results in additional friction loss.

Observations by Herbich (1962) showed that the particle velocity leaving the impeller was 4 to 5 times as large as the velocity of the fluid (Plastic beads: diameter = 3 mm, density = 1190 kg/m^3). Similar findings from theoretical calculations were reported by Fairbanks (1941). However, at the discharge end of the pump, Wiedenroth (1970) found from experimental investigations with a quarz mineral of particle sizes from 0.1 mm to 10 mm that the velocity of the components was equal.

Burgess et al. (1976) extended the variables in Eq. (5.1) to the flow of slurries in centrifugal pumps. For a particular pump, they wrote:

$$(Q, g, H, \eta, N, D, d_{50}, \mu, \rho_o, \rho_s, C) = 0 \qquad (5.9)$$

The variables were then expressed in dimensionless parameters:

$$\frac{H}{H_o N^2 D^2} = \phi \left(\frac{Q}{ND^3}, C, \frac{d_{50}}{D}, s_s\right) \qquad (5.10)$$

and

$$\frac{\eta}{\eta_o} = \phi \left(\frac{Q}{ND^3}, C, \frac{d_{50}}{D}, s_s\right) \qquad (5.11)$$

Burgess et al. assumed Eqs. (5.10) and (5.11) to be approximately independent of flow rate and pump rotary speed, a statement confirmed experimentally by Stepanoff (1965) and others. Eqs. (5.10) and (5.11) are then reduced to:

$$\frac{H}{H_o} = \phi \left(C, \frac{d_{50}}{D}, s_s\right) \qquad (5.12)$$

$$\frac{\eta}{\eta_o} = \phi \left(C, \frac{d_{50}}{D}, s_s\right) \qquad (5.13)$$

Results published by other investigators

Mc Elvain (1974) presented reduction curves, where the dependence of the density, particle size, and concentration was defined by a reduction factor K, Fig. (5.4). In an empirical approach, Mc Elvain found a linear dependence between the efficiency and head ratio and the concentration. He related the factor K to C = 0.20 (20%) and obtained:

$$\frac{H}{H_o} = \frac{\eta}{\eta_o} = 1 - K \frac{C}{0.20} \qquad (5.14)$$

Test data published by some other investigators have been listed in Table (5.1) and are compared with Eq. (5.14) in Fig. (5.4).

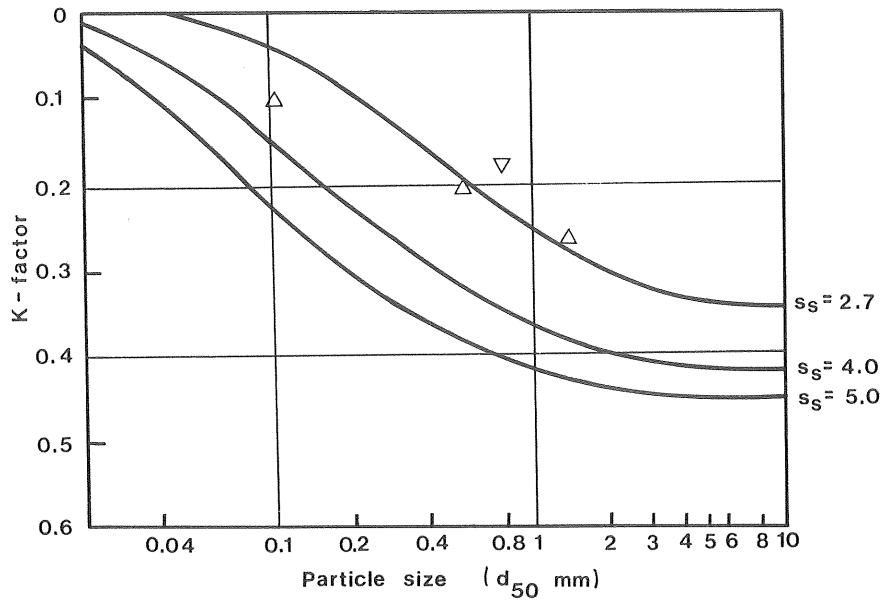

Fig. 5.4 *Curves of reduction due to the presence of solids, Mc Elvain (1974). Comparison with some other experimental data listed in Table (5.1).*

Table 5.1 Legend for comparison of investigations in Fig. (5.4)

Investigator:	Fairbanks (1941)	Vocadlo et al. (1974)
Mineral:	sand	sand
Solid density (kg/m^3):	2655	2670
Particle size: d_{50} (mm)	0.8	0.11, 0.57, 1.4
Concentration by volume (%):	20	20, 20, 20
Symbol in Fig. (5.4):	▽	△
Pump data:	0.076 m dredge pump. Metal impeller with diameter = 0.30 m. Rotary speed = 16.7 rps.	Worthington, 0.10 m slurry pump. Rubber-lined 3-vanes impeller with diameter = 0.28 m. Rotary speed = 29.6 rps.

5.3 Discussion

Fairbanks and Vocadlo et al. used pumps of different geometry and impeller design, Table (5.1). However, the comparisons in Fig. (5.4) indicate that there is only a slight influence of the individual pump design characteristics on the performance for a given slurry. Cave (1976) stated more generally that the influence of pump geometry on the reduction in head is slight for typical slurry pump proportions. Contrary to these findings, Hunt et al. (1968) demonstrated a substantial change in the efficiency reduction due to the impeller design. Their tests were carried out with woodchip slurries and different impellers.

The statements given in Eqs. (5.6) and (5.7) have been confirmed in most reported studies. However, the amount of available pump performance test data with highly concentrated industrial slurries is small.

A greater reduction in efficiency than in head was reported by Sasaki et al. (1958) when pumping coal (0-15 mm, C = 25%) with a pump having a discharge diameter of 0.076 m. The increased power consumption of rather small pumps, working at low speed or flow rate, may be explained by increased disc friction loss, especially if the slurry is composed of fine solids, Stepanoff (1965).

The functional relationships given by Eqs. (5.12) and (5.13) indicate that the relative performance of a particular slurry pump of given impeller diameter is altered by concentration, particle size, and density. However, most investigations have generally dealt with slurries composed of particles relatively close in size. It is believed that the depression in head and efficiency will be lesser for a mixture containing solids of a broad size distribution than that of a mixture of uniform solids with comparable mean particle size. The liquid and the finer particles may form a medium in which the separation between the components is reduced, which may cause a smaller change in the internal flow characteristics. Therefore it is questionable if d_{50} can be used as a representative particle size of slurries covering a considerable range of particle sizes. More generally, the solid particles may be related to a characteristic particle size, d, and a characteristic particle distribution factor, Z.

The influence of the shape, ψ , of the particles on pump performance must also be considered. For example, Wiedenroth (1970) reported greater losses in efficiency for fresh angular particles compared to more rounded particles (particle sizes from 2 to 8 mm). The fact, that centrifugal pumps cause preferential attrition in friable materials, thus may be an important factor in industrial applications. Besides,attrition has to be considered when discussing results from tests where the slurry is recirculated.

The reported observations of a large difference in velocity between the components inside the pump while leaving the impeller indicates that the performance should be related to a characteristic terminal settling velocity, w. The variables discussed previously: d, Z, ψ , and w are believed to give a better expression of the solid properties than those given in Eqs. (5.12) and (5.13). The influence of d and w can be expressed by the particle Reynolds number:

$$Re_w = \frac{w\, d\, \rho_o}{\mu_o}$$

With Re_w, ψ , and Z then Eqs. (5.12) and (5.13) can be rewritten in the following form:

$$\frac{H}{H_o} = \phi\,(Re_w,\ Z,\ \psi\ ,\ s_s,\ \frac{d}{D},\ C) \qquad (5.15)$$

$$\frac{\eta}{\eta_o} = \phi\,(Re_w,\ Z, \psi\ ,\ s_s,\ \frac{d}{D},\ C) \qquad (5.16)$$

where Re_w, Z, ψ , s_s, and d represent characteristic solid properties.

6. EXPERIMENTAL STUDY

6.1 Objectives

The overall objectives of the experimental study were the determinating of important design factors such as velocities, concentrations, and energy consumption in vertical slurry transportation of some ores and industrial minerals, and of the effect of solids on the performance of a centrifugal pump. The solids were taken directly from in-plant crushing and milling processes, thus covering a wide particle size distribution, Table (6.1). The study is intended as a part of an overall program on hydraulic transportation.

Table 6.1 Industrial minerals and ores used in the pilot-plant study. The portion of particles less than 0.07 mm varied from about 5% to about 20%.

Solids	Average solid properties			Remarks
	d_{50} (mm)	d_{max} (mm)	Density (kg/m^3)	
Coarse iron ore	2.0	8	4150	Sinter fines from the LKAB-mine at Kiruna
Primary ground iron ore	0.25	1	4000-4350	Taken from the dressing process (rod mills) at the LKAB-mine at Malmberget
Complex ore	0.17	4	3300-3500	Zink-lead-copper ore from work face at the Boliden AB-mine in Garpenberg
Lead ore	0.4	2.0	2670	Taken from the dressing process (rod mills) at the Boliden-AB mine in Laisvall
Perlite	0.35	2.0	2350	From deposit in Iceland. After processing (thermal expansion), perlite has been suggested as a substitute for asbestos.
Crushed granite	3.0	3.5	2670	From crushing plant in Göteborg

The required parameters were obtained by experimental determination and evaluation of the following hydrodynamic characteristics.

- Energy losses of the solid-water flow in a vertical pipe.
- Head and efficiency of a rubber-lined centrifugal slurry pump, mainly operated at reduced rotary speed and flow rates.

The importance of attritional effects on mineral particles in a test loop has been pointed out, and therefore special attention was given to this problem. The objectives were to quantify, to some extent:

- Time-dependent changes in pipe friction loss and pump performance with respect to repeated passages of the slurry through a pilot-scale test loop system.

The hydraulic design characteristics of horizontal parts of a hydraulic hoisting system were experimentally studied in a small horizontal test loop only. These laboratory-scale tests were limited to relatively fine-grained solids, Table (6.2).

Table 6.2 Minerals and ores used in the laboratory-scale horizontal test loop. The portion of particles less than 0.07 mm varied from 5% (beach sand) to about 60% (iron ore concentrate).

Solids	Average solid properties d_{50} (mm)	d_{max} (mm)	Density (kg/m^3)	Remarks
Primary ground iron ore	0.25	1	4000-4350	See Table (6.1)
Iron ore concentrate	0.06	0.2	4900	Pellet feed from Malmberget
Beach sand	0.15	0.6	2670	Deposit in Baskarp

Limited rheological bench tests were carried out for the finer parts of the iron ore.

6.2 Design of the pilot-test facility

The pilot-plant facility was designed for a planned enlargement. In an enlarged test-facility, a complete hydraulic transportation system from underground could be simulated by connecting a horizontal pipe to the top of a vertical pipe. The available pump was a rubber-lined centrifugal slurry pump with a 66 kW motor. If the pump was placed in the basement store-room of the laboratory, the vertical test line could be attached to a balcony floor 10 m above. Then, in an enlarged system, the pump was capable of transporting a slurry with a density of up to 2000 kg/m^3 in a pipe of a diameter of about 0.1 m. Because of these considerations, the length chosen for the vertical test pipe was 10 m, with an inner diameter of 0.094 m.

On-line continuous measurement of flow in industrial applications is often carried out with magnetic flowmeters. Worn-out or coated electrodes have hindered the use of magnetic flowmeters in connection with mineral slurries. The use of capacitance-type magnetic flowmeters, where the electrodes do not come into contact with the slurry, seems to have eliminated these problems. However, magnetic material can cause considerable inaccuracies, why the use of such flowmeters is thus limited by the content of magnetic solids in the mixture. The upper possible limit of concentration of magnetite ore in this study has been estimated to about 50% by weight.

The density inside a pipe transporting slurries can be measured by a nuclear density gauge without disturbing the flow. Nuclear gauges are sometimes used in slurry laboratories to obtain knowledge of the profile of the density inside the pipe. In the mineral industry, these are used together with a magnetic flowmeter for indirect registration of the capacity of dry solids in a pipeline. In laboratory tests the in situ density has also been obtained by weighting a flexible connected pipe section, Haas et al. (1973b).

In a closed loop small quantities of solids can be used, but the energy fed by the pump shaft is given off as a considerable amount of heat, which must be carried off by a refrigation system. Besides, it can be difficult to avoid negative pressure at the top of a vertical loop.

Because of the difficulties with closed loops and the costs of instrumentation, it was decided to design an open recirculating system, where flow rate and slurry density were measured directly by divert-

ing the flow to a calibrated volumetric weighting tank. The head loss measurements in the vertical pipe were carried out with a differential manometer containing some heavy oil. It was believed that these methods were the simplest and most accurate.

The schematic lay-out of the open loop test facility is shown in Fig. (6.1). The energy of the downcoming slurry was utilized to obtain uniform mixing in the feeding tank without baffles or circulating pump arrangements.

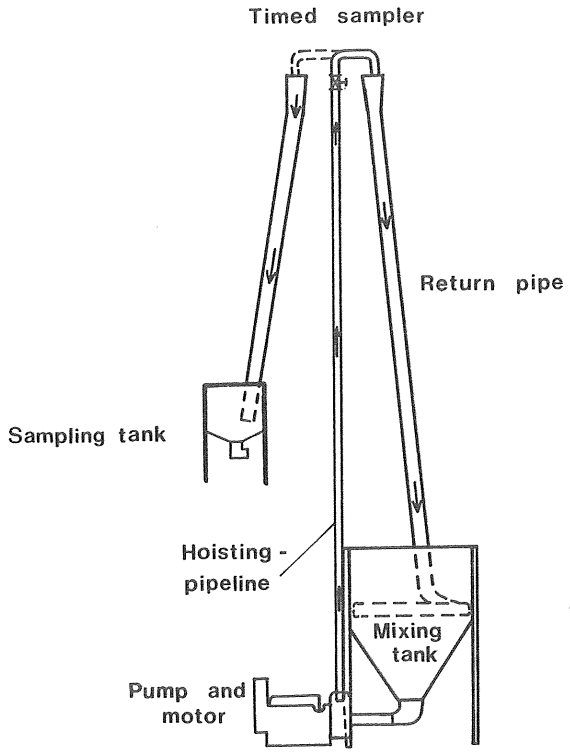

Fig. 6.1 *Open loop testing facilities - schematic lay-out.*

Effects of circulating in the test loop were intended to be studied as particle attrition, measured as changes in particle size distribution during a test period. The relative tendency of the minerals to degrade was believed to be quite different, but it is generally believed that

attritional effect, measured as changes in particle size distribution, must be registered over a relatively long period, for example at least 1 h. However, during a 1 h test-run each of the solid particles was expected to pass through the pump some 200-500 passages, which was considerably more than in a true transport situation.

The volume and the depth of the pump feeding tank must be sufficient to allow the release of entrained air. In general, pump manufacturers recommend a volume adequate for 1-2 minutes of pumping. However, the recirculation in a laboratory open loop causes continuous entrainment of air, and special attention has to be given to the discharge of the slurry in the mixing tank.

At the top of the hoisting pipe the flow could be diverted to the sampling tank, Fig. (6.1). The sampling tank must have a minimum volume to provide sufficient time intervals and prevent spills during the time of measurement. On the other hand, during sampling, the mixing tank level will be lowered by an amount equal to the volume of the sample, and this will affect the flat head curve of the pump and, consequently, the discharge rate. To ensure an overall sufficient accuracy of measurements in the system, the volume chosen for the sampling tank was 0.5 m^3 and the working volume of the conical-cylindrical pump feeding tank was 2.5 m^3 with a water surface area of 5.7 m^2.

The entire discharge was diverted into the sampling tank by a swivel elbow at the top of the hoisting pipe. The elbow was rotated over a sharp edge between two cones, which were connected to the mixing tank and the sampling tank, respectively, Fig. (6.2).

The time of discharge into the tank was measured by means of a digital counter with an accuracy of 0.01 s. The switching of the elbow was controlled by an interrupter, adjusted in such a way that it transmitted a signal to the counter whenever the flow passed a sharp edge between the cones. The sampling discharge was gravitated down a vertical pipe into the sampling tank, and spills were prevented by the flow being discharged into the tank as shown in Fig. (6.3). The inflow time into the sampling tank was between 6 and 15 s.

The volume of the discharged mixture in the sampling tank was obtained by reading a millimeter-ruler attached to the side of the tank, Fig. (6.3). The volume flowing into the tank was normally 0.2-0.3 m^3.

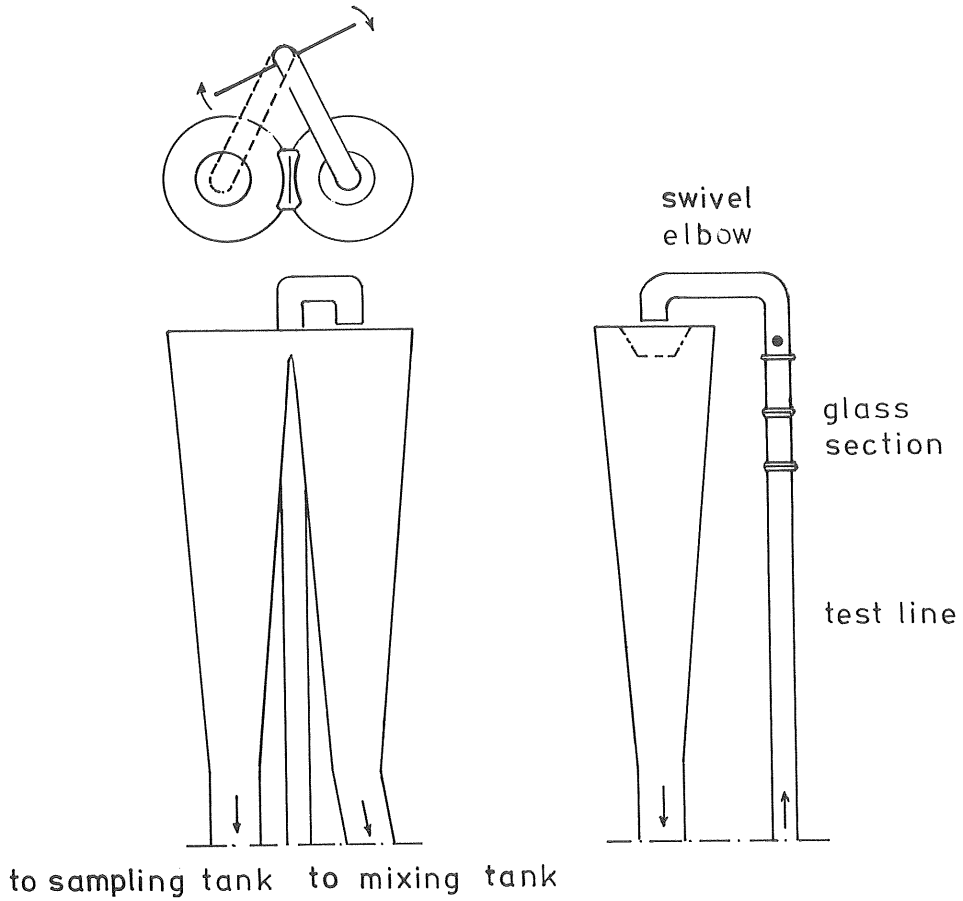

Fig. 6.2 *Swivel elbow at the top of the test line and cones connected to the mixing tank and to the sampling tank.*

The millimeter scale on the ruler therefore corresponds to a repeatability of about 10^{-3} m^3.

The weight of the filled sample tank was registered by a load cell having an accuracy of $\pm$ 0.5%. The output of the load cell was recorded on a transmitter with a resolution of $\pm$ 0.5 kg. The total accuracy of the weight determination therefore, was about 0.7%.

The flow from the cone at the top of the vertical test pipe returned to the feeding tank in a 0.20 m diameter plastic pipe with an inclination of 8^{o} to the vertical line. The return pipe discharge jet was horizon-

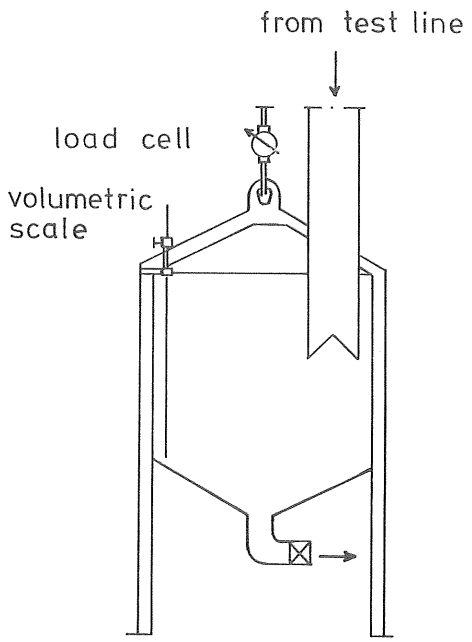

Fig. 6.3 *Sampling tank - discharge of slurry from the top of the test line.*

tally entrained into the tank for uniform mixing and prevention of air entrainment and possible vortex information. The discharged mixture in the vertical test-pipe was expected to be composed of coarser minerals than those added to the system. Coarse or dense particles would pass through the mixing tank more quickly than fine particles. The return pipe was extended around the wall of the tank so that the time of residence of coarse and dense particles would be increased. The slurry was gradually discharged by an elongated opening on the inside of the pipe, Fig. (6.4). The design is based on a liquid level placed 0.5 m below the top of the tank. Entrained air was released by perforated holes in the upper part of the discharge pipe in the mixing tank.

The lower part of the conical feeding tank was designed to allow start-ups and shut-downs without valve installations. The lay-out included cylindrical by-pass lines from the upper part of the tank, Fig. (6.5).

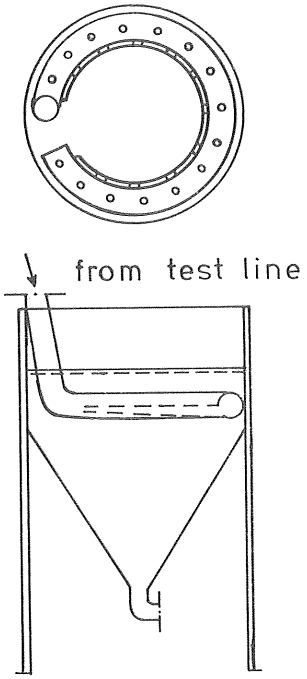

Fig. 6.4 *Discharge of slurry in the mixing tank. The return pipe was extended around the tank, and slurry was discharged by an elongated opening on the inside of the pipe.*

These cylinders and a three-hole entrance in the bottom will supress any tendency of vortex formation.

The three vertical by-pass lines are connected to a shifting axle. They were moved by an arm which was operated from the side of the tank. The vertical axle was pivoted in a nylon wheel between two steel plates in which the three discharge holes had been furned out. During shut-down, the three cylinders were switched over and the by-pass lines opened, allowing water to be drawn down from above and solids to settle onto the bottom, Figs. (6.6) and (6.7). The pump could then be started up with water only, and solids were continuosly introduced by a gradual opening of the entrance holes in the bottom.

The pressure drop test section (length 2.5 m) in the vertical pipe was preceded by an approach section of about 50 diameters of pipe

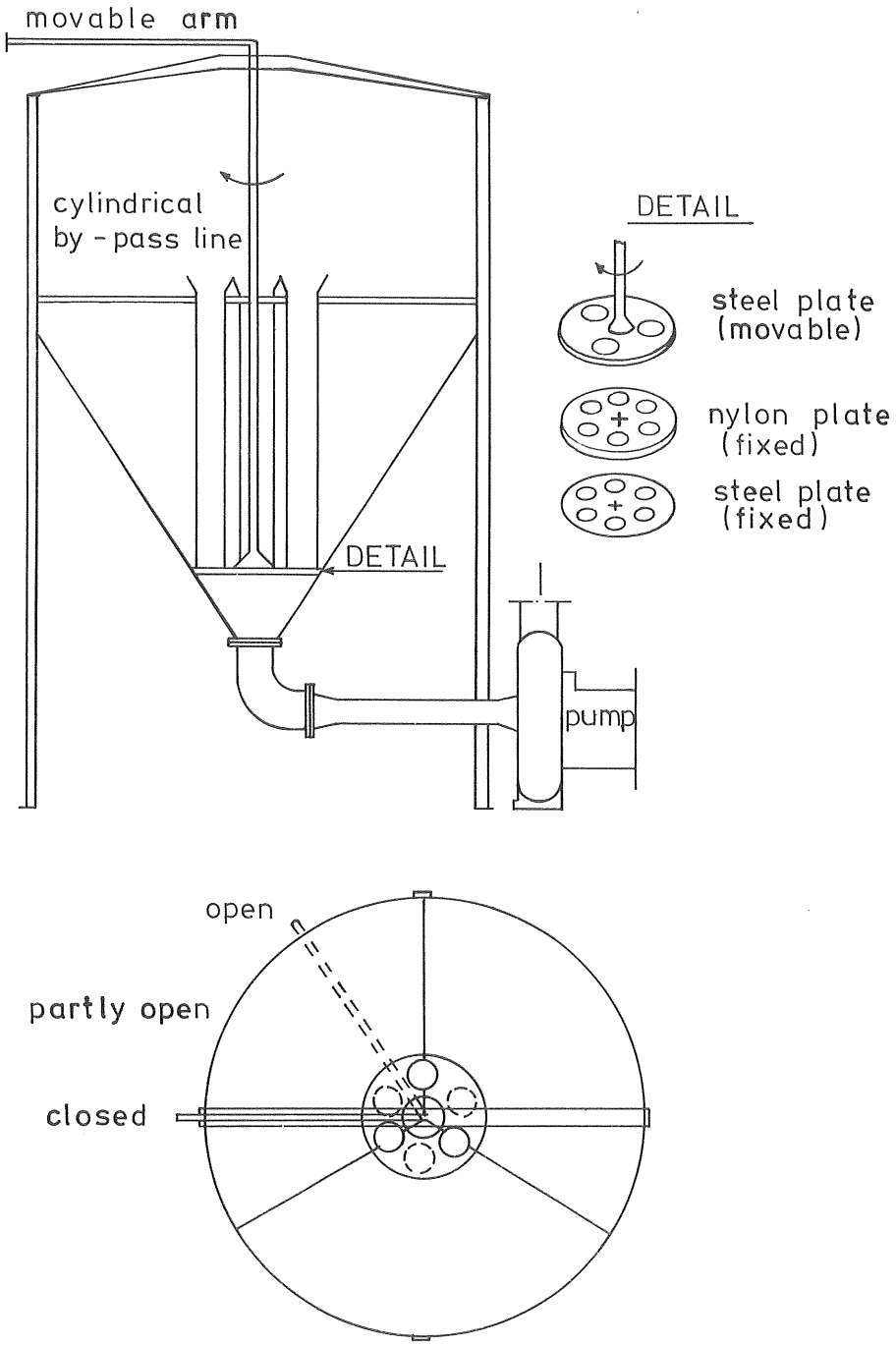

Fig. 6.5 *Lay-out of the lower part of the mixing tank.*

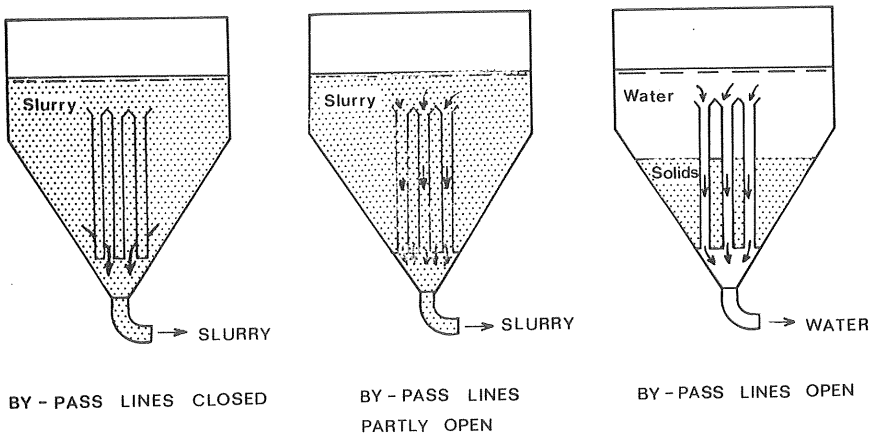

Fig. 6.6 *Principal lay-out of the by-pass facility in the mixing tank.*

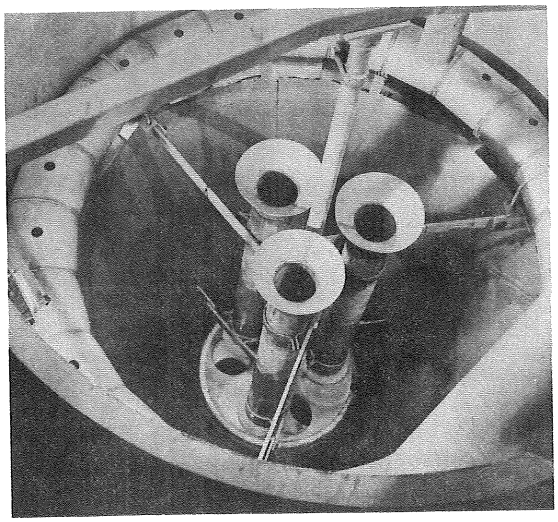

Fig. 6.7 *By-pass lines partly open in the mixing tank.*

in length. The measurements were made with a differential manometer (U-tube) containing tetrabromine methanol and water, Fig. (6.8).

The solids were prevented from plugging the pressure gauges by fitting all taps with flushing arrangements, and by injecting a small constant flow of de-aerated water into the pipe. The constant flow was obtained by a purge meter connected to a differential pressure regulator.

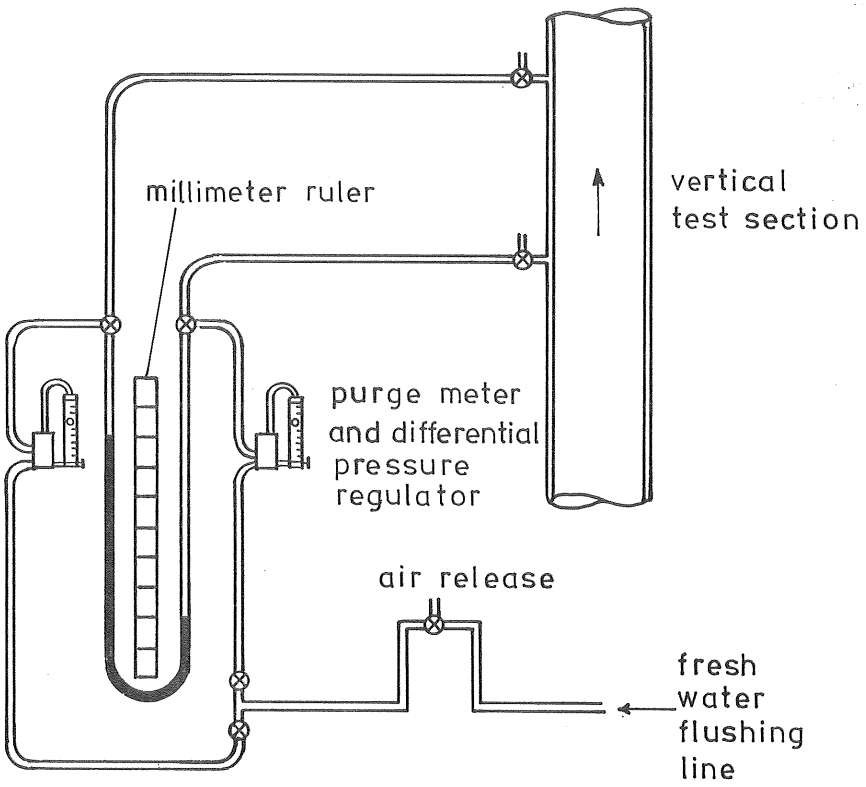

Fig. 6.8 *Schematic lay-out of the differential manometer system.*

The readings on the manometer columns were 0.4-1.2 m, which meant that the smallest division, 1 mm, on the manometer scale represented an accuracy of 0.25% of the reading.

The pump was a 0.152 m by 0.152 m hydroseal rubber-lined Morgårdshammar BC-pump[1)] with a 3-vane impeller of 0.43 m in diameter. Slurry dilution must be minimized for experimental reasons, therefore, a constant seal water flow of $3.3 \cdot 10^{-3}$ m^3/min was permitted which was considerably lower than the proposed 0.015 m^3/min. Pump discharge and suction pressure were measured with bourdon gauge manometers which were fitted with flushing water lines, Fig. (6.9).

1) manufactured under licence from the Allen-Sherman Hoff Pump Co., U.S.A.

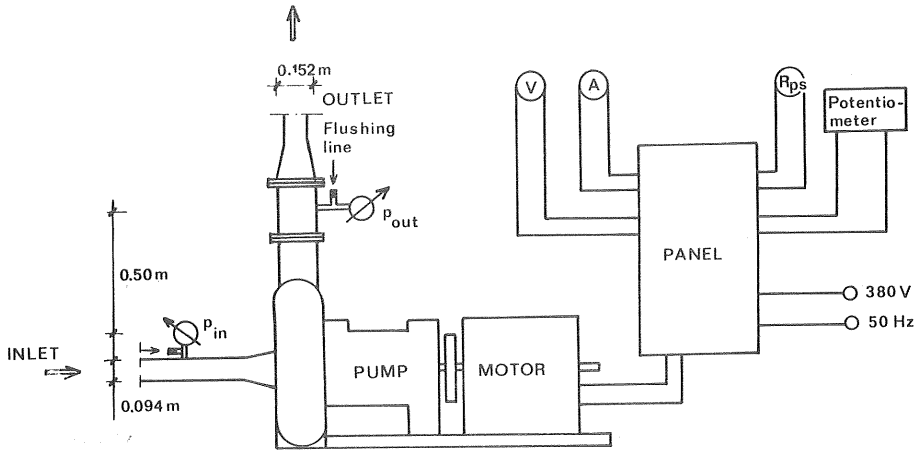

Fig. 6.9 *Schematic lay-out of the pump control and measurement facilities.*

The motor was an ASEA LD-29 DC-motor (66 kW) with the speed regulated by a thyristor converter with tachogenerator feedback, Fig. (6.10). The pump rotary speed was regulated by a potentiometer,

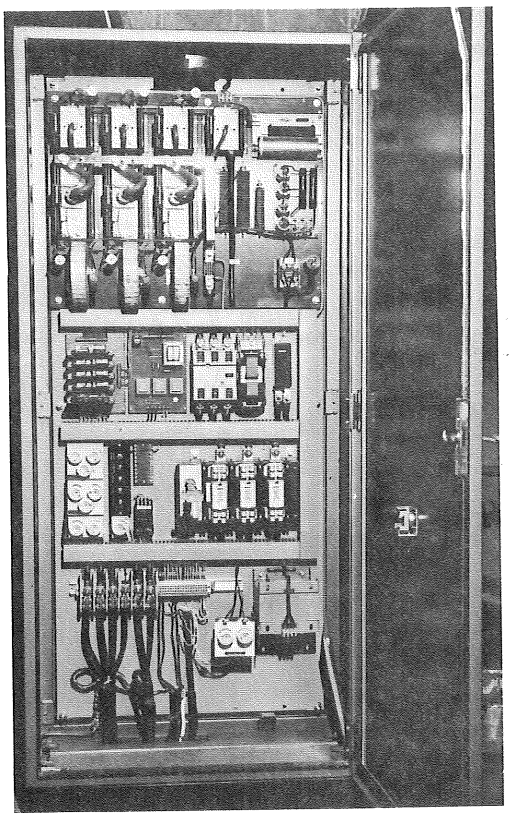

Fig. 6.10 *Thyristor converter panel for 440 V and 150 A. (Aros Electronics AB).*

and the input power consumption was determined from ampère- and voltmeter readings. The ampère- and volmeter readings gave the power consumption with an accuracy of $\pm$ 3%.

6.3 Test procedures and performance

The initial stage of the experimental work was devoted to reliability tests of the system. The observations and results from this initial test programme led to modifications of the lay-out of parts of the system and, finally, an operational procedure was established that met the requirement of fast high-accuracy registration of the hydraulic data.

Observations showed that air was released along a relatively short distance by the perforated holes in the top of the discharge pipe which was extended around the mixing tank. Visual observations through a glass section at the top of the vertical test section showed that no air entered the test section during steady-state flow conditions. No changes in pump performance were observed after hours of clear-water pumping.

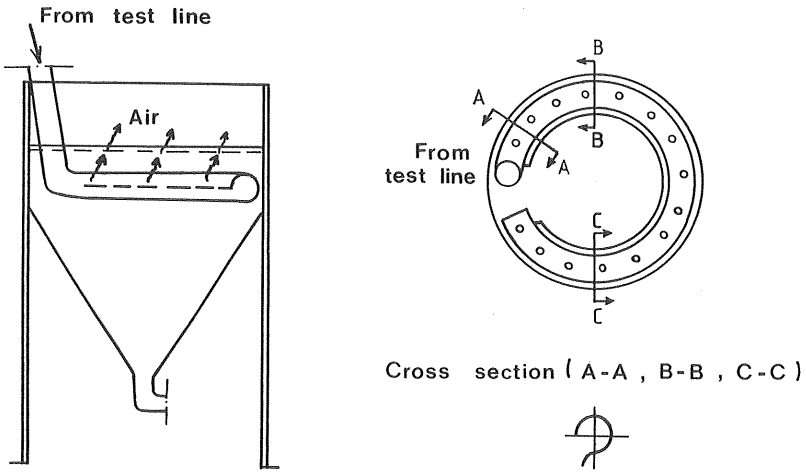

Fig. 6.11 Design of the discharge of the returned slurry into the mixing tank.

Preliminary tests showed that the elongated opening on the inside of the discharge pipe in the tank should be opened up for a more uniform discharge of the solids. The opening was adjusted to be constant along the whole length of the discharge pipe, Fig. (6.11).

The downcoming flow in the pipe and the initial part of the discharge line has a skewed distribution with a high rate of dissipation and mixing, Fig. (6.12).

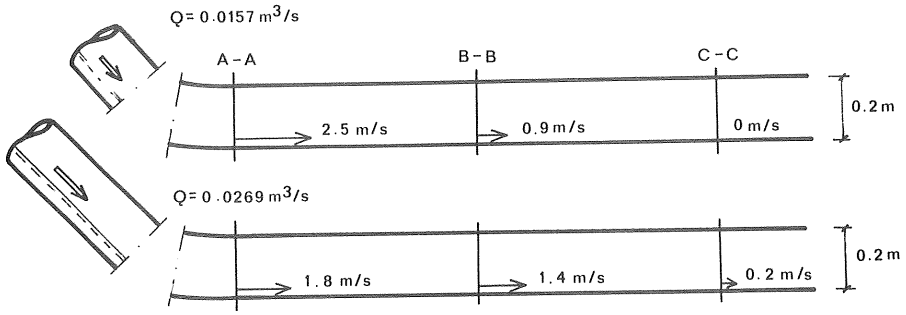

Fig. 6.12 *Distribution of velocity in the discharge pipe with clear water. Symbols from Fig. (6.11). The velocities were measured 25 mm above the bottom of the pipe with screw-type current meters.*

The temperature of the mixtures increased 2^{o}-4^{o}C during a 1h test run. Most of the data was collected at temperatures of 13^{o}C to 17^{o}C and in the evaluation of experimental data the density of water was related to 15^{o}C (999 kg/m^3), giving an error of less than 0.1%.

General test procedure

Solids were delivered to the laboratory in barrels. A representative amount of solids was taken out for particle size analysis, etc. The slurry was prepared by filling the pump feeding tank with water and then adding the predetermined amount of solids. As described earlier the pump was started and circulation was initiated by clear water from above the settled solids. Once the solids in the system were fully suspended, the flow rate was regulated to the value desired for

obtaining the first data points. A test run started at the highest desired velocity. The velocity was then reduced in steps. Discharge rate, solid concentration, and head losses were measured for each step until unstable flow conditions were reached, sometimes causing clogging of solids in the pump. The procedure was then repeated, and the solid concentration was adjusted until the desired ranges of concentrations and velocities were covered.

Most tests were carried out at constant pump speed, and therefore the operation point was varied by a conventional gate valve at the top of the vertical test line. The thyristor variable speed control made it possible to increase the flow very quickly when the system operated close to clogging conditions. However, in the beginning of the test programme there was some failure, leading to complete clogging of the pump. The pump and the lower parts of the facility had to be withdrawn and emptied manually. A non-return flap-valve on the pressure side of the pump never worked, because its moving mechanism was clogged.

Discharge measurements

The mixture density, ρ, of the delivered slurry taken out at the top of the test line was obtained from the sampling tank measurements:

$$\rho = \frac{G_1}{V_1} \tag{6.1}$$

where

G_1 = weight of the mixture in the sampling tank

V_1 = volume of the mixture in the sampling tank

The flow rate, Q, and velocity, U, in the hoisting pipe were determined from the readings of the volume and the filling time in the sampling tank:

$$Q = \frac{V_1}{t} \tag{6.2}$$

where

t = filling time

$$U = \frac{Q}{A} \tag{6.3}$$

where

A = Area of the test pipe section (0.00694 m^2).

Reliability tests with water and slurry showed that the sampling tank relative volume error was less than $\pm$ 0.5%. The weight and volume measurements yield the slurry density, Eq. (6.1), at an accuracy of $\pm$ 1.0%, while volume and time measurements give discharge within $\pm$0.5%. The mean velocity in the vertical pipe was then determined at an accuracy of less than $\pm$ 1%.

Analyses of mineral samples

Periodically the full pipe slurry was allowed to discharge into a 0.02 m^3 sampling bucket placed in the lower part of the sampling tank cone and samples were taken for analysis of particle size distribution and solid density. Some samples were also taken for pH measurement. Only a limited change of the fresh water pH = 8.2 was observed. There was a decrease of pH with time of exposure in the loop with the coarse iron ore which was exposed up to 25h. A minimum pH value of 6 was observed. With the complex ore a constant pH-value of 9.1 was observed after about 5 min.

Particle size distribution

Mineral samples were analysed by the following standard screening procedure. The finest mineral samples analyzed were 0.074 mm in size.

1. The sample was dried at a constant temperature of 95°C and then weighed.
2. The -0.074 mm sized fraction was removed by washing the sample through a 0.074 mm screen.
3. The washed sample was again dried at a controlled temperature of 95°C and the weight of the -0.074 mm fraction was determined.
4. The remaining coarse fractions were screened, using standard screens and standard testing sieve shaker equipment and procedures.

The discharge mixture at the top of the test loop contained coarser particles than solids taken directly from the barrels, because of the shorter time of residence of coarse dense particles in the mixing tank, Fig. (6.13).

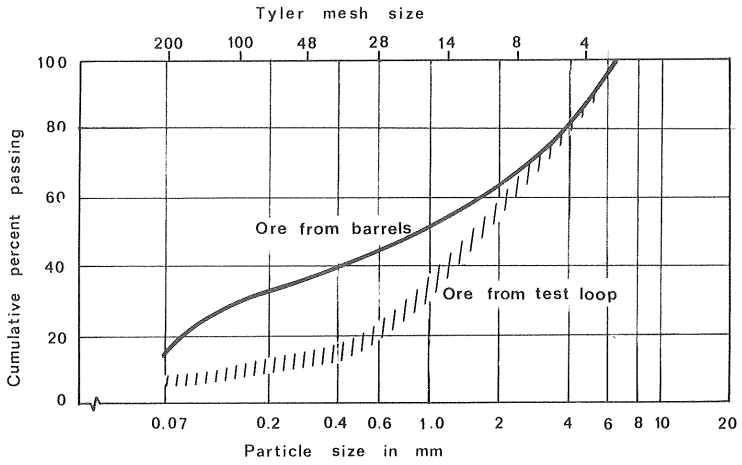

Fig. 6.13 *Maximum effect on particle size distribution due to shorter time of residence of particles in the mixing tank (Coarse iron ore: 10%<C<25%, 3,6 m/s <U<3,9 m/s).*

The effect was expected to decrease for higher concentrations due to hindered settling. However, no such trend was observed for the conditions investigated in Fig. (6.13). For slurries containing finer or lighter minerals the effect on particle size distribution, because of different time of residence was nearly negligible.

Throughout this experimental study all particle size distribution data will be related to samples taken from the flow at the test loop.

Solid density

A standard procedure (Swedish Council for Building Research, 1973) for determination of the solid density had to be modified so that the desired accuracy ($\pm$ 2%) could be reached. Alcohol was used instead of water because it has lower viscosity and thus more easily finds its way through the pores of the mineral. The tare of a standard $50 \cdot 10^{-6}$ m^3 volumetric flask was determined (G_2) and about 0.03 kg of pulverized solids was filled into the flask and the weight

(G_3) of the solids was determined. Exactly $25 \cdot 10^{-6}$ m^3 of 99.0% alcohol was now added by a burette. The flask was then taken into an ultra-sound bath for about 15 min. to force out any entrained air. Finally, alcohol (V_2) was added to the $50 \cdot 10^{-6}$ m^3 point of the flask and the density was calculated according to the following relationship:

$$\rho_s = \rho_o \frac{G_3 - G_2}{(50 - V_2) \cdot 10^{-6}} \tag{6.4}$$

where ρ_o was taken as 999 kg/m^3. The solid density was then obtained from the mean of two values determined experimentally in the manner described above.

The concentration by volume, C, was determined from Eq.(3.8),

$$s = 1 + C(s_s - 1)$$

in the form:

$$C = \frac{s - 1}{s_s - 1} \tag{6.5}$$

where

$$s = \rho/\rho_o$$

$$s_s = \rho_s/\rho_o$$

With measured values of ρ and ρ_s and with ρ_o = 999 kg/m^3 then the concentration was determined with an accuracy of 3%.

Terminal settling velocity

The terminal settling velocity of the mineral particles was measured in two perpex pipes having a diameter of 0.074 mm and length of 1 m and 4.5 m, respectively. The settling time over a length of 0.7 m and 4.0 m was registered by a time recorder. The mean terminal velocity, W_j, was determined from the individual terminal velocities of 10-20 randomly chosen particles from each sieve fraction. The terminal velocity of the finer fraction particles was observed as an average velocity of a cloud of particles. The characteristic particle size was represented by the mean of each sieve size. The wall correction factor was within the experimental error of $\pm$ 2% of the

settling velocity measurements.

Reliability of mineral sample tests

The accuracy of the particle size distribution measurement was tested by holding all other variables constant and taking samples in rapid succession from the flow at the top of the vertical test line. A representative example is shown in Fig. (6.14).

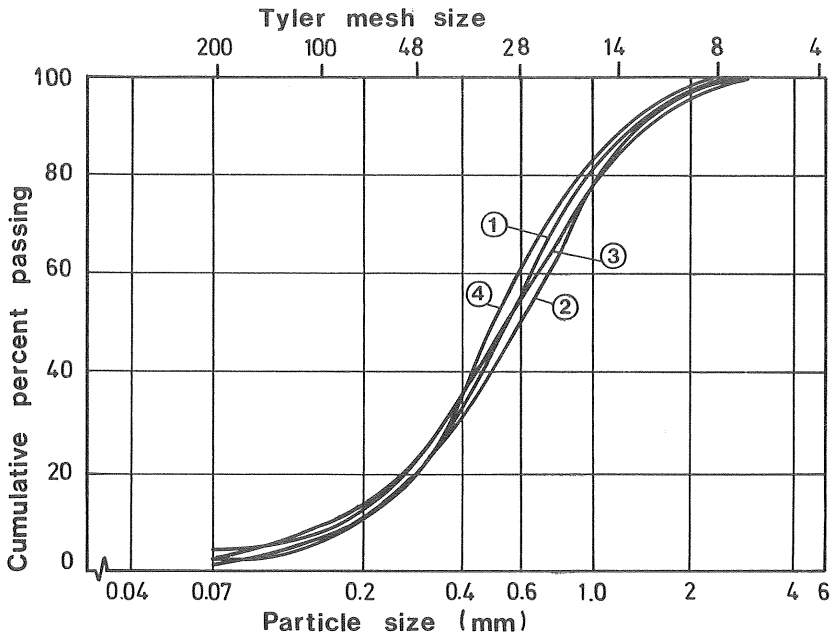

Legend: ① ② ③ ④

Measured density (kg/m^3): 2335 2361 2350 2337

Fig. 6.14 Particle size distribution and solid density accuracy test (Perlite mineral).

The above procedure generally gave an accuracy of about ± 10% of the particle size distribution. It was believed that the scatter in the particle size distributions was not only sampling or screening effects but also influence of inherent fluctuations in the slurry flow that exist even under controlled laboratory conditions. The accuracy was considerably better for the uniformly distributed crushed granite mineral. Therefore, the attrition of this angular mineral could be

uniquely demonstrated, Fig. (6.15).

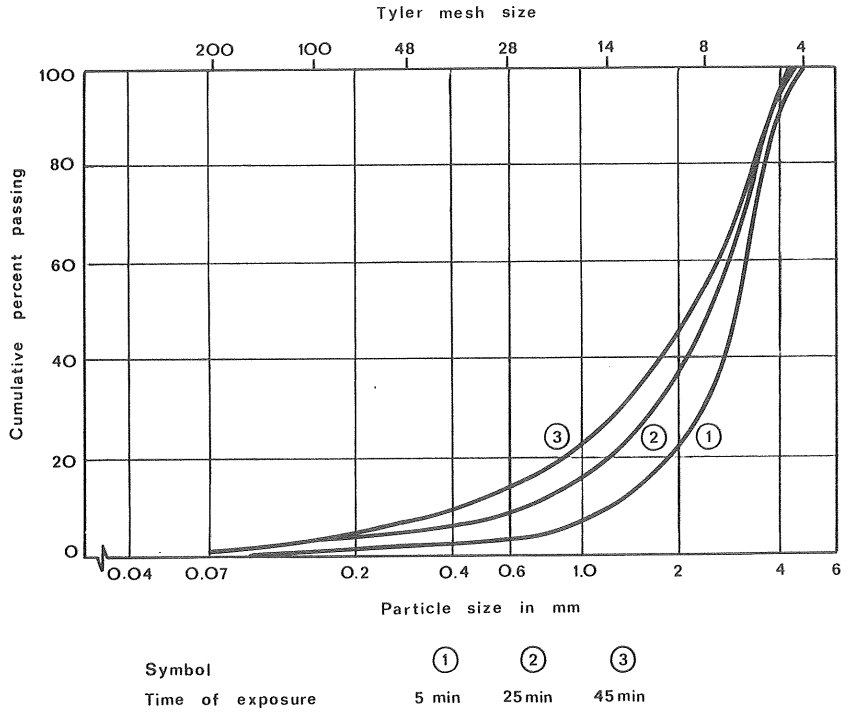

Fig. 6.15 *Attrition of the crushed granite, observed during constant flow conditions.*

The influence of flow-dependent changes of the concentration in the test pipe was investigated in the following manner. A constant amount of solids and water was circulated in the system, and samples were taken from the whole span of flow in the pipe. The test was carried out with the lead ore and the coarse iron ore. It was previously found that the attrition of these solid particles could be neglected during a short period of testing. From the measured results, Fig. (6.16), it was concluded that the influence of flow-dependent changes of the delivered concentration have no significant effect on the composition of the solids in the mixture in the pipe.

The coarse iron ore was the coarsest and heaviest solid investigated. The coarse iron ore was also the only solid tested over a relatively long period of time up to about 25 hours of exposure in the loop. The variation in observed size distribution of large particles exposed over a long period of time, was mainly a result of the rounding of their sharp edges, Fig. (6.17).

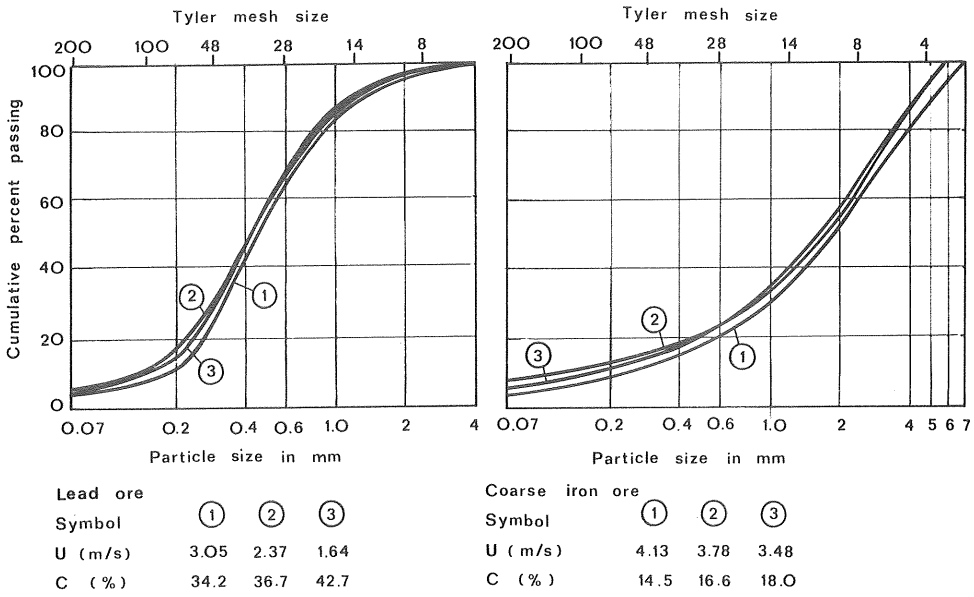

Lead ore			
Symbol	①	②	③
U (m/s)	3.05	2.37	1.64
C (%)	34.2	36.7	42.7

Coarse iron ore			
Symbol	①	②	③
U (m/s)	4.13	3.78	3.48
C (%)	14.5	16.6	18.0

Fig. 6.16 *Influence of different flow conditions on solid composition at the top of the vertical test line.*

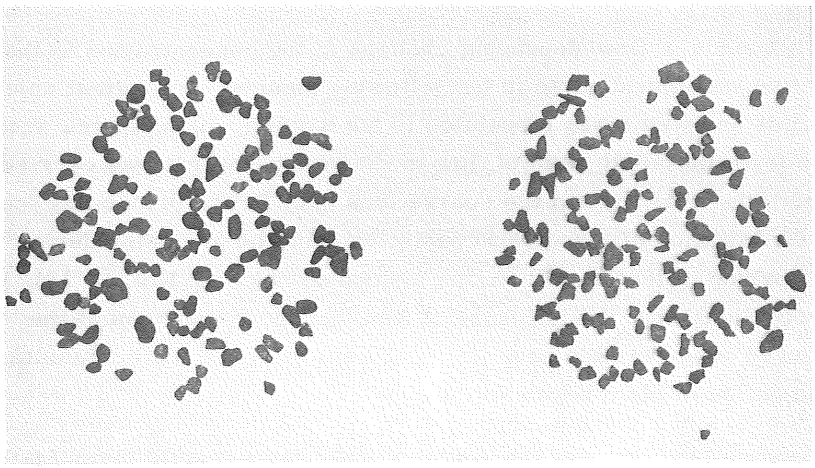

Fig. 6.17 *Rounding of coarse particles (4-6 mm) after about 10h of exposure in the loop (coarse iron ore).*

Attrition test procedure

If the data was to simulate a true transport situation, it had to be collected during a 5 min period, which is equal to about 20-40 passages through the pump, However, only limited data on such short times of exposure could be collected because of the demand for very large quantities of fresh mineral. Finally, the following operational procedure was organized to meet the demand of accuracy and fast determination of hydraulic data. "Fresh mineral" condition was defined as: "mineral exposed less than 20-30 minutes in the loop" (60 minutes with coarse iron ore). "Circulated mineral" was defined as "mineral exposed 50-90 minutes" (more than 4h with coarse iron ore). These tests were carried out with a constant pump speed = 12.67 rps. In the intermediate time between "fresh" and "circulated" mineral conditions the pump performance was tested at a maximum pump speed = 19 rps.

Pressure drop measurements

The pressure gradient required to maintain a steady-state flow between two sections of a vertical pipe was obtained from the energy equation along the centre-line streamline, Fig. (6.18),

$$i_{Tot} = \frac{p_1 - p_2}{\rho_o g L} \qquad (6.6)$$

where the gradient, i_{Tot}, is expressed in metres of water per metre of pipe and where p_1 and p_2 are the pressure in pipe section 1 and 2, respectively.

The measured pressure gradient, i_{Tot}, is obtained from the following relationship for the tetrabromine methanol system in the differential manometer:

$$i_{Tot} = 1 + \frac{(s_t - 1)\, h_t}{L} \qquad (6.7)$$

where

$s_t = \rho_t / \rho_o$

ρ_t = density of tetrabromine methanol

h_t = manometer reading (see Fig. 6.18)

The density of the tetrabromine methanol was found to be 2980 kg/m^3, and since L = 2.50 m it follows that:

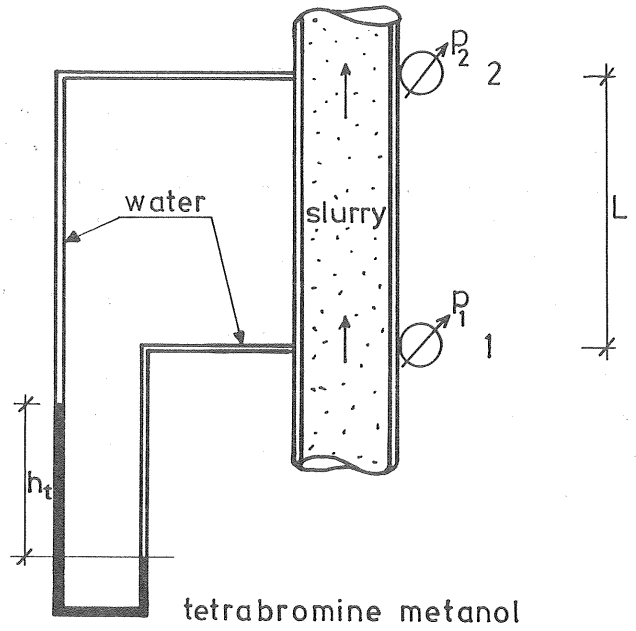

Fig. 6.18 *Schematic representation of the determination of the pressure gradient.*

$$i_{Tot} = 1 + 0.793\, h_t \qquad (6.8)$$

An average reading was estimated, since there were always minor fluctuations, especially at high velocities of coarse slurries. The overall accuracy of the U-tube system was found to be within $\pm$ 2%.

Pump performance measurements

The pump head was obtained from the pressure rise and flow rate readings. Application of the energy equation to the inlet and outlet sections of the pump, Fig. (6.9) page 101, gave:

$$H + \frac{p_{in}}{\rho g} + \frac{\alpha_{in} Q^2}{A_{in}^2\, 2g} = \frac{p_{out}}{\rho g} + \frac{\alpha_{out} Q^2}{A_{out}^2\, 2g} + 0.50 \qquad (6.9)$$

where

p_{in} = pressure reading at the suction side of the pump

p_{out} = pressure reading at the discharge side of the pump

ρ = mixture density

Q = flow rate of mixture

H = pump head in metres of mixture

α_{in} = velocity distribution correction factor at the suction side of the pump

α_{out} = velocity distribution correction factor at the discharge side of the pump

$$A_{in} = \frac{\pi D_{in}^2}{4}$$

$$A_{out} = \frac{\pi D_{out}^2}{4}$$

The correction factors, α_{in} and α_{out}, are taken here as unity. The possible error of this assumption will be negligible in the determination of the pump head.

From Eq. (6.9) it follows:

$$H = 0.50 + \frac{p_{out} - p_{in}}{\rho g} - \frac{Q^2}{A_{in}^2 2g} \cdot \left(1 - \left(\frac{D_{in}}{D_{out}}\right)^4\right) \qquad (6.10)$$

with

$$D_{in} = 0.094 \text{ m}$$

and

$$D_{out} = 0.152 \text{ m}$$

then

$$H = 0.50 + \frac{p_{out} - p_{in}}{\rho g} - 904\, Q^2 \qquad (6.11)$$

The pump head, H, will be greater than 10 m and the flow, Q, will be less than about 0.04 m^3/s. Therefore, the influence of slightly different values of α_{in} and α_{out} will be small and negligible. The pump manometer readings yield the pressure rise by the pump with, an accuracy of $\pm$ 2%. The pump head was then determined by Eq. (6.11) with an accuracy of $\pm$ 5%.

The pump efficiency characteristics were obtained from the pump

head determination and the measured values of density, flow, current and voltage. The efficiency of a centrifugal pump, η, is defined as the ratio of pump energy output to the energy input applied to the pump shaft. The total efficiency, η_{Tot}, includes the efficiency of the motor, η_{Motor}, and the efficiency of the motor-pump transmission, η_{Transm} :

$$\eta_{Total} = \eta \cdot \eta_{Transm} \cdot \eta_{Motor} \qquad (6.12)$$

$$\eta_{Total} = \frac{P_{out}}{P_{in}} \qquad (6.13)$$

where the input power, P_{in}, was obtained from the ampère- and voltmeter readings. The output power, P_{out}, was given by:

$$P_{out} = \rho g Q H \qquad (6.14)$$

From the ρ, Q and H measurements, P_{out} was then determined from Eq. (6.14) with an accuracy of about $\pm$ 10%.

The efficiency of the LD-motor, η_{Motor}, for different values of rotary speed and input current was obtained from the motor manufacturer, Fig. (6.19).

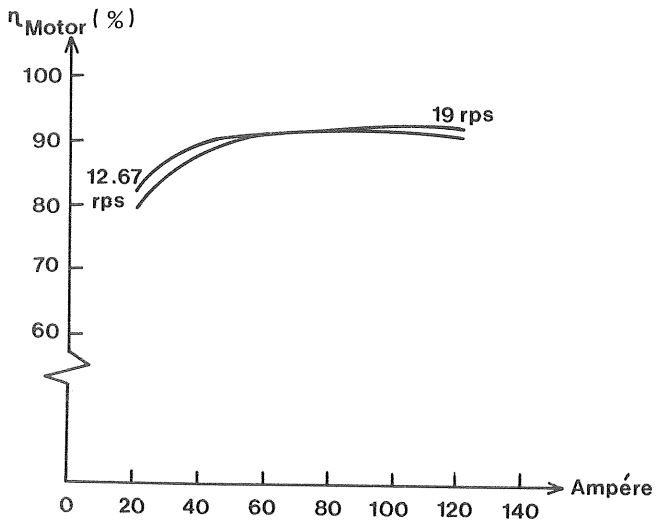

Fig. 6.19 *Efficiency of the LD-motor at 12.67 and 19 rps. The rotary speed of the pump shaft was measured with a stroboscope.*

The losses in the belt drive transmission can generally be estimated at 4% - 5%, Nilsson (1976). Therefore, a constant value of 95.5% was used for η_{Transm}. Fluctuations in the ampère-meter registration were observed. This was the main source of the error in the input power measurements during slurry tests. The indirect evaluation of η from Eqs. (6.12) and (6.13) yield pump efficiency with an accuracy of not better than about $\pm$ 15%.

The pump utilized in the study operated in the domain showed in Fig. (6.20). The pump performance test was carried out at two pump speeds, 12.67 rps and 19 rps.

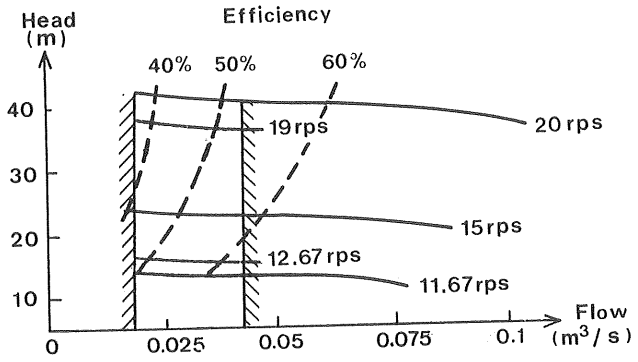

Fig. 6.20 Operational domain of the pump.

Performance of pump and pipe in water service

A summary of operational data from the whole experimental study is shown in Table (6.3).

The clear water pump characteristics were compared with a similar water test following every slurry test run. There was no noticeable difference between the water performance after about 70 h of pumping the different minerals shown in Table (6.3). Measured clear water head and efficiency are shown in Fig. (6.21), together with the clear water characteristics published by the manufacturer.

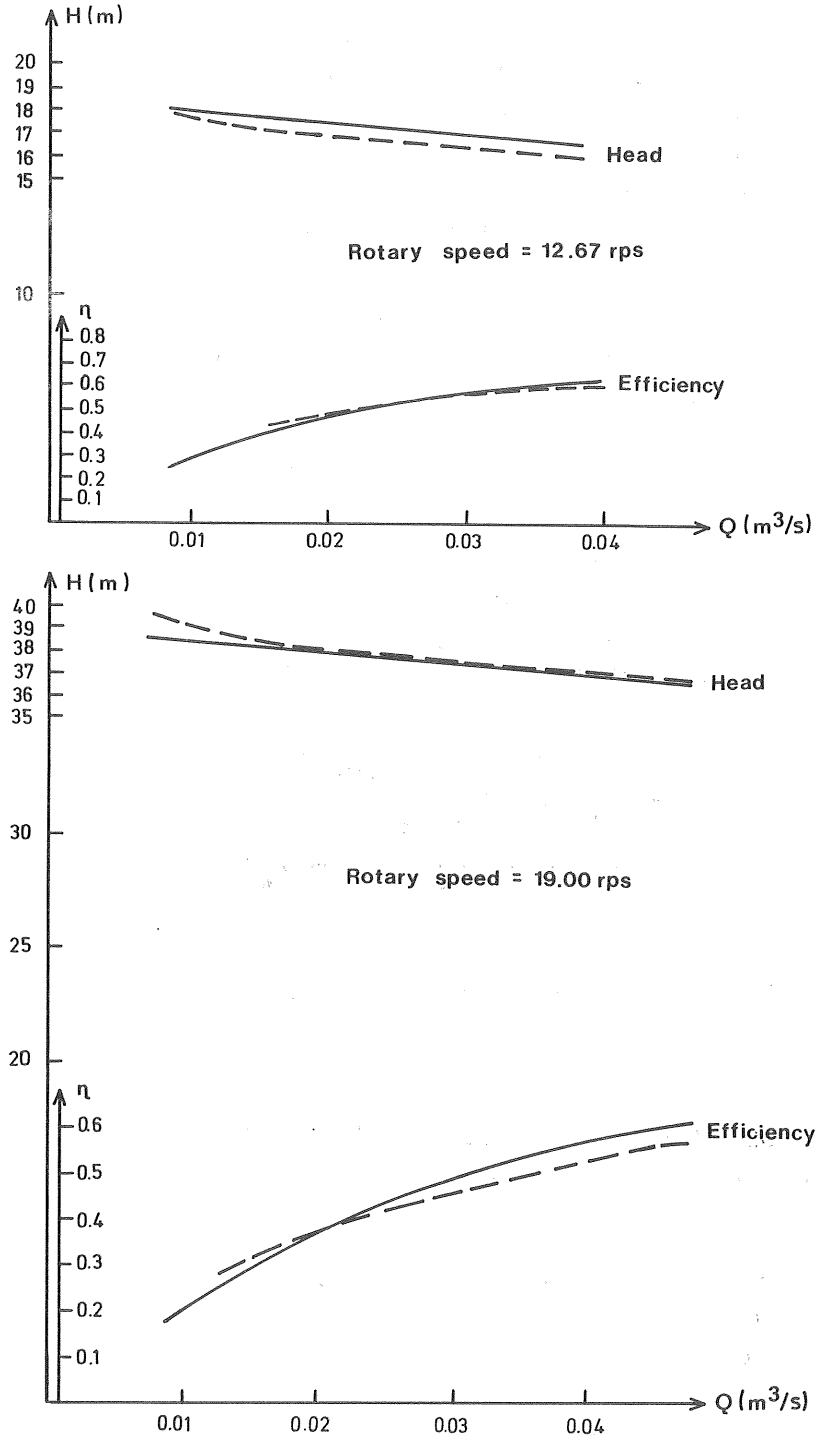

Fig. 6.21 *Measured clear water head and efficiency of the centrifugal slurry pump. The dashed lines represent clear water characteristics published by the manufacturer.*

Table 6.3 Summary of operational data

Mineral	Delivered tonnes	Average concentration by volume %	Average velocity (m/s)
Coarse iron ore	2450	15	3.3
Primary ground iron ore	290	24	3.2
Complex ore	50	11	3.2
Lead ore	150	30	3.0
Perlite	140	27	3.2
Crushed granite	25	10	3.2
Total	3105 tonnes		

The hydraulic characteristics of the water in the vertical pipe were determined throughout the range of velocities to be considered for the slurry tests. These clear water characteristics were compared with similar tests following the slurry run to determine if there was any change in the pipe roughness caused by erosion or corrosion. Visual observations of the inner surface of the pipe showed a starting formation of pits at the end of the experimental programme. However, the roughening of the surface has no measureable influence on friction losses.

The clear water friction loss was expressed in the dimensionless form of the Darcy-Weissbach friction factor and the Reynolds number. The clear water friction factor - Reynolds number relationship was within experimental error during the whole period of investigation. The pipe roughness coefficient, k, was found to be $3.0 \cdot 10^{-5}$ m. The domain of the tests is shown in the Moody-diagram in Fig. (6.22).

The formation of pits demonstrated the strong effect of corrosion. The corrosion component was high because of the presence of dissolved oxygen in the circulated water and the relative freshness of the solids.

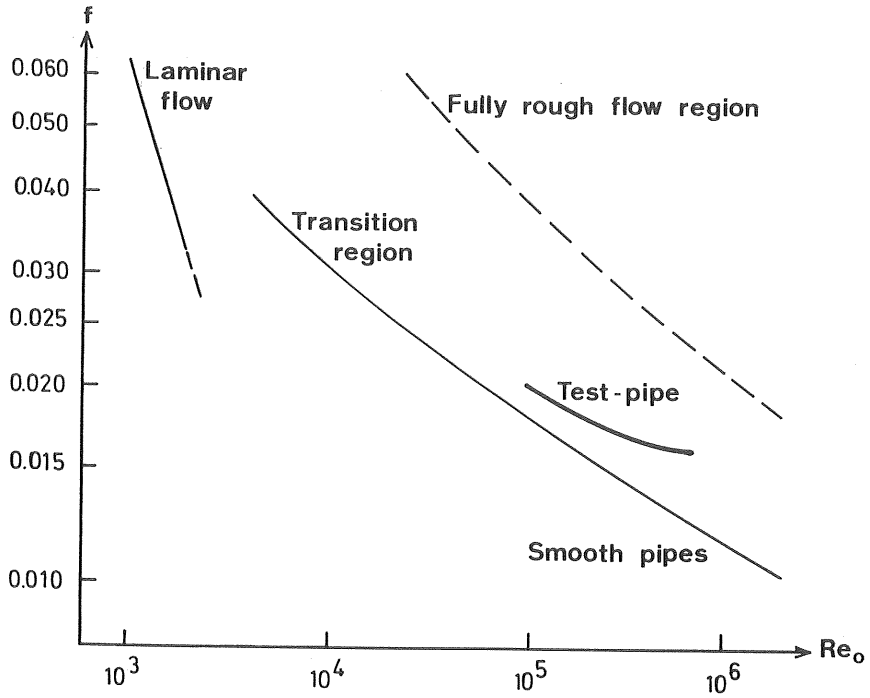

Fig. 6.22 *Domain of measured clear water friction loss in the vertical steel pipe of diameter = 0.094 m and with absolute roughness $k = 3.0 \cdot 10^{-5}$ m.*

6.4 Wear in the test loop

Approximative prediction of wear

Wear in slurry flow is caused by two distinctly different mechanisms: chemical corrosion and mechanical abrasion or erosion. Corrosion is generally due to the presence of dissolved oxygen in the slurry and low pH values. The abrasion of materials by fluid-borne solid particles is primarily caused by a combination of deformation wear (impact) and wear caused by cutting (sliding). The relative rate depends on the nature of the wearing material as well as on the angle of impingement. The solids have the effect of removing the surface film of the pipe and increasing the rate of mass transfer of oxygen. The great effect of this erosion-corrosion behaviour in slurry flow has been demonstrated by Postlethwaite (1976).

Numerous tests have shown that wear in pipes and in pump parts, etc. increases exponentially with velocity, the exponent being somewhere between 2 and 3 (Link et al. 1972, Wilson 1972). It has also been shown that wear increases linearly as particle size and density increase (Link et al. 1972). The latter also reported that when the concentration increases more than about 20% by weight, the influence of concentration on wear diminishes.

Data from wear tests in pipe bends have been published only to a small extent. The following investigational data from a steel pipe test with sand slurry was given by Schreiber (1967):

$D = 0.05$ m
$U = 7.5$ m/s
$C = 0.15$
$\rho_s = 2650$ kg/m^2 (sand)
$d_{50} = 1.8$ mm

After 1000 h of exposure, 4 mm of wall thickness loss was observed in a 90^o elbow. The wear rate per delivered tonne of sand was $0.19 \cdot 10^{-3}$ mm. Assuming equivalent concentration and velocity, one can transfer the wall thickness loss obtained in a smaller pipe to pipes of larger diameters. Faddick (1975), thus found the wear rate, We, mm/tonne, to be inversely proportional to the cross-sectional area of the pipe, i.e.

$$\frac{We_1}{We_2} = \left(\frac{D_2}{D_1}\right)^2 \qquad (6.15)$$

In the test loop the elbows at the top of the vertical test line, Fig. (6.2) page 95 , and the bend of the return pipe, Fig. (6.4) page 97, were the sections most impaired by wear. The characteristics of the flow in the initial stage of the investigational work in the test loop were assumed to be:

$D = 0.094$ m
$U = 3.3$ m/s
$C = 0.15$,
$\rho_s = 4150$ kg/m^3 (coarse iron ore)
$d_{50} = 1.8$ mm

Based on the investigational data given by Schreiber, Eq. (6.15), and assuming an exponential increase of wear with velocity (exponent 2-3) and a linear increase with particle size, d_{50}, and no influence of concentration, one can estimate the wear in the test loop elbow:

$$We_{0.094} = 0.19 \cdot 10^{-3} \cdot \left(\frac{0.050}{0.094}\right)^2 \cdot \left(\frac{3.3}{7.5}\right)^{2-3} =$$

$$= 0.01 \cdot 10^{-3} - 0.005 \cdot 10^{-3} \text{ mm/tonne} \qquad (6.16)$$

About 60 tonnes of iron ore were delivered per hour and the pipe wall thickness was 3.6 mm; thus the lifetime of the elbow at the top of the test line could be predicted to be over 1000 h.

The velocity of an iron ore slurry was estimated to be about 12 m/s when the slurry entered the steel pipe elbow in the mixing tank, because of the acceleration of the free flow in the return pipe. The flow was strongly supercritical and the energy dissipation of the submerged hydraulic jump inside the curved conduit was considerable. The wear of the bend was believed to be concentrated in a relatively small area because of the skewed distribution of the flow. The exposed area of the free surface flow in the return pipe bend (diameter = 0.2 m) was assumed to be roughly equal to that of the investigational data given by Schreiber. Again, assuming exponential increase of wear with velocity and a linear increase with particle size, then:

$$We_{0.2} = 0.19 \cdot 10^{-3} \cdot \left(\frac{12}{7.5}\right)^{2-3} = \tag{6.17}$$

$$= 0.49 - 0.77 \cdot 10^{-3} \text{ mm/tonne}$$

which gives an estimated lifespan of 75-140h (wall thickness = 3.6 mm).

The predictions given above are of course very approximative and in no way conclusive.

Observed wear

After about 1 h of pumping the angular crushed granite mineral a slight decrease in the clear water pump efficiency was observed, but the variation was hardly measurable and was within the experimental error.

Examination of the pump parts showed the beginning of wear of the lining and the wheel. "Chips" of rubber were ripped off during the test, Fig. (6.23).

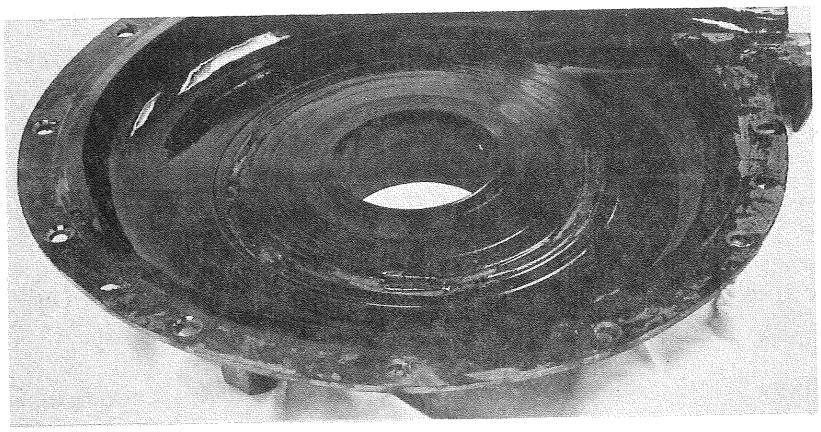

Fig. 6.23 *Observed wear in pump lining after about 1h of pumping the crushed granite.*

The return steel pipe elbow was completely worn out after about 30 h in coarse iron ore slurry service, Fig. (6.24).

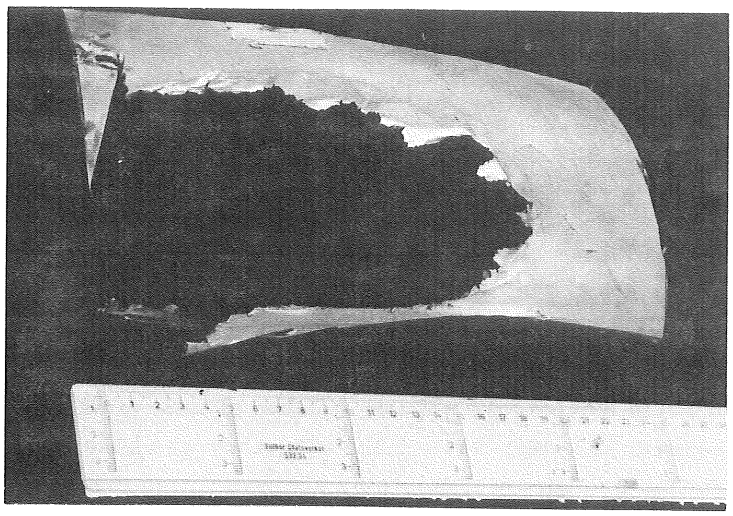

Length = 0.25 m

Fig. 6.24 Worn-out part of the bend in the return pipe.

The destroyed elbow was repaired, and the return pipe was lined with a flexible rubber hose all the way up to the top of the test line.

The 90^{o} elbow at the top at the test loop was worn out after 35 h in coarse iron ore service, which was considerably earlier than estimated. However, the fracture occurred locally at a welding joint just downstream the elbow.

6.5 Horizontal pipe test loop

The small horizontal test loop system is schematically shown in Fig. (6.25).

A glass section permitted visual observation of deposit conditions, etc. Ancillary equipment included a mixing tank, pinch valves and a U-tube manometer. Slurry temperature was controlled by circulating water. The flow and the slurry density were measured directly by diverting the flow to a sample bucket with a volume of 0.03 m^3. Average velocity and slurry concentration were determined from

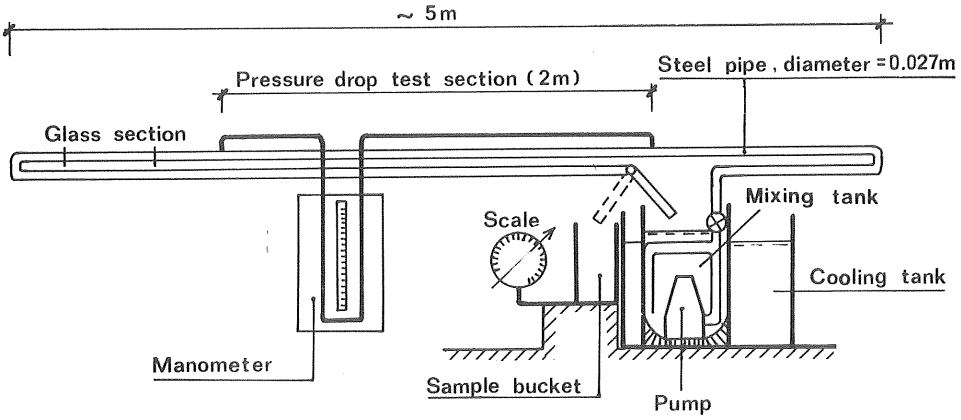

Fig. 6.25 Horizontal pipe test loop - schematic lay-out.

time interval, volume, and weight measurements.

The pressure drop in the horizontal pipe test section was measured by a similar differential manometer system as is shown in Fig. (6.8) page 100. The energy losses, i_H, measured in metres of water per metre of pipe was obtained from the following relationship:

$$i_H = \frac{(s_t - 1)h_t}{L} \tag{6.18}$$

where s_t, and h_t were defined on page 111. With $s_t = 2.983$ and $L = 2.00$ m, then it follows from Eq. (6.18) that:

$$i_H = 0.991\ h_t \tag{6.19}$$

The general accuracy of the i_H, U, and C determinations were 2% 2%, and 3%, respectively.

The pipe roughness coefficient was found to be $3.8 \cdot 10^{-5}$ m. The domain of the friction loss test is shown in the Moody-diagram in Fig. (6.26).

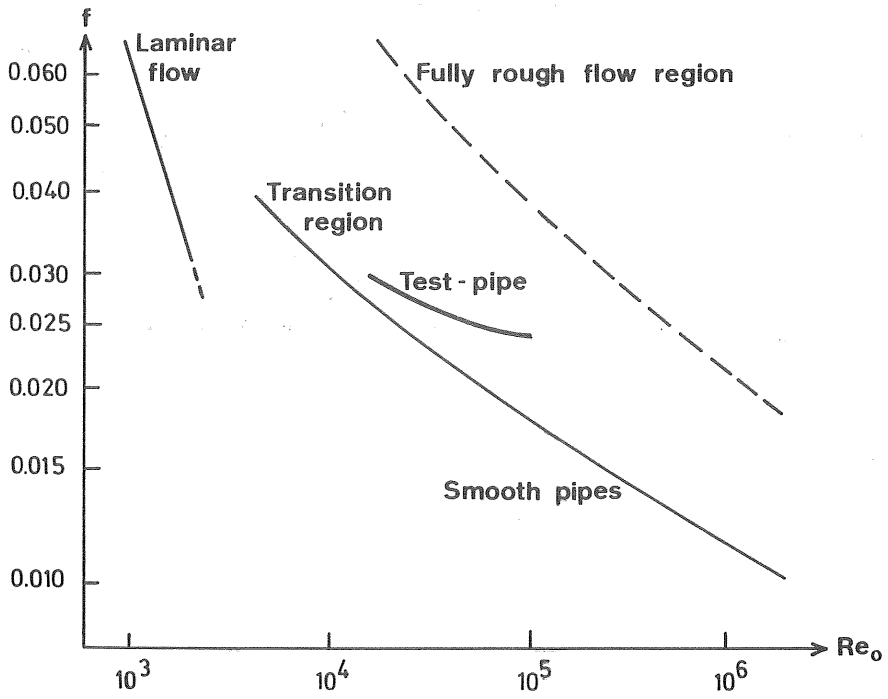

Fig. 6.26 *Domain of measured clear water friction loss in the horizontal steel pipe of diameter = 0.027 m and with absolute roughness* $k = 3.8 \cdot 10^{-5}$ *m.*

7. EVALUATION OF EXPERIMENTAL DATA

7.1 Pilot-loop test

The experimental study was carried out for concentrations by weight of up to 60% to 70% for the iron ores, perlite, and lead ore. The concentration by weight, C_w, is related to the concentration by volume, C, by the following relationship:

$$C_w = \frac{C\, s_s}{s} \tag{7.1}$$

where

s = mixture density ratio, ρ/ρ_o

s_s = solid density ratio, ρ_s/ρ_o

For the complex ore and the crushed granite no experimental data for concentrations by weight greater than 30% was available, because of limited amount of ore and limited pump motor power, respectively.

The experimentally determined density of the mixture, ρ, was obtained from Eq. (6.1):

$$\rho = \frac{G_1}{V_1}$$

where

G_1 = weight of the mixture in the sampling tank

V_1 = volume of the mixture in the sampling tank

The irreversible energy in the 2.5 m vertical test section was evaluated from Eqs. (3.31), (3.32) and (6.8), respectively

$$i_{Irr} = i_{Tot} - i_{Rev}$$

where

$$i_{Rev} = s = 1 + C\,(s_s - 1)$$

$$i_{Tot} = 1 + 0.792\, h_t$$

and where h_t is the manometer reading in metres and i_{Tot} is the measured pressure gradient in metres of water per metre of pipe. Thus, the experimentally obtained irreversible energy gradient in

metres of water per metre of pipe is:

$$i_{Irr} = i_{Tot} - s \qquad (7.2)$$

where, $s = \rho/\rho_o$,is the measured mixture density ratio. The concentration by volume is obtained from Eq. (6.5):

$$C = \frac{s - 1}{s_s - 1}$$

Mineral properties etc.

The average physical composition, solid density, particle size distribution, terminal settling velocity, and the attrition of the pumped minerals are shown in Figs. (7.1 - 7.6) on the following pages. The mean particle size distributions and terminal settling velocities shown were based on mineral taken from the test loop within 5 minutes, i.e. fresh mineral conditions. The weighted particle sizes and weighted terminal settling velocities were determined by Eqs.(3.23) and (3.24), respectively:

$$\bar{d} = \sum_{j=1}^{N} p_j d_j$$

$$\bar{w} = \sum_{j=1}^{N} p_j W_j$$

where the particle size, d_j, and the terminal settling velocity, W_j, were related to the weight fractions, p_j, defined by the standard sieve openings. W_j is an average value of randomly chosen particles from each fractional part, p_j.

In the determination of $\bar{d}$, particle sizes of less than 0.074 mm was assumed to be uniformly distributed down to 0, because the particle size distribution of the fine particle part was not investigated. In the determination of $\bar{w}$, W_j was taken = 0 for particle sizes less than 0.074 mm, a reasonable approximation because the portion of small particles in general was low. The calculated values of $\bar{w}$ and the experimentally obtained distribution curves of W_j and d_j are shown in Figs. (7.1 - 7.6). The particle size d_j corresponding to W_j was

Primary ground iron ore

(LKAB-mine in Malmberget)

Iron (magnetite)	50%[1)]
Silica	11%
Sulphur	1%
Apatite etc.	38%
Density	4003 kg/m^3

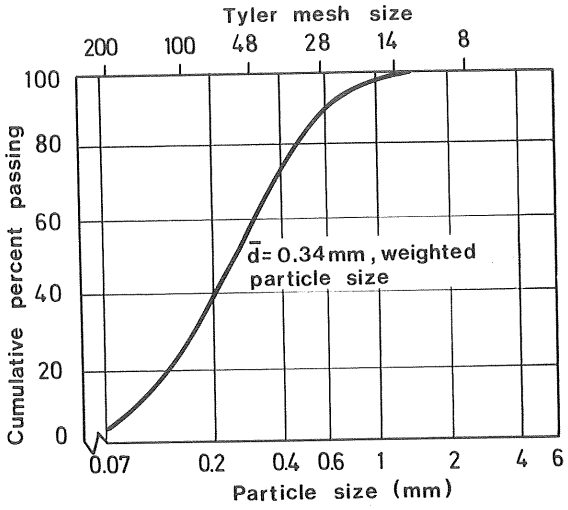

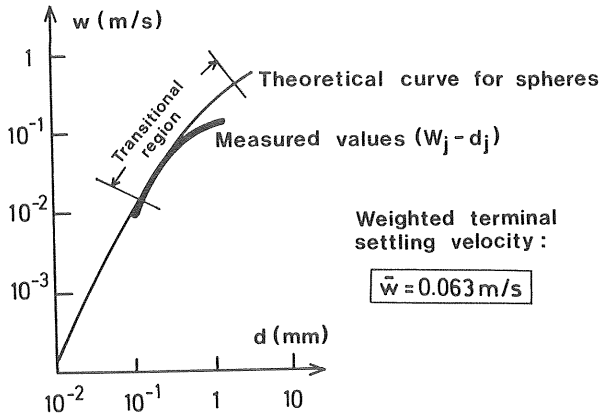

Fig. 7.1 *Average composition, particle size distribution, and terminal settling velocity of the tested primary ground iron ore.*

[1)] The average composition is given in percent by weight in Figs. (7.1 - 7.6).

Lead ore

(Boliden AB-mine in Laisvall)

Lead	3.5% - 4%
Zink	0.5% - 1%
Fluorspar, Baryt, Calcite etc.	10%
Quartz	86%
Density	2672 kg/m^3

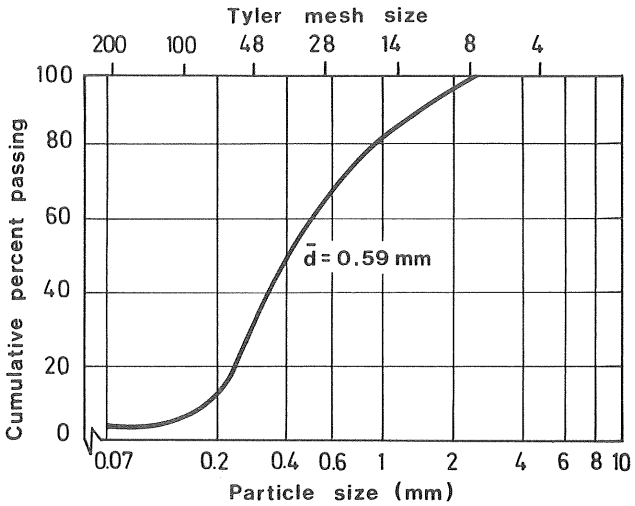

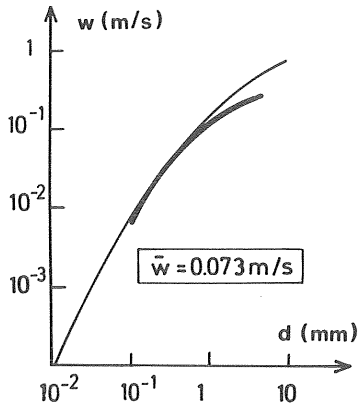

Fig. 7.2 *Average composition, particle size distribution, and terminal settling velocity of the tested lead ore.*

Perlite mineral

(Deposit in Iceland)

Quartz 70%

Oxids of Aluminium, Natrium, Potassium etc. 30%

Density 2341 kg/m^3

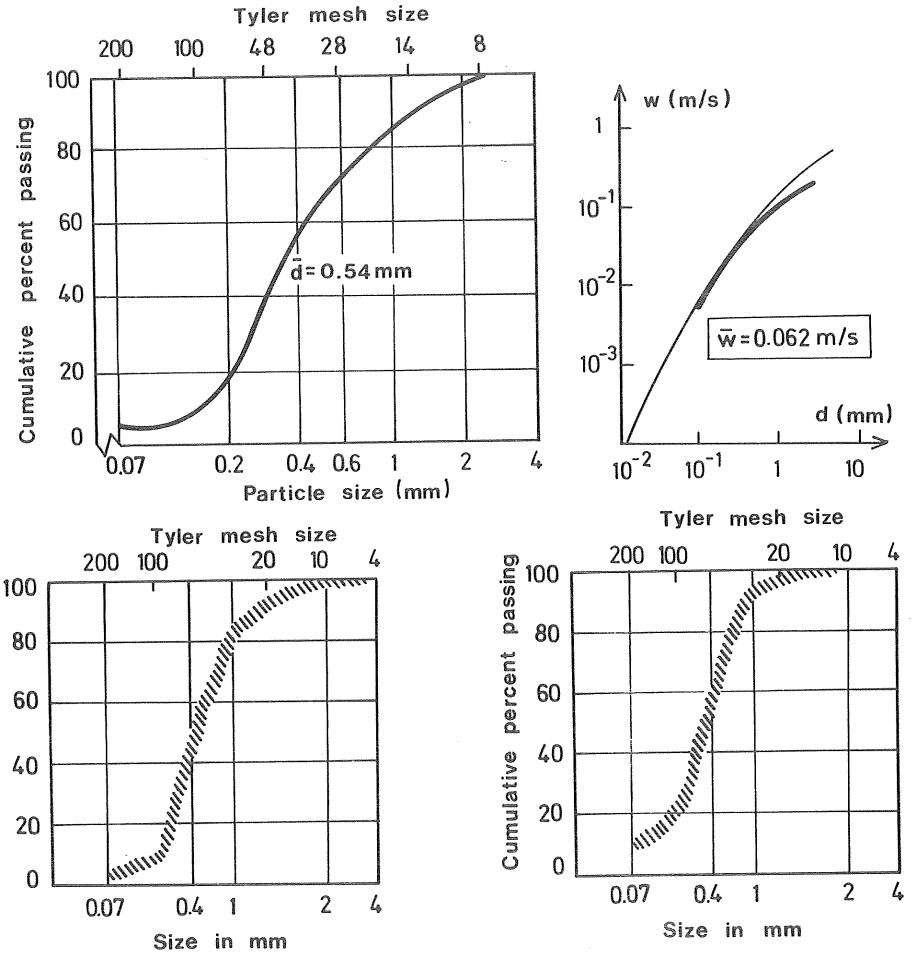

Fresh mineral - exposed
0 - 25 minutes in the loop

Circulated mineral - exposed
50 - 90 minutes in the loop.

Fig. 7.3 *Average composition, particle size distribution, and terminal settling velocity and attrition of the tested perlite mineral.*

Complex ore

(Boliden AB-mine in Garpenberg)

Copper, Lead, Zink	mainly in the form of carbonates, sulfates, silicates and hydrates	10%
Pyrite		5%
Talc		15%
Leptite, limestone etc.		70%

Density 3395 kg/m^3

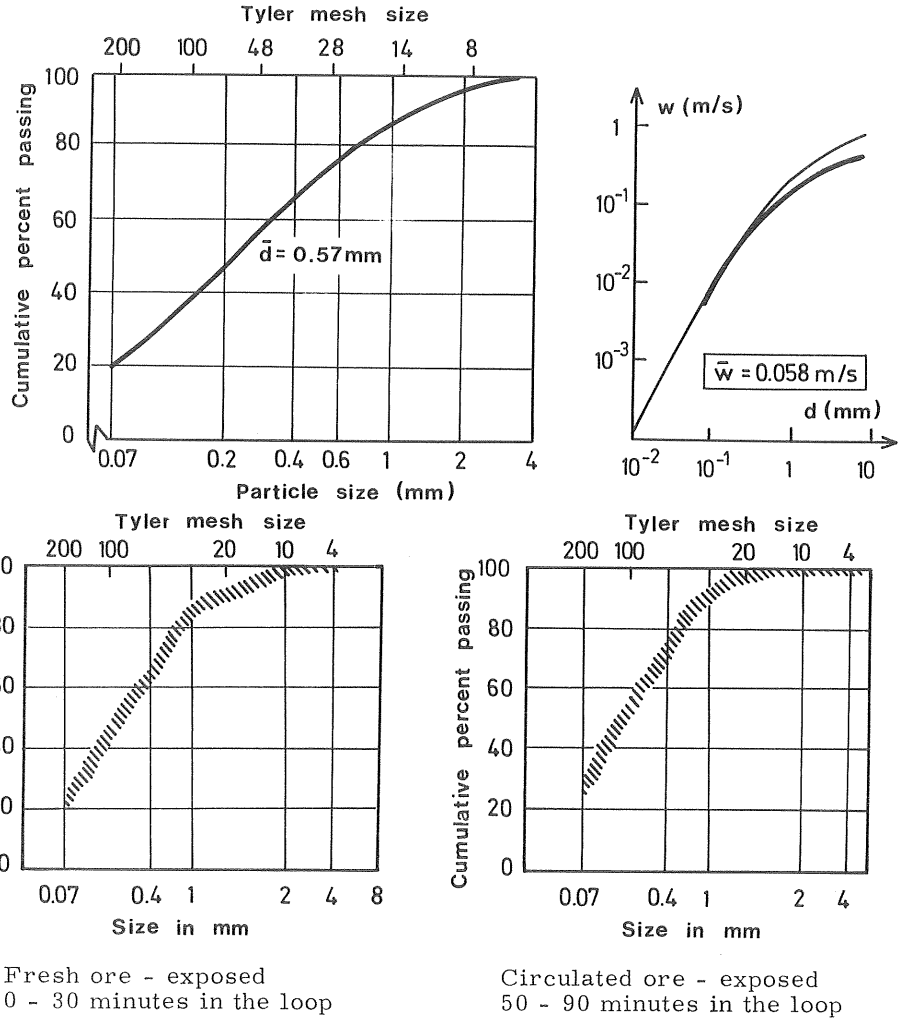

Fresh ore - exposed
0 - 30 minutes in the loop

Circulated ore - exposed
50 - 90 minutes in the loop

Fig. 7.4 *Average composition, particle size distribution, terminal settling velocity and attrition of the complex ore.*

Crushed granite

(Crushing plant in Göteborg)

Density 2676 kg/m^3

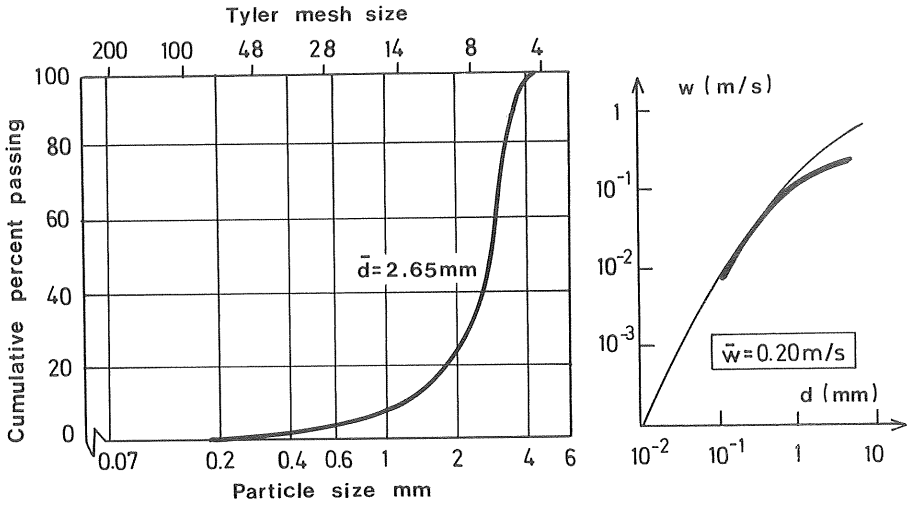

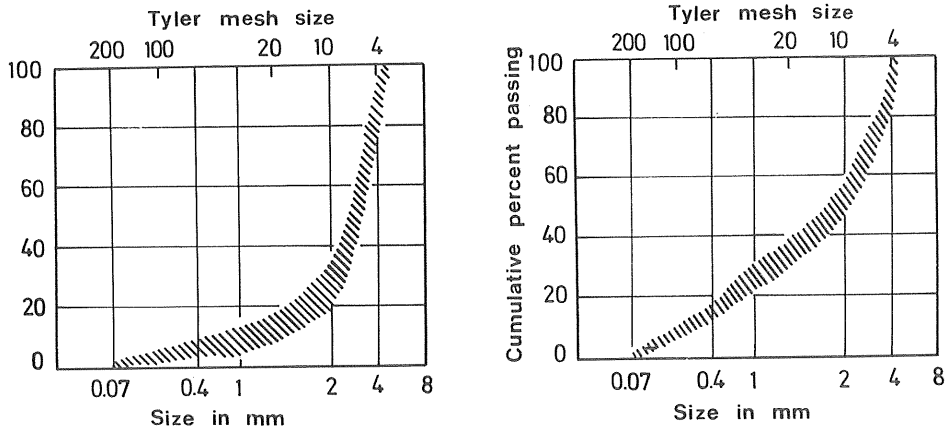

Fresh mineral - exposed
0 - 25 minutes in the loop

Circulated mineral - exposed
50 - 90 minutes in the loop

Fig. 7.5 *Average composition, particle size distribution, terminal settling velocity and attrition of the tested crushed granite.*

Coarse iron ore

(LKAB-mine in Kiruna)

Iron (magnetite)	50%
Sulphur	1%
Silica	11%
Apatite etc.	38%
Density	4150 kg/m^3

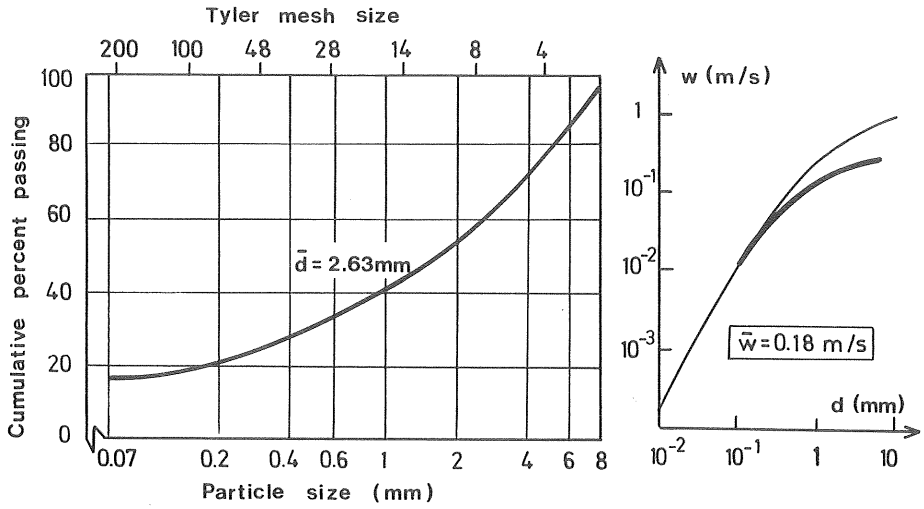

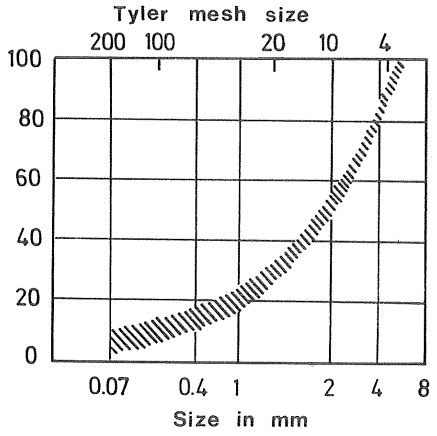

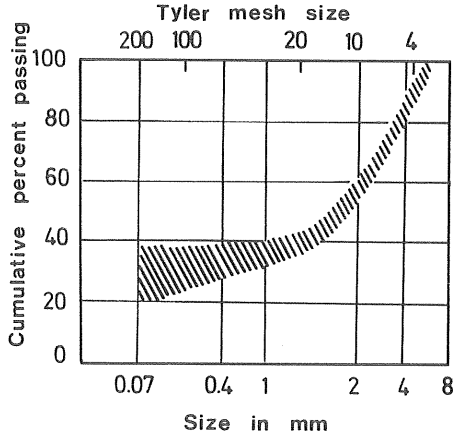

Fresh ore - exposed
0 - 1 hour in the loop

Circulated ore - exposed
4 - 25 hours in the loop

Fig. 7.6 *Average composition, particle size distribution, terminal settling velocity and attrition of the tested coarse iron ore.*

represented by the mean of each standard sieve size. For comparison, the standard C_D - Re_w relationship for spheres is represented in the form of graphs given by Weber (1973) in Figs. (7.1 - 7.6).

The relative tendency of the solids to degrade during circulation in the test loop was negligible, and was within experimental error for the primary ground iron ore and the lead ore, Figs. (7.1 and 7.2). For the perlite, the complex ore, and the granite mineral circulated up to 90 minutes, there was a trend of particle size reduction, Figs. (7.3), (7.4) and (7.5). Only with the coarse iron ore exposed up to 25 h in the test loop, a significant change in the particle size distribution occurred, Fig. (7.6).

Measured energy losses

The experimentally determined gradient, i_{Irr}, obtained from Eq. (7.2) was converted to the form of a Darcy-Weissbach friction factor. Thus, the friction factor, f, was determined with, i_{Irr}, expressed in metres of mixture per metre of pipe, i_{Irr}/s. With measured values of i_{Irr}, s, U, and D = 0.094 m inserted in Darcy-Weissbach equation, it follows that:

$$f = \frac{\left[i_{Irr}/s\right] 2g\, D}{U^2} \qquad (7.3)$$

Thus, all irreversibilities schematically expressed in Eq. (3.34 a) by:

$$i_{Irr} = (E - C)(s_s - 1) + \begin{bmatrix}\text{pipe wall}\\ \text{friction}\end{bmatrix}$$

are here expressed in the form of a Darcy-Weissbach friction factor. Based on the previous discussion in section 3.6, it was decided to define the corresponding Reynolds number using the density of the mixture but the viscosity of the water, i.e. Eq. (2.23),

$$Re' = \frac{UD\rho}{\mu_o} = s\,Re_o$$

The variables, i_{Tot}, and, s, in Eq. (7.2) were experimentally determined with a maximum error of 2% and 1%, respectively. However, the experimental error of the evaluated f values in Eq. (7.3) will be

considerable, because $i_{Irr} \rightarrow 0$ when $U \rightarrow 0$, based on fluid-like behaviour similar to the clear water f_o - Re_o relationship. Examination of the experimentally determined f-Re´ values demonstrated the large experimental scatter. Values corresponding to "fresh" and "circulated" conditions (see page 111) were uniformly distributed and no conclusions as to tendencies could be drawn, except for the coarse iron ore. With coarse iron ore exposed more than 4h, Fig. (7.6), there was a tendency towards a lower friction factor. This will be shown later.

For each mineral commodity tested, a graph of f versus Re´ was compared to the clear water curve, Figs. (7.7 to 7.13). The clear water relationship is expressed by the f_o - Re_o parameters. The concentrations in percent are shown for some points on the graphs. The lowest velocities in Figs. (7.7) to (7.13) indicate the locus below which certain operation risks occurred in the test loop. These velocities represent conditions where steady-state conditions could not be maintained, which at once led to accumulation of solids and plugging of the pump.

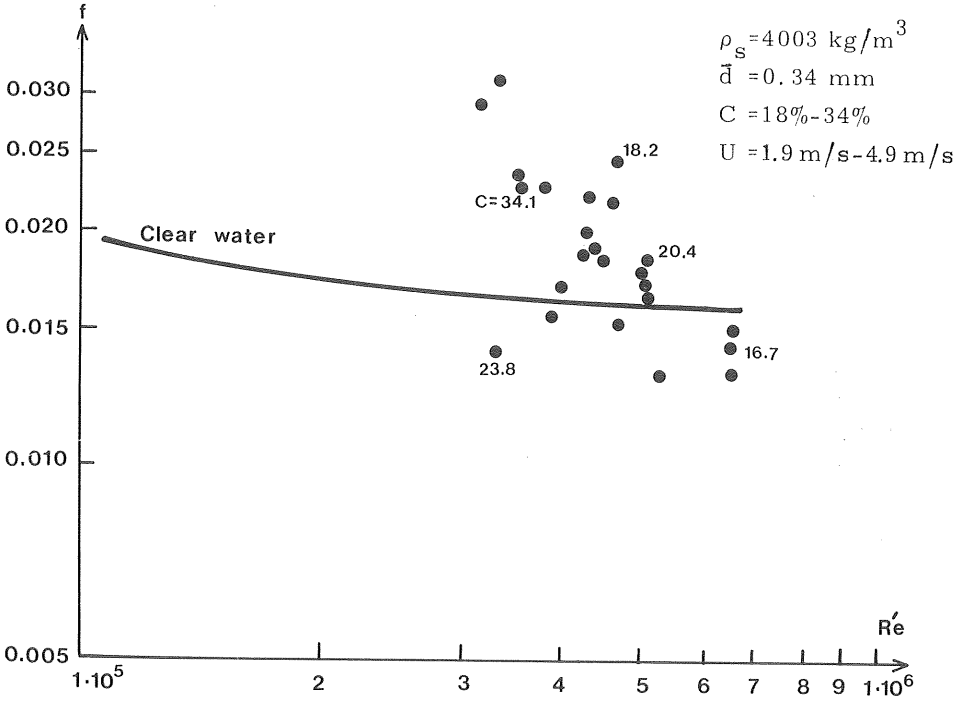

Fig. 7.7 *Mixture friction factor (f) versus Reynolds number (Re´) for the primary ground iron ore in water. D=0.094 m and water temperature T = 13°-17° C.*

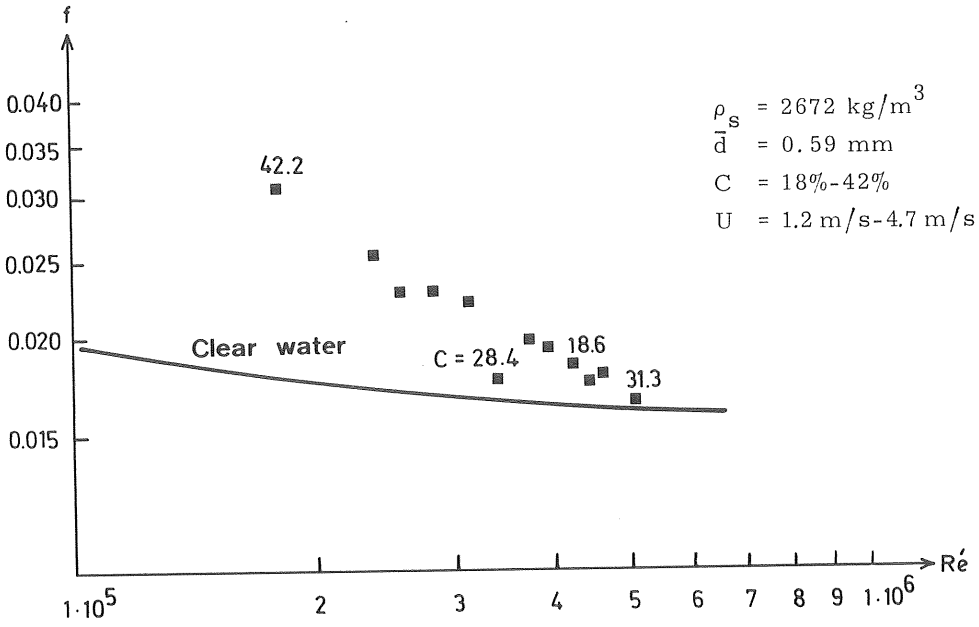

Fig. 7.8 *Mixture friction factor (f) versus Reynolds number (Re') for the lead ore in water. D = 0.094 m and T = 13°-17° C.*

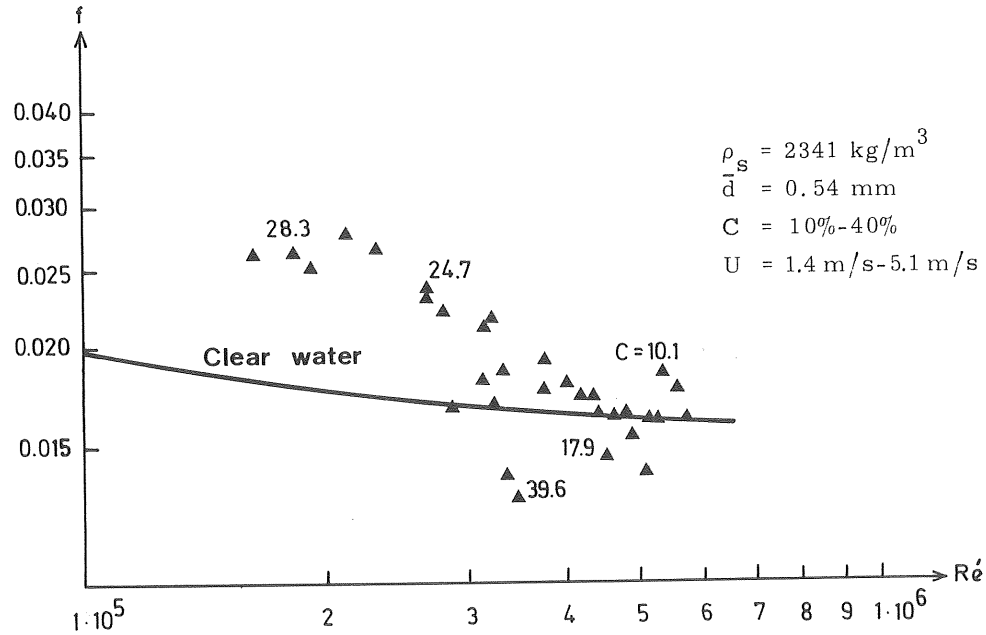

Fig. 7.9 *Mixture friction factor (f) versus Reynolds number (Re') for the perlite mineral in water. D = 0.094 m and T = 13°-17° C.*

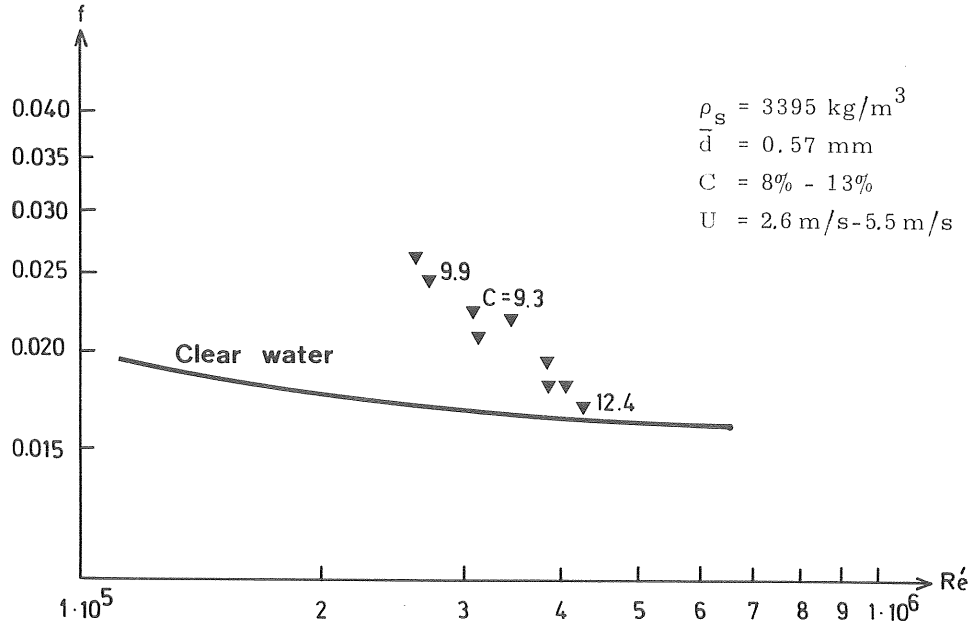

Fig. 7.10 *Mixture friction factor (f) versus Reynolds number (Re') for the complex ore in water. D = 0.094 m and T = 13°-17° C.*

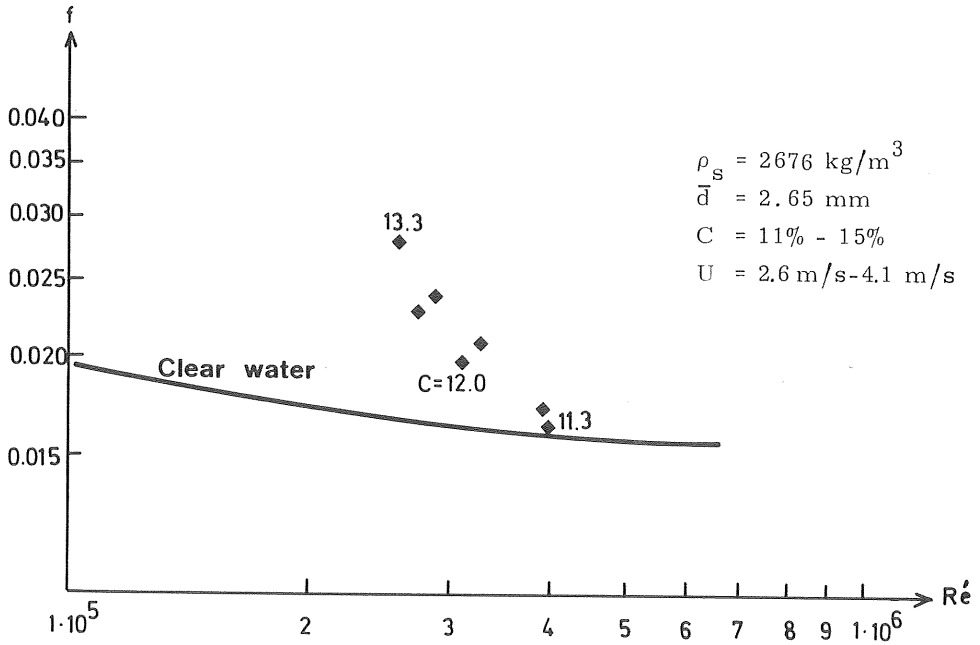

Fig. 7.11 *Mixture friction factor (f) versus Reynolds number (Re') for the crushed granite in water. D = 0.094 m and T = 13°-17° C.*

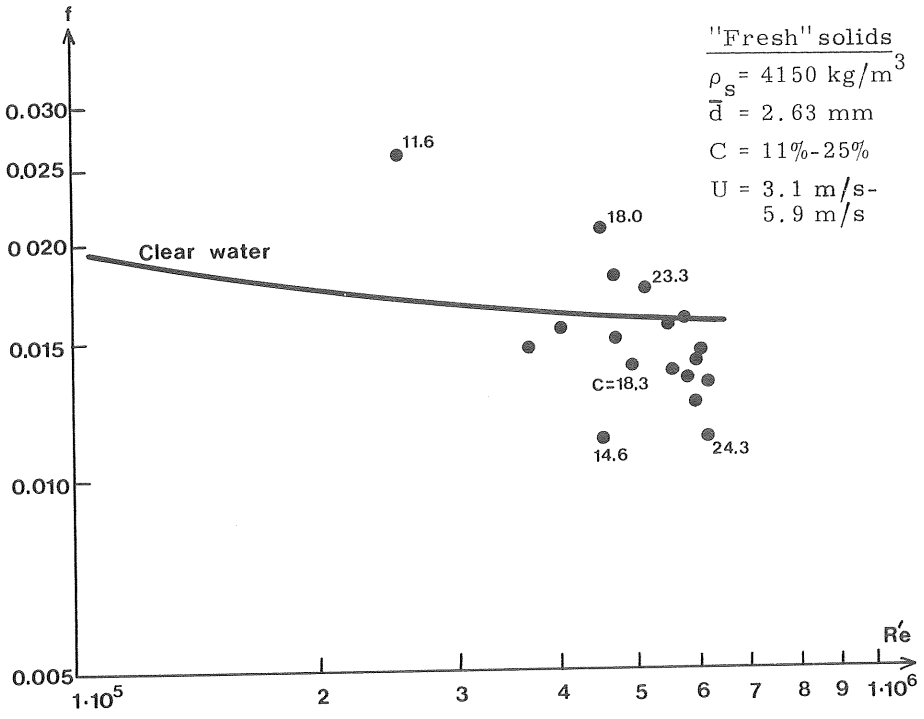

Fig. 7.12 *Mixture friction factor (f) versus Reynolds number (Re') for "fresh" coarse iron ore in water. D = 0.094 m and T = 13°-17° C.*

The f-Re' graphs in Figs. (7.7 - 7.12) show that there was a tendency for f to diverge at lower Re', corresponding to a lower operational velocity. The divergence reflects increasing irreversible energy because of slip or possible turbulent/laminar transitional (non-Newtonian) behaviour, the latter in connection with highly concentrated slurries composed of fine-grained solids.

The general tendency of the graphical representations in Figs. (7.7 - - 7.12), indicates that the energy loss of the industrial slurries investigated here will generally be greater than the energy loss of a similar flow of a Newtonian fluid which has the viscosity of water and the density of the slurry. However, there is a slight tendency of lower values of f for the coarse iron ore shown in Fig. (7.12).

The experimentally obtained friction factors for the coarse iron ore which had been circulated up to 25h in the test loop, Fig. (7.13), were mostly lower than those shown for the other mixtures in Figs. (7.7 -

- 7.12). The clear water friction factor - Reynolds number relationship for a smooth pipe has been drawn for comparison in Fig. (7.13).

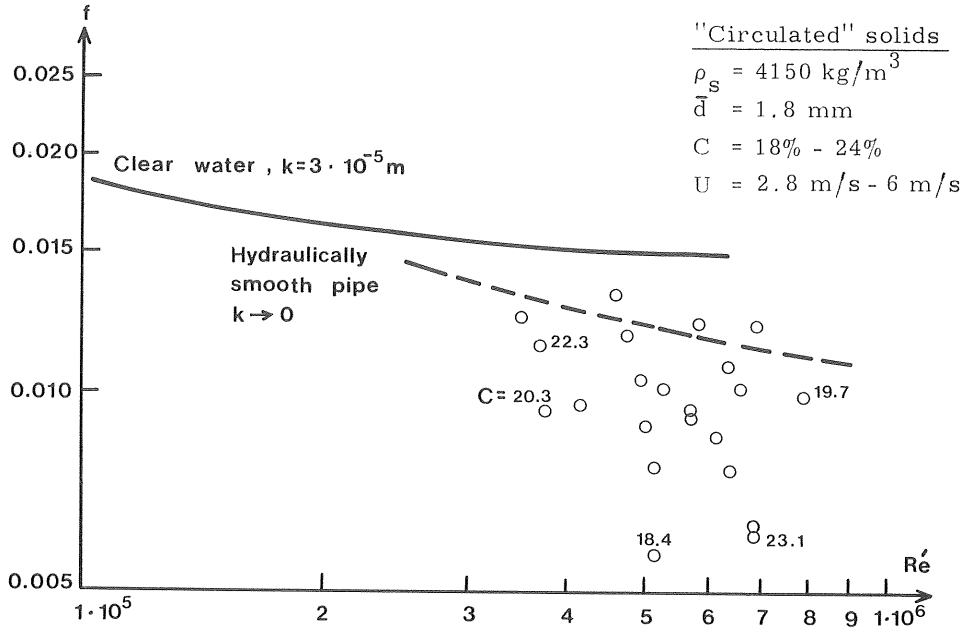

Fig. 7.13 *Mixture friction factor (f) versus Reynolds number (Re') for "circulated" coarse iron ore in water. D = 0.094 m and T = 17°-23° C. The dashed line is the clear water relationship for a smooth pipe.*

7.2 Laboratory-loop test

Mineral properties etc.

The properties of the solids were determined in a similar way as for the minerals used in the pilot-loop study. The density, particle size distribution, and the weighted terminal settling velocity of the pumped solids are shown in Fig. (7.14). The terminal settling velocity was related directly to the C_D - w relationship of spheres for particles of less size than 0.074 mm.

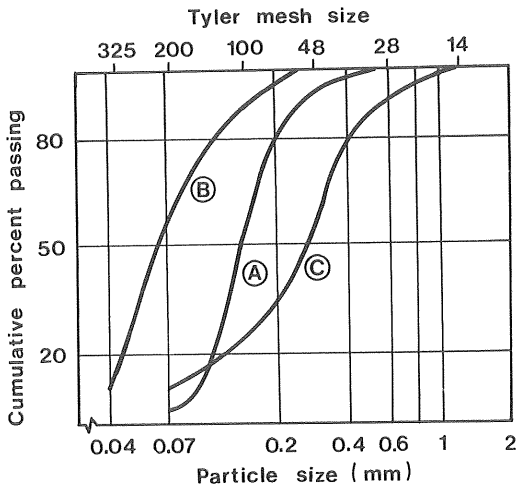

Legend	Ⓐ	Ⓑ	Ⓒ
	Beach sand (Deposit in Baskarp)	Iron ore concentrate (LKAB-mine in Malmberget)	Primary ground iron ore
$\bar{d}$ (mm)	0.20	0.08	0.34
ρ_s (kg/m^3)	2672	4947	4350
$\bar{w}$ (m/s)	0.022	0.007	0.067

Fig. 7.14 *Particle size distribution, terminal settling velocity, and density of the solids tested in the horizontal test loop.*

The physical composition of the iron ores was similar to that shown in Fig. (7.1), except the content of magnetite was higher.

Energy losses - operational conditions

In accordance with the earlier discussions on representation of measured irreversible energy, all experimental data was related to the Darcy-Weissbach friction factor and a representative Reynolds number. The friction factor was determined from the ordinary relationship in the form of Eq. (7.3) with $i_{Irr}/s = i_H/s$, i.e.

$$f = \frac{\left[i_H/s\right] 2gD}{U^2}$$

where D = 0.027 m and s and U are the measured density ratio and velocity, respectively. The gradient, i_H, is the measured energy loss in the horizontal test section, Eq. (6.19),

$$i_H = 0.991\ h_t$$

where h_t is the manometer reading in metres. The friction factor was determined with a maximum error of less than 10%.

The content of fine particles of size less than about 0.1 mm was considerably higher for the iron ore concentrate than for any other mineral tested, Fig. (7.14). However, the particle size spectrum was too large for rheological measurements in conventional viscosimeters available. It was found that a relatively stable (non settling) mixture could be obtained, if particles of size less than 0.04 mm were removed from a sample. The volumetric portion of particles of size less than 0.04 mm in a slurry of iron ore concentrate will be less than 5% if the total solid content is 30% by volume. It is generally recognized that such mixtures are essentially Newtonian in behaviour up to a concentration of about 10% to 15%. Besides, most reported measured values of the viscosity for concentrations up to about 10% are close to Eq. (2.4):

$$\mu/\mu_o = 1 + 2.5\,C + 10.05\,C^2 \ldots\ldots$$

The linear Newtonian relationship between shear stress-velocity gradient was recognized and Eq. (2.4) was approximately confirmed by some limited measurements with a Brookfield viscosimeter for an iron ore concentrate slurry of a concentration of less than 10%.

A representative viscosity of the slurry may be defined by Eq. (2.4), with C less than about 10%. The corresponding Reynolds number for the mixture is:

$$Re = \frac{UD\rho}{\mu}$$

However, taking μ_o instead of μ in this relationship, i.e. taking it as:

$$Re' = s\,Re_o$$

will have a nearly negligible influence on the friction factor, f.

Similar estimates, as shown previously in section 3.4, page 55, showed that the largest scatter of determining f based on Re´ instead of Re, with μ defined for the fine-particle content, was below 5%. Therefore, all experimentally determined values of f were related to Re´, as in the representation of the pilot-loop results.

The deposition velocity, U_D, was evaluated from direct observations of the flow through the transparent pipe section. The deposition velocity was defined as the velocity at which a stationary bed was first built-up by the stoppage of some of the larger solids, which formed a shallow and narrow band on the bottom of the pipe.

The evaluated values of f are graphically represented against Re´, and compared to the clear water curve for each mineral tested in Figs. (7.15)

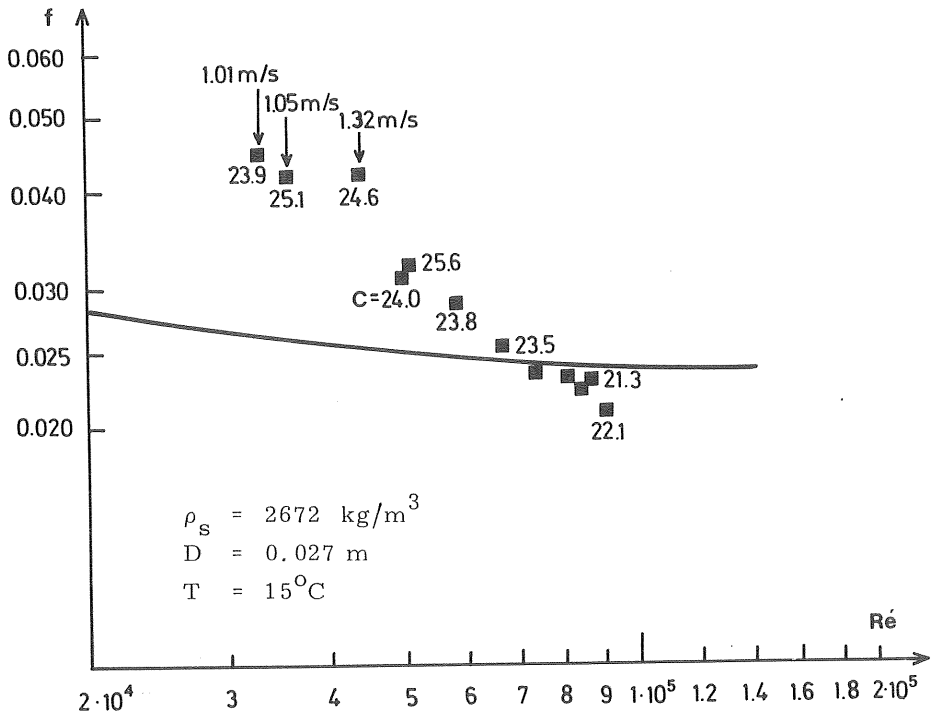

Fig. 7.15 *Mixture friction factor (f) versus Reynolds number (Re´) for the beach sand in water. The arrows show observed deposition velocities.*

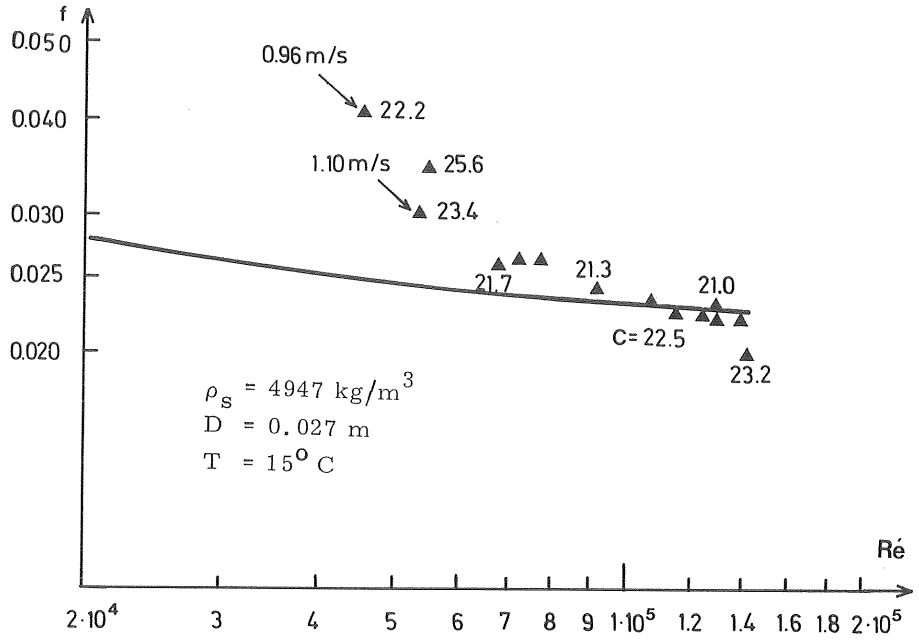

Fig. 7.16 *Mixture friction factor (f) versus Reynolds number (Re') for the iron ore concentrate in water. The arrows show observed deposition velocities.*

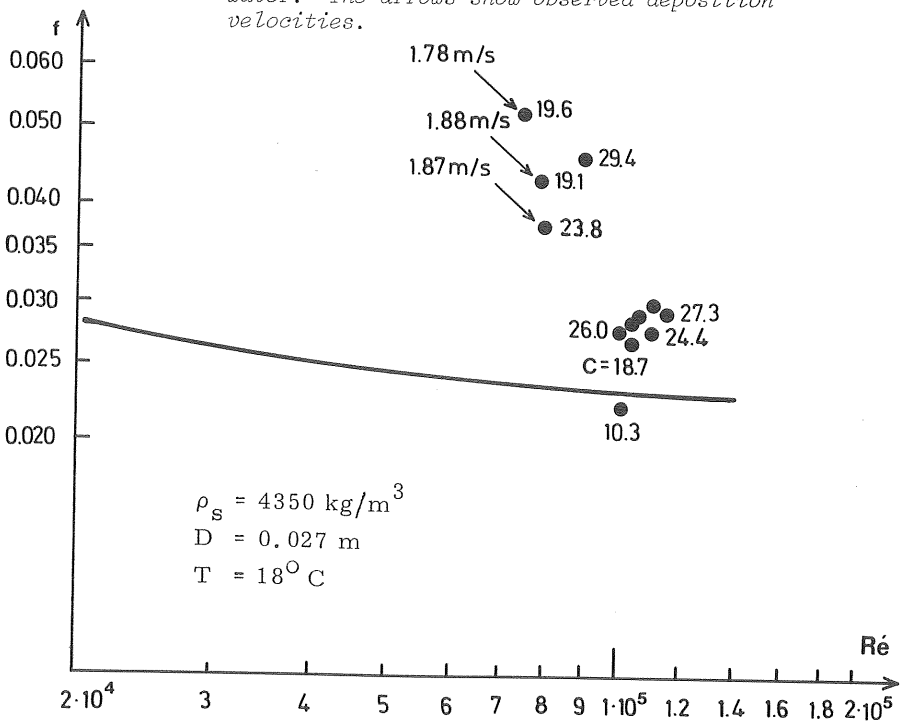

Fig. 7.17 *Mixture friction factor (f) versus Reynolds number (Re') for the primary ground iron ore in water. The arrows show observed deposition velocities.*

to (7.17). The observed deposition velocities are shown by arrows in Figs. (7.15) to (7.17). Individual concentrations are shown for some points in the graphs. The primary ground iron ore could not be transported at higher velocities than about 3 m/s because of limited available power in the test loop.

The operational conditions for the slurries tested have been compared in Table (7.1) to some of the criteria defining flow regimes and deposition velocities, given earlier by Eqs. (4.1), and (4.3).

Table 7.1 Application of some empirical criteria defining flow regimes and deposition velocities to the tested minerals in the horizontal test loop. The criteria, in the form of the velocities U_{Mb}, U_{Het}, and U_{Ph} were defined in section 4.1, page 67.

Velocities defining flow regimes and deposition	Beach sand	Iron ore concentrate	Primary ground iron ore
$U_{Mb} = 17\ \bar{w}$	0.37	0.12	1.14
$U_{Ph} = (1800\ g\bar{w}D)^{1/3}$ (Eq. 4.1 with the weighted terminal settling velocity, $\bar{w}$)	2.19	1.49	3.17
$U_D = F_L (2gD(s_s - 1))^{1/2}$ (Eq. 4.3 with F_L obtained from Fig. 4.1)	0.9	1.1	1.7

Comparison of the f-Re′ relationships determined by experiments in Figs. (7.15 - 7.17) and the calculated values in Table (7.1) indicate that the flow of the sand and the iron ore concentrate slurries can be considered to be mainly in pseudohomogeneous suspension. Furthermore, the primary ground iron ore slurry exhibit a heterogeneous flow pattern.

7.3 Pump performance test

The slurry density, flow rate, and the solid concentration were ob-

tained from Eqs. (6.1), (6.2), and (6.5), respectively, as shown previously in section 7.1. The head developed by the pump, H, in metres of slurry, was evaluated by Eq. (6.11):

$$H = 0.50 + \frac{p_{out} - p_{in}}{\rho g} - 904\, Q^2$$

where

p_{out} = pressure reading at the discharge side of the pump

p_{in} = pressure reading at the suction side of the pump

ρ = mixture density

Q = flow rate

The efficiency of the pump, η, was obtained from Eq. (6.12)

$$\eta_{Total} = \eta \cdot \eta_{Transm} \cdot \eta_{Motor}$$

where

$$\eta_{Total} = \frac{P_{out}}{P_{in}} \quad \text{(Eq. 6.13)}$$

These variables were defined in section 6.3 page 114.

A typical set of results for the primary ground iron ore, the lead ore, the perlite, and the coarse iron ore are shown in Figs. (7.18 - - 7.21), for a constant pump rotary speed equal to 12.67 rps and at solid concentrations of about 20%.

It can be seen in Figs. (7.18-7.20) that the time of exposure in the loop has only a minor influence on the pump performance which in the following will be neglected. Only for the coarse iron ore, Fig. (7.21), which was exposed more than 4h (about 500 pump passages) a more distinguishable effect of circulation was observed. However, the effect was small and it was not interpreted quantitatively. In the following analysis, the experimental results on the coarse iron ore will be limited to ore that was exposed less than 4h.

The reduction in head and efficiency increases slightly for decreased flow rates, however, for the flow rates investigated here, the head and efficiency ratio can be considered to be nearly independent of flow rate.

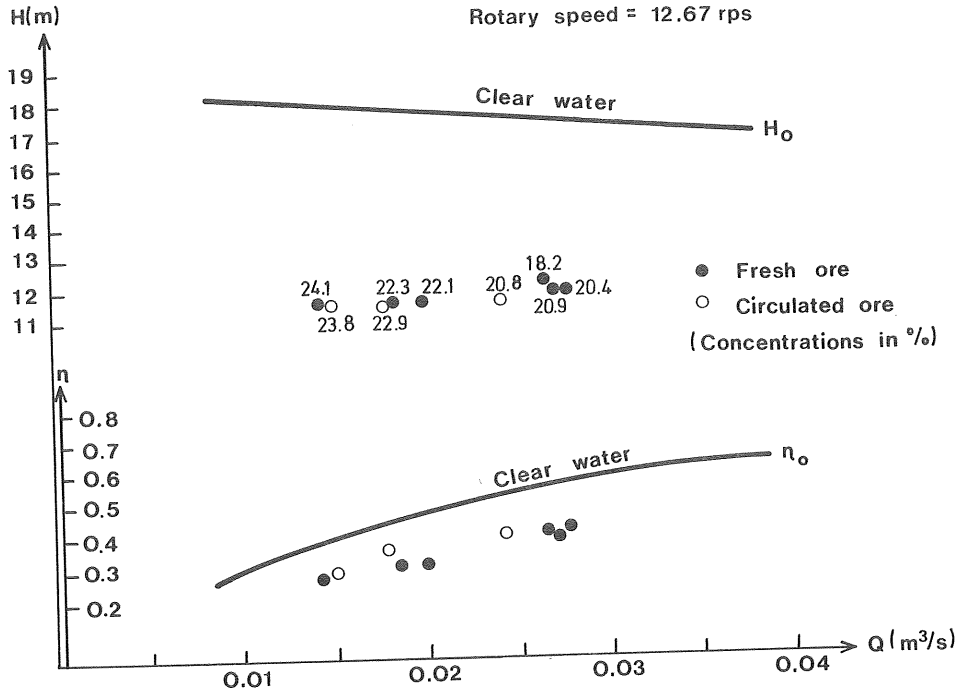

Fig. 7.18 *Depression of head and efficiency for the primary ground iron ore.*

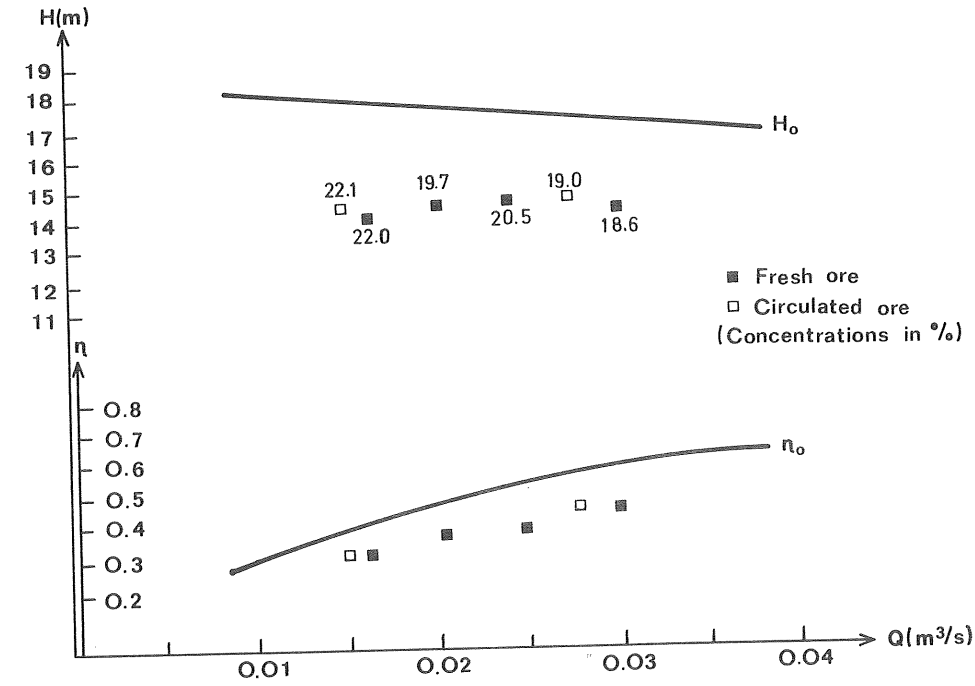

Fig. 7.19 *Depression of head and efficiency for the lead ore.*

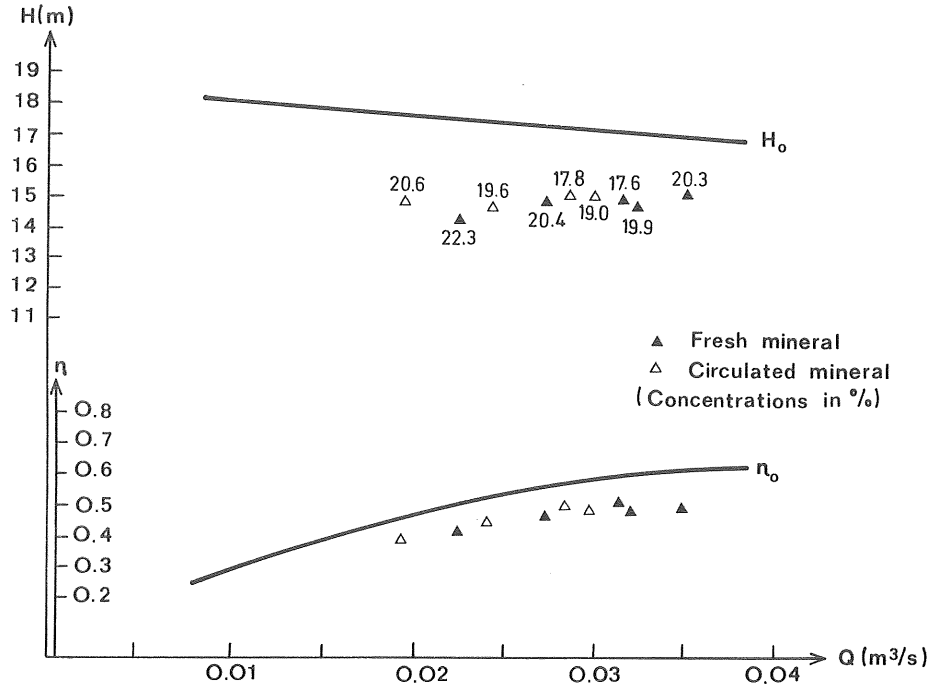

Fig. 7.20 Depression of head and efficiency for the perlite mineral.

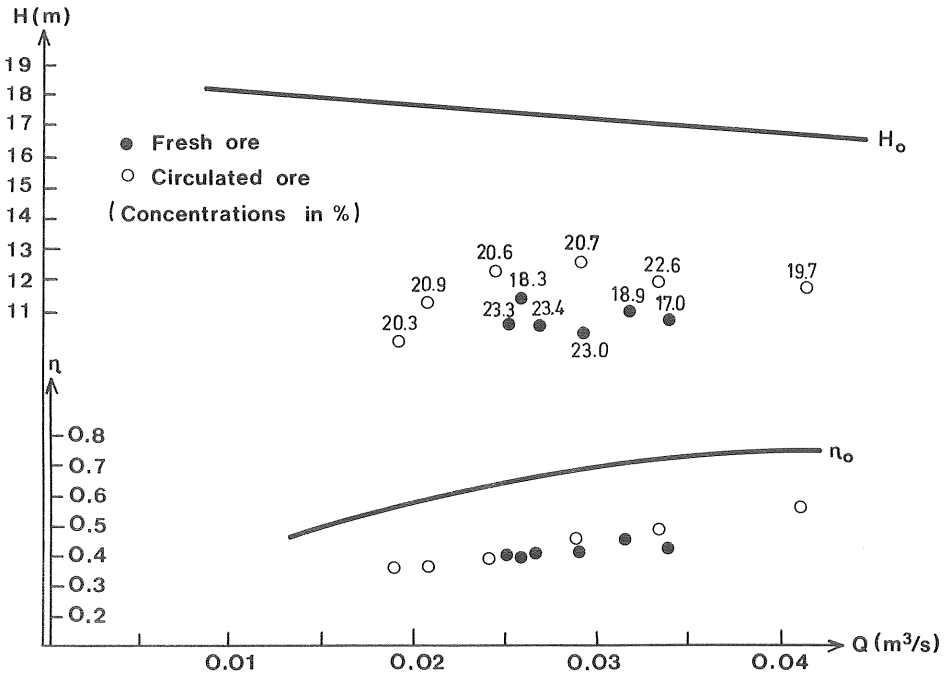

Fig. 7.21 Depression of head and efficiency for the coarse iron ore.

The experimental results with the higher pump rotary speed, 19 rps, showed a similar behaviour as was illustrated in Figs. (7.18 - 7.21) for solid concentrations of about 20%. The statement that the depression in efficiency is equal to the head depression,

$$P = s\,P_o \qquad \text{(Eq. 5.5)}$$

$$s = \rho/\rho_o = \text{mixture density ratio}$$

$$H/H_o = \eta/\eta_o \qquad \text{(Eq. 5.6)}$$

was largely confirmed by the experimental data shown in Figs. (7.18 - 7.21) and similar results were also found for the higher pump speed. The reduction in efficiency was slightly higher than the reduction in head for the coarse iron ore, Fig. (7.21). The experimental data shown in Figs. (7.18 - 7.21) and similar findings with a pump speed of 19 rps, were related to Eq. (5.14) and compared to Fig. (5.4) in Fig. (7.22). Eq. (5.14) reads:

$$H/H_o = \eta/\eta_o = 1 - K\,\frac{C}{0.20}$$

where K is a reduction factor.

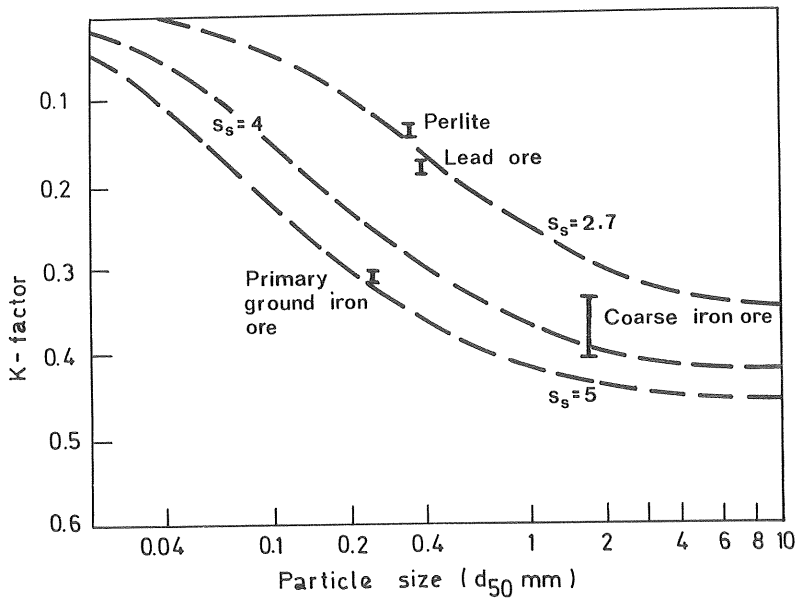

Fig. 7.22 *Comparison of measured reduction in head and efficiency of the primary ground iron ore, lead ore, perlite mineral, and coarse iron ore to the reduction curves in Fig.(5.4). Solid concentrations in the range of 20% and pump speeds of 12.67 rps and 19 rps.*

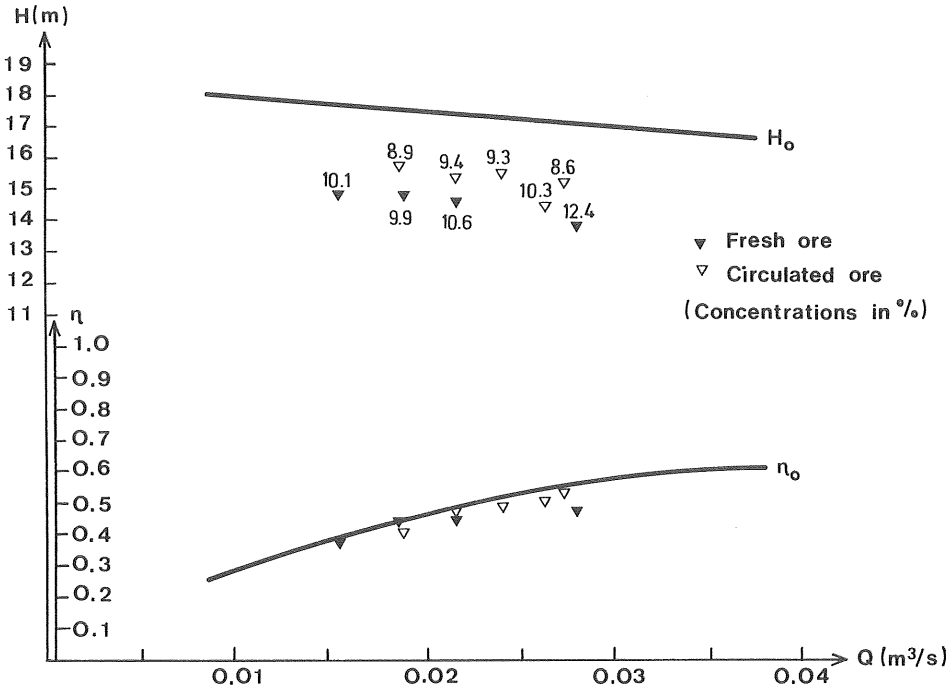

Fig. 7.23 Depression in head and efficiency for the complex ore.

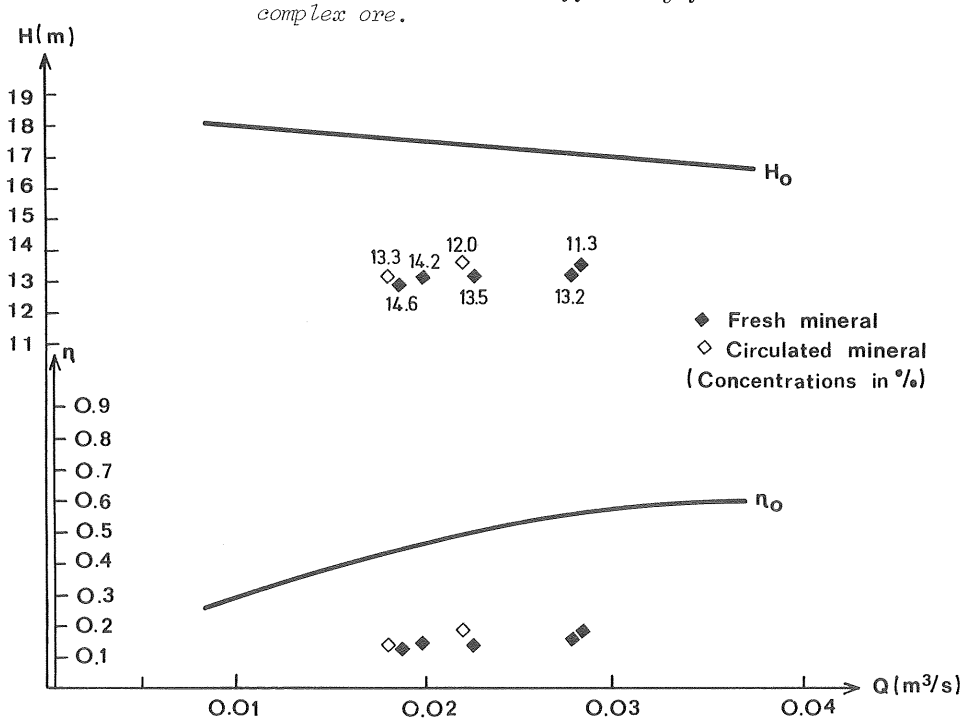

Fig. 7.24 Depression in head and efficiency for the crushed granite.

The experimental findings presented so far agree for the most part with the general trends discussed earlier and illustrated in Fig. (7.22). These general trends were, however, not in accordance with the experimental results of the complex ore and the crushed ore as can be seen in Figs. (7.23) and (7.24), respectively.

From the graphs in Fig. (7.24) it can be seen that the clear water efficiency was reduced by about 70% for the angular crushed granite. On the other hand, the drop in efficiency was only a few percent below the clear water efficiency for the complex ore, Fig. (7.23). The graphical representations in Figs. (7.23) and (7.24) indicate that Eqs. (5.5) and (5.6) do not hold uniquely for these solids. It can be seen from Fig. (7.23) that:

$$\eta/\eta_o > H/H_o$$

for a given concentration of complex ore. The corresponding power requirement is less than that given by Eq. (5.5), i.e.

$$P < s P_o$$

Furthermore, for the crushed granite in Fig. (7.24), it can be seen that:

$$\eta/\eta_o < H/H_o \tag{7.4}$$

which corresponds to:

$$P > s P_o \tag{7.5}$$

Similar results as is shown in Fig. (7.23) were obtained with the higher pump speed = 19 rps. No experimental data was available for the high pump speed with the crushed granite, because of power limitations in the experimental facility. The results shown in Fig. (7.23) and (7.24) demonstrate the complex influence on the pump performance of the physical and the chemical properties of the solid component.

The results presented so far have not included concentrations of over about 20%. For higher concentrations, it was observed that the solid concentration has a predominant influence on the pump performance.

Therefore, the dependence of the solid concentration on the relative reduction in head and efficiency was evaluated in detail.

The observed values of the efficiency ratio, η/η_o, can in some cases be correlated to Eq. (5.8),

$$\eta/\eta_o = \frac{1 - C}{s}$$

With

$$C_w = \frac{C\, s_s}{s}$$

and

$$s = 1 + C(s_s - 1)$$

in Eq. (5.8), then it follows that:

$$\eta/\eta_o = 1 - C_w \qquad (7.6)$$

The reduction in head and efficiency, dimensionlessly expressed by H/H_o and η/η_o were separately represented as functions of C_w and the two pump speeds for each mineral investigated. These relationships are graphically represented in Figs. (7.25 - 7.30) for concentrations by volume, C, from about 20% to about 40%, which correspond to concentrations by weight, C_w, in the range of 45 to 65%. For comparison, Eq. (7.6) has been plotted in Figs. (7.25 - 7.30).

It can be seen from Figs. (7.25 - 7.28) that the reduction in efficiency diverges from the drop in head for higher concentrations. The drop in efficiency is greater than the reduction in head:

$$\eta/\eta_o < H/H_o \qquad \text{(Eq. 7.4)}$$

which corresponds to a power requirement, P, of:

$$P > s\,P_o \qquad \text{(Eq. 7.5)}$$

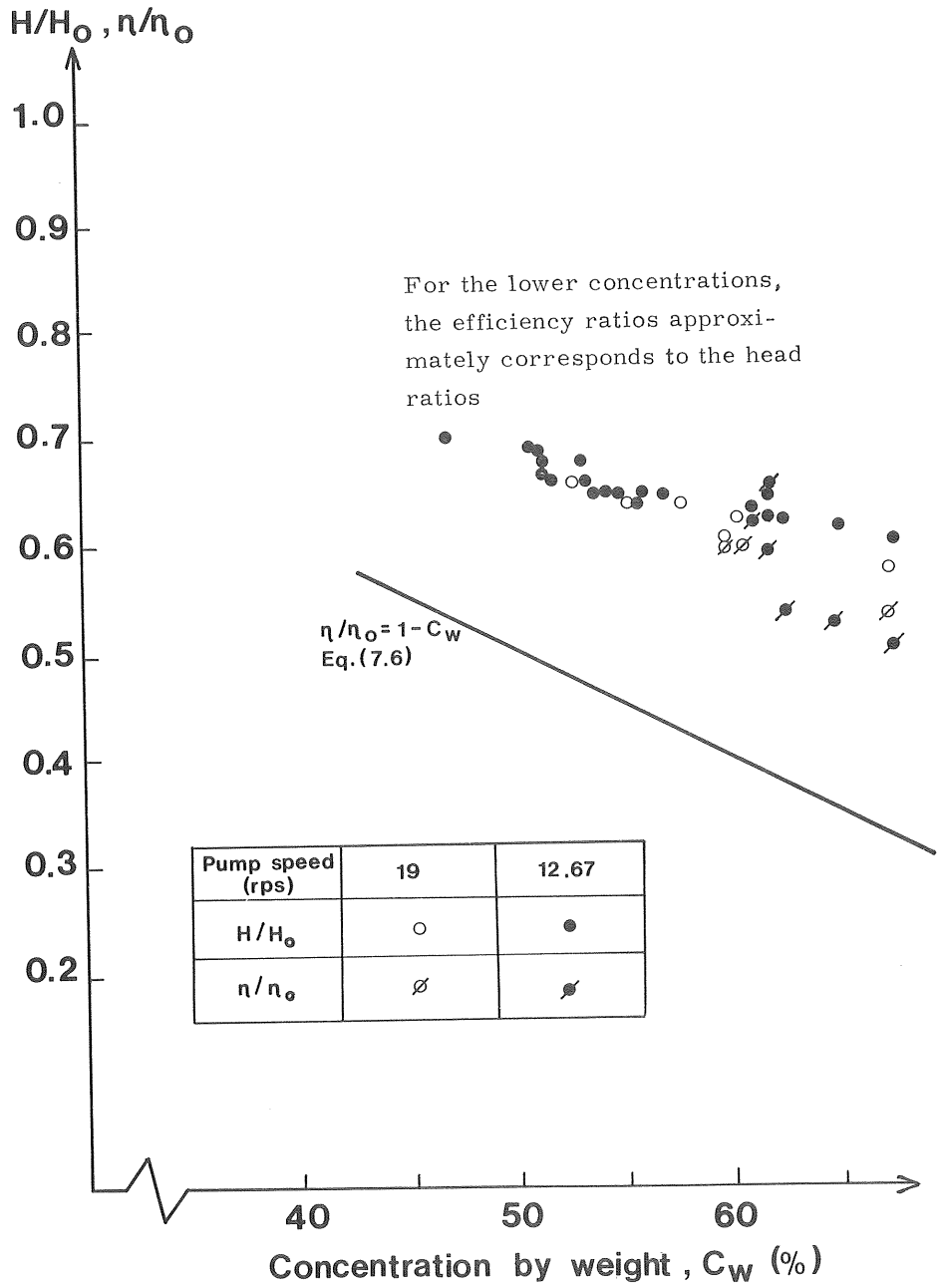

Fig. 7.25 *Relative reduction in head and efficiency versus concentration by weight for the primary ground iron ore.*

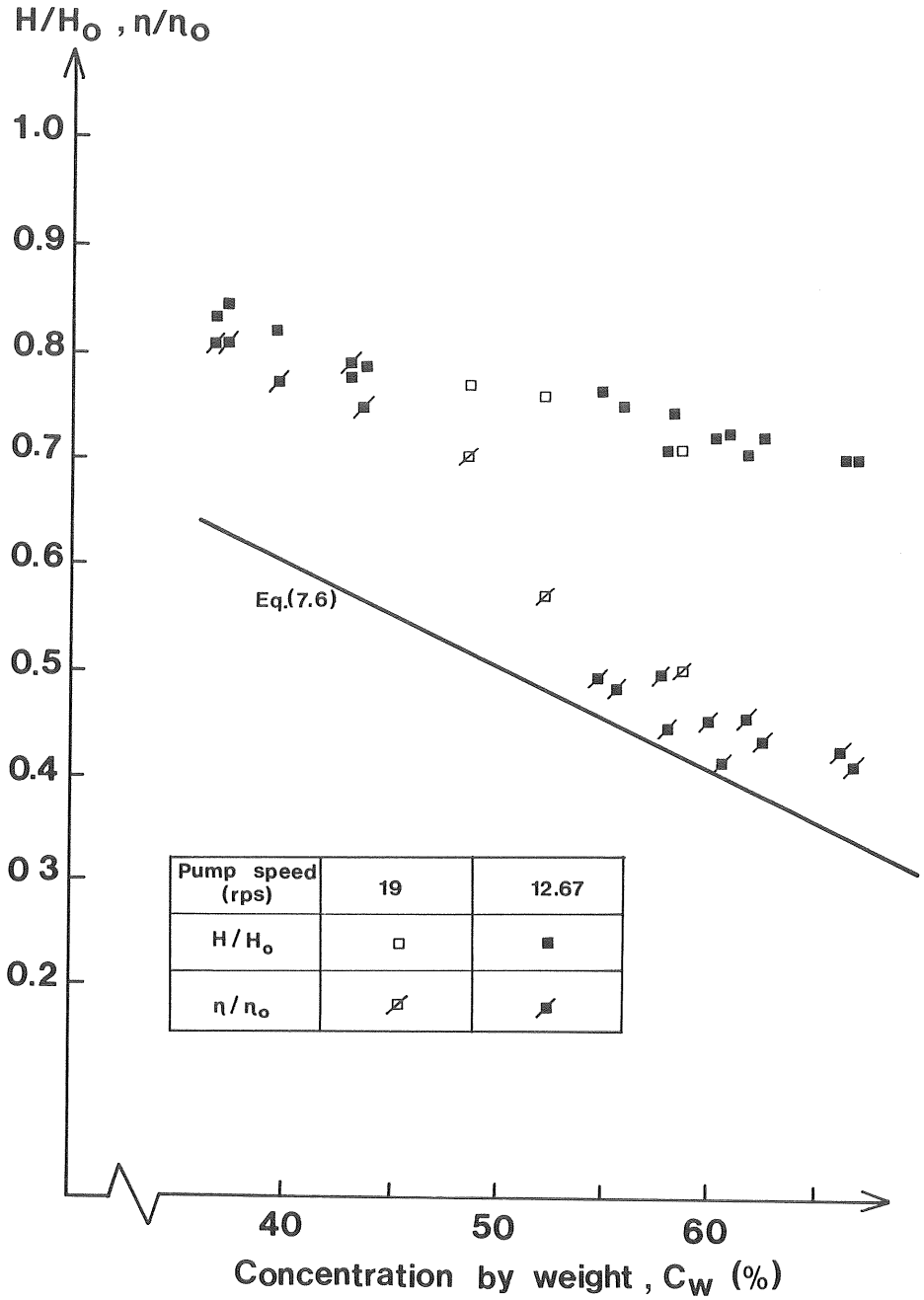

Fig. 7.26 *Relative reduction in head and efficiency versus concentration by weight for the lead ore.*

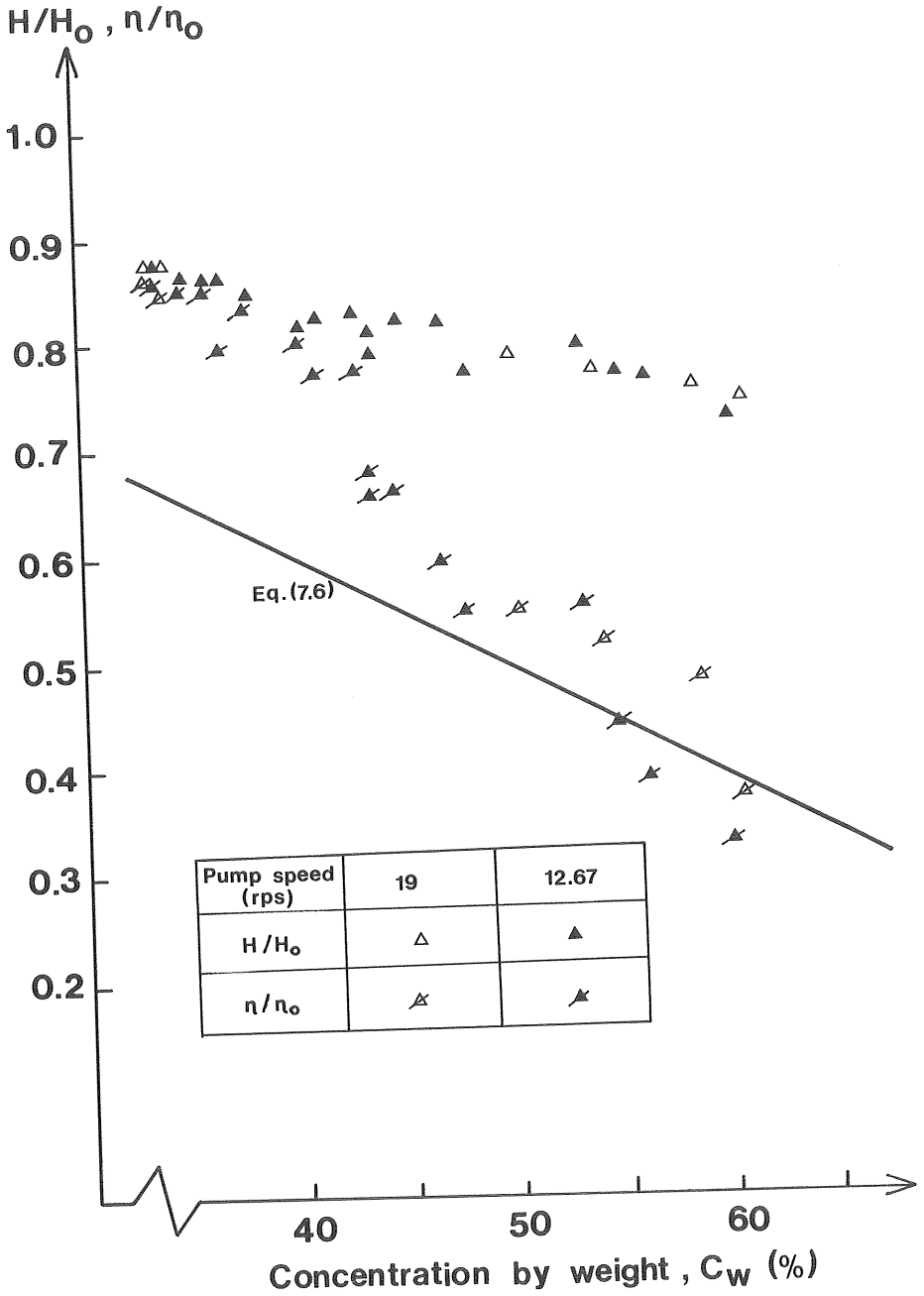

Fig. 7.27 *Relative reduction in head and efficiency versus concentration by weight for the perlite mineral.*

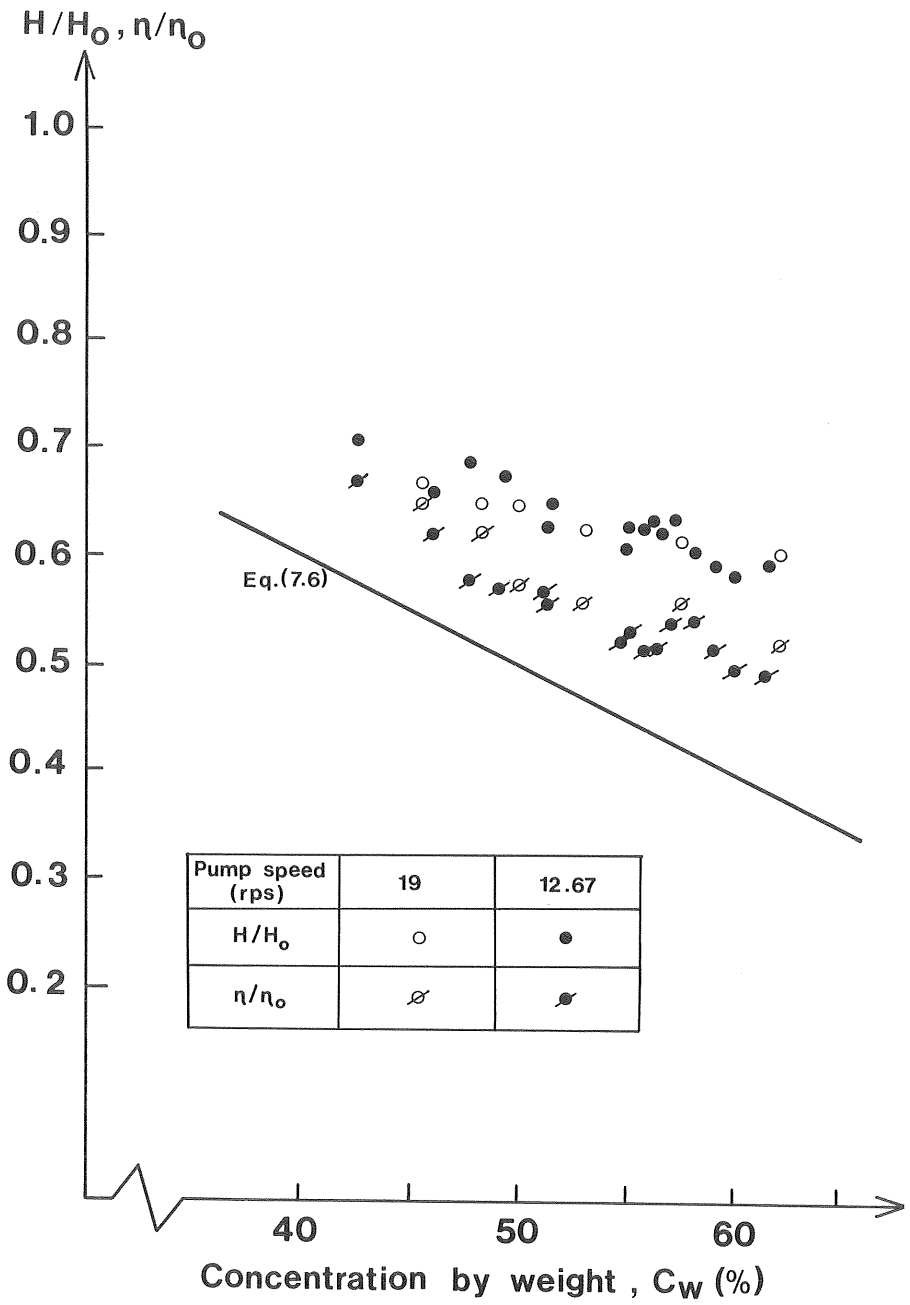

Fig. 7.28 *Relative reduction in head and efficiency versus concentration by weight for the coarse iron ore.*

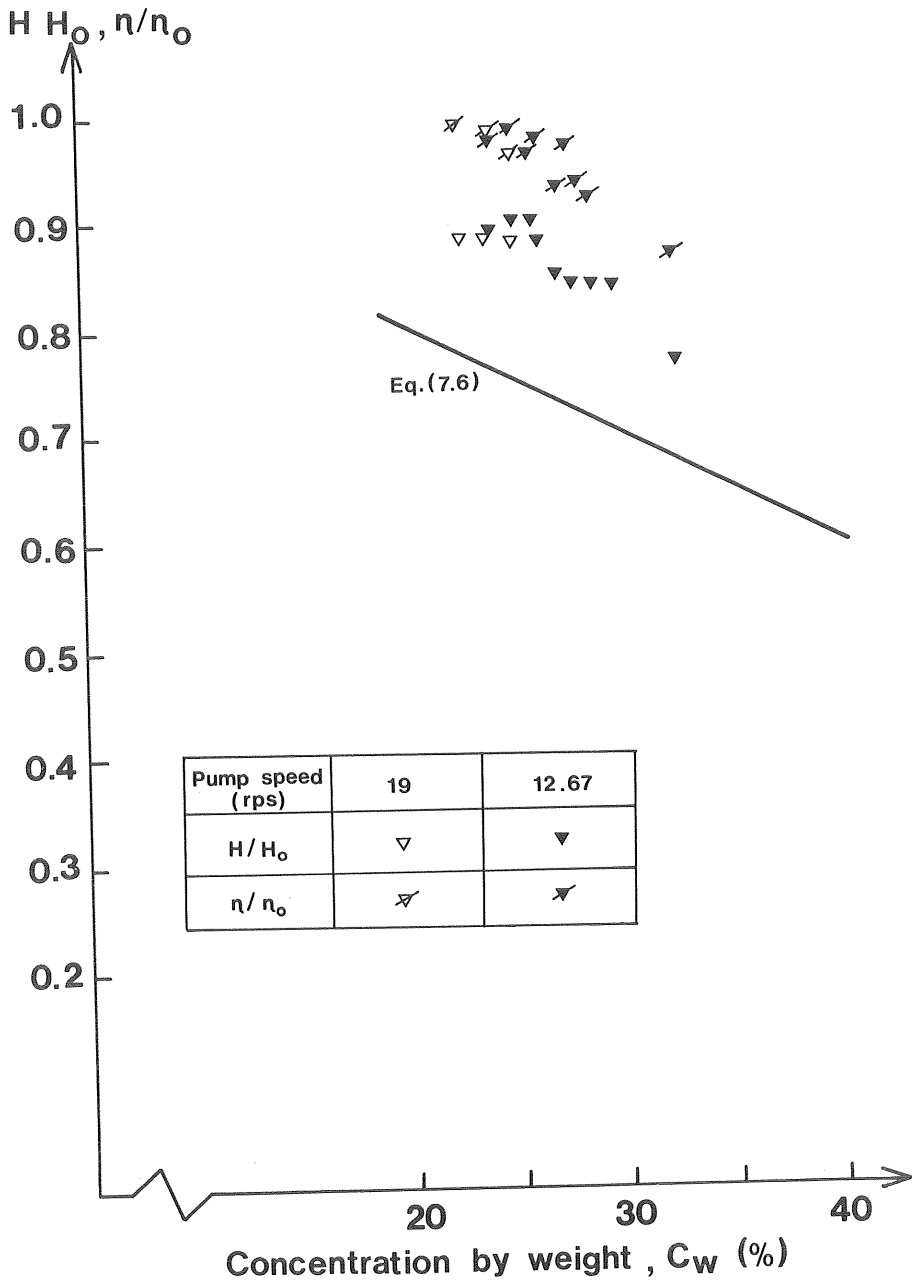

Fig. 7.29 *Relative reduction in head and efficiency versus concentration by weight for the complex ore.*

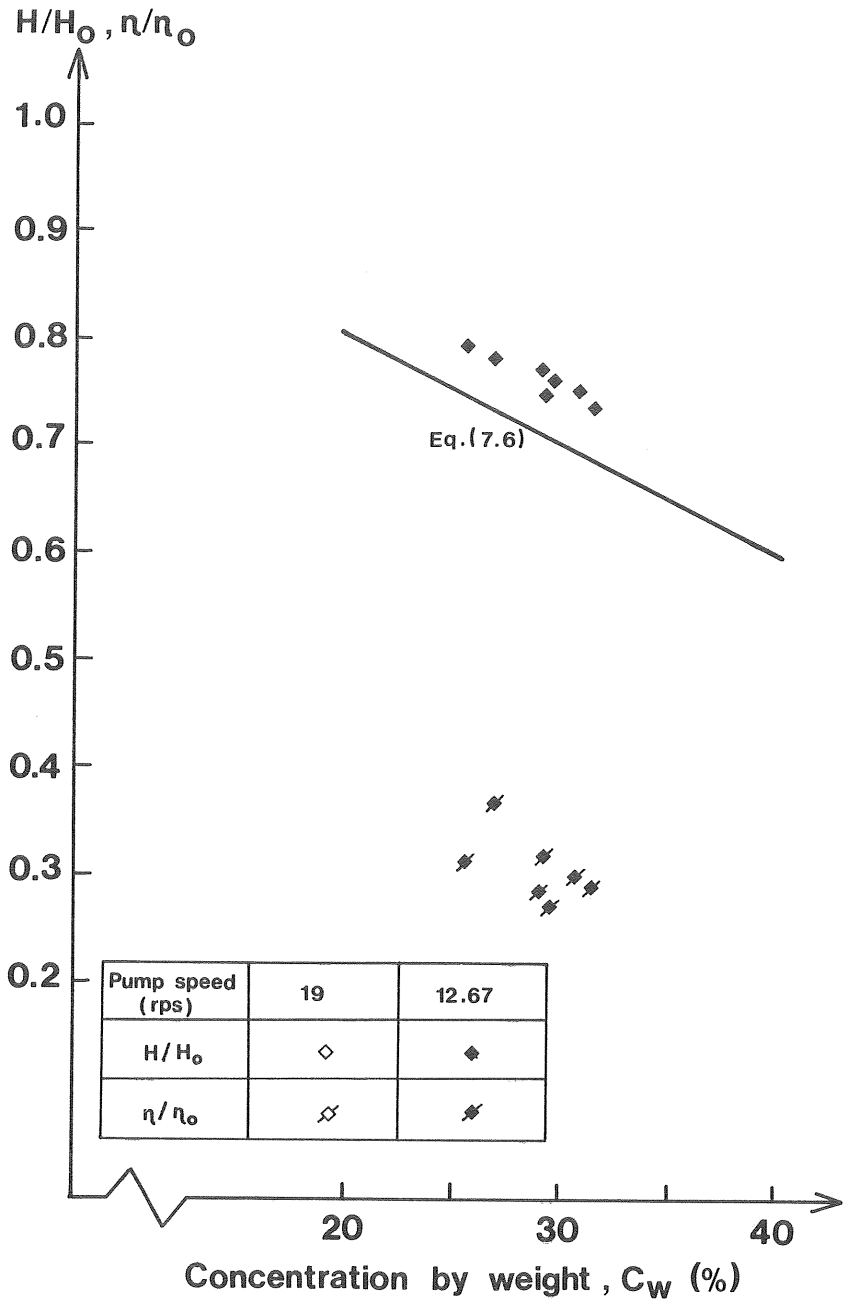

Fig. 7.30 *Relative reduction in head and efficiency versus concentration by weight for the crushed granite.*

Thus, the investigational data in Figs. (7.25 - 28) comprising high concentrations is not in agreement with Eqs. (5.5) or (5.6):

$$H/H_o = \eta/\eta_o \qquad \text{(Eq. 5.5)}$$

$$P = sP_o \qquad \text{(Eq. 5.6)}$$

The drops in head and efficiency were almost equal for concentrations close to 20%, as shown in Figs. (7.19 - 7.22). Figs. (7.25 - 7.27) show that a significant reduction in efficiency occurred at concentrations by weight of approximately 60%, 40%-45% and 45%-50% for the primary ground iron ore, perlite, and lead ore, respectively. These concentrations by weight of the three solids of different densities correspond to concentrations by volume of 20%-25%. These concentrations represent threshold values over which the drop in efficiency considerably exceeds the drop in head. For the perlite and lead ore slurries, the reduction in efficiency approaches the values given by Eq. (7.6) for concentrations by weight larger than about 50%.

The reduction in efficiency was not so significant for the primary ground iron ore, Fig. (7.25), and the coarse iron ore, Fig. (7.28). The primary ground iron ore has the smallest weighted particle size, $\bar{d}$, of the minerals investigated, while the coarse iron ore has a comparatively large $\bar{d}$-value and a wide particle size distribution.

From Figs. (7.25 - 7.29) it can be seen that the drop in head is independent of the pump speed but the small number of data points shows a slightly smaller decrease in efficiency for the higher pump speed, 19 rps.

Finally, Figs. (7.29) and (7.30) again illustrate the influence on the performance of the complex ore and the crushed granite, respectively. For the complex ore in Fig. (7.29):

$$\eta/\eta_o > H/H_o$$

and for the crushed ore in Fig. (7.30):

$$\eta/\eta_o < H/H_o$$

8. RESULTS OF EXPERIMENTS - DISCUSSION

8.1 Effects of particle attrition

In this study the characteristic dimension of the solid particles was related to the weighted value, $\bar{d}$, which gives a greater weight to the largest particles than the median value d_{50}. Most solids used have particle sizes which correspond to the transition region defined by the C_D-Re_w relationship, shown in Fig. (3.4). In this region the influence of particle shape becomes significant, as shown in the w-d graphs in Figs. (7.1 - 7.6). This was accounted for to some extent by representing the settling conditions by the weighted settling velocity, $\bar{w}$, which gives the greatest weight to the largest particles.

It was found that the circulation in the loop and the frequent passages through the pump caused change in the particle size distribution for the coarse iron ore which was exposed up to about 25h. The attrition process produced a large amount of fine particles and the intermediate size fraction almost disappeared, Fig. (7.6). This is a typical effect of pumping friable materials or of frequent passages in centrifugal pumps.

For the coarse iron ore which had been exposed up to 25h in the vertical loop, the experimentally determined f-Re´relationship, Fig. (7.13), differs from the general tendency shown in Figs. (7.7-7.12). The values of the friction factors in Fig. (7.13) are usually lower than obtained for the ore which had been exposed less than 1h, Fig. (7.12). This difference may be related to effects caused by attrition of solid particles during the long-term exposure in the loop.

The attrition of the coarse iron ore produced a large amount of particles of size less than 0.074 mm. The particle size distribution of the fine particles of sizes less than 0.074 mm was not investigated in this study. However, attrition tests with limestone slurries in centrifugal pumps have shown a shifting towards very fine particles of sizes less than 0.005 mm, Haas et al. (1973 c). The presence of such fine particles affects the rheological properties of the slurry and may introduce the turbulent dampening effects, discussed earlier in sections 2.4 and 3.6. This behaviour may be the cause of the comparatively low friction factors obtained here for the coarse iron ore slurry which was exposed up to 25h.

The rheological behaviour of a mixture of the fine particle part (particle size less than 0.074 mm) was investigated for concentrations less than 10%, which correspond to the fine particle part in a "circulated" coarse iron ore slurry with a total solid content of 30% by volume. However, limited measurements with a Brookfield viscosimeter indicated no changes of the Newtonian behaviour.

In the 25h test it was also observed that the pH-value was lowered from about 8.2 to about 6. A similar lowering of pH was not observed for the iron ore slurry exposed only up to 1 h. The pH-value of the "fresh" slurry was very close to the value for fresh water, pH = 8.2.

It is possible that the low losses of the "circulated" iron ore can be partly explained by the conditions in the loop due to the lowering in pH. The long-term test with the coarse iron ore was the first test after the initial stage of the experimental programme. After this test, no change in the friction loss of the flow of water in the vertical pipe was observed. However, this does not necessarily mean that changes did not take place during the long-term test. For this particular test, it seems reasonable to believe that the erosive action of the solids would first have produced a more polished pipe wall, which then was roughened due to corrosion. Corrosion may be magnified considerably in comparison with a neutral surrounding. Thus, some measured values may have been obtained with a smoother pipe wall surface. The rest of the test programme was carried out for solids for which the pH-value was never less than that of fresh water. No measurable influence of a change in the pipe wall roughness was observed during the entire experimental programme.

It was only for the coarse iron ore, which had been exposed for up to about 25h, that a more distinguishable effect of attrition on the pump performance was observed, Fig. (7.6). Therefore, the analysis of experimental data on the coarse iron ore, was limited to ore that was exposed less than 4h. The effect of different times of exposure on the rest of the experimental data of the pump performance was negligible, in comparison with other variables.

In summary, the effect of attrition of most solids used in this study was nearly negligible, because the solid particles were relatively

inert and because the time of exposure in the loop was not too long. However, the effect of attrition can be servere, with more friable minerals such as coal and limestone. This has to be considered in industrial applications working at optimal conditions which may be very sensitive to small changes in the particle size distribution.

In this study, the contradicting results obtained for the energy loss of the fresh coarse iron ore slurry and the ore exposed for a long time demonstrate the importance of controlling the effect of attrition and other time-dependent variables in a recirculating test-system.

8.2 Pilot-plant study of vertical transportation

Minimum operational velocity

The minimum operational velocity was related to conditions where steady state delivery of solids could not be maintained at the discharge end in the vertical test loop. The lowest observed velocities correspond to 1.3 m/s - 1.9 m/s, for concentrations in the range of 25% - 40%, for the more fine-grained mixtures of primary ground iron ore, lead ore, and perlite. The lowest possible flow for stable, steady state operation with the more coarse-grained mixtures should exceed a velocity of about 5-8 times the terminal settling velocity of the largest particles. This is roughly in agreement with in-plant experience, discussed earlier in section 3.4. However, observations of unstable flow conditions in a relatively short test loop system cannot always be transformed to a full-scale application, because of the effect of recirculation.

Estimation of the effect of slip

The representation of experimental data in the form of the f-Re' parameters in section 7.2 shows that there was a tendency towards an increasing friction factor, f, over and above f_o for decreasing values of Re'. The increasing value of f is an expression of additional irreversible energy. However, it is not possible to distinguish the different influence of pipe wall friction of water and solids, slip, and particle-particle interaction, because the behaviour of the flow inside the pipe is not known.

With highly concentrated fine-grained slurries, the increased friction factor for lower velocities may be attributed to transitional non-Newtonian behaviour. However, the influence of such phenomena can be neglected for the experimental results for the crushed granite shown in Fig. (7.11) page 136.

The crushed granite was the coarsest solid investigated, with $\bar{d}$ = = 2.63 mm, $\bar{w}$ = 0.20 m/s, and with a uniform particle size distribution without fine particles. Furthermore, the investigated concentrations were lower than 15%. The observed tendency of divergence from the Darcy-Weissbach relationship in Fig. (7.11) indicates that irreversibilities are generated by other factors than pipe wall friction due to a fluid-like behaviour.

The irreversible energy gradient, in a two-component system, i_{Irr}, can be schematically represented by Eq. (3.43):

$$i_{Irr} = (E - C)\,\phi_1 + \frac{f_o\,U^2}{2g\,D}$$

where

$$\phi_1 = (s_s - 1) + \frac{f_o\,U^2(E-C)}{2gD(1-E)^2} + \frac{f_o\,U^2}{gD(1-E)}$$

In section 3.4 it was found that:

$$1 - C/E \leqslant w/U \quad \text{(Eq. 3.38)}$$

which was based on the assumption of slip, S, to be approximately equal to a characteristic terminal settling velocity, w. Eq. (3.38) can be rewritten as:

$$E - C \leqslant \frac{w}{U}\left(1 - \frac{w}{U}\right)^{-1} C$$

Thus, in Eq. (3.43) it follows that:

$$i_{Irr}/s \leqslant \frac{w}{U}\left(1 - \frac{w}{U}\right)^{-1} C\,\phi_1 s^{-1} + \left[\begin{matrix}\text{pipe wall}\\ \text{friction}\end{matrix}\right] \qquad (8.1)$$

In order to evaluate the difference between experimentally determined f-values and the clear water relationship, the pipe wall friction term in Eq. (8.1) is related to the pseudohomogeneous f-Re´

parameters. Based on this assumption in Eq. (8.1), a maximum irreversible energy gradient, i_{Irr}^{max}, is defined by:

$$i_{Irr}^{max}/s = \frac{w}{U}\left(1 - \frac{w}{U}\right)^{-1} C\,\phi_1 s^{-1} + \\ + \frac{f\,U^2}{2g\,D}\left[\frac{\text{metres of mixture}}{\text{metre of pipe}}\right] \qquad (8.2)$$

With this expression identified to the Darcy-Weissbach equation in the form:

$$i_{Irr}^{max}/s = \frac{f^{max}\,U^2}{2\,g\,D}\left[\frac{\text{metres of mixture}}{\text{metre of pipe}}\right]$$

it then follows that the maximum friction factor is determined by:

$$f^{max} = 2g\,D\,U^{-2}\,\frac{w}{U}\left(1 - \frac{w}{U}\right)^{-1} C\,\phi_1 s^{-1} + f \qquad (8.3)$$

The friction factor, f^{max}, in Eq. (8.3) is estimated from experimentally determined values of U, s, f, and $\bar{w}$ for C = 13.2%, which is the average concentration of all measured values for the crushed granite in Fig. (7.11). The theoretically estimated f^{max} in Eq. (8.3) is graphically compared with the experimentally determined f-values in Fig. (8.1).

It can be seen in Fig. (8.1) that most experimentally determined friction factors is larger than the maximum values estimated in Eq. (8.3). If the observed extra irreversibilities are attributed to the slip-term,

$$\frac{w}{U}\left(1 - \frac{w}{U}\right)^{-1} C\,\phi_1 s^{-1}$$

in Eq. (8.2), then the estimation given earlier in Eq. (3.38):

$$1 - C/E \leqslant w/U$$

is not valid here. In fact, the comparison with the experimental results of the crushed granite indicates that:

$$1 - C/E \geqslant w/U$$

An explanation of this result may be related to the basic assumption

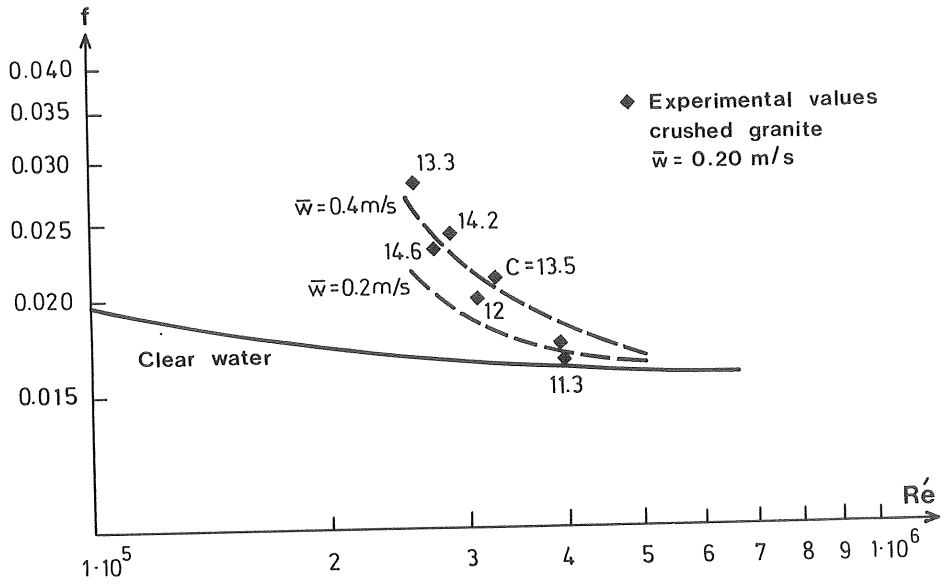

Fig. 8.1 *Theoretically estimated maximum friction factors compared with experimentally determined values for the crushed granite in water. The two dashed lines show theoretically estimated values based on weighted terminal settling velocities of 0.2 m/s and 0.4 m/s, respectively.*

of slip, $S \approx w$, where w is the terminal settling velocity in a stagnant liquid and not in a pipe with turbulent flow.

The experimental result obtained here for the crushed granite thus indicates that the settling velocity in a turbulent flow is greater than the corresponding quiescent settling velocity, i.e. the drag coefficient is lower in a turbulent flow.

The effect of a larger weighted settling velocity than the measured value, $\bar{w} = 0.20$ m/s, is illustrated in Fig. (8.1). The configuration of the curves in Fig. (8.1) indicate that the influence of slip in this case can be related to the effect of a larger terminal settling velocity in a pipe with turbulent flow.

This effect was recently confirmed experimentally in a vertical solid-water flow with particles in the transitional region, Howard (1974). The terminal settling velocity was found to be 50% to 100% greater

in a turbulent flow than in a still liquid.

The experimentally obtained results for the more concentrated slurries of iron ores, lead ore, and perlite were analysed in a similar way to the crushed granite. It was found that the estimated influence of slip on the irreversible energy was comparatively small, Fig. (8.2).

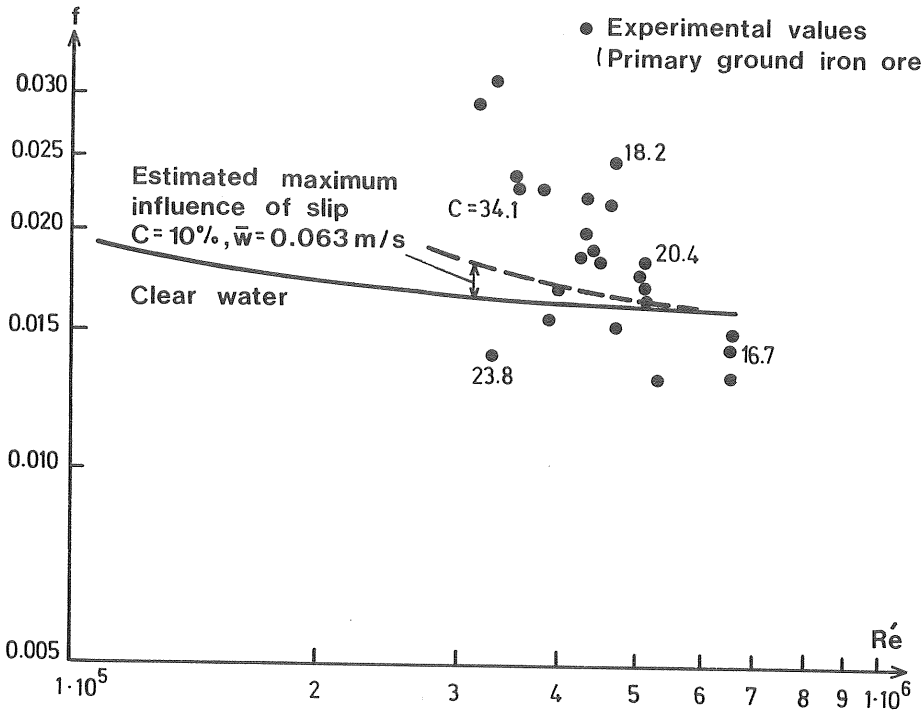

Fig. 8.2 *Theoretically estimated maximum effect of slip on the friction factor (dashed line). Comparison with experimentally determined values for the primary ground iron ore.*

The estimated maximum influence of slip for these solids can partly be related to the lower terminal settling velocities in comparison to the crushed granite. However, the greatest influence may be related to the effect of hindered settling, which is developed in highly concentrated mixtures. In a stagnant liquid the hindered settling velocity is decreased exponentially with concentration, the exponential value is larger than 2. The effect of hindered settling was omitted in the estimation of slip in Fig. (8.2). However, if this effect is included then the estimated maximum influence of slip holds for higher concentrations also.

The results obtained in this study for concentrations of industrial interest ($C > 20\%$) and experience by others indicate that $E \approx C$, provided w/U is less than about 0.1.

The effect of hindered settling illustrates the importance of having effective control of input quantities of water and solids in a vertical slurry transportation system. High concentrations dampen the growth rate of slip-induced instabilities, which for coarse particle slurries show up as a rapidly growing friction factor.

A correlation of energy losses for the iron ores, lead ore and perlite

The factors affecting the tendency towards an increased friction factor for decreasing values of Re' cannot be identified separately for the slurries of the iron ores, lead ore and the perlite. However, in order to obtain a correlation for all experiments with these solids, all data for concentrations of up to 35% was transformed, according to the homogeneous flow pattern discussed earlier in section 3.5. Thus, the experimentally determined friction factors from Eq. (7.3):

$$f = \frac{[i_{Irr}/s]\, 2g\, D}{U^2}$$

are related to the relative roughness, k/D, and the following Reynolds number:

$$Re = \frac{U D \rho}{\mu}$$

where the viscosity, μ, is obtained from Eq. (2.4):

$$\mu/\mu_o = 1 + 2.5C + 10.05\,C^2 + 0.0027 \exp(16.6\,C)$$

The experimental data for the iron ores, lead ore and perlite, thus transformed, are graphically represented in Fig. (8.3).

In spite of the large scatter encountered, the experimental results shown in Fig. (8.3) approximately confirm the homogeneous approach given in section 3.5 by Eq. (3.48):

$$i/s = \frac{f U^2}{2 g D} \quad \left[\frac{\text{metres of mixture}}{\text{metre of pipe}}\right]$$

where

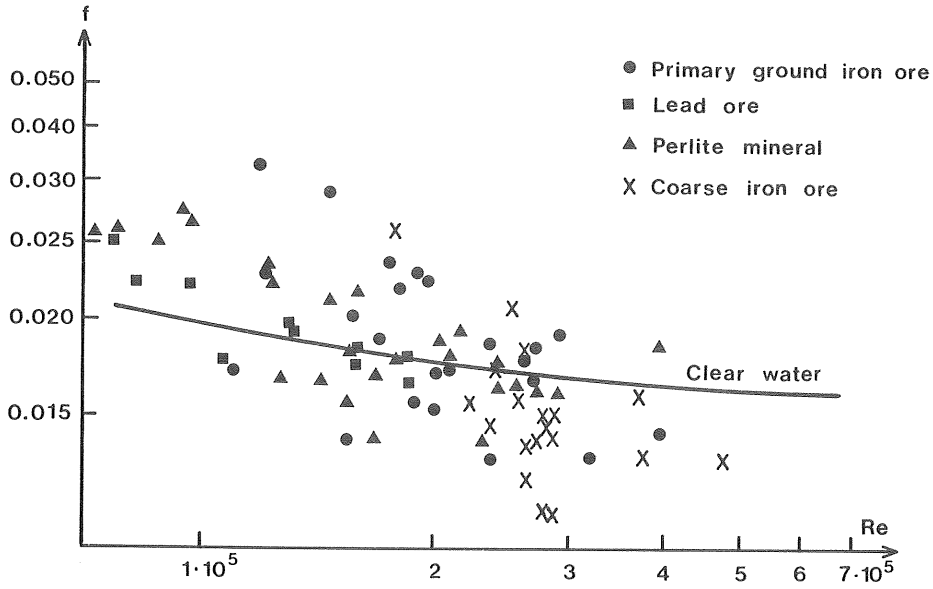

Fig. 8.3 *Representation of all experimental data in the f-Re parameters, for the iron ores, lead ore and perlite.*

i = energy loss gradient expressed in metres of water per metre of pipe

s = mixture density ratio = ρ/ρ_o

Based on the approximations discussed in section 3.5, page 56, the total pressure gradient required in most practical applications can be related to:

$$i_{Tot} = s(1+i_o) \left[\frac{\text{metres of water}}{\text{metre of pipe}}\right] \text{(Eq. 3.56)}$$

$$i_{Tot}/s = 1 + i_o \left[\frac{\text{metres of slurry}}{\text{metre of pipe}}\right] \text{(Eq. 3.57)}$$

8.3 Laboratory-scale study of horizontal transportation

Experimental results from small pipe systems cannot generally be used for designing large-sized pipe systems. However, some

experimental results obtained in this study were compared to Durand's equation and to pilot-plant data published by others. A comparison has also been made to the computational model developed by Wasp et al. (1963).

Primary ground iron ore

The experimentally derived deposition velocity for the primary ground iron ore was found to be about 1.85 m/s, Fig. (7.17). With a velocity of 2.4 m/s and C = 20.4%, the successive estimates given earlier in Table (7.1), indicate that the flow can be considered to be in heterogeneous suspension. Therefore, the experimental result with U = 2.4 m/s and C = 20.4% will be compared to Durand's equation, which reads:

$$i = i_o(1 + c_5\, C(Fr^{-2}(s_s - 1)\, C_D^{-1/2})^{3/2}) \qquad \text{(Eq. 4.4)}$$

where

c_5 = constant equal to 81

$Fr = \dfrac{U}{(g\,D)^{1/2}}$ (Froude number)

$s_s = \rho_s/\rho_o$

C_D = drag coefficient

Compared experimental or calculated data will be related to the energy loss gradient expressed in metres of slurry per metre of pipe, i/s, and to the clear water gradient, i_o, by the energy loss gradient ratio, i/si_o.

Durand's equation only applies to uniformly sized particles and doubt arises as to how the drag coefficient, C_D, should be defined in Durand's equation because C_D is a function of d and w:

$$C_D = \frac{4\,g}{3}\,\frac{d(s_s - 1)}{w^2} \qquad \text{(Eq. 3.22)}$$

The experimentally determined energy loss gradient ratio, $i/s\,i_o$, was compared to Durand's equation for the following two approaches of the C_D-coefficient:

d_{50} and the corresponding terminal settling velocity for spheres, w_o.

$$C_D = \frac{4}{3} \frac{g}{w_o^2} \frac{d_{50} (s_s - 1)}{} \qquad (8.4)$$

and

$\bar{d}$ and the measured $\bar{w}$

$$\bar{C}_D = \frac{4}{3} \frac{g}{\bar{w}^2} \frac{\bar{d}(s_s - 1)}{} \qquad (8.5)$$

The experimental result was also compared to the modified approach based on Durand's equation given by Eq. (4.5), in which the energy losses produced by each size fraction was first calculated and then added. The individual properties for each sieve size fraction, d_j, were here related to the corresponding w_{o_j}

$$C_{D_j} = \frac{4}{3} \frac{g}{w_{o_j}^2} \frac{d_j (s_s - 1)}{} \qquad (8.6)$$

Eq. (4.5) reads:

$$i = i_o (1 + c_5 (Fr^{-2} (s_s - 1))^{3/2} \sum_{j=1}^{N} C_{D_j}^{-3/4} C_j)$$

where N is the number of fractions and C_j is the volume concentration of fraction p_j. The measured energy loss gradient ratio, i/si_o, and calculated values from Durand's equation are compared in Table (8.1), based on the approaches of the drag coefficient given in Eqs. (8.4 - 8.6).

Table 8.1 Comparison of measured energy loss of the primary ground iron ore and calculated values based on different applications of the Durand's equation.

U (m/s)	C (%)	i/si_o (measured)	i/si_o from Eq. (4.4), where C_D is calculated based on: d_{50}-w_o $C_D = 4.38$	$\bar{d}$-$\bar{w}$ $\bar{C}_D = 3.22$	i/si_o from Eq. (4.5), where C_{D_j} is calculated based on d_j and the corresponding w_{o_j}
2.41	20.7	1.20	0.79	0.84	0.90

The calculated values in Table (8.1) are lower than the measured values in the pipe of diameter = 0.027 m. The empirically Durand's equation was originally developed for pipes of diameters larger than 0.05 m. The experimental results presented in Table (8.1) confirm the general tendency of Durand's equation to underestimate the energy losses in small pipes, see for example Charles et al. (1972).

Beach sand and iron ore concentrate

The energy loss gradient ratio determined from some observed beach sand data is shown in Table (8.2).

Table 8.2 Energy loss gradient ratios of some of the experimental results with beach sand.

U (m/s)	C%	i/si_o
1.77	23.8	1.107
2.03	23.5	1.004
2.27	23.4	0.938

Following the estimates given in Table (7.1), the experimental results shown in Table (8.2) mainly correspond to a pseudohomogeneous flow pattern, i.e. the solids are nearly uniformly distributed. The experimentally determined deposition velocity was approximately equal to 1.1 m/s, Fig. (7.15). The particle size distribution of the sand used in this study, Fig. (8.4), was very similar to that used in the pilot-scale test by Haas et al. (1973 a), discussed earlier in section 2.4.

The experimental results shown in Table (8.2) were compared to the reproduced pilot-plant data shown in Table (2.2), see page 28. For example, the deposition velocity for the beach sand used in this study was estimated to be about 2.2 m/s in a pipe of diameter 0.11 m, based on Eq. (4.5):

$$\frac{U_D}{(2gD(s_s - 1))^{1/2}} = F_L$$

In a pipe of diameter = 0.11 m, Haas et al. observed a deposition

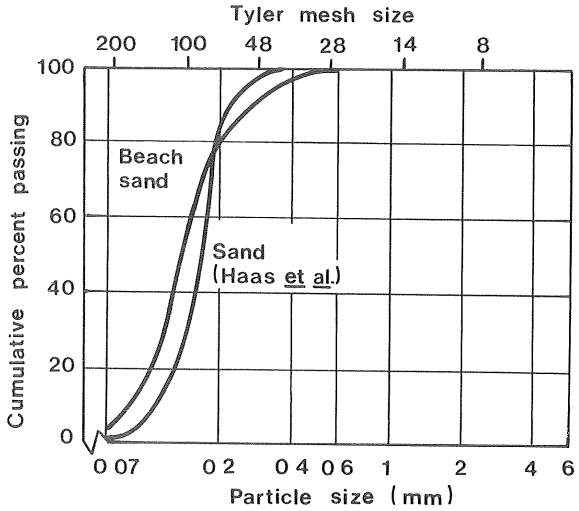

Fig. 8.4 *Comparison of the particle size distribution of the beach sand used in this study and the sand used in the pilot-plant study by Haas et al. (1973a).*

velocity of about 1.95 m/s, which was related to a velocity just above that which has been observed for moving dunes on the bottom of the pipe, see Table (2.2). However, the pipe roughness in the two investigations was not equal, a factor which may influence the deposition conditions. The overall behaviour in larger pipes of the beach sand used in this study is expected to follow the converging tendencies shown in Table (2.2).

The computational model developed by Wasp et al. (1963) described in section 4.3, was compared to some experimental data of the iron ore concentrate and the beach sand. The properties: density, particle size distribution of the solids tested, and the experimentally obtained operational data: solid concentration, velocity, pipe diameter, pipe roughness, and temperature, were given as input to the computer calculation programme of the energy losses. The iteration procedures were described and exemplified in Chapter 4. The experimentally determined and the calculated energy loss gradient ratios were compared in Table (8.3).

The compared experimental data in Table (8.3) corresponds to operational conditions without any tendency of solid deposition on the bottom of the pipe, except for the iron ore concentrate with velocity 1.09 m/s. This velocity corresponds to deposition conditions in the pipe

Table 8.3 Comparison of measured energy losses with calculated values based on the Wasp et al. computational model.

Solids	U (m/s)	C (%)	i/si_o (measured)	i/si_o (calculated)
Iron ore concentrate				
	1.95	21.3	0.978	0.967
	1.62	21.9	1.039	0.977
	1.09	25.6	1.296	1.115
Beach sand				
	2.27	23.4	0.939	0.992
	2.03	23.5	1.005	0.990
	1.77	23.8	1.111	0.993

of diameter 0.027 m, Fig. (7.16).

The heterogeneous influence on the flow for the rest of the data in Table (8.3) was small, because both the measured and calculated values indicate that the energy loss expressed in metres of slurry is approximately equal to energy loss of water flowing at an equivalent velocity, i.e.

$$i/si_o \approx 1$$

or

$$i/s \approx i_o$$

The agreement between measured and calculated values in Table (8.3) is attributed to the dominant influence of Darcy-Weissbach equation in the computational model by Wasp et al., when applied to pseudohomogeneous flows.

8.4 Pump performance study

Reduction in efficiency

It was found that the general tendencies expressed by the reduction curves in Fig. (7.22), Eqs. (5.5), and (5.6) hold approximately for the investigated slurries of iron ores, perlite, and lead ore, provided the concentration was less than about 20%. Eq. (5.5) reads:

$$P = s P_o$$

where

P = power input to pump when pumping slurry

P_o = power input to pump when pumping water

s = slurry density ratio = ρ/ρ_o

Eq. (5.6) is given by the expression:

$$\frac{H}{H_o} = \frac{\eta}{\eta_o}$$

where

H = pump head developed in slurry service, metres of slurry

H_o = pump head developed in water service, metres of water

η = pump efficiency in slurry service

η_o = pump efficiency in water service

However, the experimental results in this study demonstrate that Eqs. (5.5) or (5.6) cannot be taken as an universal statement when pumping industrial slurries. For the pump used in this study, it was thus found that the reduction in efficiency exceeds the reduction in head if the concentration exceeds 20%-25% for the primary ground iron ore, the perlite, and the lead ore, i.e.

$$\eta/\eta_o < H/H_o \qquad \text{(Eq. 7.4)}$$

or

$$P > s P_o \qquad \text{(Eq. 7.5)}$$

Increased power consumption due to high solid content here expressed by Eq. (7.4), or (7.5) has generally been related to increased disc

friction loss. However, the complex mechanism of the flow inside a centrifugal pump is not completely understood, not even with clear water flow.

As the amount of solid increases it is believed that the obstruction to the flow also will be associated with rapidly increasing additional hydraulic losses. The drop in efficiency for concentrations above 20% - 25%, for the solids shown in Figs. (7.25 - 7.27), may be related to breakaway of boundary layers in the flow in the impeller. A characteristic Reynolds number of the flow within the pump, Re_N, can be based on the rotary speed, N, and the diameter of the impeller, D, i.e.

$$Re_N = \frac{(ND)\,D\,\rho}{\mu} \tag{8.7}$$

where ND is the periphery speed. If the water viscosity, μ_o, is used to represent the viscous influence in Eq. (8.7), then the drop in efficiency can be considered to be independent of Reynolds number, because the drop was nearly independent of the rotary speed, Figs. (7.25 - 7.27). Detailed inspection of basic experimental data also indicates that the efficiency ratio, η/η_o, was almost independent of the velocity in the discharge end of the pump. Therefore, circulatory effects and breakaway of boundary layers may not be completely responsible for the accelerated drop in efficiency, observed for concentrations over 20% - 25%.

The drop in efficiency was not so pronounced for higher concentrations of the coarse iron ore, Fig. (7.28). This behaviour may be related to that a slurry composed of solids with a wide particle size distribution influence the internal flow characteristic to a lesser degree than a slurry of uniformly distributed solids.

The experimental results of the complex ore and the crushed granite, in Figs. (7.29) and (7.30), demonstrate the complex influence of not only the size, shape, and distribution of the solids but also specific mineral properties related to the basic mineral structure and the chemical composition. The influence of the different factors behind the results in Figs. (7.29) and (7.30) cannot be identified separately but the composition of the complex ore is believed to play a dominant role.

The complex ore contained a large amount of talc mineral, Fig. (7.4). Talc is a friable waxy mineral, which, when mixed with water, has a pronounced lubricating effect. The almost negligible reduction in efficiency, Fig. (7.23), may therefore be explained by a decrease of the disc friction within the rubber-lined pump, which nearly compensated the extra hydraulic loss due to solids.

It is convenient to express the influence of solids on the clear water pump performance in the form of a reduction factor. The reduction factor of the drop in efficiency is defined here by:

$$R_\eta = 1 - \eta/\eta_o \qquad (8.8)$$

The reduction of the clear water efficiency for the complex ore and the crushed granite was in the range of 0% - 10% and 60% - 75%, respectively, Figs. (7.29 - 7.30). Inspection of the experimental results of the other minerals and ores, in Figs, (7.25 - 7.28), showed that the reduction in efficiency, R_η, mainly can be estimated by:

$$1 - H/H_o \leqslant R_\eta \leqslant C_w \qquad (8.9)$$

where H/H_o is the head ratio and C_w is the concentration by weight. The right term in Eq. (8.9) refers to Eq. (7.6):

$$\eta/\eta_o = 1 - C_w$$

The expression to the left in Eq. (8.9) can be related to a reduction factor for head, R_H, defined by:

$$R_H = 1 - H/H_o \qquad (8.10)$$

Thus, Eq. (8.9) can be expressed in the following form:

$$R_H \leqslant R_\eta \leqslant C_w \qquad (8.11)$$

The experimental data showed that the influence of different parameters in Eq. (5.16) on the reduction in efficiency are interrelated in a very complex way. Eq. (5.16) reads:

$$\eta/\eta_o = \phi(Re_w, Z, \psi, s_s, \frac{d}{D}, C_w)$$

where

$Re_w = \frac{w\, d\, \rho_o}{\mu_o}$ (Particle Reynolds number)

Z = particle distribution factor

ψ = shape factor

s_s = solid density ratio = ρ_s/ρ_o

d = characteristic particle size

D = impeller diameter

C_w = concentration by weight

Therefore, no further attempts were made to correlate individual experimentally determined efficiencies, except Eq. (8.11).

Reduction in head

It can be seen in Figs. (7.25 - 7.30) that the head ratios are more uniquely related to C_w than the efficiency ratios. Besides, the drop in head is not influenced so much by individual mineral properties as the efficiency. In fact, all investigational data indicates that the head ratio may be represented by Eq. (5.15):

$$H/H_o = \phi(Re_w,\ Z,\ \psi,\ s_s,\ \frac{d}{D},\ C_w)$$

where the parameters were defined in Eq. (5.16) above.

The head ratio of a particular slurry pump is given by:

$$H/H_o = \phi(Re_w,\ Z,\ \psi,\ s_s,\ C_w) \qquad (8.12)$$

where the influence of the parameters Re_w, Z, and ψ can be related to a representative drag coefficient C_D, i.e. Eq. (8.10) can be expressed in the following way:

$$H/H_o = \phi(C_D,\ s_s,\ C_w) \qquad (8.13)$$

To obtain an expression applicable to the experimental data in this study the influence of particle shape and particle distribution is simply related to the weighted particle size, $\bar{d}$, and to the weighted

settling velocity, $\bar{w}$, i.e. the characteristic drag coefficient in Eq. (3.22) is related to $\bar{C}_D$, Eq. (8.5),

$$\bar{C}_D = \frac{4g}{3} \frac{\bar{d}(s_s - 1)}{\bar{w}^2}$$

Finally, with $\bar{C}_D$ from Eq. (8.5) in Eq. (8.13) and expressing this equation by the reduction factor given by Eq. (8.10), it follows that:

$$R_H = \phi(\bar{C}_D, s_s, C_w) \tag{8.14}$$

Eq. (8.14) was related quantitatively to all experimental data for the minerals used in this study. A preliminary comparison of the plotted experimental results of the iron ores, lead ore, and the perlite in Figs. (7.25 - 7.28) indicate that the functional relationship in Eq. (8.14) can be expressed in the following form:

$$R_H = c_6 C_w^{\beta} (s_s - 1)^{\gamma} \bar{C}_D^{\delta} \tag{8.15}$$

where c_6, β, and γ are constants ≥ 0 and δ is a constant ≤ 0. For given solid properties defined by the solid density ratio s_s and the drag coefficient $\bar{C}_D$, R_H appears to be approximately proportional to C_w^{β} with the exponent $\beta = 0.7$. The value of the coefficients c_6, γ, and δ were estimated as 0.32, 0.7 and -0.25 respectively. Thus,

$$R_H \approx 0.32\, C_w^{0.7} (s_s - 1)^{0.7} \bar{C}_D^{-0.25} \tag{8.16}$$

The validity of Eq. (8.15) in the form of Eq. (8.16) is shown in Fig. (8.5), where calculated values of R_H are graphically represented against observed values of $(1 - H/H_o)$. Error bands of $\pm$ 15% have been drawn for comparison.

The empirical expression in Eq. (8.16) overestimates the reduction in head for the complex ore and underestimate the reduction for the crushed granite, by about 30% in each case, for the experimental results with these solids in this study. It is believed that the scatter can be related to the basic structure and the chemical composition of the mineral, as discussed in connection with the reduction in efficiency. However, the influence of these individual

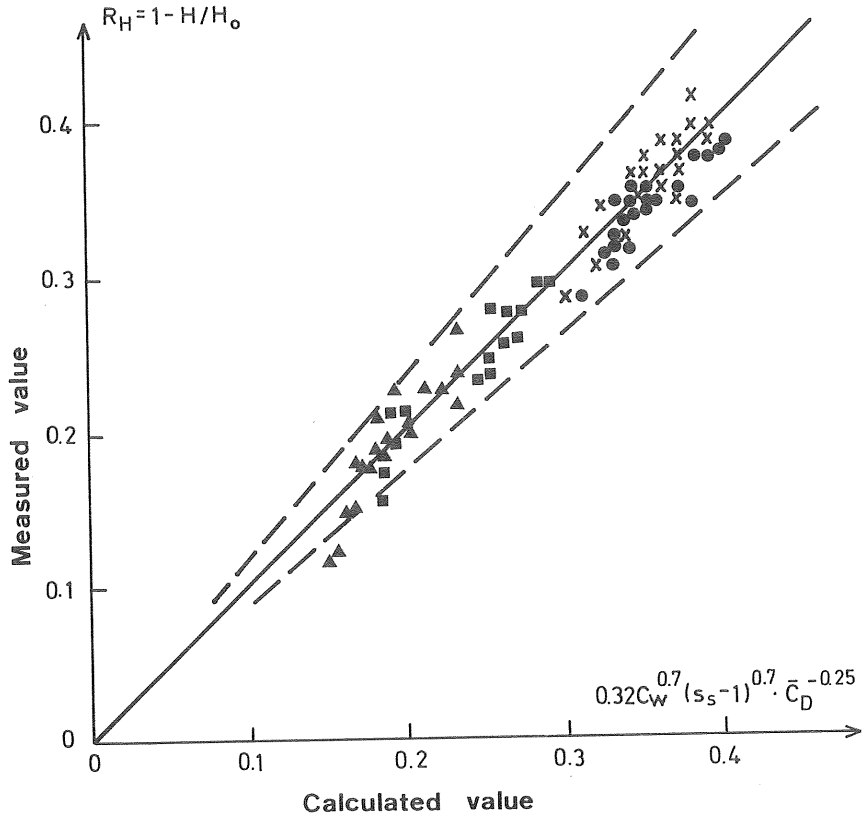

Legend

- ● Primary ground iron ore
- ■ Lead ore
- ▲ Perlite mineral
- X Coarse iron ore

Fig. 8.5 *Observed reduction factors in head versus calculated values with Eq. (8.16). The dashed lines indicate error of ± 15%.*

mineral properties on the reduction in head is more moderate than for the efficiency.

Eq. (8.15), in the form of Eq. (8.16) was also compared to experimental results given by Burgess et al. (1971), for the minerals and ores shown in Table (8.4).

The diameter of the impeller used in their study was of the same order as the impeller used in this study. However, the impeller

Table 8.4 Properties of the minerals used in the experimental study by Burgess (1971).

Mineral:	Beach sand	River sand	Ore	Ilmenite
Solid density, kg/m^3	2670	2670	4350	4630
Particle size, d_{50} mm	0.30	1.29	0.29	0.17
Pump data	Warman 0.11 m pump Hard cast iron 4-vane impeller with diameter = = 0.37 m, rotary speed = 13.3 - 21.7 rps			

design was different. The pump used here has a rubber-lined 3-vane impeller of 0.43 m in diameter. In addition, the mineral used in the Burgess et al. study, Fig. (8.6), had a more uniform particle size distribution than the solids used in this study.

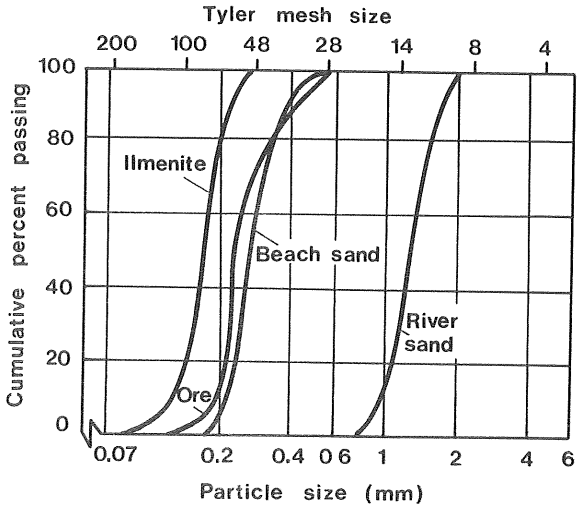

Fig. 8.6 *Particle size distribution of the solid materials used in the pump performance study by Burgess et al. (1971).*

The weighted particle size, $\bar{d}$, was determined from the particle size distributions in Fig. (8.6), but no information about terminal settling velocities was available. Therefore the drag coefficient was related to w_o for the corresponding $\bar{d}$, i.e.

$$C_D = \frac{4g}{3} \frac{\bar{d}(s_s - 1)}{w_o^2}$$

The reduction factor was then calculated with Eq. (8.16) and compared with some measured values of the reduction in head in Burgess et al. study, Fig. (8.7).

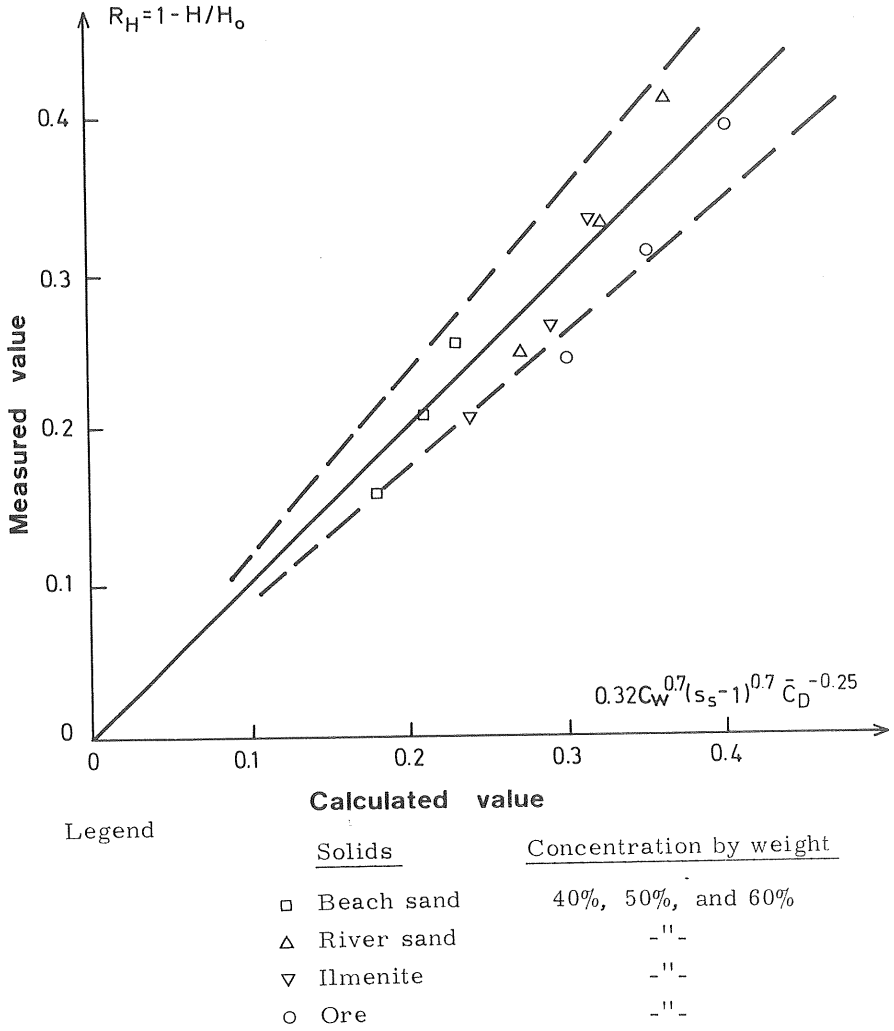

Fig. 8.7 *Observed reduction factors in head according to Burgess et al. (1971), compared with calculated values with Eq. (8.16). The dashed lines indicate error of ±15%.*

In spite of the fact that the pump used in Burgess et al. study was of different design than the pump used in this work and that the drag coefficients could not be identically defined, the scatter is not too large in comparison to Eq. (8.16) as shown in Fig. (8.7).

A correlation in the simple form of Eq. (8.15) may be a promising approach for determining the reduction in head for a large variety of industrial slurries and centrifugal slurry pumps.

The experimental results for the iron ores, lead ore, and perlite mineral used in this study show that the expression in Eq. (8.16) can be used in industrial applications for determining the reduction in head within an error of about $\pm$ 15%. The comparison with some other test data shows that Eq. (8.16) may also be valid for pumps of other design than the rubber-lined pump used in this study.

9. DESIGN PROPOSALS - EXAMPLES

A centrifugal slurry pump generally operates inside the best efficiency point developed for clear water. The choice of pump speed is an important aspect to consider in the design of a slurry system, because the wear increases exponentially with velocity, and the exponent value may be between 2 and 3. The most affected parts are usually made of special metals or lined with wear-resistant rubbers.

The influence of solids on the performance of the centrifugal pump used in this study was related to reduction factors for head and efficiency, R_H and R_η, respectively.

$$R_H = 1 - H/H_o \qquad \text{(Eq. 8.10)}$$

$$R_\eta = 1 - \eta/\eta_o \qquad \text{(Eq. 8.8)}$$

where

H = pump head developed in slurry service, metres of slurry

H_o = pump head developed in water service, metres of slurry

η = pump efficiency in slurry service

η_o = pump efficiency in water service

With the exception of the complex ore and the crushed granite, the reduction factor, R_H, for the solids tested can approximately be expressed by Eq. (8.16):

$$R_H \approx 0.32\ C_w^{0.7}\ (s_s - 1)^{0.7}\ \bar{C}_D^{-0.25}$$

where s_s is the density ratio $= \rho_s/\rho_o$ and C_w is the concentration by weight, Eq. (7.6). The value of $\bar{C}_D$ is obtained from Eq. (8.3):

$$\bar{C}_D = \frac{4g}{3}\ \frac{\bar{d}\,(s_s - 1)}{\bar{w}^2}$$

where g is the acceleration of gravity, $\bar{d}$ and $\bar{w}$ are the weighted particle size and terminal settling velocity, respectively, see page 126.

The reduction factors for the tested complex ore and the crushed granite may be obtained directly from Figs. (7.29) and (7.30), re-

spectively.

The reduction factor of efficiency, R_η , was found to be almost equal to R_H for concentrations of less than about 20% by volume of the iron ores, perlite, and lead ore, i.e. the power needed, P, in slurry service was proportional to the density ratio, i.e.,

$$P = s P_o \quad \text{(Eq. 5.5)}$$

where

s = slurry density ratio = ρ/ρ_o

ρ = slurry density

ρ_o = water density

P_o = power input to pump when pumping water

However, with higher concentrations of the above mentioned solids, the situation was less clear, but it was found that:

$$P > s P_o \quad \text{(Eq. 7.5)}$$

A rough estimate may be obtained from Eq. (8.11):

$$R_H \leqslant R_\eta \leqslant C_w$$

In general, when the solids and water component move with different velocity, the total pressure drop cannot be determined without knowledge of the mixture density and the flow behaviour inside the pipe. In-plant experiences have shown that pumping systems available at present should operate under conditions where the relative velocity (slip) between the components is negligible, i.e. with an operational velocity which clearly exceeds the largest terminal settling velocity of the solid particles. The results from slurries composed of coarse particles in this study and the experiences of many others show that the operational velocity should exceed 4-6 times the terminal settling velocity of the largest particles, in order to maintain steady-state delivery of solids. These velocities generally correspond to negligible slip in industrial applications. With highly concentrated slurries, composed of fine-grained solids, the operational velocity must be checked against the transition from turbulent to laminar flow. The rheological properties must first be identified for such

mixtures.

From the experimental results of the iron ores, lead ore, and perlite used in this study, it is concluded that the total pressure gradient required can be determined with a homogeneous approach, i.e. with the mixture considered as a true Newtonian fluid. However, the energy loss term in vertical transportation is usually small compared with the total pressure gradient. Therefore, in practical applications, the total pressure gradient, i_{Tot}, can be approximately determined by the following relationships:

$$i_{Tot} = s(1 + i_o) \qquad \left[\frac{\text{metres of water}}{\text{metre of pipe}}\right]$$

or

$$i_{Tot}/s = 1 + i_o \qquad \left[\frac{\text{metres of slurry}}{\text{metre of pipe}}\right]$$

where

$$i_o = \frac{f_o U^2}{2 g D} \qquad \left[\frac{\text{metres of slurry}}{\text{metre of pipe}}\right]$$

is the ordinary Darcy-Weissbach equation with,

$$f_o = \phi (k/D, Re_o)$$

obtained from a Moody-diagram, Fig. (9.1).

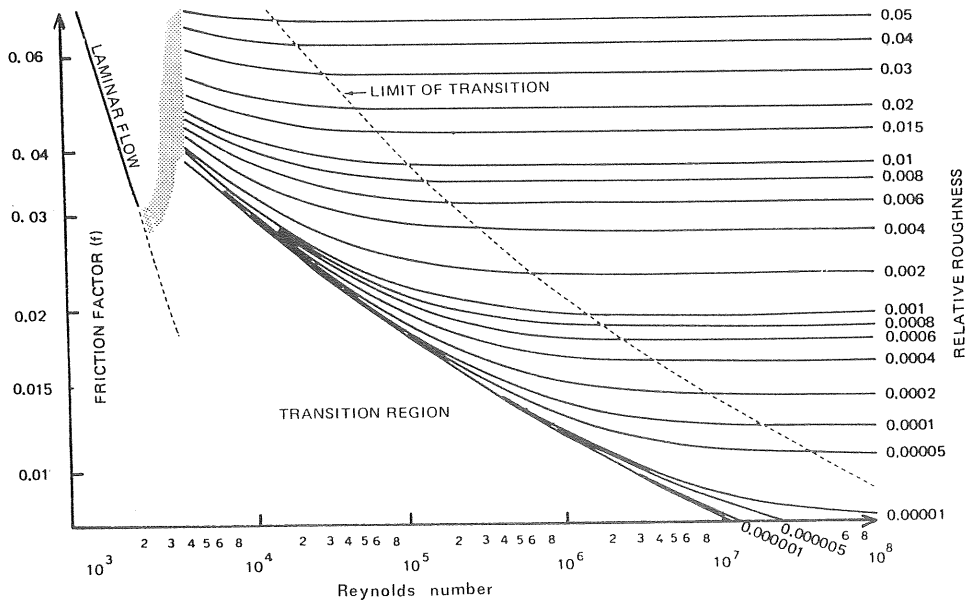

Fig. 9.1 *Pipe friction factors for turbulent flow (Moody-diagram). Adapted from Wasp et al. (1977).*

The Darcy-Weissbach equation is used in this study but, in designing, the Hazen-William formula is widely used, due to its convenience. For the flow situations studied here, the energy loss gradient, i_o, can be calculated by the Hazen-Williams formula provided that equivalent friction factors and roughness coefficients are used.

The pressure required per metre, p, to transport a solid-water mixture in a vertical pipe is:

$$p = \rho g \left[i_{Tot} / s \right] \tag{9.1}$$

where p is expressed in Pa/m and ρ is the density of the slurry in kg/m^3. The power needed is:

$$P = p Q \tag{9.2}$$

where P is expressed in W/m and where Q is the volume flow rate of mixture. The corresponding energy requirement per unit mass of solid, E, is:

$$E = \frac{P}{Q C \rho_s} \tag{9.3}$$

where E is expressed in J/kg · m and C is the concentration by volume. With E expressed in kWh/tonne · m, then it follows from Eqs. (9.1), (9.2) and (9.3) that:

$$E = 0.28 \cdot 10^{-3} \cdot \frac{\rho g \left[i_{Tot} / s \right]}{C \rho_s} \text{ kWh/tonne} \cdot \text{m} \tag{9.4}$$

The pressure and energy required, as expressed by Eq. (9.1) and (9.4), respectively, are graphically represented per 100 m of pipe versus the operational velocity in Fig. (9.2), based on the experimental results in this study for the primary ground iron ore, perlite, lead ore and coarse iron ore. The diagrams in Fig. (9.2) are related to a constant concentration of 25%.

The diagrams in Fig. (9.2) can be used for arbitrary concentrations in the following way. For a solid of given density and operation at given velocity, p is proportional to ρ, and E is proportional to ρC^{-1}. The interrelation between ρ, C, and C_w for a given ρ_s is expressed by Eqs. (3.8) and (7.1):

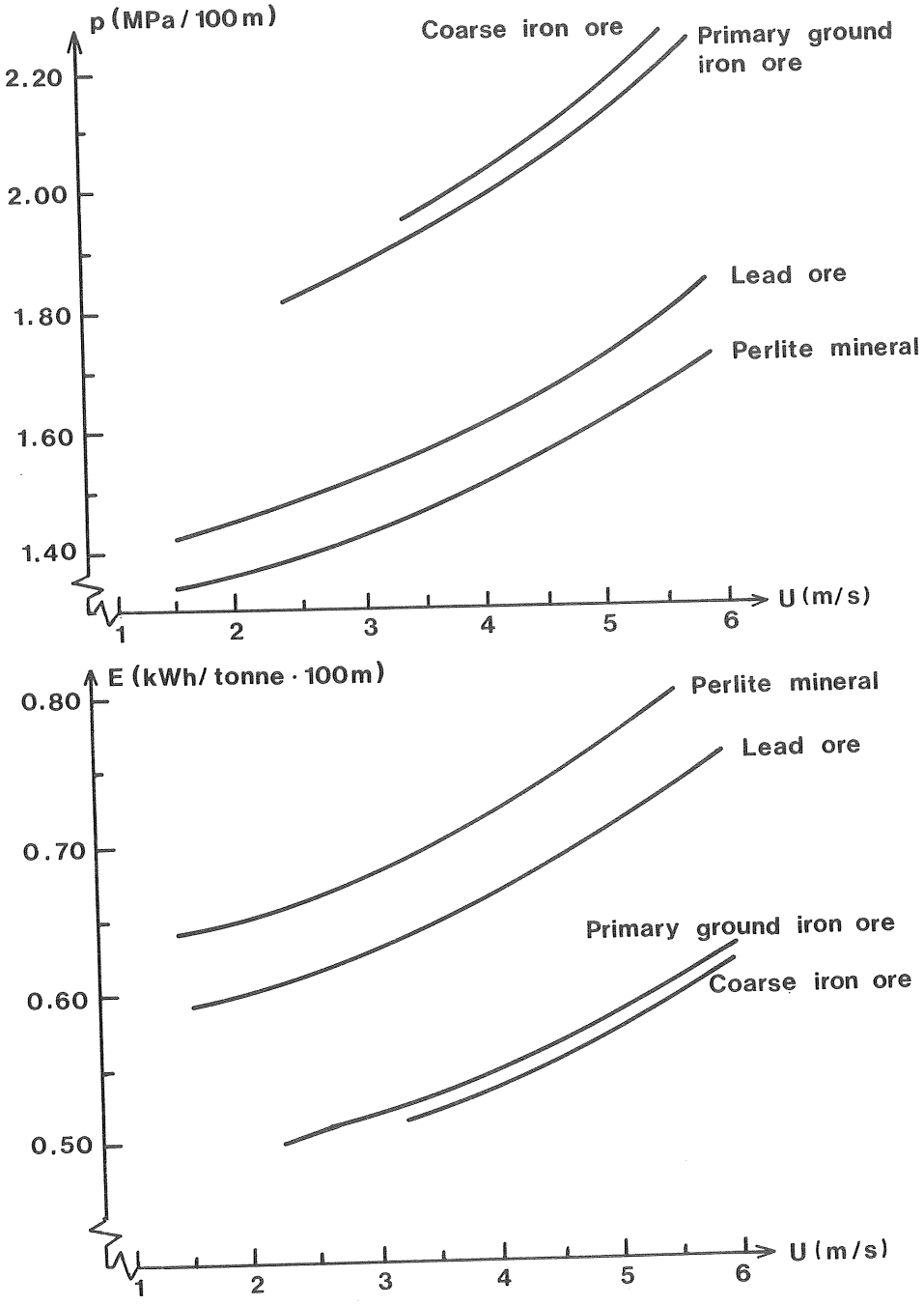

Fig. 9.2 *Pressure and energy requirements versus operational velocity of vertical transportation based on experimental results in a pipe of a diameter of 0.094 m. Pipe roughness, $k = 3.0 \cdot 10^{-5}$ m and temperature = 15°C. The graphs are related to a constant concentration by volume, C = 25%.*

$$\rho = \rho_o (1 + C(s_s - 1))$$

$$C_w = \frac{\rho_s \, C}{\rho}$$

These relations are graphically represented in Fig. (9.3) for the solids shown in Fig. (9.2).

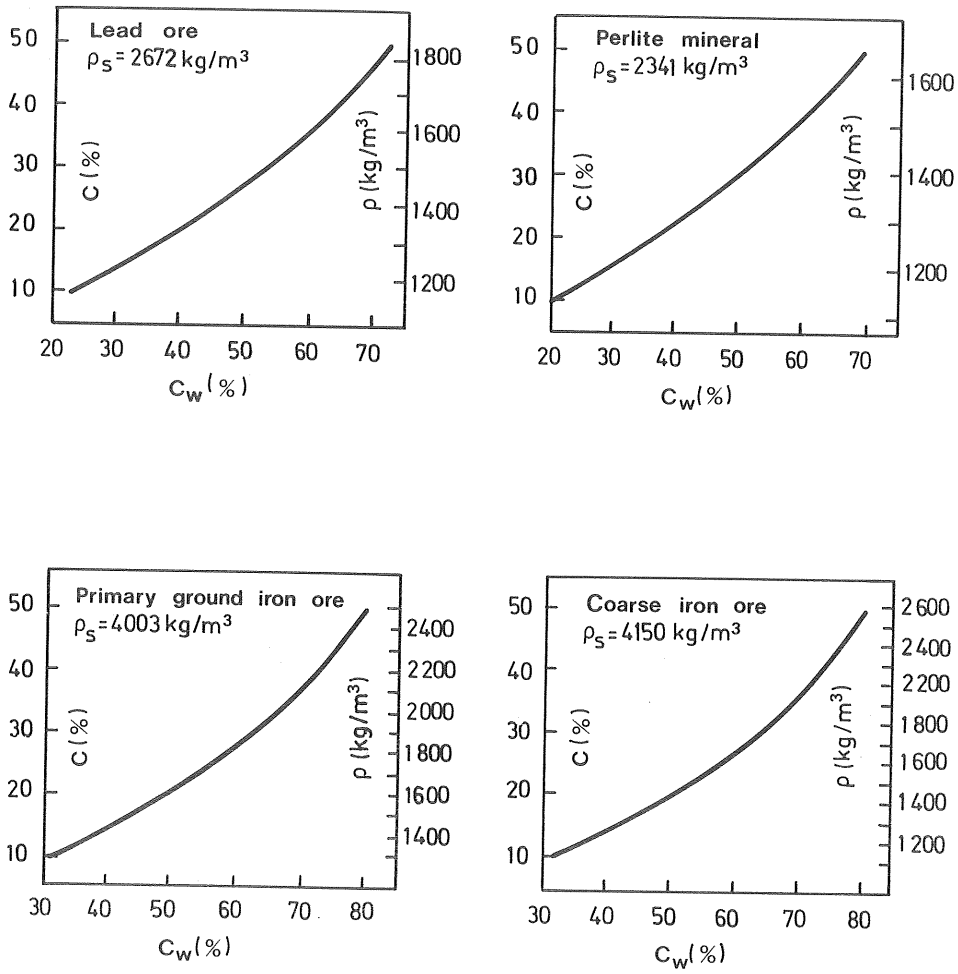

Fig. 9.3 *Graphical representation of ρ, C, and C_w for each solid material shown in Fig. (9.2).*

Example 9.1

Transportation of primary ground iron ore in a vertical pipe of diameter of 0.094 m and of length 500 m. Operational velocity = 2.6 m/s and C = 25%. Temperature = 15°C and pipe roughness, $k = 3 \cdot 10^{-5}$ m.

From readings in Fig. (9.2) it follows that:

$$p = 1.83 \frac{500}{100} = 9.15 \text{ MPa}$$

$$E = 0.51 \frac{500}{100} = 2.55 \text{ kWh/tonne}$$

Example 9.2

Similar assumptions as in Example 9.1 but with a vertical pipe length of 100 m and a concentration of 20%.

With C = 20% in Fig. (9.3) then $\rho = 1600$ kg/m^3 and $C_w = 50\%$. With C = 25% then $\rho = 1750$ kg/m^3.

The readings in Fig. (9.2) are corrected with respect to a concentration of 20%.

$$p = 1.83 \cdot \frac{1600}{1750} = 1.67 \text{ M Pa}$$

$$E = 0.51 \cdot \frac{1600}{1750} \cdot \frac{25}{20} = 0.58 \text{ kWh/tonne}$$

A centrifugal pump similar to that used in this study will be influenced by the iron ore in the following way:

The properties of the ore are obtained from Fig. (7.1):

$\bar{d} = 0.34$ mm
$\bar{w} = 0.063$ m/s
$\rho_s = 4003$ kg/m^3

With these values in Eq. (8.3),

$$\bar{C}_D = \frac{4g}{3} \frac{\bar{d}(s_s - 1)}{\bar{w}^2}$$

it follows that $\bar{C}_D = 3.36$. With $\bar{C}_D^{-0,25} = 0.74$ in Eq. (8.16):

$$R_H \approx 0.32\, C_w^{0.7} (s_s - 1)^{0.7}\, \bar{C}_D^{-0.25}$$

then for $C_w = 50\%$ it follows that:

$$R_H \approx 0.32(0.5)^{0.7}(4.0 - 1)^{0.7} \cdot 0.74 = 0.32$$

Inspection of Fig. (7.25), page 151 shows that R_η can be used as equal to R_H.

Thus, further hydraulic design must be based on a reduction of about 32% of the clear water pump head and efficiency.

Example 9.3

Transportation of lead ore 100 m vertically in a rubber lined plastic pipe of diameter of 0.16 m with absolute roughness, $k = 10^{-6}$ m. Operational velocity = 2.9 m/s and concentration, C = 24%. Slurry temperature = 15 °C. The ore was taken from the rod mill processing step with particle size distribution similar to that shown in Fig. (7.2), page 128.

The friction loss, i_o, in the relationship:

$$i_{Tot}/s = 1 + i_o \quad \left[\frac{\text{metres of slurry}}{\text{metre of pipe}}\right]$$

is obtained from the Darcy-Weissbach equation and the Moody-diagram with $Re_o = 4.03 \cdot 10^5$ and $k/D = 6.25 \cdot 10^{-6}$, see page 183. The total pressure gradient is then determined, and it follows that:

$$i_{Tot}/s = 1.041 \quad \left[\frac{\text{metres of slurry}}{\text{metre of pipe}}\right]$$

With the density of solids, $\rho_s = 2672$ kg/m^3, and the mixture density, $\rho = 1400$ kg/m^3 from Fig. (9.3), then it follows from Eqs. (9.1) and (9.4) that:

$$p = \rho g \left[i_{Tot}/s\right] = 1400 \, g \, 1.041 = 0.014 \text{ MPa/m} =$$

$$= 0.014 \cdot 100 = 1.4 \text{ MPa/100 m}$$

$$E = 0.28 \cdot 10^{-3} \cdot \frac{p}{C \rho_s} = 0.28 \cdot 10^{-3} \cdot \frac{0.014 \cdot 10^6}{0.24 \cdot 2672} =$$

$$= 0.0061 \text{ kWh/tonne} \cdot \text{m} = 0.0061 \cdot 100 =$$

$$= 0.61 \text{ kWh/tonne} \cdot 100 \text{ m}$$

The operational premises in this example correspond to those for which the energy consumption could be halved in horizontal transportation, by the use of helically ribbed pipes. This will be discussed in Chapter 10.

10. FEASIBILITY OF HYDRAULIC TRANSPORTATION FROM UNDERGROUND

Long-distance slurry transportation in pipelines

International experience has shown excellent benefits of slurry pipeline transportation, in situations where large stable volumes of fine-grained mineral are to be delivered over fixed routes. Labour supplies and pumping power to operate a pipeline represent only a small portion of the total cost, and therefore pipeline transportation is much less vulnerable to inflation than alternative modes of transportation.

Table 10.1 Average energy consumption (kWh/tonne· km) for different modes of long-distance transportation of iron ore.

Pipeline	Railroad (electric power)	Truck (diesel fuel)
0.05	0.10	0.20

Long-distance pipeline transportation also offers many safety and environmental benefits. Transportation of $2.5 \cdot 10^6$ tonnes of iron ore per year over 100 km can be carried out in a buried pipeline of a diameter of about 0.25 m. The transportation takes place without any visual or audible effects or exposure to potential traffic hazards.

10.1 Hydraulic hoisting

High pressure water jets can be used to cut the mineral in mining and tunneling operations. Small flexible monitors operate with pressures up to 3.5 MPa. For example, hydraulic mining is used in open pit mining of kaolin. (China clay, Great Britain). The hydraulically won material is pumped up from the bottom of the pit, and kaolin is then separated at the mine and pumped on for further processing.

Recent experience from some German underground coal mines has shown that direct hydraulic transport from the mine face to the preparation plant is favourable. Hydraulically won coal in steeply inclined workings is gravitated to a sump and then pumped directly to the preparation plant.

Most existing applications of hydraulic hoisting appear to be accompanied by major mine dewatering or hydraulic mining activities. Hydraulic hoisting of mineral ores has been used in mines where the ore is wet in situ, which presents difficult control problems in ore passes and feeder chutes and on belt conveyors. Principal data from some representative applications is listed in Table (10.2).

Table 10.2 Some representative applications of hydraulic hoisting.

Country:	South Africa	Federal Republic of Germany		
Mine:	Val Reef	Lengede	Carl Funke	Hansa
Mineral:	Gold ore	Iron ore	Coal	Coal
Density (kg/m^3):	2100	up to 3700	1400	1400
Capacity (tonnes/h):	35	300	60	190
Max particle size (mm):	2	30	3	100
Vertical length (m):	2200	130	760	840
Horizontal length (m):	-	-	5500	600
Pump facilities:	Mars pumps[1]	Modified[2] dredge pump	Positive displacement pump	Pipe-feeding[3] system

1) The mars pump is a reciprocating pump where the slurry is isolated from the pistons by an oil filled reservoir.

2) Extensive development work and series of full scale tests resulted in a constructional modification of a dredge pump (Habermann 250/IV). In this installation the pump works with a 0.57 m impeller at a rotary speed of 20.8 rps. Two-staged units deliver 0.08 m^3/s with a total efficiency of about 45%.

3) Feeding systems have been developed and designed for high transportation of coarse granular solids. Mostly these systems pass solids into an isolation chamber of relatively low pressure. The chamber is then sealed and pressurized and opened to a high-pressure water system. Most applications of pipe-feeding system have been reported from Japanese mines but the installations in German coal mines are based on a system developed in Hungary.

About ten hydraulic hoisting applications are at present in operation in China, Poland, and USSR. In the United States the first plant for commercial operation is under construction, Shook (1976). Continuous miners will be served by an underground haulage face system having a pipe length of about 300 m in which the coal slurry is then pumped about 300 m vertically and then 4 km overland to a preparation plant.

The demand for higher productivity as well as health and safety considerations are the main reason behind the development of hydraulic transportation from underground coal mines in the U.S.A. Underground mining is one of the most hazardous industrial occupations in both the U.S.A. and Sweden.

In the metal mining industry, conversion into a slurry of fine particles is often a part of the normal processing of the ore. In Swedish mines there is generally a considerable inflow of groundwater which has to be pumped out.

Ore transportation facilities in conventional underground mining of a steeply inclined ore body are schematically shown in Fig. (10.1).

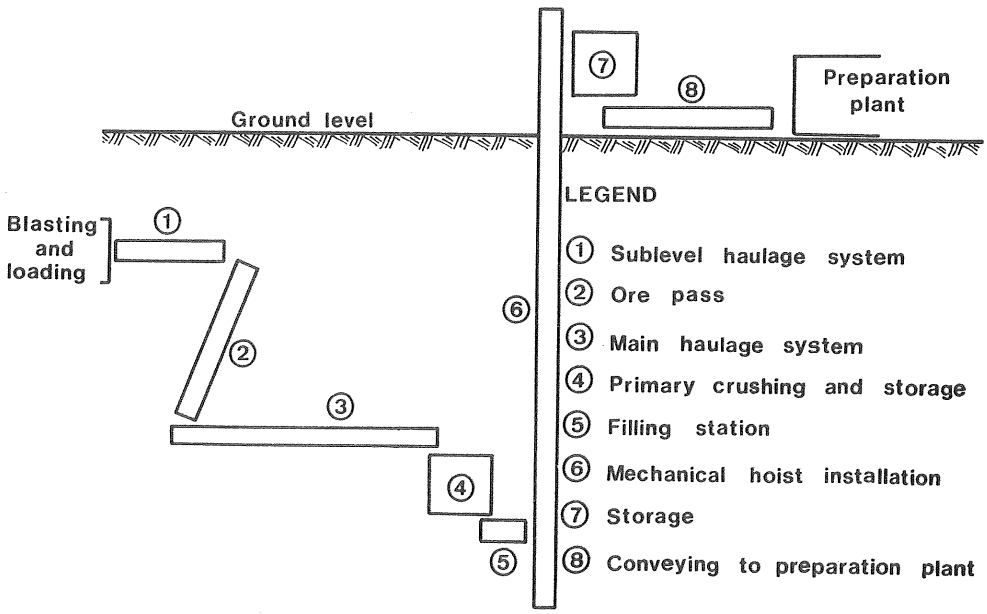

Fig. 10.1 Schematic diagram - Ore transportation facilities in underground mining.

Loose ore from the mining levels is transported to a chute leading to the main haulage level below. Front-end loaders are usually used in the loading and hauling of the boulders from the working area. On the main haulage level the ore is transported to the primary crushers where it is comminuted to a rock size of about 0.1-0.2 m. The conveying is usually trackbound with automatically controlled loading and unloading. Sometimes haulers are used as a competitive alternative.

From the storage bins the ore is transferred into skips for hoisting to the surface. The hoists are located in headframes directly above the hoisting shaft. Modern mine hoists operate at high efficiency, and automatic controls have become normal practice. Ore from the hoisting system is dumped by the skips into hoppers located in the headframe and then conveyed by belt, etc. to the preparation plant. In the preparation plant the ore is first sorted and crushed. Parts of the ore is then concentrated by various dressing methods depending on the type of mineral. The concentration process is mostly carried out by wet milling methods, where the ore lumps are grated into fine particle sizes, usually less than 0.2 mm.

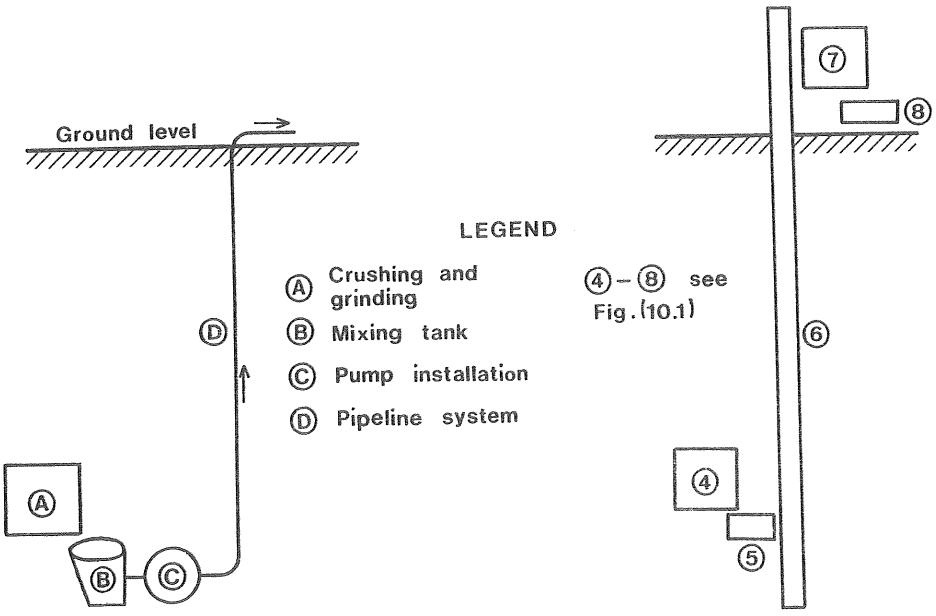

Fig. 10.2 *Schematic comparison of a hydraulic hoisting system and a shaft hoisting system.*

A hydraulic hoisting system is schematically compared with a shaft hoisting system in Fig. (10. 2). In the case of an emergency shutdown it is recommended that a sump should be provided at the bottom of the shaft so that the hoisting leg can be drained to prevent plugging at the bottom of the pipe by the settled solids.

Additional underground grinding and handling of the ore is necessary if the ore is to be hoisted hydraulically. Grinding and pumping facilities need extra room, which can be problematical in deep mines. Moving and installation of heavy, large surface-suited equipment can cause considerable problems. It is believed that operation in underground areas will be associated with some extra costs. Pumping with centrifugal or positive displacement pumps limits the maximum particle size of the mineral to about 10 and 1 mm, respectively.

The chief advantages of hydraulic hoisting are:

- The hoisting capacity can be increased without the necessity of sinking new shafts.

To increase the capacity by conventional means requires a large capital investment and takes a long time to achieve. Work on deeper and deeper levels requires the hoisting shafts to be sunk deeper. Depending on construction method, rock strength, etc, a level is eventually reached from which the same rate of production cannot be maintained. At that point other technical solutions have to be applied.

- The small pipe shaft required can be sunk near the ore-bearing area and thus a more rational utilization of the existing underground horizontal haulage system is achieved.

The hoisting shafts are not always located close to the current exploitation of the ore body. A hydraulic hoisting system can replace or partly replace the shaft hoisting system and thus influence the load carrying capacity of the main haulage system.

Some factors which operate against the use of hydraulic hoisting are:

- Conventional skip hoisting must in many cases be provided for the transport of men and equipment. Shafts are always necessary for ventilation and safety.

- The overall efficiency in hydraulic transportation of coarse heavy ores will be rather low with the technology that is available today.

10.2 Economics

The energy requirements of hydraulic hoisting will be compared with two alternative modes of transportation. The hydraulic design data is mainly based on the experimental results in this study. It is pressumed that the hydraulic system relies on presently available grinding equipment and pump facilities.

In the outlined examples it is assumed that water from the inflow of groundwater is used in the hydraulic hoisting system and that the power needed to pump out this water is excluded in a comparison with the other modes of transportation.

Example 1. Hydraulic hoisting of 140 tonnes/h of coarse iron ore by centrifugal pumps from a depth of 200 m, compared with truck transportation in inclined drifts.

Example 2. Hydraulic hoisting of 140 tonnes/h of primary ground iron ore, pumped by a positive displacement pump from a depth of 800 m, is compared with shaft hoisting from the same depth.

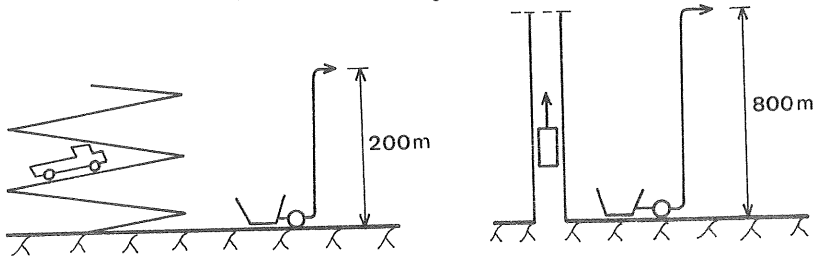

Example 1. Example 2.

Fig. 10.3 Examples, for comparison of the energy requirements of hydraulic hoisting with truck transportation and shaft hoisting.

The capacities in tonnes per hour and the pipe diameters are the the same in the two examples.

Example 1.

Concentration: In application, C=20% is believed to be a suitable average value during the time of operation.

Operational velocity: To maintain steady-state operation without plugging the pump in the test loop, the velocity had to exceed 3.3 m/s with C=20%. The design velocity is taken 0.3 m/s above this value, i.e. 3.6 m/s.

Efficiency: The pilot-plant test with the centrifugal slurry pump showed a reduction in head and efficiency of about 30%-40%, as compared with clear water values. In application, it is believed that the pump selected will have a clear water efficiency of 65%-70%.

Example 2

In order to get comparable capacity and pipe diameter with example 1, an operational velocity and concentration of 2.7 m/s and of 27%, respectively, can be considered to be suitable design values. The mechanical efficiency of a positive displacement pump in slurry service is 85%-90%, Thompson et al. (1972).

Energy consumption

	Example 1	Example 2
Vertical length (m)	200	800
Pump equipment	Staged centrifugal pumps	Positive displacement pump
Mineral	Coarse iron ore	Primary ground iron ore
Maximum grain size	8 mm	1 mm
Density (kg/m^3)	4150	4000
Capacity (tonnes/h)	140	140
Concentration by volume (%)	20	27
Concentration by weight (%)	51	60
Operation velocity (m/s)	3.6	2.7
Inner diameter of pipe (m)	0.13	0.13
Throughput of slurry (m^3/s)	0.047	0.036
Throughput of water (m^3/s)	0.038	0.026
Total efficiency (%)	40 1)	80
Installed power (kW)	402	677
Power to raise the water (kW)	122 2)	340 2)
Net power consumption (kW)	280	337
Energy (kWh/tonne of ore)	2.0	2.4
Compared alternative of transportation	Trucks in inclined drifts	Mechanical skip hoist in a vertical shaft
Vertical length (m)	200	800
Energy (kWh/tonne of ore)	1.7 3)	2.4 4)

1) based on 40% reduction of the clear water pump efficiency
2) friction loss neglected and total pump efficiency = 60%
3) based on four 16-tonne trucks in a drift with the inclination 1:10
4) based on total efficiency = 90%

It was found that the power needed to pump coarse iron ore in centrifugal pumps was slightly higher than that of truck transportation in inclined drifts. In the outlined example 2 it was shown that hydraulic hoisting of particles up to 1 mm consumes about the same amount as conventional shaft hoisting.

For particle sizes up to about 1 mm there are applications in which centrifugal pumps or positive displacement pumps both are technically feasible. The fact that positive displacement pumps have 15%-40% higher efficiency should be weighted against the higher initial cost.

Maintenance

Centrifugal pumps

Pumping of heavy coarse minerals has a substantial reductional effect on the performance curves of conventional centrifugal slurry pumps. The life-time of impellers and casings would be limited to about 1000-2000 hours in abrasive slurry handling. In the hydraulic hoisting installation at Lengede (see Table (10.2), page 191) the pump maintenance cost in 1975 was about Sw. Crowns 0.20/tonne.

Positive displacement pumps

As a rule it is advisable not to pump particles greater than 2 mm in a positive displacement pump, Faddick (1976). The price of pumping coarse solids is accelerated wear. In the outlined example 2 it was assumed that ore particles up to 1 mm would be pumped. At present the cost of maintenance and supply in such application is relatively unknown. The life-time of valve parts in abrasive long-distance iron ore service (d_{max} about 0.1 mm) will be about 500 hours according to Thompson et al. (1972). The same authors stated that typical ranges of the cost of expendable parts were Sw. Crowns 0.15-0.30/tonne and pump station. The maintenance cost in a mechanical skip hoist system can in general be estimated to be about Sw. Crowns 0.10/tonne, Bergdahl (1975).

Investment

Hydraulic system:	Pumps[1] and pipes (100% stand-by) feeders and screens, mixing tank, emergency sump, instrumentation, and controls.
Shaft hoisting system:	Driving and furnishing of production shaft. Hoist support facilities: Concrete head frames with hoist room and skip pockets, feeders, ropes, measuring pocket, instrumentation, and controls.

The investment cost of a conventional shaft hoisting system for 140 tonnes of iron ore per hour from a depth of 800 m is about $20 \cdot 10^6$ Sw. Crowns.

10.3 Future applications

Mining and tunneling on land

The trend in mining is toward giant open pit mines because of their suitability for mechanization and highly productive mining. To compete with ore from such mines, one has to find new ways of working and transportating ore from underground mines.

When hydraulic hoisting becomes a familiar and proven technique, then it will be natural to couple this concept with underground and surface hydraulic horizontal transportation systems, Fig. (10.4). This would be a natural integration of the overall mining system from an economic and process standpoint.

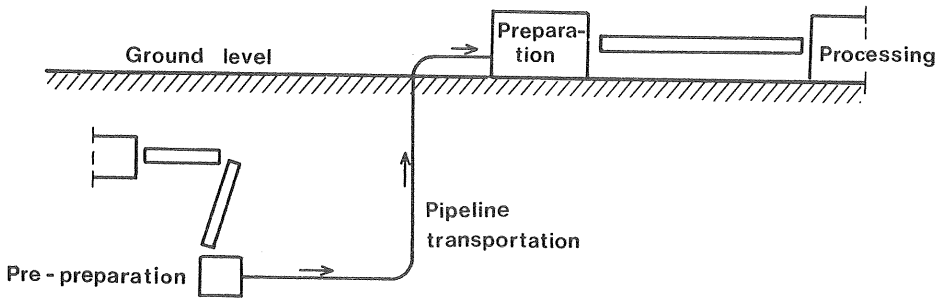

Fig. 10.4 Integration of horizontal pipeline parts in a hydraulic hoisting system.

1) The total investment cost of the positive displacement pumps in example 2 is believed to be about Sw. Crowns $4 \cdot 10^6$ (Aldrich, Ingersoll-Rand).

Continuous excavation of soft minerals by miners or tunneling machines has improved solutions to the problem of face area hydraulic haulage. The present state-of-the-art in hardrock fullface techniques and continuous mining methods in softer minerals will gain the utilization of continuous hydraulic transportation from working face to surface.

There is a general fear of long-term effects on man in the underground working environment. At present there is a growing resistance to diesel power. Recent medical research points toward the fact that exposure to carcinogenic substance is the primary source of cancer diseases, Persson (1976). A large portion of such substances come from diesel exhaust gases, and simultaneous exposure to airborne dust in an environment without photochemical activity magnifies the effect; a series of parallel influence must also be considered, e.g. exposure to radon, nitrogen dioxide, etc.

In the near future major improvements of the underground working environment have to be made. Underground hydraulic haulage is one possible solution for improving mine safety and working environment in underground mines.

Underground location of mineral dressing plants may be necessary in the future to minimize environmental impact on urban areas or ecologically sensitive areas, Fig. (10.5).

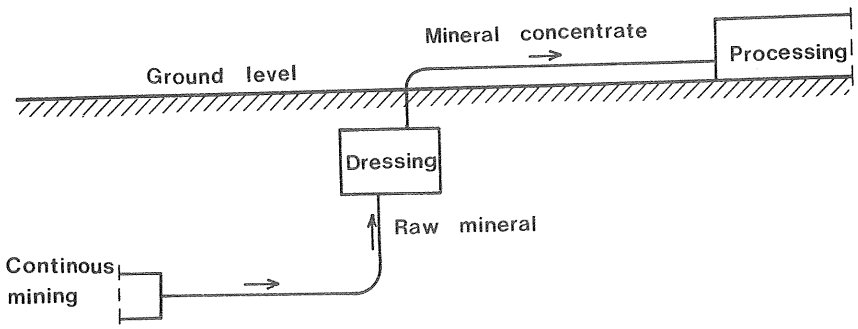

Fig. 10.5 Continuous mining and long-distance pipeline transportation to processing plant.

Small or low-grade deposits are often not profitable if conventional mining and transportation methods are used. In the development of small deposits transportable pumping and crushing units ("modules")

for hydraulic hoisting may be an useful solution. The dressing of the ore may take place at the mine in a mobilized plant, Fig. (10.6).

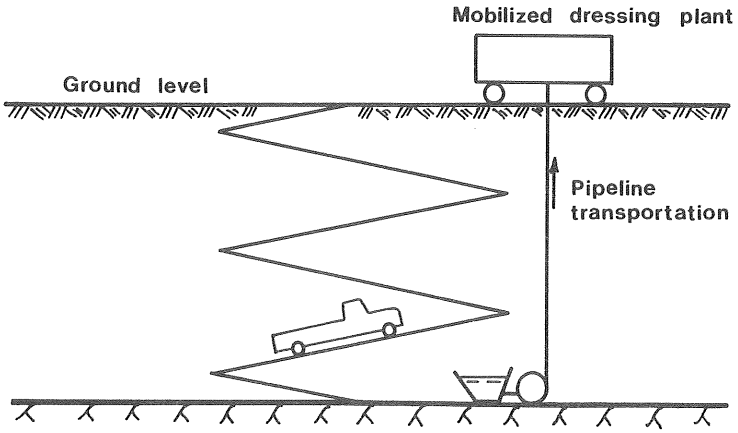

Fig. 10.6 Hydraulic hoisting of ore in a small mine.

Hydraulic hoisting and overland transportation in pipes is believed to be a competitive way for rational utilization of a relatively closely located grouping of mines. With a minimum of surface buildings and transportation facilities ore will be pumped to a large central dressing plant, which gives considerable economic and environmental benefits, Fig. (10.7).

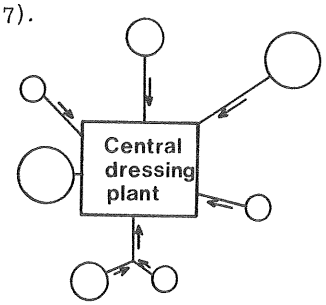

Fig. 10.7 Hydraulic hoisting and haulage to a central dressing plant from a group of underground mines.

Coarse particles transportation - Some improvements

Transportation of relatively coarse particles has been limited to short distances because of necessarily high operation velocities resulting in extensive pipe wear and excess energy consumption. Fur-

ther development of equipment and pumps is required to increase the economic feasibility of coarse mineral transportation.

The energy consumption can be reduced by creation of secondary flow by helically ribbed pipes. Hydraulics studies in Canada by Smith (1976) and Charles (1976) have demonstrated that helically ribbed pipes may have special advantages in the horizontal transportation of relatively coarse mineral. Tests conducted by Smith (1976) show that the consumption of energy could be halved in the transportation of a sand with d_{50}=0.5 mm in a ribbed pipe of diameter = 0.16 m. Wear studies by Smith indicate that the total wear produced per tonne of solids transported would be lower, mainly because of the lower possible operation velocity and the higher possible concentration.

It is believed that further development in slurry technology must include transportation of coarser particles than today. The investigational works citied above represent interesting improvement upon the feasibility of such systems. Laboratory tests with helically ribbed pipes and in-plant tests of a new wear-resistent rubber-lined plastic pipe and a high pressure pump without large external devices and with a minimum of moving parts is carried out in Sweden in light of the system-oriented development work mentioned earlier in the Introduction.

Mining at sea

Marine mining activities can be expected to increase as the shortage and cost of land-based mineral resources grow. From an economic point of view it is expected that the exploration of an underwater ore deposit can be compared to the opening of deep underground land deposits.

Consolidated deposits occur as hard rock on the continental shelves. It is anticipated that deposits of hard minerals in the bedrock occur with the same frequency as they appear under similar conditions on land. The Swedish potential of consolidated ore deposits is believed to be limited to complex sulphide ores in the gulf of Bothnia, where the depth is mainly between 25 and 100 m. Areas close to the shore generally have depths of less than 25 m. Prospecting for minerals in the sea presents complex problems. Before any potential of these

minerals can be realized, the technological capabilities of locating and assessing them must be improved.

It is believed that land-developed underground mining methods can be used, but precautions must be taken with regard to overhead cover. Cut- and fill mining methods seem to be preferable.

Ore deposits located near land can be exploitated by driving tunnels from shoreside. To get acceptable economical and technical solutions for longer distances, artificial islands for ventilation and access shafts must be provided. Mine development from artificial islands has also been proposed as an alternative in shallow water. In deeper water (up to about 100 m) platform rigs and cassion structures may be used such as the ones developed and utilized in the exploration of offshore oil and gas resources.

The mined ore can be barged or pumped in pipeline to a shoreside processing plant. Today the building of undersea pipelines for oil and gas has been accomplished at depths of up to a hundred meters. If tailings are to be used for building artificial islands or to be filled back into the mine, great savings in transportation costs could be made by pre-preparation of the ore at the offshore mine site.

The methods outlined previously for land-based underground mines is believed to be applicable to slurry transportation from future Swedish mining of consolidated undersea ore deposits.

Unconsolidated deposits on the continental shelf may be defined as seabed deposits of heavy minerals, sand, gravel, etc. These deposits are generally found in water depths of the order of 100 m or less. Therefore different dredging methods probably could be used for exploitation of these deposits. In the deep-ocean basins, manganese nodules contain the deep sea mineral most likely to be exploited in the future. Considerable commercial activity exists in developing these resources for their major component ores: nickel, copper, cobalt, and manganese. Nodules from the Norteast Pacific have attracted great attention. These modules are generally located in water depth of 2600 m - 5500 m.

There are basically two types of deep water dredges, mechanical and hydraulic. The mechanical dredge digs and lifts the mineral in

a container. The hydraulic dredge lifts the mineral as a slurry in a contained stream of upward-moving water. Most deep-water dredges have been designed around hydraulic systems with variations in the means of introducing solids into the pipe, in the design of the gathering device and in the means of imparting horizontal motion to the system on the seabed.

Vertical slurry flow may be induced by:

- the injection of air or light weight materials in the pipe
- feeding and pumping directly from the seabed
- feeding at the seabed and pumping in a loop with the pump at the surface (dual-pipe system).

The dual-pipe system has also been suggested for hoisting applications from underground mines, Fig. (10.8). Land-based commercially available feeding systems are dealt with briefly in Table (10.2), page 191.

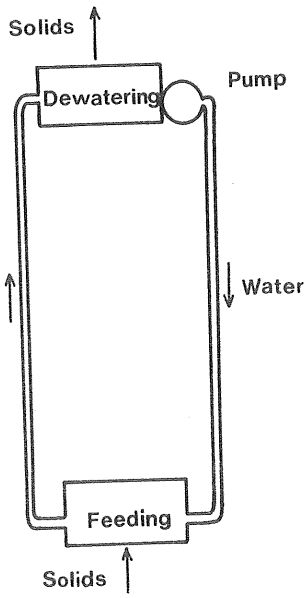

Fig. 10.8 Schematic representation of a dual-pipe feeding system.

The water is pumped from the dewatering facility at the top down the downflow pipe. The pump can work with high efficiency because no solids pass through it. The difference in density in the up-and-down flow pipe and the friction losses must be overcome in the balanced leg system.

LIST OF TABLES

LIST OF FIGURES

LIST OF NOTATIONS

A	cross-sectional area of pipe
A_s	cross-sectional area of pipe occupied by the solids
A_{in}	cross-sectional area of pipe at the suction side of the pump
A_{out}	cross-sectional area of pipe at the discharge side of the pump
C	delivered volumetric concentration
C_D	drag coefficient
C_j	fractional delivered volumetric concentration
C_w	delivered weight concentration
C_{D_j}	fractional drag coefficient
C_{max}	maximum delivered volumetric concentration
C^{Het}	delivered volumetric concentration (heterogeneous part)
C^{Hom}	delivered volumetric concentration (homogeneous part)
C_j^{Het}	fractional delivered volumetric concentration (heterogeneous part)
C_j^{Hom}	fractional delivered volumetric concentration (homogeneous part)
$\bar{C}_D$	weighted drag coefficient
D	pipe diameter
D	impeller diameter
D_{in}	pipe diameter at the suction side of the pump
D_{out}	pipe diameter at the discharge side of the pump
D_1	diameter of pipe 1
D_2	diameter of pipe 2
E	spatial volumetric concentration

E	energy
F	force of average pipe wall shear stress
F_L	diagram factor
F_y	transversal force
G_1	weight of mixture in the sampling tank
G_2	weight of flask for determination of sample density
G_3	weight of solid sample for determination of sample density
H	pump head developed in slurry service, metres of slurry
H_o	pump head developed in water service, metres of water
K	power law coefficient
K	reduction factor
L	pipe length
M	delivered mass flow rate of mixture
M_o	delivered mass flow rate of water
M_s	delivered mass flow rate of solid
N	number of fractions
N	pump rotary speed
P	power
P	power input to pump when pumping slurry
P_o	power input to pump when pumping water
P_{in}	input power to pump motor at run
P_{out}	output pump power at run
Q	volume flow rate of mixture
Q_o	volume flow rate of water
Q_s	volume flow rate of solids
R_H	reduction factor for pump head
R_n	reduction factor for pump efficiency
S	slip velocity

T	temperature
U	average mixture velocity
U_D	deposition velocity
U_o	average velocity of water
U_s	average velocity of solids
U_{Mb}	velocity, separating heterogeneous flow from flow with moving bed
U_{min}	minimum operational velocity in a vertical pipe
U_{max}	maximum velocity in a circular pipe section
U_{Ph}	velocity, separating heterogeneous flow from pseudo-homogeneous flow
U_1	velocity in pipe 1
U_2	velocity in pipe 2
V_1	volume of mixture in the sampling tank
V_2	volume of alcohol for determination of sample density
W_j	fractional average terminal settling velocity
Y	exponent
Y_j	fractional exponent
Z	particle size distribution factor
c	local concentration of solid particles at level z
c_o	local delivered concentration of solids at level z=o
c_{z_o}	local delivered concentration of solids at level z_o
c_1	constant
c_2	constant
c_3	constant
c_4	constant
c_5	constant
c_6	constant

$c_{0.08\ D}$	delivered volumetric concentration 0.08 D below the top of a pipe	
$c_{0.50\ D}$	delivered volumetric concentration 0.50 D below the top of a pipe	
d	differential operator	
d	characteristic particle size	
d_j	fractional particle size	
d_{max}	maximum particle size	
d_o	diameter of a spherical particle	
d_{50}	particle median sieve size	
$\bar{d}$	weighted particle size	
e	internal energy	
f	Darcy-Weissbach friction factor for mixture flow	
f_o	Darcy-Weissbach friction factor for water flow	
f^{max}	estimated maximum Darcy-Weissbach friction factor for mixture flow	
g	acceleration due to gravity	
h	water depth	
h_t	column of tetrabromine methanol in manometer reading	
i	energy loss gradient of mixture	$\left[\frac{\text{metres of water}}{\text{metre of pipe}}\right]$
i_H	measured energy loss gradient of mixture, horizontal pipe	-"-
i_o	energy loss gradient of water	-"-
i_s	excess energy loss gradient due to the solids in the mixture	-"-
i^{Het}	energy loss gradient of mixture, heterogeneous part	-"-
i^{Hom}	energy loss gradient of mixture, homogeneous part	-"-
i_{Irr}	irreversible energy gradient of mixture transported vertically	-"-
i_{Rev}	reversible energy gradient of mixture transported vertically	-"-

i_{Tot}	total pressure gradient required in a pipe of constant diameter	$\left[\frac{\text{metres of water}}{\text{metre of pipe}}\right]$
i_j^{Het}	fractional energy loss gradient of mixture, heterogeneous part	-"-
i_{Irr}^{max}	estimated maximum irreversible energy gradient of mixture transported vertically	-"-
j	particle size fraction index	
k	absolute roughness coefficient	
n	power law coefficient	
p	pressure	
p_j	weight fraction of solid particles	
p_1	pressure in pipe section 1	
p_2	pressure in pipe section 2	
p_{in}	pressure reading at the suction side of the pump	
p_{out}	pressure reading at the discharge side of the pump	
s	mixture density ratio (delivered)	
s_s	solid density ratio	
s_t	tetrabromine methanol density ratio	
t	filling time	
u	local average velocity	
$\hat{u}$	local instantaneous velocity	
u'	local velocity fluctuation	
u'_y	local velocity fluctuation in the y-direction	
u'_z	local velocity fluctuation in the z-direction	
u_*	friction velocity	
y	distance from pipe wall	
y_b	thickness of buffer layer	
y_s	thickness of viscous sublayer	
z	vertical coordinate	

z_o	vertical constant level
w	characteristic terminal settling velocity
w_j	fractional terminal settling velocity
w_o	terminal settling velocity of a sphere
w_{max}	maximum terminal settling velocity
w_{o_j}	fractional terminal settling velocity of a sphere
w'	hindered terminal settling velocity
$\bar{w}$	weighted terminal settling velocity
$\bar{w}_o$	weighted terminal settling velocity of spheres
ψ	particle shape factor
ϕ	indicates, "function of"
ϕ_o	a function
ϕ_1	a function
α	exponent
α_{in}	velocity distribution correction factor at the suction side of the pump
α_{out}	velocity distribution correction factor at the discharge side of the pump
β	diffusion coefficient proportionality factor
β	exponent
γ	exponent
δ	exponent
ε	coefficient of turbulent diffusion
ε_s	coefficient of diffusion of solid particles
$\varkappa$	von Karman constant
η	pump efficiency in slurry service
η_r	coefficient of rigidity
η_o	pump efficiency in water service
η_{Motor}	efficiency of pump motor

η_{Transm}	efficiency of pump motor transmission
η_{Tot}	total efficiency
θ	pipe inclination
λ	turbulent microscale
μ	dynamic viscosity of mixture
μ_o	dynamic viscosity of water
μ^{Hom}	dynamic viscosity of mixture, homogeneous part
μ_j^{Hom}	fractional dynamic viscosity of mixture, homogeneous part
ξ	integration variable
ρ	density of mixture (delivered)
ρ_o	density of water
ρ_s	density of solids
ρ_t	density of tetrabromine methanol
ρ^{Hom}	density of mixture, homogeneous part
ρ'	density of mixture (spatial)
τ	average shear stress
τ_y	yield shear stress
τ_w	average wall shear stress of slurry
τ_{w_o}	average wall shear stress of water
Fr	Froude number
Re	Reynolds number of mixture
Re_B	Bingham Reynolds number
Re_N	Reynolds number of flow in a centrifugal pump
Re_c	"critical"Reynolds number of mixture
Re_o	Reynolds number of water
Re_w	particle Reynolds number
Re'	modified Reynolds number of mixture
We_1	wear rate in pipe 1
We_2	wear rate in pipe 2

$We_{0.094}$	wear rate in a pipe of diameter 0.094 m
$We_{0.20}$	wear rate in a pipe of diameter 0.20 m

REFERENCES

Adam, I. (1968): The Distribution of Solids in Hydraulic Transportation of Heterogeneous Suspensions in Horizontal Pipes, Dissertation, TH Karlsruhe, 1968 (in German).

Aude, T.C., Cowper, N.T., Thompson, T.L., and Wasp, E.J., (1971): Slurry Piping Systems: Trends, Chemical Engineering, June, 1971.

Aziz, K., and Govier, G.W., (1972): The Flow of Complex Mixtures in Pipes, Van Nostrand Rheinhold, 1972.

Bergdahl, S.G., (1975): Comparison of Different Alternatives of Transportation of Rock from Underground Cavity, Meeting, Swedish Mining Association, 1975 (in Swedish).

Blasius, H., (1913): VDI - Forsch.- Heft 131, Berlin, 1913 (in German).

Brebner, A., and Wilson, K.C. (1964): Theoretical Considerations of Vertical Pumping of Mine Products, Civil Eng. Dept, Queen's Univ., Kingston (Ontario), Rept. No. 33, 1964.

Brühl, H. (1976): Influence of Fine Particles on the Slurry Transport in Pipelines, Report No. 43, Franzius-Institut, TU Hannover, 1976 (in German).

Burgess, K.E., (1971): A Study of the Effects of Sizing, Specific Gravity and Concentration of Solids on the Characteristics of a Centrifugal Slurry Pump, Univ. of New South Wales, B.E. thesis, 1971.

Burgess, K.E., and Reizes, J.A., (1976): The Effect of Sizing, Specific Gravity and Concentration on the Performance of Centrifugal Slurry Pumps, The Inst. of Mech. Eng. Vol. 190, No. 36, 1976.

Cave, I., (1976): Effect of Suspended Solids on the Performance of Centrifugal Pumps, Paper H3, Fourth International Conference on the Hydraulics Transport of Solids in Pipes, BHRA Fluid Engineering, Cranfield, Bedford, U.K., May, 1976.

Cave, I., (1978): Some Practical Aspects of Slurry Pipe Line Testing, Paper A3, Fifth International Conference on the Hydraulic Transport of Solids in Pipes, BHRA Fluid Engineering, Cranfield, Bedford U.K., May, 1978.

Charles, M.E., and Vocadlo, J.J., (1972): Prediction of Pressure Gradient for the Horizontal Turbulent Flow of Slurries, Paper G1, Second International Conference on the Hydraulic Transport Solids in Pipes, BHRA Fluid Engineering, Cranfield, Bedford, U.K., May, 1972.

Charles, M.E., and Singh, V.P. (1973): The Flow of Sand-Water Slurries in Horizontal Pipes with Internal Spiral Ribs Can. J. Chem. Eng., No 4, 1976.

Cheng, D.C., and Whittaker, W., (1972): Application of the Warren Spring Laboratory Pipeline Design Method to Settling Suspension, Paper C3, Second International Conference on the Hydraulic Transport of Solids in Pipes, BHRA Fluid Engineering, Cranfield, Bedford, May, 1972.

Condolios, E., Chapus, E.E., and Couratin, P., (1963): Pumping Ores up Vertical Shafts, The Canadian Mining and Metallurgical Bulletin, March, 1963.

Cruger, C.O., and Pollak, F., (1974): Pumps, No. 96, 1974.

Duckworth, R.A., (1974): Introductory Lectures I and II, Slurry Pipelining Course, BHRA Fluid Engineering, Cranfield, Bedford, U.K., May, 1974.

Durand, R., (1953a): The Flow of Solid-Liquid Mixtures in Vertical Pipes, La Houille Blanche, No special A, 1953 (in French).

Durand, R., (1953): Basic Relationship of the Transportation of Solids in Pipes - Experimental Research, Proceedings, Minnesota International Hydraulics Conference, Minneapolis, Minn., Sept., 1953.

Einstein, H.A. and Graf, W.H. (1966): Loop System for Measuring Sand-Water Mixtures, Proc. Am. Soc. Civ. Engrs., Vol 92, HYI, 1966.

Eriksson, B., and Sellgren, A., (1976): Slurry Pipeline Transportation of Iron Ore from Pajala to Luleå . Teknisk Tidskrift, No. 6, 1976 (in Swedish).

Eriksson, B., and Sellgren, A., (1978): Development of Slurry Transportation Technology in Sweden, Paper I5, Fifth International Conference on the Hydraulic Transport of Solids in Pipes, BHRA Fluid Engineering, Cranfield, Bedford, U.K., May, 1978.

Faddick, R.R., (1972): A Mineral Slurry Data Bank, Part I: Report, Colorado School of Mines Research Institute, March, 1972.

Faddick, R.R., (1975): Pipeline Wear from Abrasive Slurries, Paper G3, First International Conference on the Internal and External Protection of Pipes, BHRA Fluid Engineering, Bedford, Sept., 1975.

Faddick, R.R., (1976): Pumps, Course Notes-Solids Pipelining, BHRA Fluid Engineering in Conjunction with the Univ. of Calgary, The Alberta Research Council, and the Colorado School of Mines, Banff, Canada, May, 1976.

Fairbanks, L.C., (1941): Solids-in-Suspension Trans. A.S.M.E. Vol. 64, 7, 1941.

Frazier, D.M., (1968): New Solids Pumping Techniques and Analyses, Paper 21, International Symposium in Solid-Liquid Flow in Pipes and its Applications, Philadelphia, U.S.A. 1968.

Gaessler, H., and Prettin, W., (1976): Bases of Calculation and Planning for the Hydraulic Transport of Run-of-Mine Coal in Pipelines According to the Results of the Hydraulic Plants of the Ruhrkohle AG. Paper E2, Fourth International Conference on the Hydraulic Transport of Solids in Pipes, BHRA Fluid Engineering, Cranfield, Bedford, U.K. May, 1976.

Gauvin, W.H., and Torobin, L.B., (1960): Fundamental Aspects of Solid-Gas Flow pt. IV, Can. J. Chem. Eng. Vol. 38, 1960.

Graf, W.H., and Acaroglu, E.R. (1967): Homogeneous Suspensions In Circular Conduits, Proc. Am. Soc. Civil Engrs, Vol. 93, No. 2, 1967.

Graf, W.H., (1971): Hydraulics of Sediment Transport. McGraw-Hill, 1971.

Haas, D.B., Husband, W.H.W., Schrick, W., and Smith, L.G. (1973a): Experimental Studies on the Transport of Two Different Sands in Water in 2, 4, 6, 8, 10, and 12 Inch Pipelines, Report VII, Saskatchewan Research Council, 1973.

Haas, D.B., Husband, W.H.W., Schrick, W., and Smith, L.G.(1973b): Slurry Pipeline Research Facilities at the Saskatchewan Research Council, Report I, Saskatchewan Research Council, 1973.

Haas, D.B., Husband, W.H.W., Schrick, W., and Smith, L.G. (1973c): Experimental Studies on the Hydraulic Transport of Limestone, Report II, Saskatchewan Research Council, 1973.

Hansen, G., (1967): Fluid Mechanics, John Wiley and Sons., Inc., 1967.

Herbish, J.B., (1962): Modifications in Design Improve Dredge Pump Efficiency, Fritz Engr. Lab., Report, No. 277-35, 1962.

Hinze, J.O. (1959): Turbulence, An Introduction to Its Mechanism and Theory, McGraw Hill, 1959.

Ho, H.W., (1964): Fall Velocity of a Sphere in a Field of Oscillating Fluid, Thesis, Univ. of Iowa, June, 1964.

Holdner, D.N. and Postlethwaite, J. (1975): Wall Mass Transfer in Horizontal Slurry Pipelines, The Can.J.Chem.Eng., Vol 53, Feb. 1975.

Holdner, D.N., and Postlethwaite, J. (1976): Wall Mass Transfer in Vertical and Horizontal Slurry Pipelines, The Can.J.Chem. Eng. Vol. 54, 1976.

Howard, N.M., (1974): Experimental Measurements of Particle Motion in a Turbulent Pipe Flow, Dissertation, Univ. of Illinois, Urbana, 1974.

Hunt, W.A., and Faddick, R.R., (1968): The Effects of Solids on Centrifugal Pump Characteristics, Paper 20, International Symposium in Solid-Liquid Flow in Pipes and its Applications, Philadelphia, U.S.A., 1968.

Ilseder Hütte (1969): Hydraulic Hoisting of Iron Ore, Report, Ilseder Hütte/Peine, 1969 (in German).

Ingebo, R.D., (1956): Drag Coefficients for Droplets and Solid Spheres in Clouds Accelerating in Airstreams, NASA-TN3762, 1956.

Ismail, H.A., (1952): Turbulent Transfer Mechanism and Suspended Sediment in Closed Conduits, Transactions, ASCE, Vol.117, Paper No. 2500, 1952.

Jeffrey, R.C., and Pearson, J.R.A., (1965): Particle Motion in Laminar Vertical Tube Flow, J.Fluid Mech. Vol. 22, No. 4, 1965.

Kazanskij, I., (1976): Contribution, Session A, Fourth International Conference on the Hydraulic Transportation of Solids in Pipes, BHRA Fluid Engineering, Cranfield, Bedford, U.K., May, 1976.

Kazanskij, I., (1978): Hydraulic Transportation of Solids in Pipes, Course, BHRA Fluid Engineering, Frazius Institut TU Hannover, April, 1978.

Kindlundh, P.J., and Nilsson, A., (1977): Application of a Computational Model for Determination of Friction Losses in a Horizontal Slurry Pipeline - A Study of Hydraulic Filling with Sand in Underground Mines, M.Sc. thesis, No. 4, Dept, of Hydraulics, Chalmers University of Technology, 1977.

Kostuik, S.P., (1966): Hydraulic Hoisting and the Pilot-plant Investigation of the Pipeline Transport of Crushed Magnetite, The Canadian Mining and Metallurgical Bulletin, Jan., 1966.

Kranenburg, C., and Geldof, H.J., (1974): Concentration Effects on Settling Tube Analyses, Journal of Hydraulic Research, No.3, 1974.

Landel, R.F., Moser, R.G., and Bauman, A.J., (1963): Fourth Int. Congr. on Rheology, Brown Univ. Proc. Part 2, Interscience Publishers, New York, 1963.

Laubscher, B., (1973): A Study of the "Hydro-lift" Feeder for Introducing Solids into a Hydraulic Hoisting Installation. CSIR Report ME 1197. National Mechanical Engineering Research Institute Council for Scientific and Industrial Research, Pretoria, South Africa, 1973.

Laufer, J., (1954): Natl. Advisory Comm. Aeronaut. Tech. Repts., No. 1174, 1954.

Lavingia, N.J., and Faddick, R.R., (1974): Investigation of a Slurry Bench Test, Paper H2, Third International Conference on the Hydraulic Transportation of Solids in Pipes, BHRA Fluid Engineering, Cranfield, Bedford, U.K., May, 1978.

Lazarus, J.H., and Neilson, I.D., (1978): A generalised Correlation for Friction Head Losses of Settling Mixtures in Horizontal Smooth Pipelines, Paper B1, Fifth International Conference on the Hydraulic Transportation of Solids in Pipes, BHRA Fluid Engineering, Cranfield, Bedford, U.K., May, 1978.

Link, J.M., and Tuason, C.O., (1972): Pipe Wear in Hydraulic Transport of Solids, Mining Congress Journal, Vol 58, July, 1972.

McElvain, R.E. (1974): High Pressure Pumping, Skillings Mining Review, Vol. 63, No. 4, 1974.

Newitt, D.M., Abbot, M., Richardson, J.F., and Turtle, R.B., (1955): Hydraulic Conveying of Solids in Horizontal Pipes, Trans. Inst. Chem. Engrs., Vol. 33 No. 3, 1955.

Newitt, D.M., Richardson, J.F., and Gliddon, B.J., (1961): Hydraulic Conveying of Solids and Vertical Pipes, Trans. Inst.Chem.Engrs., Vol. 39, No. 2, 1961.

Nilsson, A., (1976): oral information, Dept. of Machine Elements, Chalmers University of Technology, 1976.

O´Brien, M.P., (1933): Review of the Theory of Turbulent Flow and Its Relation to Sediment Transportation, Transactions, American Geophysical Union, Washington, D.C., April, 1933.

O´Brien, M.P., and Folsom, R.G., (1937): The Transportation of Sand in Pipelines, Publication in Engineering, Vol. 3, Univ. of Calif., Berkeley, Calif, 1937.

Persson, B., (1976): Impact of Urban Traffic on Man and Environment-Carcinogenic Substances in Vehicle Exhaust, Report No. 76, Dept. of Town Planning, Chalmers University of Technology, 1976.

Postlethwaite, J., Tinkee, E.B., and Brady, B.J., (1976): Studies of Erosion-Corrosion Wear Patterns in Pilot-plant Slurry Pipelines, Paper J2, Fourth International Conference on the Hydraulic Transportation of Solids in Pipes, BHRA Fluid Engineering, Cranfield, Bedford U.K., May, 1976.

Pouska, G.A., and Link, J.M., (1978): Investigation of Head Losses in Coarse Oil Shale Slurries, Paper H2, Fifth International Conference on the Hydraulic Transport of Solids in Pipes, BHRA Fluid Engineering, Cranfield, Bedford, U.K., May, 1978.

Sasaki, Kato, Ueki, and Kajiwara (1958): Characteristics of Pump Pumping Coal, Journal of Japanese Mining Industry Association, Vol. 74, 1958.

Schreiber, W., (1967): Elbow Wear in Steel Pipes and Plastic Pipes, for the Flow of a Sand-Water Mixture. Farbwerke Hoechst, Frankfurt a.m., 1967 (in Germany).

Sellgren, A., (1975): Hydraulic Transportation of Solids in Pipes, a state-of-the-art-study, Report, Department of Hydraulics, Chalmers University of Technology, 1975 (in Swedish).

Sellgren, A., (1977): Hydraulic Hoisting of Crushed Ores. A Feasibility Study on Coarse Iron Ore Transportation by Centrifugal Pumps, Report, Series B:3, Department of Hydraulics, Chalmers University of Technology, 1977.

Shook, C.A., (1976): Development in Hydrotransport. The Can. J. Chem. Eng., Vol. 54, Febr./April, 1976.

Smith, L.G., (1976): A Study of Slurry Flow and Erosion in Helically Ribbed Pipes, M.Sc.thesis, Dept. of Mechanical Engineering, Univ. of Saskatchewan, 1976.

Stepanoff, A.J. (1965): Pumps and Blowers Two-Phase Flow, John Wiley and Sons Inc., New York, 1965.

Swedish Council for Building Research (1973): Density, Water Content, and Pore number. Draft of Geotechnical Laboratory Instructions, B5, 1973 (in Swedish).

Thomas, D.G., (1962): Transport Characteristics of Suspensions, Part IV, AIChE Journal, Vol. 8, May, 1962.

Thomas, D.G., (1965): Transport Characteristics of Suspensions: Part VIII. A note on the Viscosity of Newtonian Suspensions of Uniform Spherical Particles, J.Colloid Sci., 20, 267, 1965.

Thompson, T.L,. Frey, R.J., Cowper, N.T., and Wasp, E.J., (1972): Slurry Pumps - A Survey, Second International Conference on the Hydraulic Transport of Solids in Pipes, BHRA Fluid Engineering, Cranfield, Bedford, U.K., May 1972.

Toda, M., Konno, H., Saito, S., and Maeda, S., (1969): Hydraulic Conveying of Solids Through Horizontal and Vertical Pipes. Kagaku, Kogaku, 1969 (in Japanese).

Vocadlo, J.J., Koo, J.K., and Prang, A.J., (1974): Performance of centrifugal pumps in slurry service. Paper, Third International Conference on the Hydraulic Transport of Solids in Pipes, BHRA Fluid Engineering, Cranfield, Bedford, U.K., May, 1974.

Wallis, G.B., (1969): One-Dimensional Two-Phase Flow, McGraw-Hill Book Co., New York, 1969.

Wasp, E.J., Regan, T.J., Withers, J., Cook, P.A.C., and Clancey, J.T., (1963): Cross Country Coal Pipe Line Hydraulics, Pipe Line News, July, 1963.

Wasp, E.J., Aude, T.C., Seiter, R.H., and Thompson, T.L.,(1968): Hetero-Homogeneous Solids-Liquid Flow in the Turbulent Regime, Paper 13, International Symposium in Solid-Liquid Flow in Pipes and Its Application, Philadelphia, U.S.A.,1968.

Wasp, E.J., Gandhi, R.L., and Kenny, J.P., (1977): Solid-Liquid Flow, Slurry Pipeline Transportation, Trans Tech Publ.,1977.

Weber, M., (1974): Strömungs-Fördertechnik, Krausskopf-Verlag, 1974, (in German).

Wiedenroth, W., (1970): The Influence of Sand and Gravel on the Characteristics of Centrifugal Pumps, some Aspects of Wear in Hydraulic Transportation Installations, Paper E1, First International Conference on the Hydraulic Transportation of Solids in Pipes, BHRA Fluid Engineering, Cranfield, Bedford, U.K., May, 1970.

Willetts, B. B., (1970): Shifts of Sediment Concentration in a Vertical Pipe, Journal of Hydr. Research, No. 1, 1970.

Wilson, G., (1972): The Design Aspects of Centrifugal Pumps for Abrasive Slurries, Paper H2, Second International Conference on the Hydraulic Transport of Solids in Pipes, BHRA Fluid Engineering, Cranfield, Bedford, U.K., May, 1972.

Zandi, I., (1967): Decreased Head Losses in Raw-Water Conduits, J. Am. Water Works Ass., Vol. 59, No. 2, Feb. 1967.

Institutionen för Vattenbyggnad

CHALMERS TEKNISKA HÖGSKOLA

Meddelanden

78. Cederwall, K.: Havet som recipient. Hydrodynamiska synpunkter.
Föredrag vid Sv. Havsforskningsföreningens årsmöte i Stockholm, mars 1975.

79. Sellgren, A.: Hydraulisk transport av fasta material i rör. 1975.

80. Andreasson, L. och Cederwall, K.: Rubbningar av grundvattenbalansen i urbana områden.
Hydrologisk konferens, Sarpsborg, 1975.

81. Cederwall, K.: Bräddning av avloppsvatten och effekten av utjämningsbassänger. "Världen, Vattnet och vi", Elmia 1975.

82. Cederwall, K.: Gross Parameter Solutions of Jets and Plumes. ASCE, HY5, May 1975.

83. Larsson, Sören och Lindquist, Per: Kalkning av försurade sjöar. Del I: Problembeskrivning samt utvärdering av kalkningen av Östra Nedsjön. Ex.arb. 1974:5.

84. Cederwall, K. och Svensson, T.: "Sediment flushing after dredging in tidal bays". 1975.

85. Göransson, C-G. och Svensson, T.: Strömkorsmätningar. Datorprogram för utvärdering inkl. korrektion för avdrift. Mars 1976.

86. Rahm, L. och Häggström, S.: Oskarshamns Kärnkraftverk. Modellstudier avseende kylvattenspridning vid framtida utbyggnad. Maj 1976. Del I Huvudrapport. Del II Bilagedel.

87. Sjöberg, A.: Beräkning av icke stationära flödesförlopp i reglerade vattendrag och dagvattensystem. Aug. 1976.

Slut på Meddelande-serien.

Institutionen för Vattenbyggnad

CHALMERS TEKNISKA HÖGSKOLA

Report Series A

A:1 Bergdahl, L.: Physics of ice and snow as affects thermal pressure. 1977.

A:2 Bergdahl, L.: Thermal ice pressure in lake ice covers. 1978.

A:3 Häggström, S.: Surface Discharge of Cooling Water. Effects of Distortion in Model Investigations. 1978.

Report Series B

B:1 Bergdahl, L.: Beräkning av vågkrafter. 1977.

B:2 Arnell, V.: Studier av amerikansk dagvattenteknik. 1977.

B:3 Sellgren, A.: Hydraulic Hoisting of Crushed Ores. A feasibility study and pilot-plant investigation on coarse iron ore transportation by centrifugal pumps. 1977.

B:4 Ringesten, B.: Energi ur havsströmmar. 1977.

B:5 Sjöberg, A. och Asp, T.: Brukar-anvisning för ROUTE-S. En matematisk modell för beräkning av icke-stationära flöden i floder och kanaler vid strömmande tillstånd. 1977.

B:6 Annual Report 76/77.

B:7 Bergdahl, L. och Wernersson, L.: Calculated and Expected Thermal Ice Pressures in Five Swedish Lakes. 1977.

B:8 Göransson, C-G. och Svensson, T.: Drouge Tracking-Measuring Principles and Data Handling. 1977.

B:9 Göransson, C-G.: Mathematical Model of Sewage Discharge into confined, stratified Basins - Especially Fjords. 1977.

B:10 Arnell,V. och Lyngfelt,S.: Beräkning av dagvatten-avrinning från urbana områden. 1978.

B:11 Arnell, V.: Analysis of Rainfall Data for Use in Design of Storm Sewer Systems. 1978.

B:12 Sjöberg, A.: On Models to be used in Sweden for Detailed Design and Analysis of Storm Drainage Systems. 1978.

B:13 S.Lyngfelt: An Analysis of Parameters in a Kinematic Wave Model of Overland Flow in Urban Areas. 1978.

B:14 Sjöberg, A. och Lundgren, J.: Manual för ILLUDAS (Version S2) Ett datorprogram för dimensionering och analys av dag-vattensystem.